

The role of Poly (ADP-ribose) polymerase in the regulation of innate recognition of immunological receptors expressed on human macrophages.



Kamaran Karim Mohamad

A thesis submitted for the degree of PhD in Immunology

School of Biological Sciences

University of Essex

October 2016

AKNOWLEDGEMENTS

First of all, I praise Allah, the almighty for providing me with this opportunity and the ability to successfully complete my PhD. Secondly, I would like to express my gratitude to my supervisor Professor Nelson Fernandez for his scientific guidance and encouragement throughout my studies. Also I would like to thank my colleagues in lab 4.13 for their help when I needed. I also have to thank my family for their support during my study. Finally, I also would love to dedicate this success to my father's soul who would always encourage me through my education and loved to see my successes.

ABSTRACT

In order to combat harmful pathogens the innate recognition part of the immune system uses a variety of receptors including CD14, TLR4, TLR2 and SR (MARCO). These receptors are expressed on most human monocytes and macrophages. CD14 recognizes and bind lipopolysaccharide (LPS), the main causative agents of sepsis and endotoxic shock. Signaling from CD14-LPS and TLR4/MD-2 complex activate the nuclear factor kappa B (NF- κ B) family of transcription factors and JNK, a member of MAP kinase (MAPK) family. This signaling results in the production of the proinflammatory cytokines such as TNF- α and IL-1 β among others. In addition, LPS also activates the DNA-repair and protein modifying enzyme poly (ADP-ribose) polymerase-1 (PARP-1). Consequently, the effect of PJ-34, a potent inhibitor of PARP on PARP-1 activation induced by LPS was studied on THP-1 cells. In response to LPS, PJ-34 reduced the PAR formation and down regulates the expression of CD14, TLR2 and TLR4. However, MARCO expression was up regulated. It was also observed that PJ-34 reduced the production of TNF- α , IL-1 β and No in response to LPS. PJ-34 was also involved in a reduction of the activation of NF- κ B in response to LPS but, did not have an effect in JNK activation. The physical association of CD14 and MARCO receptors was examined in response to LPS. It was found that PJ-34 reduced the colocalisation of these pair of receptors and regulates their expression at gene level. Furthermore, PJ-34 regulates expression of a number of proteins on the THP-1 cells in response to LPS.

TABLE OF CONTENTS

AKNOWLEDGEMENTS	i
ABSTRACT	ii
TABLE OF CONTENTS	iii
LIST OF FIGURES	vi
LIST OF TABLES	x
ABBREVIATIONS	xi
CHAPTER1: Introduction	1
1.1 Innate immunity.....	2
1.2 Pathogen-associated molecular patterns.....	4
1.2.1 Properties of lipopolysaccharide.....	5
1.2.2 The structure of LPS	6
1.2.3 The biological importance of LPS	7
1.3 Pattern-recognition receptors.....	8
1.3.1 Cluster of differentiation 14 (CD14)	9
1.3.2 Toll-like receptors (TLRs)	15
1.3.3 Scavenger receptors	23
1.4 Regulation of cytokine and chemokine gene expression	28
1.4.1 The nuclear factor kappa B (NF- κ B)	29
1.5 The mitogen-activated protein kinase family (MAPK).....	34
1.5.1 JNK subfamily proteins	35
1.5.2 JNKs and inflammation	35
1.6 Poly (ADP-ribose) polymerases (PARP)	37
1.6.1 Structure and types of PARP enzymes	37
1.6.2 Poly (ADP-ribose) polymerase-1 (PARP-1).....	39
1.6.3 PARP enzymes and mechanisms of proinflammatory cytokine production	40
1.7 Role of CD14 and PARP enzymes in diseases.....	42
1.8 Role of CD14 and PARP in sepsis/septic shock	42
1.9 Pharmacological effect of anti-CD14 and PARP enzymes	43
1.9.1 Anti-CD14 antibody	43
1.9.2 PARP inhibitors	43
AIM OF THE STUDY	45

CHAPTER 2: Materials and Methods	46
2.1 Materials	47
2.1.1 General Laboratory chemicals	47
2.1.2 Tissue culture	47
2.1.3 Antibodies	48
2.2 Methods	49
2.2.1 Tissue culture.....	49
2.2.2 Proliferation studies	51
2.2.3 Flow cytometry to detect cell surface receptors	53
2.2.4 Immunofluorescence labelling of antigens for microscopy.....	54
2.2.5 Confocal microscopy	56
2.2.6 Protein Immunoblotting assay	62
2.2.7 Enzyme-link immunosorbent assay (ELISA)	65
2.2.8 Polymerase chain reaction PCR.....	66
2.2.9 LPS uptake assay	69
2.2.10 Nitric oxide determination by Gries reaction.....	70
2.2.11 Co-Immuno-precipitation assay.....	71
2.2.12 Proteomic analysis of THP-1 cell line	72
CHAPTER 3: The role of the poly (ADP-ribose) polymerase inhibitor PJ-34 on the expression of LPS receptors on THP-1 cells.....	78
PART I: Immunofluorescence analysis of poly (ADP-ribose) polymer synthesis PMA-differentiated THP-1 cells in presence and absence of PJ-34 in response to H₂O₂.....	79
3.1.1 Introduction.....	79
3.1.2 Method and materials.....	80
3.1.3 Results.....	81
3.1.3.2 Poly ADP ribose synthesis in THP-1 cells after treatment with different concentrations of H ₂ O ₂	81
3.1.4 Conclusion	88
PART II: The role of PJ-34 in the expression of LPS receptors on differentiated THP-1 cell in response to LPS.....	90
3.2.1 Introduction.....	90
3.2.3 Results.....	93
3.2.4 Conclusion	106

CHAPTER 4: Measurement of production of cytokines and nitric oxide by THP-1 cells	107
4.1 Introduction	108
4.2 Method.....	110
4.2.1 ELISA	110
4.2.2 Western blotting.....	111
4.2.3 Nitric oxide measurement	112
4.3 Results.....	112
4.3.1 Secretion of TNF- α and IL-1 β in undifferentiated and.....	112
differentiated THP-1 cells in response to LPS.....	112
4.3.2 The effect of PJ-34 on TNF- α and IL-1 β production by THP-1 and.....	116
PD/THP-1 cells after LPS exposure.	116
4.3.3 The role of CD14, TLR2, TLR4 and MARCO in the production of	120
TNF- α and IL-1 β by PD/THP-1 cells in response to LPS	120
4.3.4 The effect of PJ-34 and activation of NF- κ B and JNK on TNF- α	126
and IL-1 β secretion by PD/THP-1 cells after LPS stimulation	126
4.3.5 Role of PJ-34 in NF- κ B and JNK activation in response to LPS	129
4.3.6 The effect of PJ-34 on production of nitric oxide in response to LPS.....	133
4.4 Conclusion.....	134
CHAPTER 5: The role of CD14 and MARCO receptors in response to LPS.....	137
5.1 Introduction	138
5.2 Methods	140
5.2.1 Flow cytometry	140
5.2.2 Colocalisation	140
5.2.3 Real time PCR (qRT-PCR).....	141
5.2.4 Immunoprecipitation.....	142
5.3 Results	143
5.3.1 The effect of PJ-34 on the expression of CD14 and SR (MARCO) in.....	143
response to LPS	143
5.3.2 Confocal microscopy	146
5.3.3 Interaction of CD14 and SR (MARCO) in response to LPS	153
5.3.4 The effect of PJ34 on mRNA CD14 and mRNA SR (MARCO)	155
expression in response LPS	155
5.3.5 The effect of PJ-34 on LPS uptake	157

5.4 Conclusion.....	159
CHAPTER 6: Proteomic analysis of PMA-differentiated THP-1 cells stimulated with LPS in presence and absence of PJ-34.....	160
6.1 Introduction	161
6.2 Methods	162
6.2.1 Cells growth conditions	162
6.2.2 Two-Dimensional gel electrophoresis	163
6.3 Results	163
6.3.1 Two dimensional gel analysis of the effect of PJ-34 on PMA-differentiated THP-1 cells in response to LPS.....	163
6.4 Conclusion.....	170
CHAPTER 7: Discussion.....	171
7.1 Discussion.....	172
References	187

LIST OF FIGURES

Figure 1-1: Schematic structure of LPS.....	7
Figure 1-2: The structure of CD14.....	11
Figure 1-3: The N-terminal region of CD14.....	12
Figure 1-4: The signal cascade via CD14 during the inflammatory response to LPS..	15
Figure 1-5: The structure of toll like receptor (TLR).....	17
Figure 1-6: Schematic structure of toll like receptors (TLRs).....	18
Figure 1-7: Schematic overview of the Toll-like receptor TLR4 signaling pathway...	22
Figure.1-8: Schematic structure of the different classes of scavenger receptors.....	24
Figure 1-9: The schematic structure of NF- κ B family proteins and their inhibitory molecules (I κ B).....	30
Figure 1-10: The structure of the active form of NF- κ B	31
Figure 1-11: Activation and translocation of NF- κ B into the nucleus.....	33
Figure 1-12: Schematic structure of some members of the PARP family of enzymes.	39

Figure 2-1: Colocalisation detection and quantification of CD14 and MARCO receptors on PMA-differentiated THP-1 cells.....	59
Figure 3-1: Poly ADP-ribose formation in PMA-differentiated THP-1 cells after treatment with different concentrations of H ₂ O ₂	83
Figure 3-2: The effect of H ₂ O ₂ on poly ADP-ribose formation in PMA-differentiated THP-1 cells.....	84
Figure 3-3: The effect of PJ-34 on poly ADP-ribose synthesis in PMA-differentiated THP-1 cells stimulated by H ₂ O ₂	86
Figure 3-4: The effect of PJ-34 on poly ADP-ribose synthesis in PMA-differentiated THP-1 cells stimulated by H ₂ O ₂	87
Figure 3-5: The effect of PJ-34 on THP-1 cell viability.....	88
Figure 3-6: The expression of CD14, MARCO, TLR4 and TLR2 in THP-1 cells, assessed by flow cytometry.....	95
Figure 3-7: Differentiation of THP-1 cells with Vit.D ₃ and PMA.....	96
Figure 3-8: The effect of different concentrations of PMA on the expression of CD14, MARCO, TLR4 and TLR2 in THP-1 cells, assessed by flow cytometry.....	98
Figure 3-9: Bar figure represents the effect of different concentrations of PMA on the expression of CD14, MARCO, TLR4 and TLR2 in THP-1 cells, assessed by flow cytometry.....	99
Figure 3-10: The effect of different concentrations of Vit.D ₃ on the expression of CD14, MARCO, TLR4 and TLR2 in THP-1 cells, assessed with flow cytometry...	100
Figure 3-11: Bar figure represent the effect of different concentrations of vit.D ₃ on the expression of CD14, MARCO, TLR4 and TLR2 in THP-1 cells assessed by flow cytometry.....	101
Figure 3-12: The expression of CD14, MARCO, TLR4 and TLR2 in THP-1 cells in response to PMA and vit.D ₃ time course.....	102
Figure 3-13: The effect of PJ-34 on CD14, MARCO, TLR4 and TLR2 expression in PMA-differentiated THP-1 cells THP-1 cells in response to LPS.....	104
Figure 3-14: Bar figure represents the effect of PJ-34 on CD14, MARCO, TLR2 and	

TLR4 expression in PD/ THP-1 cells in response to LPS. ar figure represents.....	105
Figure 4-1: The TNF- α secretion by undifferentiated cells, vit.D ₃ and PMA differentiated THP-1 cells in response to LPS.....	114
Figure 4-2: The IL-1 β - α secretion by undifferentiated cells, vit.D ₃ and PMA differentiated THP-1 cells in response to LPS.....	115
Figure 4-3: The effect of PJ-34 on TNF- α secretion by undifferentiated THP-1 cells in response to <i>E. coli</i> LPS.....	117
Figure 4-4: The effect of PJ-34 on TNF- α secretion by PMA-differentiated THP-1 cells in response to <i>E. coli</i> LPS.....	118
Figure 4-5: The effect of PJ-34 on IL-1 β secretion by undifferentiated THP-1 cells in response to <i>E. coli</i> LPS.....	119
Figure 4-6: The effect of PJ-34 on IL-1 β secretion by PMA-differentiated THP-1 cells in response to <i>E. coli</i> LPS.....	120
Figure 4-7: The TNF- α secretion by PMA-differentiated THP-1 cell in response to <i>E.</i> <i>coli</i> LPS.....	122
Figure 4-8: The TNF- α secretion by PMA-differentiated THP-1 cell in response to <i>E.</i> <i>coli</i> LPS.....	123
Figure 4-9: Secretion of IL-1 β by PMA-differentiated THP-1 cells in response to <i>E.</i> <i>coli</i> LPS.....	124
Figure 4-10: Secretion of IL-1 β by PMA-differentiated THP-1 cells in response to <i>E.coli</i> LPS.....	125
Figure 4-11: The TNF- α production by PMA-differentiated THP-1 cells in response to <i>E. coli</i> LPS.....	127
Figure 4-12: The production of IL-1 β by PMA-differentiated THP-1 cells in respons to <i>E. coli</i> LPS.....	128
Figure 4-13: The effect of PJ-34 on the activation of NF- κ B in response to LPS.....	131
Figure 4-14: The effect of PJ-34 on the activation of JNK-1 in response to LPS.....	132
Figure4-15: The effect of PARP inhibitor PJ-34 on NO production in THP-1 cells in	

response to LPS.....	134
Figure 5-1 (I) & (II): Represents the expression of CD14 on PMA-differentiated THP-1 cells in response to LPS in presence and absence of PJ-34.....	144
Figure 5-2 (I) & (II): Represents the expression of SR (MARCO) on PMA-differentiated THP-1 cells in response to LPS in presence and absence of PJ-34.....	145
Figure 5-3: A representative of single cell image acquired by Nikon confocal microscope.....	147
Figure 5-4: Confocal microscopy images of unstained cells and negative control samples of undifferentiated and PMA-differentiated THP-1 cells.....	148
Figure 5-5: Colocalisation of CD14 and SR (MARCO) on the cell surface of undifferentiated and PMA-differentiated THP-1 cells, determined by confocal microscopy analysis.....	150
Figure 5-6: Colocalisation The effect PJ-34 on the percentage of CD14 and SR (MARCO) receptors by undifferentiated and PMA differentiated THP-1 cell in response to LPS.....	152
Figure.5-7: Immunoprecipitation of CD14 and co-immunoprecipitation to study the interaction of CD14 and SR (MARCO) in undifferentiated THP-1 cells.....	154
Figure 5-8: Immunoprecipitation (IP) of CD14 and coimmunoprecipitation (Co-IP) to study the interaction of CD14 and SR (MARCO) in PMA-differentiated THP-1 cells.....	154
Figure 5-9: Expression of CD14 mRNA in PMA-differentiated THP-1 in response to LPS in presence and absence of PJ-34 using RT-qPCR.....	156
Figure 5-10: Expression of MARCO mRNA in PD/THP-1 cells in response to LPS in presence and absence of PJ-34 using RT-qPCR.....	157
Figure 5-11: The effect of PARP inhibitor PJ-34 on the up taking of LPS labelled FITC by SR (MARCO).....	158
Figure 6-1: Two-dimensional gel images of cell lysate proteins from PD/ THP-1 cells	

treated with LPS in presence and absence of PJ-34.....	165
Figure 6-2: Reference image of cells only (control) showing all differentially expressed polypeptide spots.....	166
Figure 6-3: 3dimensional views of polypeptide spots derived from PMA-differentiated THP-1 cells, analysed by Progenesis SameSpot software.....	167

LIST OF TABLES

Table. 1-1: Microbial Ligands of human TLRs.....	19
Table. 6-1: Summary of polypeptides obtained from reference image showing all differentially expressed spots by untreated PMA-differentiated THP-1 cells (Control) by their IP and molecular.....	168.
Table. 6-2: Representatives and Comparison of polypeptides spots expressed by untreated PMA-differentiated THP-1 cells (control) and cells treated with LPS in the presence and absence of PJ-34 PARP inhibitor.....	169

ABBREVIATIONS

Ab	Antibody
AGE	Advanced glycation end
APC	Antigen presenting cells
APS	Ammonium persulfate
AP-1	Activator protein-1
BSA	Bovine serum albumin
^o C	Celsius
C-terminal	The Carboxyl terminal
Co-IP	Co-immunoprecipitation
CAMs	Cell adhesion molecules
CD14	Cluster of differentiation 14
cDNA	Complementary deoxyribonucleic acid
CO ₂	Carbon dioxide
DAPI	4', 6'-diamino-2-phenylindole, di-hydrochloride
DBD	DNA binding domain
DCs	Dendritic cells
2DE	Two-dimensional gel electrophoresis
DNA	Deoxyribonucleic acid
dNTPs	2'-deoxynucleoside-5'-triphosphates
DTT	Dithiothreitol
ER	Endoplasmic reticulum
ERK	Extracellular-signal-regulated kinases
FCS	Fetal calf serum
FITC	Fluorescein isothiocyanate
FL	Fluorescence
FSC	Forward scatter
FACS	Fluorescent activated cell sorter
H ₂ O ₂	Hydrogen peroxide
hr	Hour
HPACC	Health protection agency culture collection
IgG	Immunoglobulin G

I κ B	Inhibitory kappaB
IL	Interleukine
iNOS	Inducible nitric oxide synthase
IRFs	Interferon regulatory factors
JNK	c-Jun terminal kinase
Kb	Kilo base pair
KDa	Kilo Daltons
LPS	Lipopolysaccharide
LBP	LPS-binding protein
LRR	Leucine-rich repeat
mAb	Monoclonal antibody
mCD14	Membrane bound CD14
ml	Millilitre
min	Minute
MAPK	Mitogen- activated protein kinases
MFI	Mean fluorescence intensity
mg	Milligram
M/M	Monocytes/Macrophages
mRNA	Messenger ribonucleic acid
MS	Mass spectrometry
MyD-88	myeloid differentiation factor 88
NAD ⁺	Nicotinamide adenine di-nucleotide
NF- κ B	Nuclear factor kappa-light-chain-enhancer of activated B cells
ng	Nano gram
NLS	Nuclear localization signal/sequence
NK	Natural killer
NO	Nitric oxide
N-terminal	The amino terminal
OD	Optical density
PAGE	Polyacrylamide gel electrophoresis
PAMPs	Pathogen associated molecular patterns
PAR	poly ADP-ribose
PARP	poly (ADP-ribose) polymerase

PBS	Phosphate buffered saline
PCR	Polymerase chain reaction
PD\THP-1 cells	PMA-differentiate THP-1 cells
PFA	Paraformaldehyde
PJ-34	<i>N</i> -(6-oxo-5,6-dihydrophenanthridin-2-yl)- <i>N,N</i> -dimethylacetamide Hydrochloride
PMA	Phorbol 12-myristate 13-acetate
PRR	Pattern recognition receptors
PS	Phosphatidylserine
rpm	Rotation per minute
RPMI-1640	Roswell park memorial institute-1640
RT	Room temperature
RNA	Ribonucleic acid
sCD14	Soluble form of CD14
SDS	Sodium dodecyl sulphate
SR(MARCO)	Scavenger receptor(Macrophage receptor with collagenous structure)
SSC	Side scatter
STAT	Signal transducer and activator of transcription
TEMED	<i>N,N,N,N</i> -tetramethylethylenediamine
TLR2	Toll like receptor 2
TLR4	Toll like receptor 4
T _m	Annealing temperature
TNF	TNF-receptor-associated factor
TNF- α	Tumour necrosis factor- α
V/V	Volume / Volume
Vit. D ₃	1,25-dihydroxyvitamin D ₃
W/V	Weight by volume
α -Tubulin	Alpha-Tubulin
μ l	Microlitre
μ M	Micromole

CHAPTER1: Introduction

1.1 Innate immunity

The immune system plays an important role in tissue repair after injury and inflammation-mediated damage. It removes internal debris, dying and malignant cells and protects against aggression from external sources.

The immune system in vertebrates consists of two subsystems, the innate and adaptive immune systems, constituting two main immune strategies. Innate immune responses are non-specific to a particular pathogen, but can develop rapidly after antigen exposure. The adaptive immune system, however, requires time to develop and is characterised by being highly specific. The adaptive immune response generates immunological memory, distinguished by enhanced immunity against a specific pathogen after subsequent encounters with that pathogen

The innate immune system requires the coordinated action of several effector cells and serum proteins. For example, bacterial infections are controlled by phagocytic neutrophils, monocyte/macrophages (M/M) and dendritic cells (DCs), which patrol the blood and immune organs to encounter and engulf the bacteria. Monocytes release large amounts of cytokines (e.g., TNF-alpha, IL-1beta, IL-6, IL-8), complement factors as well as proteolytic enzymes which contribute the onset of early systemic inflammatory response associated with acute and chronic diseases. Furthermore, monocytes also facilitate the transendothelial migration of macrophages to the site of injury (Antoniades et al., 2008). During a bacterial infection macrophages play an important role in both innate and adaptive immune responses in which blood circulating macrophages migrate from the vasculature in to extracellular compartment under influences of different endogenous and exogenous factors (Martinez, 2008). Intracellular bacterial or viral infections generally cannot be detected by phagocytes, and are controlled by natural killer (NK) cells, which

detect and destroy infected cells. Innate immune cells recognise and interact with microbes by responding to germ line-encoded pattern recognition receptors (PRRs) such as cluster of differentiation 14 (CD14), toll-like receptor 2 (TLR2), toll-like receptor 4 (TLR4), the scavenger receptor macrophage receptor with collagenous structure (MARCO) and MD-2 (Doyle et al., 2004; Arredouani et al., 2006; Areschoug & Gordon, 2009). These receptors detect conserved microbial structures that are not found in the host, designated pathogen-associated molecular patterns (PAMPs), which include mannans and zymosan in the yeast cell wall, and a variety of bacterial cell-wall components, such as lipopolysaccharide (LPS), lipopeptides, lipoteichoic acid and peptidoglycans (Aderem & Ulevitch, 2000; Uematsu & Akira, 2008; Xagorari & Chlichlia, 2008; O'Neill et al., 2013). Many of these components are able to stimulate the innate immune system. LPS is one of the most potent among these, inducing production of cytokines such as interleukins (ILs), and tumour necrosis factor (TNF) in mononuclear phagocytes, and it represents a central component in the pathogenesis of septic shock syndrome. Innate antimicrobial defence is significantly assisted by several serum proteins which detect and bind to microbes, thereby promoting the uptake and destruction of microbes by immune cells. For example, binding of LPS to CD14 is enhanced by serum LPS-binding protein (LBP) (Schumann, 1992; Thompson et al., 2003; Hamann et al., 2005; Schröder & Schumann, 2005). The engagement of LPS by the host cell triggers the production of proinflammatory cytokines such as tumour necrosis factor alpha (TNF- α) and interleukins (Correia et al., 2001; Cohen, 2002; Kim & Krueger, 2015). TNF- α is one of the earliest major proinflammatory mediators released by macrophages when stimulated with LPS in vivo and in vitro. Elevated serum levels of TNF- α is associated with the pathogenesis of several inflammatory conditions, including sepsis (Dufour et al., 2003; Esposito & Cuzzocrea, 2009; Kasimanickam et al., 2013; Koppolu et al., 2013),

rheumatoid arthritis (Edrees et al., 2005), and multiple sclerosis (Gregory et al., 2012). Suppression of TNF- α production has been suggested as a possible therapy in these diseases. The intracellular events that mediate LPS-induced TNF- α secretion have been the subject of intense research. Nuclear factor kappa B (NF- κ B), a protein complex that controls transcription of DNA has been found to have an important role in the transcriptional regulation of many proinflammatory cytokines genes. Several stimulants, including bacterial LPS, can activate NF- κ B which, once activated, translocate from the cytoplasm to the nucleus (Kim et al., 2010; Gupta et al., 2011). NF- κ B family members are rapidly inducible, and play an important role in immune and inflammatory responses. NF- κ B is critical in the production of proinflammatory cytokines as a response to injury and inflammatory stimuli (Bonizzi & Karin, 2004; Qi et al., 2012; Kumar et al., 2014). The poly (ADP-ribose) polymerase (PARP) protein family is a group of enzymes mainly involved in DNA repair that are also necessary for mammalian apoptosis (Soldani & Scovassi, 2002; Bürkle, 2005). PARP-1 can interact with many transcriptional factors (Hassa et al., 2001), and has been postulated to play a role in the regulation of NF- κ B transcriptional activity (Meder et al., 2005; Pacher & Szabó, 2007; Cohausz & Althaus, 2009; Kraus & Hottiger, 2013).

1.2 Pathogen-associated molecular patterns

Pattern-recognition receptors (PRRs) are used by the innate immune system to differentiate harmful pathogens (non-self) from “self”. PRRs detect conserved structures on microbes that are absent from the host (Janeway & Medzhitov, 2000; Postel & Kemmerling, 2009; Kumar et al., 2011) termed pathogen-associated microbial patterns (PAMPs). PAMPs include lipoteichoic acid (LTA) and LPS that are common components

of gram-positive and gram-negative bacteria, respectively. In addition, double-stranded RNA is a structural signature of several groups of RNA viruses and mannans, which are components of yeast cell walls (Akira et al., 2006; Veckman, 2007).

PRRs can be classified into families based on the domains the receptors possess. The most common are lectin, cysteine-rich and leucine-rich repeat domains (Medzhitov and Janway 2000). PRRs can also recognize endogenous ligand in the host. These receptors, therefore, play a vital role in tissue homeostasis and host defence (Gordon, 2002; Kawai & Akira, 2010; Di Gioia & Zanoni, 2015). PRRs can bind a very wide range of molecular ligands, including proteins, lipids, carbohydrates and nucleic acids from endogenous and exogenous sources. A single PRR is often able to recognize multiple ligands through relatively weak interactions. Some ligands, such as LPS, can bind to several distinct PRRs. Furthermore, different PRRs can cooperate as a receptor complex for a particular ligand. For example CD14, TLR4 and MD2 form a receptor complex for LPS.

1.2.1 Properties of lipopolysaccharide

LPS is also termed endotoxin, an important structural component of the outer membrane of Gram-negative bacteria (Haziot et al., 1996; Gronow & Brade, 2001; Trent et al., 2006). LPS is vital to protect bacteria from hydrolytic degradation by other organism, and plays a role in the pathogenicity of bacterial infection (Hacker & Kaper, 2000; Hacker & Carniel, 2001;). LPS is released from the bacteria during cell division, cell death, or as a result of antibiotic treatment against bacterial infection (Rice & Bayles, 2008; Tanouchi et al., 2013). Upon its release, LPS is recognized by M/M cells of the innate immune system, and it activates them. The LPS molecule is not toxic when it is released in small amounts, but after endotoxin reaches the blood stream and spreads in the body the

immune system begins to release proinflammatory cytokines such as TNF- α , interleukins such as IL-1, and others (Beishuizen & Thijs, 2003; De La Garza, 2005). High levels of endotoxin can be life-threatening, frequently causing endotoxic or septic shock (Wanecek et al., 2000; Wu et al., 2004; Hiromura et al., 2007).

1.2.2 The structure of LPS

The LPS molecule is made up of hydrophobic and hydrophilic domains and forms part of the outer membrane of the cell wall of gram-negative bacteria, which is impermeable to large molecules and hydrophobic compounds. Its function is to protect gram-negative bacteria from hydrophilic degradation by the other organisms in the environment. Figure 1.1 illustrates the three component parts of LPS, (i) Lipid A, (ii) core oligosaccharide and (iii) O-specific side chain or O-antigen (Skurnik & Bengoechea, 2003; Loutet et al., 2006; Hagelueken et al., 2015). Lipid A, which binds to CD14 epitopes, contains two acylated GlcNAc-P residues (GlcN). The core part is made of 3-deoxy-D-manno-octulosonic acid (KDO), heptoses (Hep), and neutral sugars such as galactose. The outer O-antigen is made of repeating units of two to eight sugars.

LPS is composed of common and unusual sugars (Fig.1.1). The polysaccharide domain is hydrophilic in nature and consists of two regions, the O-antigen and core oligosaccharide. The O-antigen is important for distinguishing between gram-negative bacteria serotype strains (Reyes et al., 2009; Wang et al., 2010). The core oligosaccharide is divisible into an inner and outer core based on the sugar groups present. The inner core is a carbohydrate structure made up of 3-deoxy-D-manno-2-octulosonic acid (KDo), L-glycero-D-mannoheptose (Heptose), phosphate and ethanolamine residues. The outer core is made up of more common hexoses, such as glucose and galactose. Lipid-A (endotoxin), the hydrophobic anchor of LPS, is formed of glucosamine-based

phospholipids that make up the outer monolayer of the outer membrane of most Gram-negative bacteria. The lipid A moiety of LPS is responsible for the toxic effects of LPS (Schromm et al., 2000; Raetz et al., 2007).

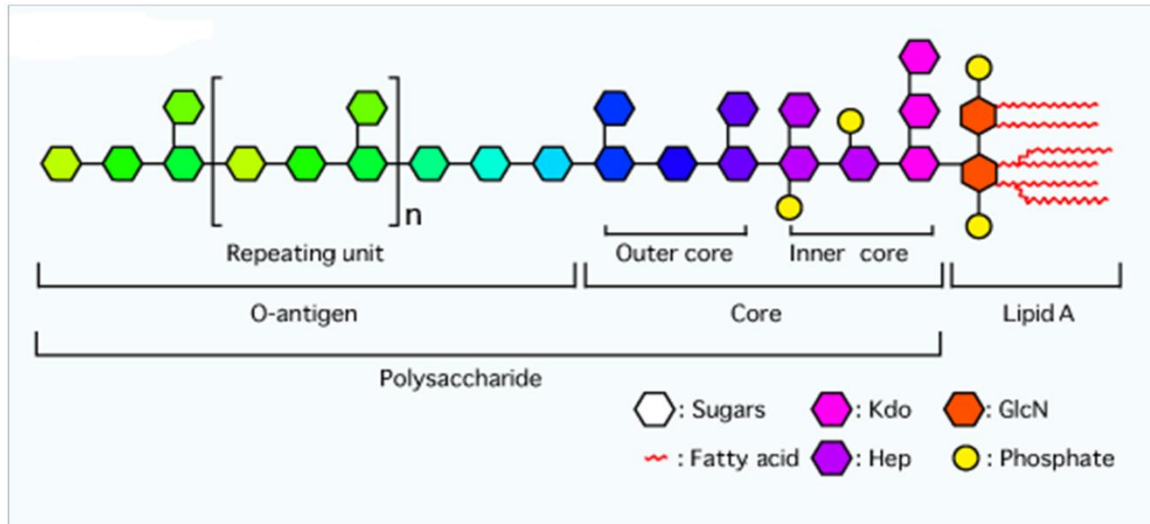


Figure 1-1: Schematic structure of LPS. LPS is composed of three main parts: The O-antigen, the core and lipid A, which interacts with epitopes of CD14, and contains of two acylated GlcNac-P residues (GlcN). The core part of LPS consists of KDO, heptoses and galactose. The O-antigen is comprised of repeating units of two to eight sugars. (Source from Glycoforum: Masahito Hashimoto, 2003).

1.2.3 The biological importance of LPS

LPS at low concentrations, is able to act as an adjuvant due to its immunostimulatory action, causing polyclonal B-cell expansion (Hamann et al., 2005; Xu et al., 2008). However, high levels of LPS can have an adverse effect. High LPS levels can cause life-threatening endotoxin shock or systemic inflammatory response syndrome (Huber et al., 2006). CD14 is the most prominent cell protein believed to be involved in the binding of LPS, after LPS is released into the blood stream. CD14 is expressed mainly on monocytes and macrophages and triggers the production of proinflammatory cytokines (Moore et al., 2000; Guha & Mackman, 2001; Auffray et al., 2009; Rossol et al., 2011).

1.3 Pattern-recognition receptors

PRRs bind their ligands through opsonization. Functionally, PRRs can be classified into three types: Humoral proteins (soluble) circulating in the plasma, endocytic receptors expressed on the cell surface, and signaling receptors expressed either on the cell surface or intracellular such as CD14, TLRs, scavenger and complement receptors which are cell surface receptors (Gordon, 2002; Lee & Kim, 2007).

Effector cells of the innate immune system that express PRRs include surface epithelial cells, monocytes, macrophages and DCs. PRRs that are expressed by innate immune cells recognize ligands on invading organisms directly by recognition of different conserved molecular patterns. In contrast, in the context of adaptive immunity, PRRs expressed in lymphocytes, are structurally and functionally heterogeneous proteins, germline-encoded, expressed by all cells, and are able to distinguish self from non-self-molecules (Janeway & Medzhitov, 2002).

Soluble PRRs include soluble CD14, LBP, bacterial permeability increasing protein (BPI), lysozyme, C-reactive protein (CRP), defence collagens (mannose binding lectin, MBL) and complement (Kumagai & Akira, 2010; Gauglitz et al., 2012). Signaling via PRRs activate signaling pathways that induce upregulation of costimulatory molecules, antimicrobial effector responses and inflammation upon recognition of PAMPs. The only known signaling PRRs expressed on cell surface are members of the TLR family (Kopp and Medzhitov, 1999). However, some PRRs, such as mitogen-activated protein (MAP) kinases, are expressed in the cytosol, and they are able to detect intracellular pathogens and initiate responses that block the pathogen's ability to replicate (Symons et al., 2006).

1.3.1 Cluster of differentiation 14 (CD14)

CD14 is one of the most important molecules of the innate immune system, having a wide-range of functions. It is well known that CD14 serves as a pattern recognition receptor in the innate immune system for many ligands, ranging from parts of microbial cell walls to whole bacteria (Arroyo-Espliguero et al., 2004; Manukyan et al., 2005). CD14 has been shown to be the receptor for LPS of Gram-negative bacteria, for peptidoglycan (Dziarski et al., 2000), lipoteichoic acids of gram-positive bacteria (Cleveland et al., 1996) and lipoarabinomannan of mycobacteria (Elass et al., 2007; Mishra et al., 2011). The binding of CD14 to LPS is enhanced by the serum protein LBP (Kitchens & Thompson, 2005; Tsukamoto et al., 2010). The role of LBP appears to be that of enabling LPS to dock at the LPS receptor complex by initially binding LPS and then forming a ternary complex with CD14. However, it has been demonstrated that in mice LBP is not required in vivo for the clearance of LPS from the circulation, but is required for the rapid induction of an inflammatory response after exposure to LPS in small amounts (Gonzalez-Quintela et al., 2013).

1.3.1.1 The structure of CD14

CD14 was first described as a myeloid differentiation antigen in 1981 (Griffin et al., 1981). It has molecular weight of 55-KDa, possesses multiple leucine-rich repeats and is encoded on chromosome 5 (5q) in a region that also codes for growth factors, such as granulocyte macrophage colony stimulating factor and vascular endothelial growth factor receptor. CD14 is present in soluble form (sCD14) in blood and as a membrane-bound form (mCD14) in myeloid lineage cells, anchored to the plasma membrane by a glycosyl-phosphatidylinositol (GPI) moiety (Lee et al., 1993), thus CD14 is not a transmembrane

protein but is attached to the plasma membrane via the GPI-tail (Zanoni & Granucci, 2013). Based on its cDNA sequence, CD14 is composed of 356 amino acids and a 19 amino acid-long N-terminal leader peptide. After translation, the C-terminal leader sequence of 28–30 amino acids is replaced by the GPI anchor. The LPS-binding site is located on the N terminal site of the protein (Iovine et al., 2002; Kim et al., 2005).

CD14 occurs as a structurally symmetrical dimer that possesses a horseshoe-like structure. Figure 1.2 shows that the monomeric subunit of CD14 contains thirteen β strands, 11 of them, from β 3 to β 13, overlapped with conserved leucine-rich repeat (LRR) domains which consist of 5 to 45 motifs, each 20-30 amino acids in length, that generally fold into horseshoe shapes (Kim et al., 2005). All major classes of LRR proteins have curved horseshoe structures with a parallel sheet on the concave side and mostly helical elements on the convex side. The main significance of LRRs is that repeats from different subfamilies never occur simultaneously and have most probably evolved independently (Enkhbayar et al., 2004).

The concave surface of the horseshoe-shaped structure of CD14 consists of a large β -sheet of 11 parallel and two antiparallel beta strands. The convex surface contains both helices and loops, in no regular pattern. As a result, it is rough rather than smooth and contains several grooves and pockets that are crucial for ligand binding. Dimerization in the crystal is mediated by residues in β 13 and in the loop between β 12 and β 13. Parallel β -sheets from the two monomers interact in an antiparallel fashion and form a large and continuous β -sheet encompassing the entire CD14 dimer. The concave face and the adjacent loops are the most common protein interaction surfaces on LRR proteins. The elongated and curved LRR 3D structure provides an outstanding frame work for achieving diverse protein-protein interactions (Kobe and Kajava, 2001). The N-terminal hydrophobic pocket is located on the side of the horseshoe near the NH_2 terminus, and it is entirely hydrophobic

except for the rim. The pocket including the sub-pocket has a total volume of 820 Å³ and hence is large enough to accommodate at least part of the lipid chains of LPS. The residues on the hydrophilic rim of the main pocket are highly flexible (Kim et al., 2005). The N-terminal region of CD14 may be critical for binding of LPS (Jerala, 2007).

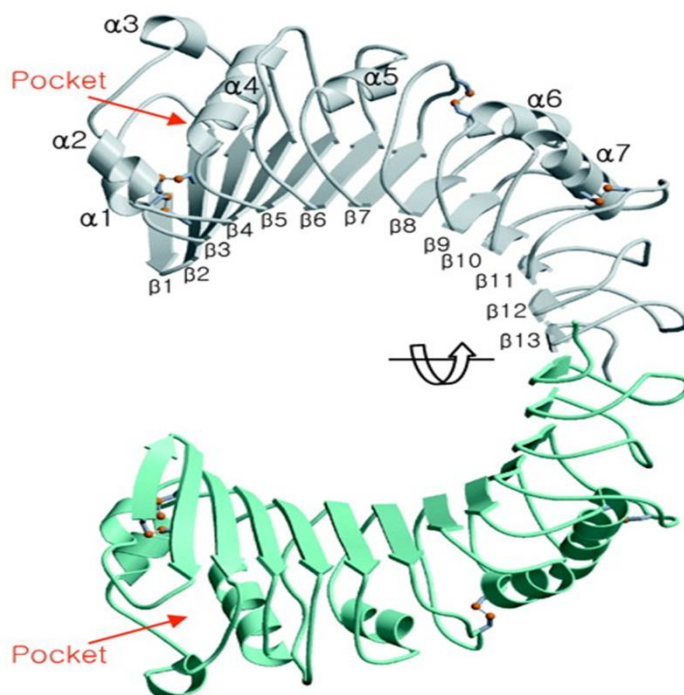


Figure 1-2: The structure of CD14. Two monomers of CD14 in the crystal are colored in gray and cyan. Disulfide bridges are shown in orange. The position of the NH₂-terminal pocket is indicated by an arrow (Adapted from Kim et al., 2005).

1.3.1.2 LPS binding site on CD14

The CD14 receptor contains binding sites that bind several anti-CD14 monoclonal antibodies (mAbs) (Wright et al., 1990). Four regions of the binding sites for LPS and CD14 have been identified within the NH₂-terminal of CD14. Residues from the turn between the $\beta 1$ and $\beta 2$ strands constitute region one. Region two is the loop between the

β 2 strand and the one alpha helix. LPS binding is inhibited by mAbs that recognize this area (Kim et al., 2005). Region three consists of residues from the β 3 strand which is the most frequent target of LPS blocking antibodies. There are at least nine monoclonal antibodies that recognize the β 2 and β 3 strands that restrict binding of LPS by sCD14. Region four includes residues from the loop connecting α 2 and α 3 helices (Kim et al., 2005).

TPEPCEL**DDEDF**FRVCVCFNFSE**PQPD**WSEAFQCVSA**VEVEI**HAGGLNLEPFLKR

VDADAD**PRQY**ADTVKALR...

Figure1-3: The N-terminal region of CD14. The amino acids in bold are the ones that have been deleted (Adopted from Viriyakosol and Kirkland, 1995).

1.3.1.3 Different forms of CD14 protein

The membrane form of CD14 protein (mCD14) is strongly expressed in human monocytes/macrophages present in peripheral blood, in lymph nodes and spleen. Other non-myeloid cell types, such as hepatocytes and several epithelial cell types, also express mCD14. Human monocytes express high levels of CD14 and elicit 100000 receptors per cell, whereas neutrophils express approximately 3000 receptors per cells (Antal-Szalmas et al., 1997). The soluble form of CD14 (sCD14), produced in human plasma by shedding from cell-membrane (Kitchens et al., 2001; Duncan et al., 2004), and present at concentrations of 12 μ g/mL (Ward et al., 2014).

Administration of LPS has been shown to upregulate the expression of CD14 within the first 3 hrs following LPS binding to CD14. This followed by a decrease after 3-6 hrs and then, remarkably, the expression of CD14 increases within the first three days of gram negative septic shock (Landmann et al., 1996; Antal-Szalmas, 2000). The first rapid

increase is associated with the translocation of intracellular CD14 to the plasma membrane. The second upregulation is associated with *de novo* protein synthesis and might correlate with monocyte differentiation (Landmann et al., 1996; Antal-Szalmas, 2000). The synthesis and expression of CD14 is regulated by several mediators.. In monocytes, the anti-inflammatory cytokines IL-4 and IL-13 reduce CD14 expression at the transcriptional level within the first two days (Ruppert et al., 1991).

1.3.1.4 The biological functions of CD14

One of the main functions of CD14 is recognition of and binding to LPS or LPS-LBP complex (Wright et al., 1990; Perera et al., 2001). Studies shows that CD14-deficient mice are hyporesponsive to low concentrations of LPS and highly resistant to LPS at a lethal dose or LPS-induced shock (Haziot et al., 1996). Teo & Hughes (2003), showed that CD14 is important for the recognition and phagocytosis of apoptosed cells, and in preventing the release of proinflammatory cytokines during phagocytosis. These results indicated that clearance of apoptotic cells is mediated by a receptor which interacts with 'non-self' components (LPS) and 'self' components (apoptotic cells) produce distinct macrophage responses. Furthermore, CD14 also has the ability to regulate apoptosis in monocytes; studies on normal monocytes have revealed that the downregulation of CD14 molecules results in monocyte apoptosis whereas increased expression of CD14 protects these cells from apoptosis (Heidenreich et al., 1997). However, upregulation of CD14 caused by LPS stimulation resulted in decreased apoptosis in monocytes (Heidenreich et al., 1997; Carracedo et al., 2002)

1.3.1.5 Role of CD14 in proinflammatory cytokine production

Sepsis is one of the most common causes of morbidity and mortality in hospital intensive care units. This condition is characterised by temperature alterations and elevation of various cytokines in blood (Gustot et al., 2009). In gram-negative bacterial infection, LPS or the LPS-LBP complex binds to CD14. LBP is not essential for the binding of LPS to CD14, but it accelerates its binding, probably serving as a transfer protein (Wurfel et al., 1995). Since CD14 is a GPI-linked protein, it is incapable of signal transmission across the plasma membrane. Thus a membrane cofactor(s) is necessary to affect LPS-mediated transmembrane signaling, toll-like receptor TLR4 and myeloid differentiation factor 2 being utilized (Akashi et al., 2000).

The CD14-LPS complex associates with TLR4, transmitting 'downstream' signals which contribute to nuclear translocation of NF- κ B and production of proinflammatory mediators such as TNF- α , IL-1 and IL-6 (Jiang et al., 2005). In addition to the CD14-TLR4-LPS complex, another glycoprotein, MD-2, is required for the optimal functioning of TLR4 (Lu et al., 2008a; Schnabl et al., 2008). CD14 is also required for TLR4-MD-2 complex interaction with LPS (Shuto et al., 2005; Lizundia et al., 2008).

Once the LPS is bound and the CD14-TLR4/TLR2 complex is formed, intracellular signaling cascades depend on different sets of adapters. An early response to LPS, which involves MyD88 and MyD88-like adapter (Mal), results in the activation of NF- κ B and AP1. Later response to LPS utilizes the TIR-domain-containing adapter-inducing interferon- β (TRIF) and TRIF-related adapter molecule (TRAM), which leads to the late activation of NF- κ B and IRF3, and production of cytokines, chemokines, and other transcription factors. Figure 1.4, shows immediate response occurs after LPS binds directly to the cell surface, and it takes approximately 30 minutes for LPS-induced actions to initiate, such as cytokine release and adhesion, after LPS binding. This suggests that a

time consuming process such as internalization is necessary to enable signaling (Wurfel et al., 1995).

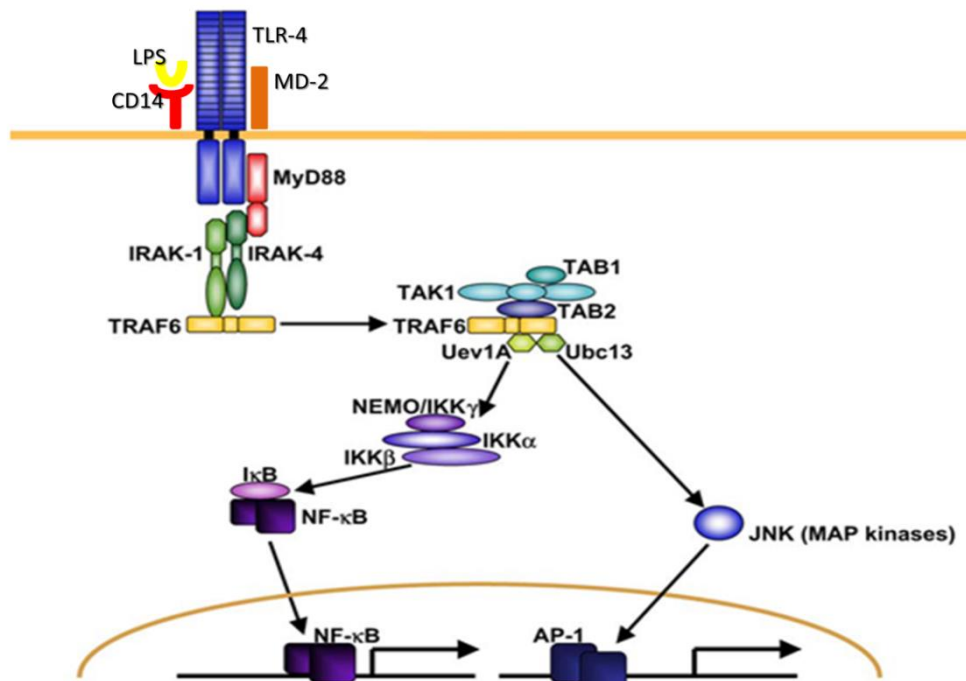


Figure 1-4: The signal cascade via CD14 during the inflammatory response to LPS. In gram-negative bacterial infection, LPS binds to CD14, and then the consequent complex binds to TLR4 which initiates a signal cascade initiated in the presence of MD-2. The LPS-mediated signaling leads to activation of transcriptional factors, including NF-κB and AP-1, and release proinflammatory cytokines (Adapted from Takeda and Akira, 2004).

1.3.2 Toll-like receptors (TLRs)

TLRs are ancient receptors, associated with wide range of activities and their involvement in innate immunity was first demonstrated in *Drosophila melanogaster*, which has only innate immune responses. In *Drosophila*, TLRs are essential in responses to fungal and bacterial infection; two signaling cascades are utilized, a toll pathway and an immune

deficiency pathway (Singh et al., 2003). Subsequently, TLR homologs were described in humans (Da Silva Correia et al., 2001). Currently 12 mammalian TLRs are known (Akira, et al., 2006) which contribute to signal transduction induced by PAMPs (Sabroe et al., 2003; Singh et al., 2003). Each TLR member activates a different signaling pathway in response to PAMPs, which then induce a specific response such as inducing production of proinflammatory cytokines. In addition, TLRs control multiple dendritic cell functions and activate signals that are critically involved in the initiation of adaptive immune responses (Jiang et al., 2000; Singh et al., 2003; Iwasaki & Medzhitov, 2004). Up-regulation of TLRs in response to microbial such as LPS or loss of negative regulation of TLR signaling, as well as recognition of self-molecules by TLRs, are strongly associated with the pathogenesis of inflammatory and autoimmune diseases (Akira, et al., 2006). The TLR4 is involved in signaling pathway initiated in response to a wide variety of endogenous and exogenous molecules, especially LPS, and it may associate with increasing the risk of septic shock (Andonegui et al., 2002; Song et al., 2001)

1.3.2.1 Toll-like receptor expression and structure

TLRs are most prominently expressed by professional antigen-presenting cells, including macrophages and DCs. They are expressed by epithelial or endothelial cells, but at low or undetectable levels. TLRs are germ line-encoded type I integral membrane glycoproteins, display an extracellular domain (amino terminus), contain LRR and intracellular domains (Carboxyl-terminus), and have a conserved cytoplasmic portion that is essential for intracellular signaling (Fig.1.6). The cytoplasmic signaling domain of TLRs is homologous to the human IL-1 receptor (Figure 1.5) and thus named the Toll/IL-1R (TIR) domain. The extracellular domain of IL-R1 contains IgG-like proteins (Singh et al., 2003).

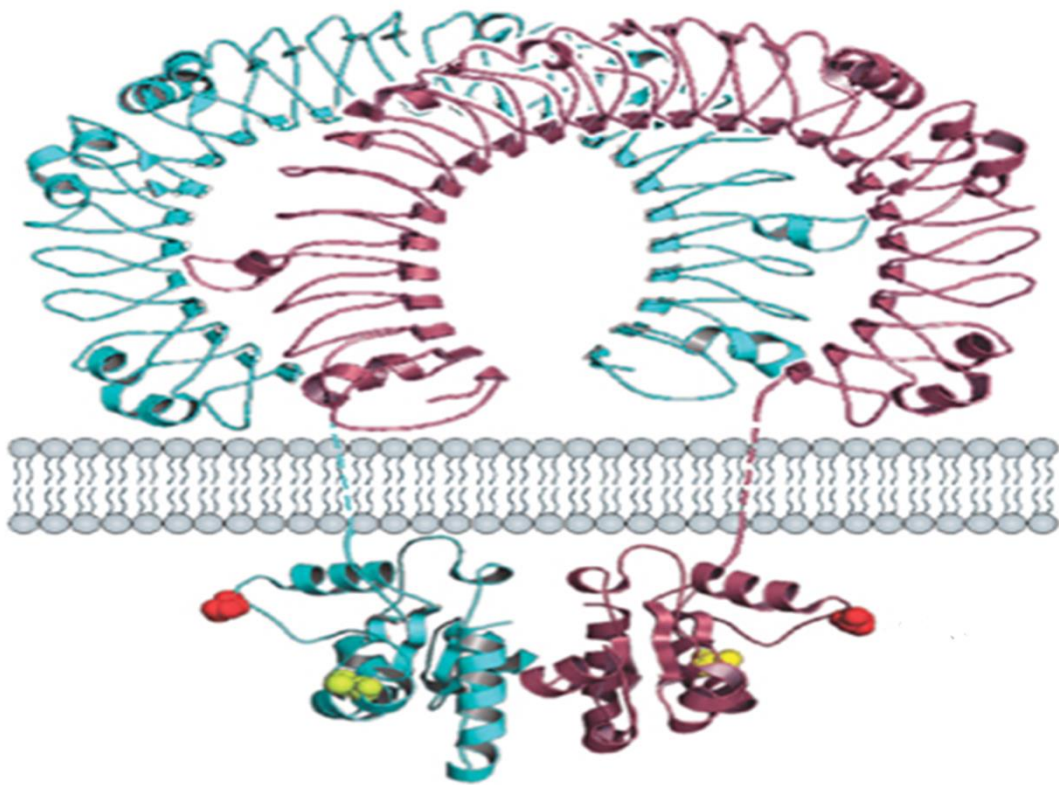


Figure 1-5: The structure of toll like receptor (TLR). A transmembrane domain connects to an extracellular domain that is folded to form a prominent c-shaped component. A cytoplasmic domain projects below the cell membrane. Two identical TLR proteins coded in blue and red, associate to form a homodimer.

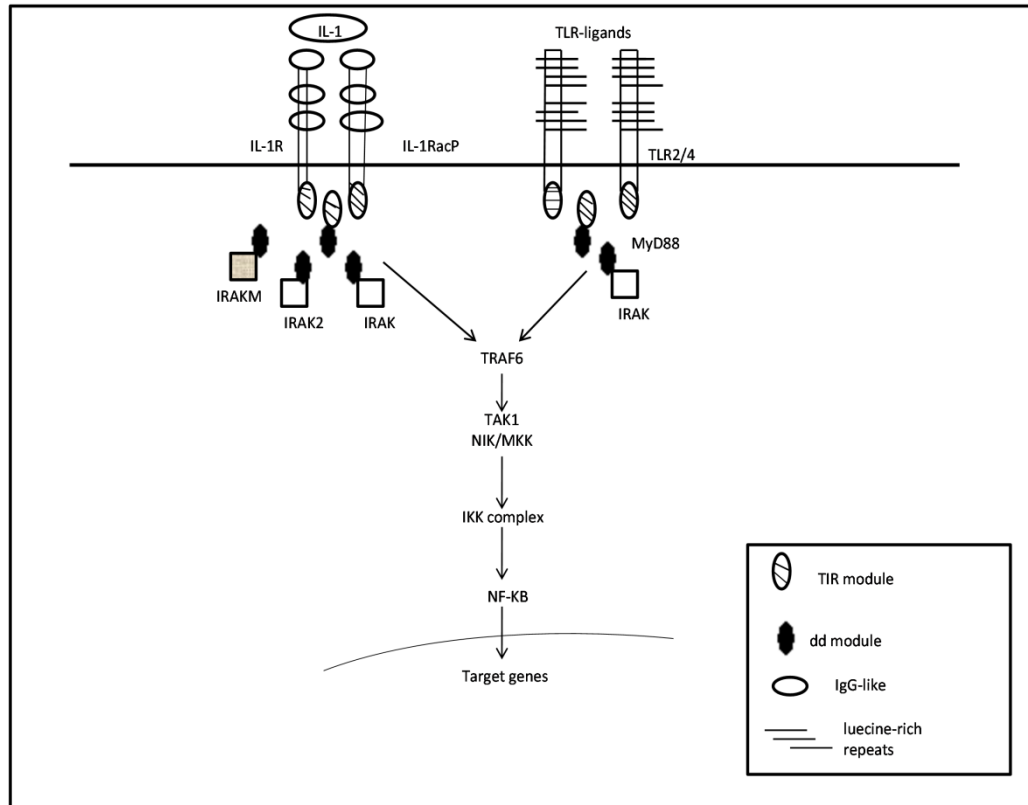


Figure 1-6: Schematic structure of toll like receptors (TLRs). The extracellular domain of TLRs contains β Leucine rich repeats, and the cytoplasmic domain contains proteins which are similar to the cytoplasmic domain of IL-R1. The extracellular domain of IL-R1 contains IgG-like proteins. TLR family members, except TLR3, use the adaptor MyD88 to activate NF- κ B, leading to production of proinflammatory cytokines. Adapted from Biochemsoctrans: (Muzio et al., 2000).

The first TLR ligand described was bacterial LPS, which is detected by TLR4. In recent years the ligands for several TLRs have been identified (summarized in Table 1.1). Significant variability in the structures of TLR ligands exists and they can consist of lipids, proteins or nucleic acids. Interestingly, some TLRs can detect ligands from several of these categories. Further fine-tuning on the ligand specificity is achieved by formation of TLR heterodimers. For example the TLR1/TLR2 dimer detects bacterial triacyl lipopeptide, while TLR2/TLR6 recognizes diacyl lipopeptide structures (Takeda & Akira, 2004).

Receptor	Ligand	Origin of ligand
TLR1 +TLR2	Triacyl lipopeptides	Bacteria and Mycobacteria
TLR2	(Peptidoglycan)	Gram-positive bacteria
	Porins	Neisseria
	Lipoarabinomannan	Mycobacteria
	Phospholipomannan	Candida albicans
	Glucuronoxylomannan	Cryptococcus neoformans
	Hemagglutin protein	Measles virus
	Not known	HSV1, HMCV
	tGPI-mutin	Trypanosoma
TLR3	dsRNA	RNA viruses
TLR4	LPS	Gram-negative bacteria
	Mannan	Candida albicans
	Glucuronoxylomannan	Cryptococcus neoformans
	Envelope proteins	RSV
	HSP60, 70	Host
	Fibrinogen	Host
TLR5	Flagellin	Flagellated bacteria
TLR2+TLR6	Lipoteichoic acid	Group B Streptococcus
	Diacyl lipopeptides	Mycoplasma
	Zymosan	Saccharomyces cerevisiae
TLR7/8	ssRNA	Viruses
TLR9	CpG-DNA	Bacteria, mycobacteria and viruses

Table 1-1: Microbial Ligands of human toll like receptors (TLRs).

At least some TLRs require accessory molecules for PAMP detection. For example TLR4 requires MD2, CD14 and LBP for efficient signal transduction, while CD36 mediates the detection of diacylglycerols by TLR2/TLR6 dimer (Poltorak et al., 1998; Hoebe et al., 2005). The cellular location of TLRs varies. TLRs 1, 2, 4, 5 and 6 are expressed on the cell surface while TLRs 3, 7, 8 and 9 are found intracellularly in endosomes (Akira et al., 2006). Intracellular TLRs detect nucleic acids which are also produced by the host. Thus, it is likely that the endosomal location of these TLRs prevent uncontrolled immune activation by endogenous nucleic acids.

1.3.2.2 Function of TLRs

TLR4 binds LPS (Lu et al., 2008; Peri et al., 2010) or the LPS-LBP-MD-2 complex (Park et al., 2009; Peri & Piazza, 2012) and CD14 (Levy et al., 2009; Peri et al., 2010), leading to receptor dimerization and activation, and proximate nuclear translocation of NF- κ B (Guha & Mackman, 2001; Park et al., 2004). Kim & Kim, (2014) reported that hyporesponsiveness and hyperresponsiveness to LPS are entirely dependent on CD14 and associated TLR4. Both TLR4-deficient mice and mice that possess a disrupted TLR4 gene are resistant to the immunostimulatory and pathophysiological effects of LPS (Arbour et al., 2000; Shi et al., 2006). Previous studies have shown that CD14 is upregulated by LPS (Zanoni et al., 2009). Silva et al. (2010), reported that TLR4 expression is also upregulated by LPS, and the physical proximity between CD14 and TLR4 trigger LPS signaling, activate and translocate of NF- κ B into nucleus. Inhibition of the activation of human TLR4 by LPS is considered to have potential for the development of innovative drugs for the treatment of sepsis and septic shock (Visintin et al., 2005; Peri & Piazza, 2012).

1.3.2.3 TLR activation and signaling

TLR4 is the signal transducing receptor for LPS (Beutler, 2000; Sekine et al., 2006). LPS recognition by the innate immune system involves as the first step binding of the LBP to the LPS, which recognize by CD14. The complex then binds to TLR4 with present of MD-2 molecules; TLR4 triggers LPS signaling and activate the MyD88-dependant or independent signaling pathway of TLR4 (Fig.1.7). TLR4 transduces the signal through the association of intracellular TIR domain, recruiting the adaptor proteins. TIR-domain-containing adaptor molecules are recruited to the intracellular domain of TLR4. Five adaptor molecules have been identified: myeloid differentiation factor 88 (MyD88), TIR-domain-containing adaptor inducing IFN- β (TRIF), TIR-domain-containing adaptor protein (TIRAP; also known as MyD88 adaptor-like, Mal), TRIF-related adaptor molecule (TRAM) and sterile alpha and HEAT/Armadillo motif protein (SARM). Among these MyD88 and TRIF are significant in TLR signaling, both mediating activation of downstream signaling (Akira, et al., 2006; Jerala, 2007). MyD88 is used by all TLRs except TLR3, while TRIF signaling is used by TLR3 and TLR4. TIRAP/Mal is required for interaction of MyD88 with TLR2 and TLR4, while TRAM enables TLR4-TRIF interaction (Akira, et al., 2006; Tanimura et al., 2008). The fifth adaptor protein SARM was recently shown to negatively regulate TRIF signaling (Carty et al., 2006; Peng et al., 2010). Downstream TLR signaling includes several phosphorylation and ubiquitination steps where TNF receptor-associated factor family proteins and IRAKs, together with cellular ubiquitination machinery, play a key role (Akira, et al., 2006; Lu et al., 2008). Ultimately, TLR signaling results in the activation and nuclear translocation of NF- κ B, interferon regulatory factors (IRFs) and mitogen-activated protein kinase (MAPK)-regulated transcription factors. These transcription factors regulate the expression of a vast

majority of anti-microbial genes including proinflammatory cytokines, chemokines and IFNs.

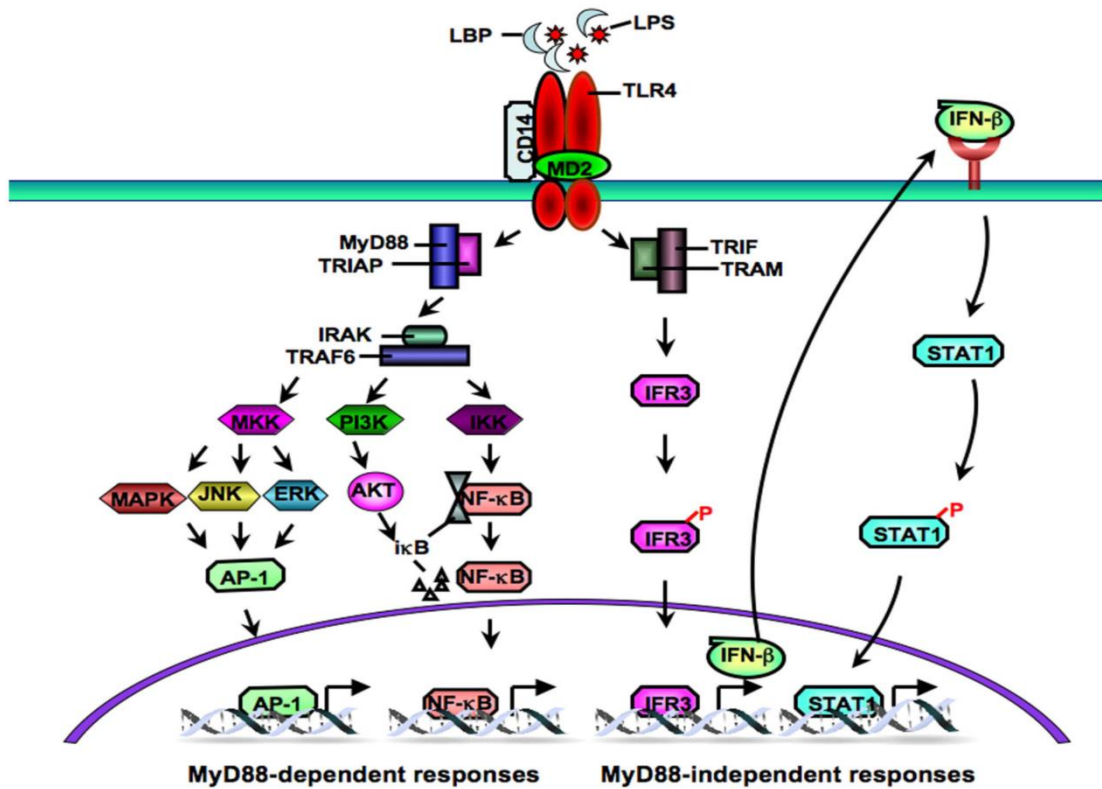


Figure 1-7: Schematic overview of the Toll-like receptor TLR4 signaling pathway. LPS binds to LPS-binding protein (LBP) and then binds to TLR4 on the cell membrane with two co-receptors (CD14 and myeloid differentiation protein (MD-2), activating myeloid differentiation factor 88 (MyD-88)-dependent and MyD-88-independent TLR4 signaling via different adaptor proteins. The MyD88-dependent pathway signals through activation of IκB kinase (IKK) and mitogen activated protein kinase (MAPK) pathways, which in turn leads to activation of the transcription factors nuclear factor (NF)-κB and activator protein (AP)-1, respectively. These control the expression of proinflammatory cytokines and other immune related genes. In addition, phosphatidylinositol 3-kinase (PI3K) and AKT are also important factors downstream of MyD88 that mediate NF-κB activation. The MyD88-independent pathway is mediated by the TIR domain-containing adaptor inducing interferon-β (TRIF), which activates interferon regulatory (IRF) 3 and induces the expression of interferon (IFN)-β and IFN-responsive genes.

1.3.3 Scavenger receptors

Scavenger receptors (SRs) were originally identified and named based on their ability to bind and internalize modified lipoprotein (Greaves & Gordon, 2005). The SR family is comprised of large type I and type II transmembrane glycoproteins expressed at high levels by macrophages and DCs, and at a low level by some endothelial cells. SRs have the capacity to bind modified low-density lipoprotein (LDL) and other polyanionic ligands. SRs have been divided into eight classes, A to H (Fig.1.8), based on congruity of structure (Plüddemann et al., 2007).

Since the SR superfamily is too large to describe each family member. Class A (SR-A) scavenger receptors have been shown to recognise a range of polyanionic molecules and play a vital role in microbial recognition and clearance. These SRs have been shown to bind both gram-positive and gram-negative bacteria (Thomas et al., 2000). Hampton and colleagues (2000) proposed that SR-A might be involved in antimicrobial host defence, based on their observation that SR-A could bind lipid A, an integral part of LPS. SR-A also recognises the gram-positive cell-wall component LTA (Dunne et al., 1994). SR-A has been shown to play a role in both infection and inflammation. SR-A-deficient mice show increased susceptibility to *Staphylococcus aureus* and *Streptococcus pneumoniae* infection (Thomas et al. 2000; Arredouani et al., 2006). However, these animals were more susceptible to endotoxic shock as a result of increased proinflammatory cytokine secretion in response to additional LPS challenge.

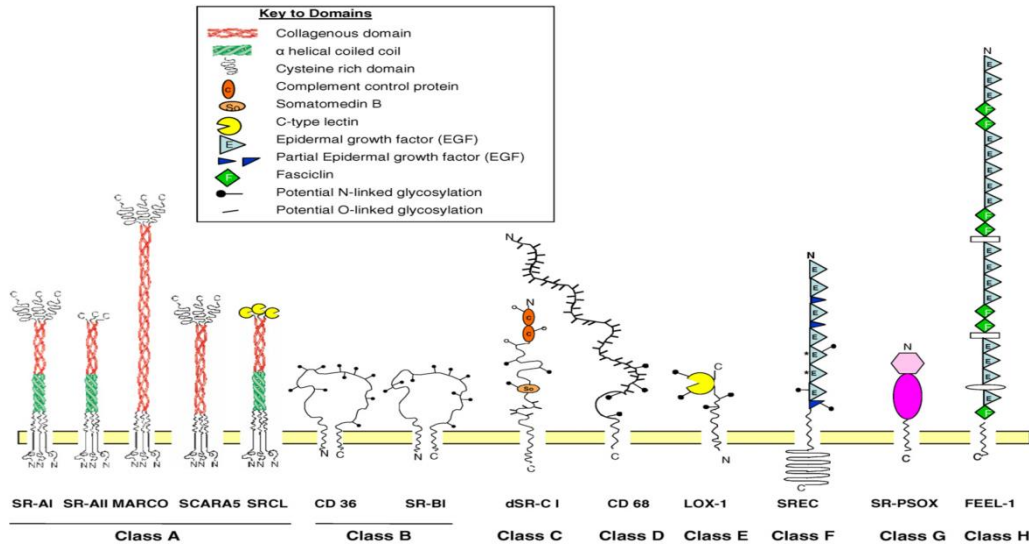


Figure1-8: Schematic structure of the different classes of scavenger receptors. Scavenger receptors are grouped together into classes based on their structural homology and are structurally very diverse. The domains are indicated in the key. Adapted from (Pluddemann et al 2006)

1.3.3.1 The structure of class A SRs

Class A SRs are homotrimeric type II transmembrane glycoproteins SR-A1(Gough et al., 1998; Nakamura et al., 2001) (Fig. 1.8), which has a short N-terminal cytoplasmic domain, a single transmembrane domain, and large extracellular protein comprised of a spacer, an α -helical-coiled-coil domain, a collagenous domain, and C-terminal scavenger receptor cysteine-rich (SRCR) domain (Martínez et al., 2011; Qiu et al., 2013). SR-AII is shorter than SR-AI as it lacks of the SRCR domain (Sarrias et al., 2004). MARCO is structurally similar to SR-AI, but lacks an α -helical coiled-coil domain and has a much longer collagenous domain (Sankala et al., 2002). In comparison to SR-AI, SRCL-I contains a C-terminal c-type lectin domain instead of a SRCR domain, and an additional extracellular serine/threonine-rich region. The SRCL- II isoform lacks the c-terminal lectin domain (Nakamura et al., 2001). Jiang et al. (2006) suggested that SCARA5 has

five domains and its extracellular portion is composed of a long spacer, a short collagenous domain and a SRCR domain.

1.3.3.2 Scavenger receptor localisation

SRs are most abundantly expressed in macrophages, particularly Kupffer cells, alveolar macrophages, and macrophages in the spleen and lymph nodes (Murray & Wynn, 2011; Hussell & Bell, 2014). Fibroblasts, endothelial cells, smooth muscle cells and DCs also express SRs (Husemann et al., 2002). Transient expression of bovine SRs on cultured cells shows that SRs are mainly expressed in the ER, nuclear envelope, and Golgi apparatus of non-macrophage cells, whereas in macrophages and macrophage-like cells they are present on the plasma membrane but also localize to endosomes (Naito et al., 1991). The expression and activity of SR-A were reported to be downregulated by LPS in the human monocyte cell line (THP-1), through TNF- α secretion. In contrast, their expression is upregulated by LPS in both peritoneal macrophage and mouse cell lines J774 and RAW264.7 (Fitzgerald et al., 2000).

1.3.3.3 Role of MARCO and SR-A in host defence

SR-AI/AII that are associated with atherosclerosis express on macrophage-derived foam cells during atherogenesis, which suggests the role of these types of SR in this process (Linton & Fazio, 2001; Van Eck et al., 2005). MARCO expression in the atherogenesis plaque has not been proven. SR-A has been implicated in several diseases, including Alzheimer disease and diabetes. It binds to β -myeloid protein and advanced glycation end product (AGE) modified protein (Granucci et al., 2003; Canton et al., 2013). AGE is a heterogeneous group of proteins or lipids linked to both oxidative stress and inflammation

and they are found in many tissues. AGE are involved in protein cross linking and have been identified in pathological tissues, such as the kidney of patients with diabetic nephropathy and chronic renal failure, atherosclerosis lesions and amyloid fibrils in haemodialysis-related amyloidosis (Basta et al., 2004; Hodgkinson et al., 2008). Macrophages from SR-A deficient mice show a decrease in the phagocytosis of apoptotic thymocytes. Therefore, it was proposed that SR-A may play a role in the removal of apoptotic cells (Platt et al., 2000). SRs were originally identified based on their ability to scavenge modified lipoproteins, these molecules have been shown to recognize and bind to modified and unmodified host derived molecules or microbial components. As a major subset of innate pattern recognition receptors, scavenger receptors are mainly expressed on myeloid cells and function in a wide range of biological processes, such as endocytosis, adhesion, lipid transport, antigen presentation, and pathogen clearance. Scavenger receptor has been implicated in the clearance of LPS in macrophage-like J774 cells (Czerkies et al., 2013). Also LBP and mCD14 augment LPS clearance (Gutsmann et al., 2001a). It seems likely from these and other studies that LPS clearance is a separate event from LPS signal transduction (Leon-Ponte et al., 2005). In addition, scavenger receptors play a crucial role in maintenance of host homeostasis, in the pathogenesis of a number of diseases, e.g., atherosclerosis, neurodegeneration, or metabolic disorders. Emerging evidence has begun to reveal these receptor molecules as important regulators of tumour behaviour and host immune responses to cancer (Yu et al., 2015). MARCO also has a role in the regulation of the cellular response to heat shock protein (Kobayashi et al., 2000), and plays a role in adhesion and spreading processes. The expression of MARCO in spleen macrophages in the spleen marginal zone contributes to retention of marginal zone B cells (Karlsson et al., 2003; Kellermayer et al., 2014). Evidence for this came from specific binding of soluble MARCO to these cells, and inhibition of the

binding with antibody against MARCO. The ligand for MARCO in marginal zone B cells has not been identified (Karlsson et al., 2003). Besides LPS, SR-A also binds lipoteichoic acid from gram-positive bacteria or the bacteria, such as *Staphylococcus aureus* and *Mycobacterium tuberculosis* (Dunne et al., 1994; Thomas et al., 2000). MARCO is able to bind gram-negative and gram-positive bacteria (Peiser et al., 2002; Huang et al., 2012). Cross-competition studies with LPS and several other SR ligands have shown other SRs, expressed on Kupffer and liver sinusoidal endothelial cells, involved in the binding of LPS (Knoll et al., 1995; Nedredal et al., 2003). SRs have been implicated in the clearance of damaged and apoptotic cells (Terpstra & van Berkel, 2000; Yu et al., 2015). This recognition by SRs may be explained by the structural similarities between cell membranes and lipoproteins. Both consist of phospholipids, cholesterol, and glycoprotein. Oxidative damage to a lipoprotein particle may create epitopes that resemble the epitopes exposed by cells that undergo apoptosis or by senescent erythrocytes, such as membrane phosphatidylserine (PS). PS is, under normal conditions, confined to the inner leaflet of cell membranes, but on apoptosis or aging, when the aminophospholipid asymmetry is destroyed, PS becomes exposed on the outer leaflet, providing a signal for removal (Züllig et al., 2007). Some SRs have been shown to bind liposomes containing PS (Plüddemann et al., 2007) and SR ligands, such as oxidized low density lipoprotein and poly I, inhibit the binding of damaged and apoptotic cells (Terpstra & van Berkel, 2000), further suggesting a role of SRs in the removal of damaged and apoptotic cells. MARCO is also described as a ligand for uteroglobulin-related protein-1, which is expressed on bronchial epithelial cells (Heinzmann et al., 2003).

In addition to microbial components, MARCO and SR-A recognize unopsonized environmental particles, such as TiO₂, FeO₂, SiO₂ and latex beads (Shifu & Gengyu, 2005; Kanno et al., 2007). MARCO appears, in fact, to be the major receptor on lung

alveolar macrophages (AM) for these particles. This notion is based on the work of Palecanda et al. (1999) who showed that particle binding by SRs is sensitive to general SR inhibitors. In addition, binding is largely retained in SR-A-KO AMs. Palecanda et al. (1999) generated an antibody that blocked binding of the unopsonized particles by hamster AMs. This antibody was found to be directed against MARCO (Palecanda et al., 1999). Recently, a similar approach was used to demonstrate the major role that MARCO confers in particle binding in human AMs (Arredouani *et al.*, 2005a). Studies with SR-A and MARCO-KO mice have provided direct evidence that these SRs afford a protective role in the host defence. SR-A KO mice were more susceptible than wild-type controls to infection with *Listeria monocytogenes* and *staphylococcus aureus* (Blanchet et al., 2014; Thomas et al., 2000), and with the viral pathogen HSV-1 (Auerbuch et al., 2004). The study with *S. aureus* indicated that opsonin-independent bacterial phagocytosis is significantly decreased in macrophages lacking SR-A. This might be the reason for the susceptibility of SR-A KO mice to the infection with this bacterial strain (Thomas et al., 2000). LPS-treated SR-A KO mice primed with Bacille Calmette-Guerin, a live attenuated *Mycobacterium bovis* vaccine, were highly susceptible to a subsequent LPS challenge, with increased production of TNF- α and IL-6 (Haworth et al., 1997).

1.4 Regulation of cytokine and chemokine gene expression

Microbial infection leads to rapid production of inflammatory cytokines and chemokines. The expression of these genes is regulated mainly at a transcriptional level by binding of transcription factors to their target elements on gene promoters. Generally cytokine and chemokine genes are regulated by activation of transcription factors such as NF- κ B, interferon regulatory factors, AP-1 and STAT. Transcription factor pathways, mainly

activated via pattern recognition receptors and cytokines which activate these transcription factors, thereby creating positive (and negative) feedback mechanisms. Both direct PRR-mediated and indirect cytokine-mediated mechanisms are involved in the regulation of cytokine and chemokine production during microbial infections.

1.4.1 The nuclear factor kappa B (NF- κ B)

Nuclear factor kappa B (NF- κ B) is a family of inducible gene transcription factors, expressed in most cells. Salminen et al., (2008) showed that NF- κ B is a master regulator of inflammatory and innate immune responses. It has been implicated in several inflammatory diseases due to its function as a regulator of proinflammatory gene expression (Li & Verma, 2002; Kravchenko et al., 2008). The present study investigates innate immune mechanisms of severe sepsis. NF- κ B plays a vital role in sepsis, involving innate immune receptors and poly (ADP-ribose) polymerase (PARP) enzymes.

1.4.1.1 Structure of NF- κ B family members

The NF- κ B family in mammals consists of five proteins (Fig. 1.9): NF- κ B1 (p105/p50), NF- κ B (p100/p52), ReL-A (p65), ReL-B and c-ReL. All members of the NF- κ B family have a conserved ReL-homology domain (RHD) (Li and Verma, 2002; Vallabhapurapu & Karin, 2009). The DNA binding domain, nuclear localization signals (NLS), dimerization domains and the I κ B binding domain are located within a REL-homology domain. The NF- κ B proteins c-ReL, ReLB and p65 (REL-A) also contain a transactivation domain. NF- κ B refers to a heterodimer of two proteins, a p65 subunit (also called ReL-A) and a p50 subunit, and it is most abundant form of the protein (Sasaki et al., 2005) (Fig. 1.10). p50–c-ReL dimers also occur (Sarnico et al., 2009). Both p50–ReL-A and p50–c-ReL

dimers are regulated by interactions with inhibitor of κ B (I κ B) proteins, which maintain their cytoplasmic localization. ReL-B can act as a transcriptional activator and a repressor of NF- κ B dependent gene expression, while REL-A is responsible for most of NF- κ B transcriptional activity, due to the presence of a strong transactivation domain (Ramakrishnan et al., 2013).

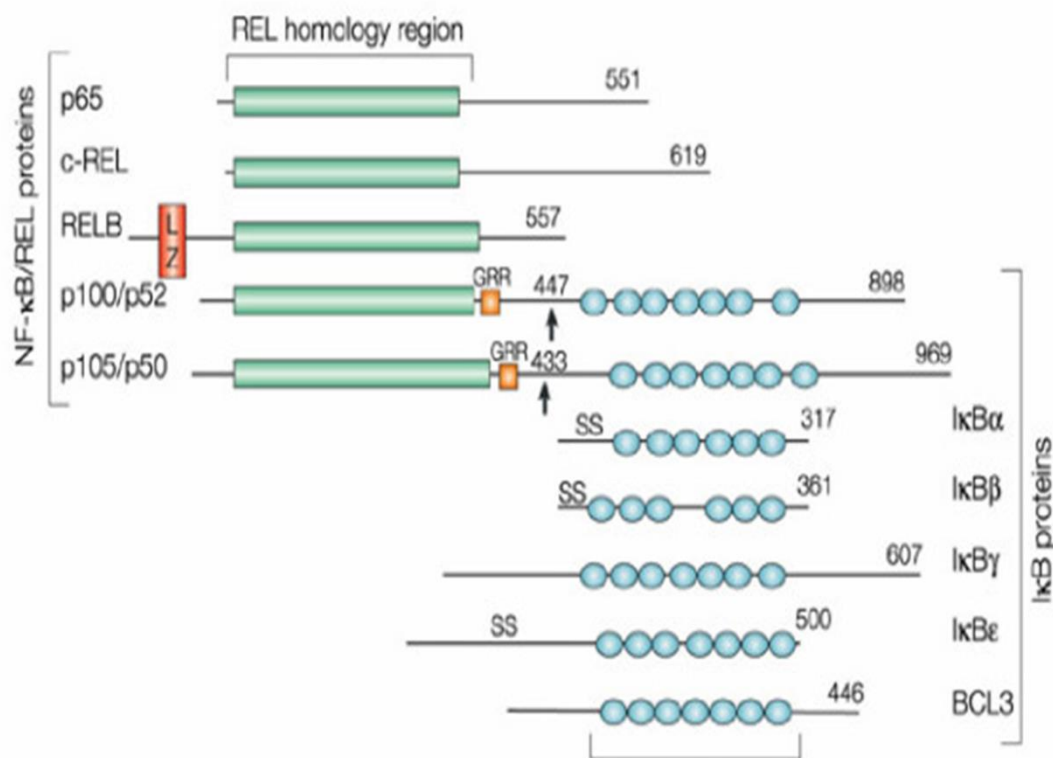


Figure 1-9: The schematic structure of NF- κ B family proteins and their inhibitory molecules (I κ B). Abbreviations; LZ (red) leucine zipper, RHD (green) REL-homology domain, GRR (orange) glycine rich regions and I κ B (blue) inhibitor of κ B proteins. (Source: Li and Verma, 2002).

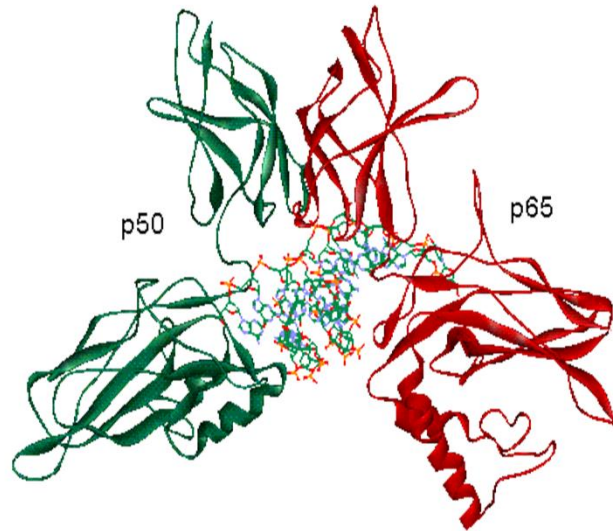


Figure 1-10: The structure of the active form of NF- κ B. The most active form of NF- κ B consists of two subunit, p50 (green) and p65 (red)

(Source: from <http://www.web books.com/MoBio/Free/Ch4H3.htm>).

Under unstimulated conditions NF- κ B proteins are retained in the cytoplasm in association with I κ B proteins. Upon activation, the inhibitory proteins are phosphorylated by I κ B kinases (IKK $\alpha/\beta/\gamma$) that subsequently enable the translocation of NF- κ B dimers into nucleus (Li & Verma, 2002). In the nucleus NF- κ B dimers bind to their target DNA sequences and associate with co-activation proteins such as cAMP responsive element binding protein to enhance transcription. The NF- κ B pathway is induced by a variety of factors, including cytokine action, activity following PRR-mediated microbe detection, and DNA damage (Kawai & Akira, 2007; Salminen et al., 2008).

1.4.1.2 Role of NF- κ B in inflammatory responses

NF- κ B is one of the key regulators of proinflammatory gene expression and mediates the transcription of proinflammatory cytokines (TNF α , IL-1, IL-2, IL-6, IL-12, and GF-CSF) (Souza et al., 2008; Lawrence, 2009), chemokines (RANTES, MIP-1 α , MCP1) (Holgate

et al., 1997; Vilá et al., 2007; Yi et al., 2014) adhesion molecules (ICAM-1, VCAM, E-selectin) (Lawrence, 2009; Zhong et al., 2012; Xiao et al., 2014) and inducible factor enzymes or proinflammatory enzymes like COX-2, hemeoxygenase-1, iNOS (Surh et al., 2001; Ferrante et al., 2008).

NF- κ B is normally retained in the cytoplasm ; it is in an inactive form associated with the inhibitory molecules of KappaBs (I κ Bs) (Li & Verma, 2002). Activation of NF- κ B occurs by two different pathways: the classical and the alternative pathway (Orange et al., 2005). The classical pathway of NF- κ B activation (Fig. 1.11), is the most relevant to this study and is triggered by signaling through TLRs. Activation of NF- κ B occurs upon cell exposure to stimuli, for example cell stress, the effect of proinflammatory cytokines such as TNF- α , ILs, LPS, and viral infection. LPS activate NF- κ B via phosphorylation of inhibitor of NF- κ B kinase subunit alpha (IKK1) and sometimes inhibitor of NF- κ B kinase subunit beta (IKK2) in the inhibitory kappa β -kinase complex. The activator factors may directly activate the IKK, which causes phosphorylation and degradation of I κ B, which results in the freeing of NF- κ B heterodimers. The heterodimers then translocate into the nucleus and bind to the appropriate promoter regions. These results in expression of transcriptional factor genes are responsible for production of proinflammatory cytokines such as IL1, IL6, IL8 and TNF- α (Orange et al., 2005).

The activation of NF- κ B occurs after a signal from TLR4, transmitted via the MyD88 pathway, which initiates when CD14 binds to LPS and then transfers to TLR4. Activation of TLR4 causes phosphorylation of I κ B by IKK (I κ B kinase). The degradation of I κ B occurs through the ubiquitin system. The freed NF- κ B (p50-ReL-A) translocates into the nucleus and activates gene expression. The newly synthesized I κ B can enter the nucleus, where it is helps to remove the NF- κ B from the DNA and export it back to the cytoplasm where it normally resides (Hinz et al., 2012; Schuster et al., 2013). It has b

been found that PARP enzymes, especially PARP-1 are required for NF- κ B activation (Hassa et al., 2001; Nakajima, 2004; Veuger et al., 2009; Castri et al., 2014). Castri et al. (2014) found that PARP-1 plays an important role in the activation and relocation of NF- κ B to the cytoplasm.

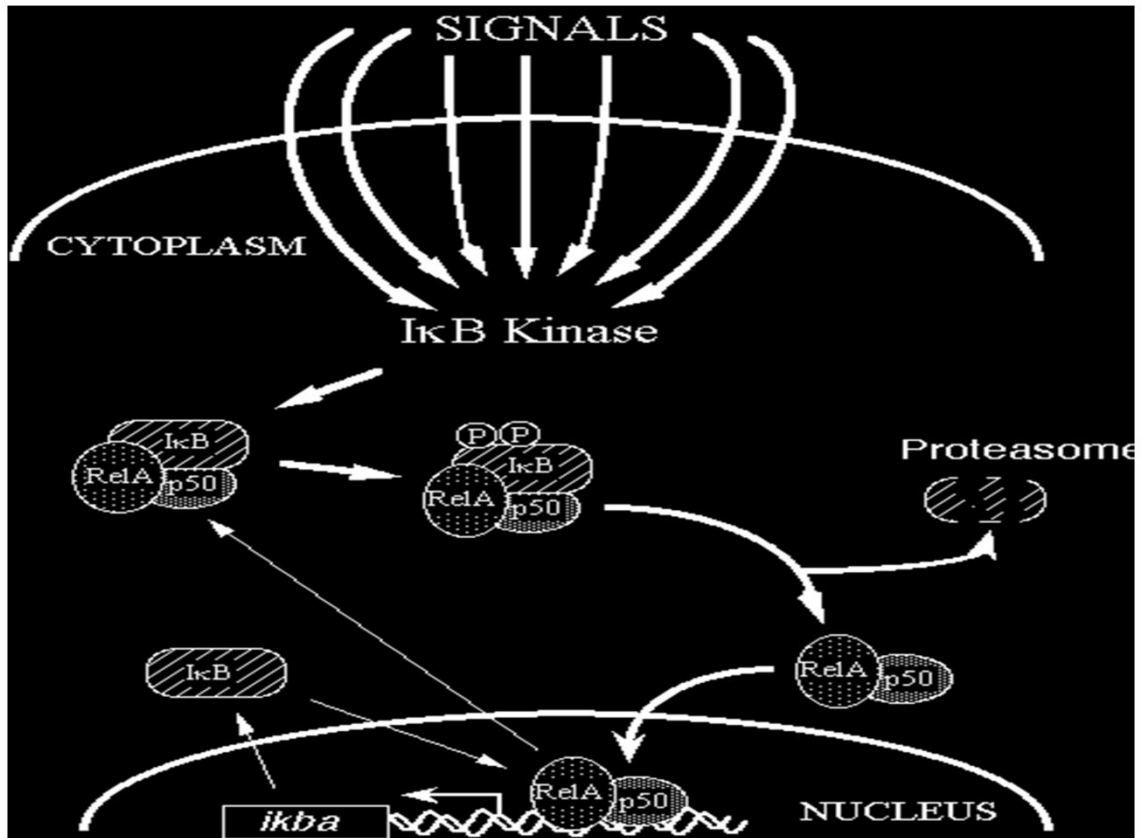


Figure 1-11: Activation and translocation of NF- κ B into the nucleus. This schematic diagram shows that NF- κ B is retained in the cytoplasm by I κ B. TLRs transmit the signal from the LPS/CD14 complex via the MyD88 pathway and cause phosphorylation of I κ B by IKK (I κ B kinase). Freed NF- κ B (p50-ReL-A) enters the nucleus and activates gene expression. The newly synthesized I κ B can enter the nucleus, pull NF- κ B off DNA and export NF- κ B back to the cytoplasm (Source: Gilmore, 1999).

1.5 The mitogen-activated protein kinase family (MAPK)

Protein kinases are enzymes that have the ability to modify other proteins by covalently attaching a phosphate group to them. The most common protein kinases, serine/threonine kinases, act on serine and threonine, tyrosine kinases act on tyrosine, while dual-specificity kinases act on all three amino acids. Such phosphorylation of proteins can affect their enzymatic activity, protein-protein interaction, protein location in the cell, or their propensity for degradation by proteases such as mitogen-MAPKs (Widmann et al., 1999). Responses to LPS are characterized by activation of multiple intracellular pathways, including the MAPK, NF- κ B and AP-1 pathways (Chen et al., 2012; Lu et al., 2012).

Mitogen-activated protein MAPKs include the extracellular signal-regulated kinases (ERKs), c-Jun N-terminal kinases (JNKs), and p38 MAPK-activated protein kinases (Johnson et al., 2002; Roux & Blenis, 2004). MAPKs phosphorylate specific serines/threonines of target protein substrates. The resultant signals transduce to downstream pathways and activate numerous transcription factors, with induction of genes encoding inflammatory molecules (Raman et al., 2007; Huang et al., 2009). The elicited cytokines are believed to be responsible for cell proliferation, differentiation, immunoregulation, and cytotoxicity of bacteria (Lamkanfi et al., 2007). MAPKs are key mediators driving the production of inflammatory cytokines during sepsis (Liu et al., 2012; Frazier et al., 2012). Activation of the MAPK pathway occur after LPS stimulation in MyD88 knockout mice, with delayed kinetics compared with wild type mice, suggesting MyD88 involvement, but not essential, in LPS-induced MAPK activation and that other MyD88-independent pathways exist (Andreacos et al., 2004; Bandow et al., 2012). Recently an adaptor molecule homologous to MyD88, Mal/Tirap, has been shown to be involved in the activation of MAPK by TLR4 (Andreacos et al., 2004; Laird et al.,

2009). In a fashion similar to that of MyD88 knockout mice, Tirap knockout mice demonstrate delayed activation of MAPK after LPS exposure (Kawai et al., 1999; Kaisho et al., 2001). These findings point to the presence of other pathway independent of MyD88 and Mal/Tirap, which lead to the activation of the MAPK after LPS stimulation.

1.5.1 JNK subfamily proteins

JNK proteins are encoded by three genes, JNk1, JNk2 and JNk3. JNk1 and JNk2 encode ubiquitously expressed JNK proteins, whereas the JNk3 protein product is primarily found in the brain, heart and to a lesser extent in the testis (Kumar et al., 2015). Alternative splicing of the jnk transcripts results in 10 different JNK isoforms, each of which may target different transcription factors (Dreskin et al., 2001; Manassero et al., 2012) JNK1 and JNK2 have four isoforms each ($\alpha 1$, $\alpha 2$, $\beta 1$ and $\beta 2$). JNK1 $\alpha 1$, JNK1 $\beta 1$, JNK2 $\alpha 1$ and JNK2 $\beta 1$ isoforms all have a molecular weight of 46 kDa, whereas JNK1 $\alpha 2$, JNK1 $\beta 2$, JNK2 $\alpha 2$ and JNK2 $\beta 2$ isoforms are larger due to an extended C-terminus and their molecular weight is 54 kDa. JNK3 has two isoforms, JNK3 $\alpha 1$ (46 kDa) and JNK3 $\alpha 2$ (54 kDa) (Dreskin et al., 2001). In this study the effect of PARP inhibitor PJ-34 on the activation of the JNK cascade, after induction of PARP-1 activity by LPS, was investigated.

1.5.2 JNKs and inflammation

LPS binds to LBP in the plasma and is delivered to the cell surface receptor CD14. Next, LPS is transferred to the transmembrane signaling receptor toll-like receptor 4 (TLR4) and its accessory protein MD2. LPS stimulation of human monocytes activates several intracellular signaling pathways that include the IkappaB kinase (IKK)-NF- κ B pathway

and three mitogen-activated protein kinase (MAPK) pathways: extracellular signal-regulated kinases (ERK) 1 and 2, C-Jun N-terminal kinase (JNK) and p38. These signaling pathways in turn mediate multiple downstream events leading to the activation of AP-1 and NF- κ B, which results in induction of a range of inflammatory cytokines (Guha & Mackman, 2001; Kim & Kim, 2014). Therefore, inhibition of the activation of MAPKs, Akt, NF- κ B and AP-1 may have potential therapeutic applications (Park et al., 2011). JNKs have been isolated and characterized as stress-activated protein kinases on the basis of their activation in response to inhibition of protein synthesis (Mehan et al., 2011). They were found to bind and phosphorylate the DNA binding protein c-Jun and to increase its transcriptional activity. C-Jun N-terminal kinase is a component of the AP-1 transcription complex, which is an important regulator of gene expression. AP-1 contributes to the control of many cytokine genes and is activated in response to environmental stress, radiation, and growth factors of all stimuli that activate JNKs. Regulation of the JNK pathway is extremely complex and is influenced by many MAP kinase kinase kinases (MKKKs). As depicted in the Signal Transduction Knowledge Environment JNK Pathway Connections Map, there are 13MKKKs that regulate the JNKs. This diversity of MKKKs allows a wide range of stimuli to activate this MAPK pathway. JNKs are important in controlling apoptosis (Chen, 2012). The inhibition of JNKs enhances chemotherapy-induced inhibition of tumour cell growth, suggesting that JNKs may provide a molecular target for the treatment of cancer. JNK inhibitors have also shown promise in animal models for the treatment of rheumatoid arthritis (Bogoyevitch, 2005). The pharmaceutical industry is bringing JNK inhibitors into clinical trials for both diseases.

1.6 Poly (ADP-ribose) polymerases (PARP)

Poly (ADP-ribose) polymerase (PARP), also known as poly (ADP-ribose) synthetase (PARS), is an abundant nuclear enzyme located in the nucleus of eukaryotic cells, and becomes active in the presence of DNA damage. PARP activation results in cleavage of NAD⁺ to nicotinamide and poly (ADP-ribose) to form long or branched (ADP-ribose) polymers (PAR) on glutamic acid residues of a number of acceptor proteins. These proteins are associated with chromatin and PARP itself. PARP-catalysed NAD⁺ polymerization is referred to as poly ADP-ribosylation (Soriano et al., 2001; Tentori & Graziani, 2005). Over activation of PARP is considered to play a role in various pathophysiological conditions, including septic shock, via activation of NF- κ B in response to LPS (Soriano et al., 2001; Cuzzocrea, 2005).

1.6.1 Structure and types of PARP enzymes

The PARP family contains 17 members that differ from one another in structure, serving different functions in the cell (Fig. 1.12). PARP-1, which is involved in repair of single-stranded DNA (ssDNA) breaks, consists of three main domains: the N-terminal DNA-binding domain (DBD), the auto-modification domain (AMD) and the C-terminal catalytic domain. The DBD domain contains two zinc fingers which are responsible for DNA binding and some protein-protein interaction (angelier et al., 2011; Sun et al., 2014). Some PARP enzymes (PARP-1 and Vault PARP) have an auto-modification domain containing a BRCT motif, which is common in DNA repair and cell-cycle proteins (Nguewa et al., 2005). The catalytic domain contains the active site of PARP-1, also termed the 'PARP signature' (highly conserved in eukaryotes), which consists of a

50-amino acid sequence. The 'PARP signature' is characteristic of all types of PARP enzymes (Bürkle, 2005).

Apart from PARP-1, PARP-2 is the only PARP isoform that it is activated by DNA strand breaks. Despite the absence of the auto-modification domain from PARP-2, it displays auto-modification properties similar to PARP-1, but its DNA binding domain is very different from that of PARP-1 (Huber et al., 2004). The DBD domain of PARP-2 differs from that of PARP-1 in size and it lacks the two zinc fingers and the BRCT motif. PARP-2 is targeted to the nucleus. The catalytic domain of PARP-3 is similar to that of PARP-2, but PARP-3 displays a smaller DNA-binding domain (Bürkle, 2005). The vault/PARP-4 has a BRCT domain similar to that in the auto-modification domain of PARP-1 (Hassa & Hottiger, 2005). The DBD domain of tankyrase-1 contains a His-Pro-Ser-rich (HPS) domain, and the C-terminus of tankyrase displays homology to the PARP-1 catalytic region (Bürkle, 2005). Tankyrase-2 displays a domain structure that is similar to tankyrase-1 except for the N-terminal HPS domain, which is missing in tankyrase-2 (Bürkle, 2005). The tankyrase-2 enzyme was reported to interact with several other proteins such as insulin-responsive amino peptidase (IRAP) (Sbodio et al., 2002). Poly (ADP-ribose) glycohydrolase (PARG) is an important enzyme that possesses both endoglycosidic and exoglycosidic activity. It is responsible for the catabolism of the poly (ADP-ribose) polymer (Min & Wang, 2009; Finch et al., 2012). As a result of the combined action of PARPs and PARG, poly (ADP-ribose) undergoes a dynamic turnover in live cells (Bürkle, 2005).

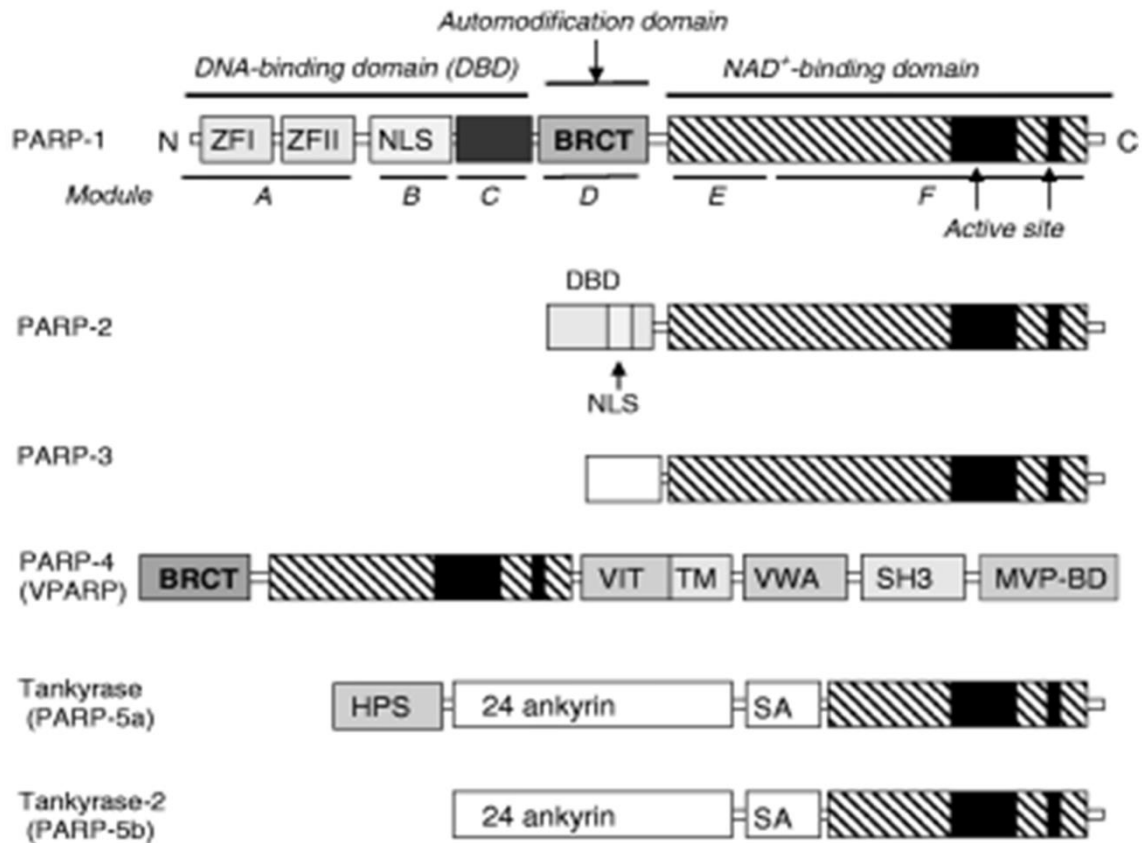


Figure 1-12: Schematic structure of some members of the PARP family of enzymes. Different types of PARP enzymes and their domains are represented. Abbreviations: BRCT, BRCA1 C-terminus; DBD, DNA-binding domain; HPS, His-Pro-Ser-rich domain; MVP-BD major vault binding domain; NLS, nuclear localization signal; SAM, sterile α -module; SH3, src homology region; TM, transmembrane domain; VIT, vault protein inter α -Trypsin domain; VWA, von Willebrand factor type A domain; ZF; zinc finger. (Source: Bürkle, 2005).

1.6.2 Poly (ADP-ribose) polymerase-1 (PARP-1)

PARP-1 appears to play a critical role in many biological processes. These include DNA repair and maintenance of genomic stability, transcriptional regulation, centromere function and mitotic spindle formation, centrosomal function, structure and vault particles, telomere dynamics, trafficking of endosomal vesicles, apoptosis and necrosis (Bürkle, 2005). PARP-1 and PARP-2 are activated by ssDNA breaks and serve important functions in DNA repair and expression of both PARP-1 and PARP-2 and/ or DNA

strand break-dependent poly(ADP-ribosyl)ation is essential during early embryo- genesis (Schreiber et al., 2002). PARP-1 or PARP-2 knock out mice provided evidence for these roles. When PARP-1/-2, inactivated the cell susceptibility to DNA damaging agents increases and strand break re-joining is inhibited (Tentori and Graziani, 2005). One of the PARP-1's most important functions, which is relevant to this study, is the regulation of the production of inflammatory mediators (; Sodhi et al., 2010; Liu et al., 2012; Scalia et al., 2013). Activation of PARP-1 plays an important role in the upregulation of inflammatory cascades through interactions with transcription pathways such as NF- κ B, JNK, AP-1 (Hunter et al., 2012; Scalia et al., 2013).

1.6.3 PARP enzymes and mechanisms of proinflammatory cytokine production

Poly (ADP-ribosyl)ation is a posttranslational modification of DNA binding protein in eukaryotic cells (Yung et al., 2004; Schreiber et al., 2006; Ahel et al., 2008). PARP-1 is activated by DNA strand breaks. Subsequently, PARP-1 synthesizes polymers of poly ADP-ribose from NAD⁺ to promote DNA repair (Kim et al., 2005b; Schreiber et al., 2006). Over-activation of PARP-1 depletes NAD⁺ and adenosine triphosphate (ATP) and eventually leads to necrotic cell death by energy failure (Ying et al., 2003; Alano et al., 2010). There is evidence that PARP acts as a co-activator in NF- κ B-mediated transcription (Nakajima et al., 2004). (Hunter et al., 2012) have indicated the likelihood that NF- κ B is regulated by PARP-1. Several reports have shown that PARP-1 plays a pivotal role in NF- κ B activation independently of energy depletion by binding directly to NF- κ B (Hassa et al., 2005; Hunter et al., 2012)or poly ADP-ribosylating it (Oliver et

al., 1999; Laudisi et al., 2011) and that inhibition of PARP-1 can attenuate this activation (Shaposhnikov et al., 2011).

NF- κ B is activated and translocate to the nucleus by a specific signal from TLR4 after binding to the CD14-LPS complex. It has been shown that treating mice with LPS results in rapid activation of NF- κ B in macrophages from PARP positive mice (Oliver et al., 1999). Activation of PARP has been shown to occur upon endotoxin administration (Oliver et al., 1999; (Shall & De Murcia, 2000). This result in degradation I κ B, an inhibitor of NF- κ B, permitting its nuclear translocation, upon which NF- κ B activates genes concerned with inflammatory or immune responses, such as inducible nitric-oxide synthases, IL-1, IL-6, and TNF- α (Oliver et al., 1999; Cuzzocrea, 2005). PARG and poly (ADP-ribosy) lation play a critical role in the re-localization of nuclear p65/NF- κ B to the cytoplasm in addition to its possible effect on NF- κ B-dependent transcription (Cuzzocrea, 2005; Shaposhnikov et al., 2011).

1.7 Role of CD14 and PARP enzymes in diseases

CD14 receptor has been reported to be related to many diseases, and regulation of CD14 gene expression plays a critical role in many inflammatory diseases. Antal-Szalmas, (2000) reported that diversion of mCD14 and sCD14 expression levels from their normal range is associated with many diseases. PARP activation plays a role in the pathogenesis of various cardiovascular and inflammatory diseases (Murakami et al, 2004). Published research suggests that CD14 and PARP may significantly contribute to the overall inflammatory response related to LPS. Since PARP and CD14 receptors are related to many diseases, this study will discuss only those diseases that might be related to the CD14 receptors and PARP via activation of NF- κ B-mediated transcription. This knowledge will help to expand the options for effective intervention, so that inflammatory diseases can be treated or prevented. Activation of CD14 and PARP has been shown to contribute to the pathogenesis of Gram-negative sepsis and various inflammatory diseases.

1.8 Role of CD14 and PARP in sepsis/septic shock

Gram-negative bacterial infection, which results in overproduction of proinflammatory cytokines such as IL-1, IL-6, and TNF- α and eventually results in multiple organ failure (Frink et al., 2009). Septic shock is a severe form of sepsis, defined as sepsis-induced hypertension. Septic shock is associated with elevation in body temperature and collapse in heart and respiratory rate (Annane et al., 2005; Hunter & Doddi, 2010; Schortgen et al., 2015).

1.9 Pharmacological effect of anti-CD14 and PARP enzymes

One might predict that blocking of CD14 and PARP with inhibitors will reduce the inflammatory response to LPS, because both are key regulators of the pathogenesis of inflammatory diseases. It has been suggested that anti-CD14 and PARP inhibitors may be valuable for treating septic shock or other inflammatory diseases (Freeman & Natanson, 2000; Veres et al., 2003; Annane et al., 2005; Szabo, 2007; Peralta-Leal et al., 2009).

1.9.1 Anti-CD14 antibody

CD14 is a receptor for LPS, and blocking of CD14 activity by anti-CD14 is an important therapeutic strategy. It has been found that anti-CD14 antibodies protected rabbits from death and prevented hypotension in LPS injected rabbits (Haziot et al., 1996). Furthermore, mice with over-expression of CD14 had an increased susceptibility to LPS-induced shock (Ferrero et al., 1993; Furusako et al., 2001; Nakamura et al., 2003), while a recombinant anti-CD14 monoclonal antibody significantly decreased LPS-induced shock in animal models and that caused by human endotoxaemia (Verbon et al., 2003; Kim & Kim, 2014). Furthermore, inflammatory responses such as cytokine release and granulocyte activation were strongly inhibited by anti-CD14 monoclonal antibodies (Verbon et al., 2003)

1.9.2 PARP inhibitors

Several studies have reported that PARP inhibition has an anti-inflammatory effect. For instance, PARP-1 plays a role in transcriptional control during CD14 activation, and

PARP-1 activity-dependent regulation of NF- κ B is a novel pharmacological target in the better management of the treatment of inflammatory disorders (Szabo, 2002). Evidence indicates that PARP-1-deficient mice are resistant to lethality induced by LPS, and inhibitors of PARP-1 are promising tools for therapeutic intervention (Cepeda et al., 2006; Pacher & Szabó, 2007; Godon et al., 2008). Inhibition of PARP improves the survival rate of mice subjected to endotoxin (Szabó et al., 2004; Godon et al., 2008). A specific PARP inhibitor, PJ-34, based on a modified 6 (5H) phenanthridinone structure, increased endotoxic shock survival rate and had various anti-inflammatory effects in animal models of endotoxaemia (Huang, 2009; Chevanne et al., 2010; Mazzone & Nistri, 2011; Scalia et al., 2013). Use of PARP inhibitors may be a promising approach to alleviate asthma attacks (Cuzzocrea, 2005; Virág, 2005). This research study was intended to improve our understanding of the role of innate immunity and CD14-PARP interactions in complex inflammatory diseases.

AIM OF THE STUDY

1. To assess the role of PARP activation in the regulation of CD14, TLR4, TLR2 and SR receptor expression in human macrophages, following treatment with LPS, in the presence and absence of PARP inhibitor.
2. To determine whether the presence of LPS can overcome the effect of the PARP inhibitor.
3. To investigate CD14 and SR receptor associations on the cell membrane with or without the presence of LPS.

CHAPTER 2: Materials and Methods

2.1 Materials

2.1.1 General Laboratory chemicals

All chemicals used in this study including tissue culture reagents were purchased from Fisher scientific (UK). DMSO and poly (ADP-ribose) polymerase inhibitor (PJ-34), Lipopolysaccharide (LPS) from *E. coli*, serotype EH100, Phorbol 12-myristate 13-acetate (PMA), 1,25-dihydroxyvitamin D₃ (VitD₃) and actinase were purchased from (Sigma Aldrich, UK). ELISA kit for measuring TNF- α and IL-1 β were bought from e bioscience (UK). A nuclear extract kit was purchased from active motif kit (UK).

2.1.2 Tissue culture

2.1.2.1 Cell line

The human monocytic cell line (THP-1), is cell line derived from acute monocytic leukaemia patient with distinct monocytic markers, was purchased from Health protection agency culture collection (HPACC) (UK). The cell was grown in different size tissue culture grade flasks, which were purchased from NUNC (Denmark).

2.1.2.2 Cell culture media

Human monocytic Leukemia THP-1 cells were grown in suspension culture in RPMI-1640 (PAA, UK), which was supplemented with 10% (v/v) heated- inactivated fetal calf serum (FCS) (PAA, UK), the culture was maintained at 37°C in an air humidified atmosphere of 5% (v/v) CO₂.

2.1.3 Antibodies

Antibodies Purified monoclonal Mouse anti- human either anti-CD14 (Clone 26ic, H14), anti-human TLR4 (Clone HTA 125), anti-human TLR2 (Clone TLR2.1), anti-human SR (Clone PLK1), poly clonal rabbit anti-human NF- κ B , poly clonal rabbit anti-human JNK and FITC goat anti-mouse IgG antibody all were purchased from (Biolegend, UK) and PE donkey anti-rabbit and FITC goat anti-mouse antibodies were purchased from (Sigma, UK). Goat anti mouse antibodies conjugated with Alex 488 (green) or Alex 555(red) were purchased from (Biolegend, UK).

2.2 Methods

2.2.1 Tissue culture

2.2.1.1 Thawing of cells

Cryogenic vials with 1×10^6 cells/ml in a 9:1(v/v) solution of FCS: dimethyl sulfoxide (DMSO) was removed from liquid nitrogen. Special precautions were taken which included using a protective mask and heavy padded gloves. Cells were thawed rapidly at 37°C and then transferred using a sterile glass pipette to a 10ml centrifuge tube containing 5ml of fresh complete medium to dilute out the DMSO. After centrifugation for 5 minutes at 1300 rpm (34 xg), the medium was removed, the cell pellet was resuspended in 5 ml of fresh medium, and the number of the cells was counted using a haemocytometer. A final concentration of 1×10^5 cells/ml was transferred to either a flask or cell culture plate. Cells were cultured at 37°C in humidified a tissue culture incubator with 5% (v/v) CO₂.

2.2.1.2 Routine passaging and prolongation of cell culture

THP-1 cells are suspension cells, growing continuously in RPMI-1640 supplemented with 10% (v/v) FCS. Cells were sub cultured twice a week when the culture reached about 70-80% of maximum density, either by dilution of the old cell culture to fresh medium or by increasing the volume of the stock culture by adding a fresh medium. The cell suspension was transferred to a centrifuge tube and was centrifuged for 3 minutes at 1300 rpm (32 xg). After that the medium was removed, the cell pellet was re-suspended in 5 ml of fresh medium and a proper mixing was carried out by continuous pipetting up and down to avoid the formation of cell clumps. Finally, the cells number was counted by using a

haemocytometer and diluted to a final concentration of 1×10^5 cells/ml. Cells were cultured at 37°C in a humidified incubator with 5% (v/v) CO₂

2.2.1.3 Determination of cell number

The cells were resuspended thoroughly by pipetting up and down the cell suspension, using a pipette, and then the cell suspension was transferred to a haemocytometer and drawn under the cover slip by capillarity. The cells in an average of 5 to 10 squares were counted using the 10X objective. The number of cells was calculated by averaging these counts and dividing by the number of the squares, and finally that number multiplied by 1×10^4 to obtain the number of the cells per/1ml of stock.

2.2.1.4 Cell viability assay

The cells viability was determined by mixing equal amount (100µ l) of 4% (w/v) trypan blue exclusion and THP-1 cell culture, mixed and left for 5 mins. After that cells from the mixture were transferred to a haemocytometer and drawn under the cover slip and cells were counted as indicated above. The cells stained with blue color were counted as dead cells and unstained cells counted as viable cells. From these counts the percentage of cell viability can be determined as following: $(\text{total cells} - \text{dead cells}) \times 100 / \text{total cells}$ (Butler and Spearman, 2007).

2.2.1.5 Freezing of cells

A cell line which is free from contamination can be stored for long term as a frozen stock in liquid nitrogen. The cells were frozen down by culturing them to grow to log phase, and the suspension prepared for freezing down with DMSO (Cryopreservative agent). After determine cell number per ml in the cell suspension, the cell suspension was centrifuged for 5 mins at 1300 rpm (32 xg) and the supernatant discarded, the cell pellet was resuspended in a 9:1 (v/v) mixture solution of FCS: DMSO. One ml of mixture solution was added to 1×10^7 cells/ml in cryogenic tube. The cryotubes were sealed tightly to avoid any leakage and wrapped up with cotton were to provide a sufficient insulation to slow down the freezing process, then placed into a box which was transferred immediately to be stored in a freezer at -80°C . Finally, after reaching this temperature, the cryotubes were transferred to liquid nitrogen to be stored at -196°C for long term storage.

2.2.2 Proliferation studies

2.2.2.1 The effect of PARP inhibitor PJ-34 on the THP-1 cell viability

To assess the cytotoxic effect of PARP inhibitor PJ34 on THP-1 cells, THP-1 cells at density of 5×10^4 cells/ml were plated in 30 mm cell culture plate and after 24 hours of seeding, different concentrations of (5, 10, 20, and 30 μM) of PARP inhibitor PJ34 were added to the cultured cells. Cells were counted at 48 hrs and 72 hrs from seeding time. Trypan blue was used to stain the dead cells by mix equal amount of cell culture with trypan blue and incubate for 3-5 mins and haemocytometer were prepared and cell counted. The percentage of cell viability was calculated as following: Total cell number-

dead cell number divided by total cell number x 100. Dead cells stained with trypan blue and live cells remain unstained (Fig. 3.5).

2.2.2.2 Treatment of THP-1 cell with hydrogen peroxide to induce DNA damage

THP-1 5×10^4 were differentiated in chamber slide with PMA 5 ng/ml for 72 hrs then the media replaced with fresh media incubated with different concentrations (0, 50, 100 and 250 μM) of H_2O_2 for 10 mins and cell then washed and fixed with paraformaldehyde 4% w/v for 15 min on ice and then washed and incubated with monoclonal mouse anti-human PAR antibody for 45 min and washed. Afterward cells were incubated with goat anti-mouse antibody labelled FITC for another 30 mins. The slide was examined under confocal microscopy. Bio-Rad Radiance 2000 and images were analysed by using image-J software.

2.2.2.3 Cell differentiation

THP-1 cells were differentiated with two differentiation inducer reagent, phorbol 12-myristate 13-acetate (PMA) and 1, 25-dihydroxyvitamin D_3 (vit. D_3) for different concentrations and time course were carried out. THP-1 cells at final density of 5×10^5 cells/ml were treated with different concentrations (0, 5, 10, 20, and 30 ng/ml) of PMA and incubated for 72 hrs, concentration of 5 ng/ml was used for time course experiment (24, 48, 72 and 96 hrs). For differentiation with vit. D_3 , cells at density of 2×10^5 cells/ml were treated with (0, 50, 100, 150 and 200 nM) of vit. D_3 and incubated for 72 hrs and concentration of 100 nM was used for time course experiment (24, 48, 72 and 96 hrs).

The difference in the cells number used with each differentiation inducer was because PMA inhibit cell proliferation, whereas Vit.D3 not affecting the cell proliferation. For flow cytometry experiments, adherent cells were detached from the plastic surface with accutase.

2.2.3 Flow cytometry to detect cell surface receptors

Flow cytometry was used to detect cell surface receptors, this was achieved by passing the cells in suspension buffer fluid sheath and exposure them to a beam of laser. Flow cytometry uses different lasers for illumination, during exposure of the cells to the laser beam, they are characterized individually based on their scattered light and emitted fluorescence, which collected and filtered and finally converted to digital value and the quantities of the labelled cells can be analysed using computer. There are two types of light-scattering, forward scattering related to the cell size and side scattering related to the cell granularity. Samples run and (10,000 cells) was acquired for each sample and analysed with specific software and geometric mean of each sample was calculated

2.2.3.1 Cell surface staining for flow cytometry

Indirect immunofluorescence staining was used to prepare cells for flow cytometry analysis. This method includes two steps: The first step includes incubation of cells with specific primary antibody to detect the antigen of interest and the second step includes incubation of cells with secondary antibody labelled to fluorochrome which binds to the primary antibody to locate the antigen. Differentiated cells were washed twice with phosphate-buffered saline (PBS) and incubated with accutase for 5-7 mins at 37⁰C. Cell

suspensions (2.5×10^5 cells/ml) per sample were centrifuged at 1200 rpm for 2-3 minutes, supernatants were discarded. The cell pellets resuspended in cold blocking buffer [PBS supplemented with 0.1% (w/v) bovine serum albumin (BSA)] for 10-20 min. The cells were incubated with concentration of 0.5mg/ml at 1:50 dilutions of primary monoclonal mouse anti-human either (anti-CD14 clone 26ic or anti-TLR4 clone HTA 125 or anti-TLR2 clone TL2.1 and anti-MARCO for 45 mins at 4⁰C, after washing twice with blocking buffer. Cells were incubated with secondary antibody goat anti mouse IgG labelled FITC for further 30 mins and washed twice with blocking buffer. Afterward cells were fixed with 4% formaldehyde for 15-20 mins on ice, washed and resuspended in 350 μ l blocking buffer. Finally, cells were transferred into FACS tubes and analysed by flow cytometry (Aria cell sorter or Accuri 6) and results analysed with Flo-Jo software version 8.8.6 (Tree Star Inc., Ashland, OR, USA).

2.2.4 Immunofluorescence labelling of antigens for microscopy

2.2.4.1 Immunofluorescence labelling methods

Immunofluorescent labelling was achieved by two ways, direct and indirect. The first way, is direct immunofluorescence can be achieved by using antibody against the molecule of interest is chemically conjugated to a fluorochrome. The second way is indirect immunofluorescence, which includes two steps, in which the first step is using a primary antibody specific for the antigen of interest is unlabelled and the second step using secondary antibody tagged with a fluorochrome. The secondary antibody should be raised against the animal in which the primary antibody was produced. Interaction of the primary antibody with the secondary antibody which labelled with a fluorochrome can then be visualised using ultra violet and laser equipped microscopy techniques.

2.2.4.2 Single immunofluorescence labelling of antigen

THP-1 cells were differentiated in Lab-Tek 8 well slides (Thermo Fisher Scientific) at a density of 7.5×10^4 cells/well, for three days with PMA (5 ng/ml). The culture medium was aspirated from the wells and cells were incubated with different concentrations of H_2O_2 for 10 min, and then washed with PBS pre-warmed at $37^\circ C$. The cells were fixed with 4% (w/v) paraformaldehyde for 15 mins on ice and permeabilized with 0.01% Triton 100X and washed with PBS after each step. The cells were blocked with blocking buffer [2% (w/v) BSA in PBS] for 1 hr at $4^\circ C$. Cells were incubated with 100 μl antibody dilutions per well primary mouse anti-human mAbs: anti-PAR (clone 10H) at a dilution of 1 $\mu g/100 \mu l$ in blocking buffer [1% (w/v) BSA in PBS] for 1 hr at $4^\circ C$. After the incubation, samples were washed three times with PBS and then incubated for 1 h with goat anti-mouse IgG antibodies conjugated with Alexa Fluor® 448 (Invitrogen, Carlsbad, CA, USA) at a dilution of 0.25 $\mu g/100 \mu l$. The cells were thoroughly washed with PBS thereafter, chamber disassociated and removed from the slides. The slides were air dried in the dark and then mounted with Vectashield Hardest Mounting Medium (Vector Laboratories, Burlingame, CA, USA), covered with the coverslips number 1.5 and the slides were visualised using confocal microscopy Bio-Rad Radiance 2000.

2.2.4.3 Detection of cell surface receptors by immunofluorescence doubles labelling

Un-differentiated THP-1 or THP-1 cells were differentiated in Lab-Tek 8 well slides (Thermo Fisher Scientific) at a density of 7.5×10^4 cells/well with PMA (5 ng/ml) for 72 hrs. The culture medium was aspirated from the wells and the cells were washed with

PBS pre-warmed at 37⁰C. The cells were fixed with 4% (w/v) paraformaldehyde for 15-20 mins on ice and washed with PBS. All subsequent steps were carried out at room temperature, otherwise stated. Cells were incubated with blocking buffer [2 % (w/v) BSA in PBS] for 1 hour. Staining was done in sequence for each antigen. The cells were incubated with 100 µl antibody dilutions per well using the following primary mouse anti-human mAbs: anti-CD14 (clone 26ic) and mouse anti-human MARCO (clone PLK1) at a dilution of 1 µg/100 µl in blocking buffer[1% (w/v) BSA in PBS] for 1 h at 4⁰C. After the incubation cells were washed twice with PBS. Cells were then incubated for 30-45 mins with goat anti-mouse IgG antibodies conjugated with Alexa Fluor® 555 or Alexa Fluor® 488 (Invitrogen, Carlsbad, CA, USA) at a dilution of 0.25 µg/100 µl. Cells were blocked again with 2% blocking buffer before second round of primary and secondary antibody staining. For staining cell nuclei, 4',6-diamidino-2-phenylindole (DAPI) (Sigma-Aldrich) was used at a 1:250 dilution in PBS. The cells were thoroughly washed with PBS thereafter, chamber disassociated and removed from slides. The slides were air dried in the dark and mounted with vectashield hardest mounting medium (Vector Laboratories, Burlingame, CA, USA), covered with the coverslips number 1.5 and cells images obtained with Nikon Air confocal microscope.

2.2.5 Confocal microscopy

2.2.5.1 Principle of confocal microscope

The confocal laser scanning microscopy is a valuable instrument that uses a laser to provide an excitation light attached to computer to build up and analyse digitalized images to observe only at the plane of focus. The laser confocal microscopy provides three-dimensional images by reconstructing the serial optical sections of thick specimen.

The laser light reflected off a dichroic mirror and hits two mirrors which are mounted on motors, and these motors scan the laser across the sample. The dye in the sample fluoresces, and the emitted light gets descanted by the same mirrors used to scan the excitation light from the laser. Then only the emitted light passes through dichroic mirror and focused onto the pinhole, and the light that passed the pinhole is measured by detector. The fluorescent light signal transformed into an electrical signal by a computer. A cell or tissue images can be sectioned optically, and these images at different depths can be compared. These images can be analysed individually, or regenerate three dimensional images by assembling a stack of these two dimensional-images from successive focal planes, and the presented image pixel corresponds to the relative intensity of detected fluorescent light. The confocal microscope provides clear images by excluding all out of focus information. In this study two different types of confocal microscopes were used a Bio-Rad Radiance 2000 and images were analysed by using image J software and Nikon A1R laser scanner use software NIS-elements AR 4.13.01

2.2.5.2 Image acquisition

For colocalisation study cell images were acquired using a Nikon A1R confocal microscope with a plan-apochromatic violet corrected (VC) 1.4 numerical aperture (N.A.) 60x magnifying oil-immersion objective. Cell images were acquired in four different channels, using one-way consecutive line scans. The Alexa Fluor 488 was excited at 488nm with laser power 7.8 Arbitrary Units (AU), its emission collected at 525/50nm with a PMT gain of 140 AU (Green channel). The Alexa Fluor 555 signal was excited at 561nm with laser power 2.1 AU, and collected at 595/50nm with a PMT gain of 117 AU (Red channel). The DAPI was excited at 405nm with laser power 3.2 arbitrary units (AU), and its emission collected at 450/50nm with a PMT gain of 118 AU. Finally the

differential interference contrast images were acquired using the transmitted light detector at a gain of 103 AU. The scan speed used was ¼ frames/s (Galvano scanner) and no offset was used. The pinhole size was 34.5µm, approximating 1.2 times the Airy disk size of the 1.4 N.A. objectives at 525nm. Scanner zoom was centred on the optical axis and fixed to a lateral magnification of 55nm/pixel and a Nyquist factor of 2.54 and 2.79 for Alexa Fluor 488) and Alexa Fluor 555 respectively. The axial step size was 140nm, with 40-50 image planes per z-stack. Single or isolated cells with reasonable signal strength in both channels were examined letting accurate quantitation of the flat plasma membrane and uncrowded receptor distribution.

In order to validate a reliable colocalisation with this method, optimisation of samples were achieved with taking in account the following conditions. First, saturated pixels were avoided, because it may represent lost information thus not used for quantitation. Therefore, all the values above the dynamic range were not recorded. Second, Using datasets that acquired with the correct sampling parameters as described by the Nyquist-Shannon reconstruction theorem (Nyquist, 1928; Shannon, 1949). Briefly, the smallest structure in an image, as determined by the microscope's resolution using Abbe's criterion, should be represented by at least two pixels and higher sampling (three to four pixels) is also acceptable, while under sampling must be avoided. Third, aberrations were minimised in the imaging setup. This was done by using objectives corrected for spherical ('plan') and chromatic aberrations (achromatic, apochromatic and apochromatic violet-corrected (VC), depending on the number of colours corrected for). In addition, uni-, not bi-directional scanning, zooming in to the centre of the field of view, and separating colours in line scanning rather than full-frame mode was done as measures for minimising aberrations.

2.2.5.3 Colocalisation analysis

A novelty method mentioned in (Jabeen et al., 2013) was followed for this analysis. The colocalisation approach uses MATLAB software (version R2010b with Image Processing Toolbox; Math Works Inc., Natick, Massachusetts) and is based on a 3D blob-like feature detection algorithm introduced by Obara and coworkers (2013). All steps are based on analysis in 3D. The algorithm is divided into two stages: candidate location detection, and candidate location pruning. After acquisition of separate datasets for both molecules, the fluorescent intensity of particles is enhanced while suppressing the noise by convolving the image with a 3D Laplacian of Gaussian (LoG) kernel. The LoG kernel size is controlled by user-defined radius r . Local maxima, detected by morphological opening, are then used to define all locations of particles brighter than their immediate surroundings. This process continues until a user-defined low intensity bound T (separate for each channel, to allow for datasets where noise levels are markedly different) is reached. This is the threshold below which no particles can be safely identified because of image noise. In order to accurately measure colocalisation of particles in the dual colour fluorescence images, their centroid positions were pinpointed at subpixel resolution using weighted centroids. A local matching procedure then performed an exhaustive search for correct matches between the two vectors of intersecting positions, using the expected average radius of the surrounding circle of light r . For each position in one channel, we calculated the Euclidean distance for every position in the other channel. If the distance of the closest pair is smaller than the maximum colocalisation distance d , then the pair is added to the list of matches and removed from the input vectors. All candidate locations are pruned to eliminate spurious locations due to image noise. The procedure is repeated until there are no more matches satisfying the maximum colocalisation distance condition. Receptor pairs were deemed to colocalise if they did not exceed the diameter

determining the approximate size of a single particle's PSF. A tight boundary was chosen for this PSF, measuring 165nm in x and y, and 412nm in z. Receptor pairs with their centroids further apart than 165nm were classified as non-colocalising. These remaining positions in both datasets are then labelled as unmatched.

2.2.5.4 Visualisation

After loading the program's Graphical User Interface (GUI) and a 3D dataset for each channel, the algorithm is run by pressing the 'Colocalisation' button. Results can then be viewed in five different ways: **1) Stacks:** Centroid positions of all identified particles are marked by red dots in the image stacks, and sliders (in the 'Stacks' box of the GUI) allow moving through the different z-planes. To verify how exactly a super-resolved centroid is positioned inside a fluorescent blob, a high zoom can be applied. **2) Maximum intensity projections.** To visualise an entire dataset in one image, projections of each image stack are available ('Projection 1' and 'Projection 2' in the 'Plot' box) figure 2.1, with green and red asterisks marking unmatched (non-colocalising) particles, green and red asterisks with blue circles indicating colocalisations. **3) Scatterplot:** Produces an isometric perspective view of particles shown as asterisks (green and red for each channel), and colocalisations encircled in blue. The numbers for colocalisations and particles detected in each channel are also indicated. **4) Distance map:** A colour-coded 3D distance map is used to visualise colocalisations. Each colocalisation is shown as a single sphere, with a coded colour indicating the distance between the two colocalising particles (Fig. 2-1).

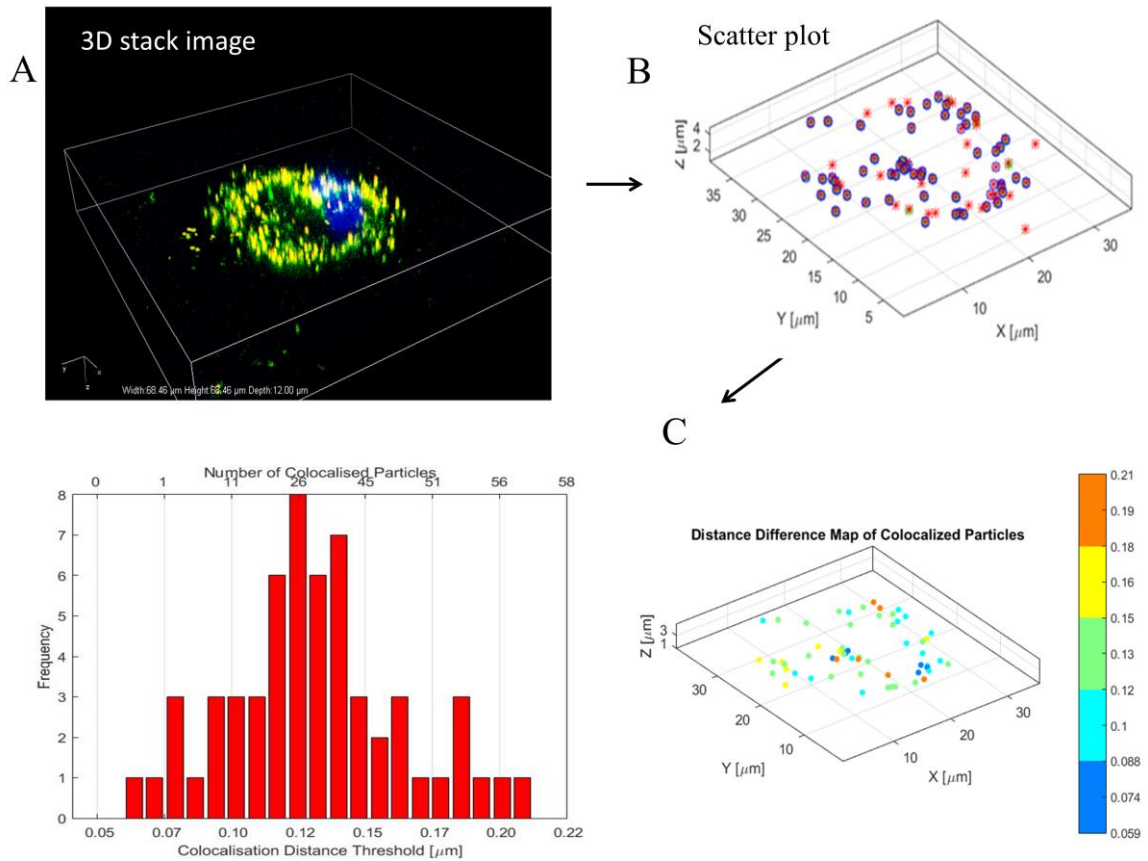


Figure: 2-1: Colocalisation detection and quantification of CD14 and MARCO receptors on PMA-differentiated THP-1 cells. (A) Three-dimensional image of PMA-differentiated THP-1 cell showing blue (nucleus), green (SR), red (CD14), and yellow/orange possibly colocalised particles. (B) Three-dimensional scatter plot of single cell depicting the relationship between SR (MARCO) (green asterisks) and CD14 (red asterisks). Blue circles designate colocalised CD14 and SR molecules. Total number of red, green and colocalised spots per cell is quantified. (C) Colour-coded 3D scatter plot for Euclidean distance map of colocalised particles. The colour scale indicates the distance between the centroids of colocalised pairs ranging from 0.059 μm -0.21 μm (colocalisation distance threshold $d=0.22 \mu\text{m}$). The corresponding histogram represents colocalisation distance on the x-axis and the number of colocalisations on the y-axis. Note that grid for cellular dimensions uses microns.

2.2.6 Protein Immunoblotting assay

Protein Immunoblotting assay also known as western blotting, is one of the most commonly used techniques in bioscience laboratories for the detection of specific proteins in cell culture supernatants and cell lysates. This assay is assembly of size-based protein separation and antibody based protein detection. This assay is involves multi-step process and described as follows

2.2.6.1 Preparation of cell lysate and protein quantification

Cell pallet from suspension cells or adherent cells, were washed twice with PBS lysed or frozen down at -80°C until used for cell lysates. To prepare whole or cytoplasmic cell lysate active nuclear kit was used. Cells pellet from suspension cells culture or adherent cell after detached with using accutase were washed twice with PBS by centrifugation for 5 mins at 1300 rpm (32 xg). Cell lysate was prepared according Active Motif kit manufacture protocol was followed. Total protein concentration was determined by the Bradford Assay (Sigma Aldrich, UK) following the manufacturer's instructions.

2.2.6.2 SDS polyacrylamide gel electrophoresis (SDS-PAGE)

Proteins are able to move in an electric field at rate which is determined by their charge mass and their shape. Proteins can be separated according to their mass by treating them with sodium dodecyl sulphate (SDS). At neutral pH, one SDS molecule binds to each amino acid, and because SDS molecule carries negative charge, therefore SDS bound amino acid repel each other, so that protein chain will remain unfolded and strengthened.

The change in the protein chain and its mass will determine the rate of the movement in the gel. In the SDS-PAGE two types of gels are used; first, a stacking gel which has a low concentration of acrylamide, subsequently proteins will move rapidly through it. Second, the running or resolving gel which uses a higher concentration of acrylamide, therefore proteins move slower through it giving better resolution.

2.2.6.3 SDS-PAGE system

The mini gel apparatus was assembled as indicated in the Bio-Rad instruction for casting discontinuous polyacrylamide gels. Two glass plates were assembled using four clamps the outer glass 8.3cm× 10.2cm and inner glass 7.3cm ×10.2cm with a space of 0.75mm between them for the comb and a mark was drawn underneath each of the teeth of the comb to facilitate loading. To prepare 12% w/v running gel, the mixture of running gel solution was poured between the glass plates until the mark, then distilled water was poured on the top of the running gel to line up the edge of the gel, and allowed to polymerize for 45 mins at room temperature. After that the water was removed by tipping up the gel plates and the surface carefully dried with filter paper. The stacking solution 5% w/v was then prepared and overlay at the top of the resolving gel, a comb inserted and was left to set for 25 mins. One well per gel was loaded with 5µl of molecular weight marker proteins (Sigma Aldrich, UK). The remaining wells were loaded with 15µg cell lysate mixed with sample buffer at ratio of 4:1 (total volume 25µl). At the start the gels were run at 50 volts for 45 mins and then after, at 100 volts until the dye front almost reached the bottom of the plate, at that point the electrophoresis was terminated.

2.2.6.4 Western blotting

When the SDS-PAGE approached the end of its run, the protein bands transferred to a polyvinylidene difluoride (PVDF) membrane (Immobilon-FL, Merck Millipore, Merck KGaA, Darmstadt, Germany) and this known as western blotting which carried out with Bio-Rad transfer system. The (PVDF) membrane was beforehand soaked in methanol for 1 min and then washed with distilled water and soaked in transfer buffer. Whatman filter paper, gel and filter pads were pre-soaked in transfer buffer. The cassette was placed in a shallow tray containing transfer buffer, the pre-wetted filter pad was placed on the black side of the cassette and a sheet of Whatman filter paper was placed on the filter pad. The gel was removed from the electrophoresis chamber after the lower corner of gel marked with blade and the gel inverted on the Whatman filter paper. Then PVDF membrane placed on the gel after cutting the lower corner to match the gel. The sandwich was completed by placing another piece of Whatman filter and filter pad on the top of PVDF membrane. The cassette was locked properly with the white latch and placed in the electrophoresis module. Finally the cassette was placed in the tank filled with transfer buffer pre chilled to 4°C and the cooling buffer help to keep the temperature as low as possible during the transferring. The transferring was run at 30 volts overnight or for 1hr and 20 mins and after completion of the run, PDVF membrane was removed from the gel keeping the protein side upside. The membrane was then blocked with 5% skimmed milk blocking buffer for 1 hr at room temperature with constant rocking. After that the membrane was incubated in 10 ml of fresh tPBS containing 10µl of the primary antibody at dilution 1:1000 for 2-3 hrs at room temperature with constant rocking. The membrane was then washed for 30 mins with wash buffer, changing the wash buffer each 10 mins. Afterward the membrane was incubated with 10µl of secondary antibody labelled FITC at dilution 1:1000 for 30 mins; the membrane was washed for 30 mins with wash buffer,

changing the wash buffer each 10 mins with constant rocking, then the membrane scanned with ODYSSEY infrared imaging system (Li-Cor Bioscience). PageRuler™ Plus Pre stained Protein Ladder from Fermentas (Thermo Fisher Scientific) was used and this prestained protein MW marker is designed for monitoring the progress of SDS-polyacrylamide gel electrophoresis, for assessing transfer efficiency onto PVDF, nylon and nitrocellulose membranes, and for estimating the approximate size of separated proteins that have been made visible with gel stains or Western blot detection reagents.

2.2.7 Enzyme-link immunosorbent assay (ELISA)

This technique is one of the most common immunological assays which highly characterized with its versatility, sensitivity and specificity and ease of automation. The colored product formed indicated for directly proportional to the amount of antigen that bond to antibody. In this the technique, a standard curve with known concentrations of antigen of interested can be plotted in order determine the unknown antigen in experimental samples. ELISA kits ready set go supplied from e-biosciences were used to measure accurately and precisely the TNF- α , IL-1 β level produced by cells.

2.2.7.1 Assay procedure

TNF- α , IL-1 β level were measured in culture supernatants by ELISA ready set go (e-biosciences, Cambridge, UK) following the manufacture recommendations. In brief 96-well microplates (Nunc MaxiSorp) were coated with capture antibody overnight. The plate were aspirated and washed three times with wash buffer, then inverted and blotted

on absorbent paper to remove any residual buffer. Following washing the wells blocked with 200 μ l/well of 1x assay diluent and incubated for 1 hr at RT followed by washing as previously. 100 μ l/well of diluted standard (500 pg/ml of TNF- α , IL-1 β) were added to appropriate wells in order to plot standard curve, 2-fold serial dilution carried out and 100 μ l/well of experimental samples were added to the rest of the wells. The plate was sealed and incubated at 4⁰C overnight followed by a total of 5 washes then, the detection antibody (100 μ l) diluted in 1X assay diluent was added and the plate was incubated at RT for another hour. Followed washing, 100 μ l/well of Avidin-HRP diluted in 1X assay diluent was added into each well and the sealed plate was incubated at RT for 30 minutes. Followed aspiration and washing 7 times. Substrate solution (tetramethylbenzidine) added to each well and plates were incubated for 15 mins at room temperature and the reaction was stopped by adding 50 μ l of 1M H₃PO₄. The optical density of each well was measured at 450 nm using micro plate reader (Versa Max).

2.2.8 Polymerase chain reaction PCR

The polymerase chain reaction (PCR) or some called "Molecular photocopying" is one of cheap and fast technique used in molecular biology which eased copy or amply a single target segment of DNA and generate thousands or millions of particular DNA sequence. The technique used in medical and biological research laboratories for variety applications such as DNA cloning for sequencing or functional analysis of genes, diagnosis of hereditary diseases, identification of genetic fingerprints used in forensic science and DNA paternity test and detection and diagnosis of infectious diseases.

PCR procedure involves three steps carried out in repeated cycles. The first step is (denaturation), during this step the denaturation, or separation, of the two strands of the

DNA molecule is achieved by heating the starting material to temperatures of about 95°C, and the two strands become a template on which the new strands will built up. The second step is (annealing) during this step the temperature is reduced to about 55°C, so that the primers can anneal to the template. The third step (extension) in this step the temperature is raised to about 72°C, and the DNA polymerase begins adding nucleotides onto the ends of the annealed primers. At the end of the cycle, which lasts about five minutes, the temperature is raised and the process begins again. The number of copies doubles after each cycle. Usually 25 to 35 cycles produce a sufficient amount of DNA.

2.2.8.1 Primer design

The pearl primer software was used to design the forward and reverse primers for CD14, MARCO and cyclophilin. In design of the primer all the factors that have a vital role in the PCR reaction and product generating such as whether the primers are for standard or real time PCR, length of the primers, the repeated and the amount of GC pairs in the primer, the annealing temperature (T_m). The designed primers were supplied by Fisher scientific (Invitrogen).

2.2.8.2 RNA extraction

Total RNA from undifferentiated and PMA-differentiated THP-1 cells grown in a 100 mm glass culture plate was extracted using TRI-reagent (Sigma Aldrich) according to the manufacturer's instructions. Briefly, cells lysed directly by adding 1 ml of TRI-reagent to glass culture plate and cell lysate homogenized by contentious pipetting, finally the

mixture transferred to 2 ml eppendorf tube and left to stand for 5 mins at room temperature. Afterward 200 μ l of chloroform was added to each tube and shaken vigorously for 15 secs and allowed to stand for another 2-15 mins and mixture at centrifuged at 12,000 xg for 15 mins at 2-8°C, the mixture separated in three phases, red organic phase containing, and proteins, an interphase containing DNA, and a colorless upper aqueous phase containing RNA. The aqueous phase transferred to a clean tube and 0.5 ml of 2-propanol per ml of TRI-reagent used was added to each tube and mixed and allowed to stand for 5-10 mins, afterward the tubes centrifuged at 12,000xg for 10 mins at 2-8°C, the RNA in the sample at the end of centrifugation form a pellet on the side and the bottom of the tube. The supernatant was removed and the pellet washed with 1 ml of 75% ethanol per 1 ml of TRI-reagent used in the sample preparation, the sample vortexed and centrifuged at 7000 xg for 5 mins at 2-8°C, the RNA pellet dried for 5-10 mins by air-dryer or under vacuum. Finally, appropriate volume of sterile double distilled water added to the RNA pellet and mixed by pipetting up and down with Gilson pipette on a water bath at 55-60°C for 10-15 mins and stored at -80°C until used. The concentration and quality of RNA were assessed with Nano drop machine and the purity of RNA extract were examined by run the RNA extract in 1% agarose gel.

2.2.8.3 Preparation of cDNA

Appropriate volume of RNA containing 2 μ g of was mixed with 1 μ l of random hexamer (Thermo scientific, UK) in PCR tube and the volume of the mixture made-up to 12 μ l with sterile double distilled water and tubes were placed in PCR machine (GeneAmp™ PCR system 9700) and heated to 65°C for 10 mins. As soon as the 10 mins finished the sample tubes were placed on ice straight away as any dealing will renaturation of the

secondary structures. With sample on the ice 4 µl of 5x buffer (enzyme buffer), 2 µl of 10 mM of dNTPs (Thermo scientific, UK), 1 µl of water and 1 µl of the reverse transcriptase enzyme (Thermo scientific, UK) were added to PCR tube, with keeping all the reagent on the ice. Finally, the PCR tubes were placed again in PCR machine and run on program as following, 37°C for 2 mins, 42°C for 1 hr, 70°C for 5 mins (to inactivate the enzyme) and at 12°C forever and the cDNA kept on ice or stored at -20°C.

2.2.8.4 Real time polymer chain reaction (qRT-PCR)

Real time PCR (qRT-PCR) was carried out utilizing 20µl of PCR reactions for each sample which is prepared as following; 10 µl master mix of SyBr Green (SensiFAST™) real time PCR kit (Bioline, UK) aliquot in 96 well PCR plate, 1.6 µl of primer mix consisting of the forward and reverse primers each present at a concentration of 5 µM, sterile distilled water 7.4 µl and 1 µl of cDNA. An RT-PCR film seal was properly placed and the plate spun briefly to insure that the liquid placed in the bottom of the wells and then the plate was placed on the qRT-PCR machine (CFX 96, Bio-Rad) run for specific number of cycling and temperature.

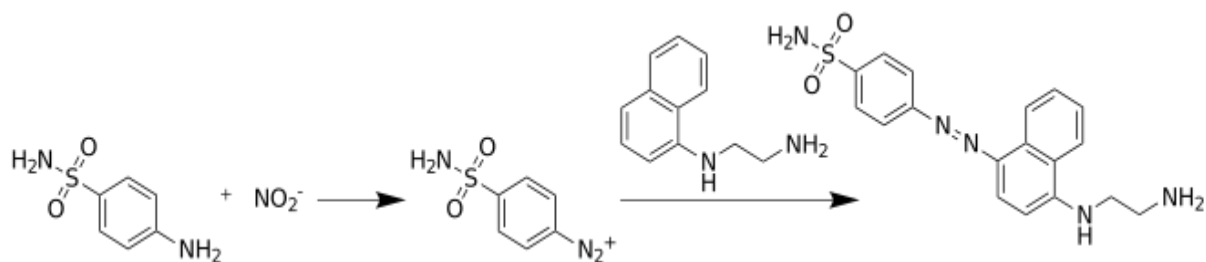
2.2.9 LPS uptake assay

THP-1 cells at density 1×10^5 cells /ml were differentiated in 8 wells chamber slides (Lab tech, Millipore) with PMA (5 ng/ml) for 72 hrs then the media was removed and chamber slide washed with sterile PBS and cells were stimulated with media free serum for

another 24 hrs. Afterward cells were stimulated with LPS 055: B5 100 ng/ml labelled FITC (Sigma Aldrich, UK) in present and absence of PARP inhibitor PJ-34 10 μ M 30 mins prior to stimulation with LPS for (15, 30, 60 and 120 mins). The slide then washed with PBS and fixed with 4% paraformaldehyde for 15 mins on ice and washed with PBS and air dried in dark. Mounting media was placed on the slide then cover with cover slip with consideration of no air bubble trapped between the slide and the cover slip. The cover slip sealed with Marabu Fixogum rubber cement (Marabuwerte GmbH & Co. KG, Tamm, Germany). The slide was examined and imaged with Nikon (wide field microscope).

2.2.10 Nitric oxide determination by Griess reaction

Nitric oxide (NO) production reflect an important immunological response, which can be detected by chemiluminescence, citrulline assay and electron paramagnetic resonance (EPR). The Griess reagent is the most common technique used to detect NO in biological samples and this system described for the first time by Griess in 1879 and this system based on the fact that NO degrades in aqueous solution to nitrite (NO_2^-) one of two primary stable formation of NO. This system is used a chemical reaction of sulfanilamide and N-1-napthylethylenediamine dihydrochloride (NED) under acidic conditions and can be used to detect NO in biological samples like tissue culture medium and plasma. Nitrite is detected in samples by formation red pink colour which formed initially as a reaction between the NO_2^- in the biological sample with sulphanilimide which form diazonium salt and with adding the azo dye agent (NED) the pink colour develop.



2.2.10.1 Procedure for determination of nitrite concentration

A stock nitrite standard solution of a 100 μM nitrite solution (Promega; CAT#G2930) was prepared by diluting 0.1 M nitrite standard 1:1000 in the RPMI-1640 medium, supplemented with 10 % FCS. Serial dilution of twofold were performed in triplicate to generate the nitrite standard reference curve (100, 50, 25, 12.5, 6.25, 3.13 and 1.56 μM), then 50 μl of the samples were dispensed in triplicate in wells allocated for the samples.

50 μl of the sulfanilamide solution (Promega; CAT#G2930) was added to all experimental samples wells by using a multichannel pipetter, and incubated for 10 mins at room temperature and finally 50 μl of N-1-naphthylethylenediamine dihydrochloride (NED) solution (Promega; CAT#G2930) was added to all wells and incubated for 10 mins at room temperature and protected from light. Absorbance was measured using a Versa Max microplate reader equipped with 520 nm and 550 nm filters.

2.2.11 Co-Immuno-precipitation assay

To study the interaction of CD14 and MARCO receptors on PMA-differentiated THP-1 cells in presence and absence of PJ-34 in response to LPS 100 ng/ml. Cells were lysed as

described in section 2.2.4 and 1 mg cell lysate of each sample was incubated with 4 µg of anti-CD14 antibody overnight at 4°C. Afterward 40 µl of protein A/G agarose (Santa Cruz,) was added and kept overnight on a rotator at 4°C. The samples were spun down for 30 seconds at 1500 rpm and the supernatant was discarded. The beads then were washed three times using cold PBS. Loading buffer containing DTT 50 µl were added to each sample and then boiled to 90°C for 5 mins. Then 20 µl of each sample was loaded in each well of SDS-PAGE gel and they were left for 30 mins at 50 V and the rest was 120 V. The gel was then transferred to PDVF membrane for 1 hr. and 20 mins at 100 V on ice. The membranes were then blocked 5 % of non-fatty milk for 1 hr. followed by washing in tPBS for 30 mins. The membranes were then incubated either with anti-CD14 or anti-MARCO for 3-4 hrs. The membranes washed with tPBS three times 10 mins each with changing the tPBS. The membranes were then incubated with secondary goat anti-mouse antibody for 30 min followed by washing with tPBS for three times each time for 10 mins with changing the tPBS. The membranes were finally scanned using the Odyssey Infrared Imaging System from Li-cor Biosciences.

2.2.12 Proteomic analysis of THP-1 cell line

2.2.12.1 Preparation of cell lysate

THP-1 cells cultured and differentiated in 100 mm cell culture dishes (Nunc, UK) with PMA (5 ng/ml) for 72 hrs, and 1×10^7 cells were used per sample for cell lysate. Cells were detached from culture dishes by accutase, counted and washed with PBS as described earlier (Section 2.2.1.2). Cell lysate was prepared by resuspended the cell pellet in 1 ml of the protein extraction buffer prepared in the Lab. (Urea 7 M, Thiourea 2 M, CHAPS 4%, 50 mM Tris base, all reagents were purchased from (Sigma Aldrich, UK).

Cells were vortexed and kept on ice for 5 min. Cell lysates were spun at 20,000 ×g for 20 mins; supernatant was transferred into prechilled clean micro centrifuge tube and stored at -80°C until further used. Protein concentration of cell lysates was determined with Bradford assay using Bradford reagent (Sigma Aldrich, UK) following manufacturer's instructions.

2.2.12.2 First dimensional gel Isoelectric electrical focusing (IEF)

Immobiline dry strip gel pH 4-7NL, 17cm (Bio-Rad, UK) used in this study was rehydrated in immobiline dry strip reswelling tray. The dry strip was rehydrated overnight at room temperature in 300ul of rehydration buffer (Urea 7 M, Thiourea 2 M, CHAPS 4%, protease inhibitor cocktail 1X, DTT 20 mM, ampholyte 1%, bromophenol blue 0.1 %, SDS 0.05%) containing 50 µg of sample proteins. The IPG strip was covered by using 2~3ml of (immobiline Plus One dry strip cover fluid) (GE Healthcare Bio-Sciences AB). After rehydration, the IPG strip was briefly rinsed with double distilled water to remove crystallized urea.

Isoelectric focusing step was performed in clean IPG-Phor washed and cleaned with Strip holder cleaning solution (GE Healthcare Bio-Sciences AB). The Ettan IPG Phor manifold was covered with 108 ml of Immobiline PlusOne dry strip cover fluid and each rehydrated strips were placed in individual lanes of Ettan IPG strip holder (GE Healthcare Bio-Sciences AB) under the fluid using tweezers with keep the positive end of the strip towards the anode end of the manifold. Hydrated filter wicks in cathode (-ve) end were hydrated with 150 µL of 100 mM DTT placed between the IPG strips and the electrodes. Whereas, the anodic (+ve) filter wick was hydrated with 150 µL double distilled water.

The lid was closed and IPG-Phor programme was run according to the programme below.

A holding step at the end was added to so that it could be left overnight.

Step1	200 V	500 V hrs
Step2	500 V	500 V hrs
Grad3	1000 V	800 V hrs
Grad4	10,000 V	16,500 V hrs
Step5	10,000 V	6,200 V hrs
Step6	200 V	24 hrs

At the end of the programme, computer was disconnected and IPG-Phor was stopped. The paper wicks were removed with tweezers and discarded. The IPG strips were placed in a petri dish, after rinsed deionized water, labelled and stored at -80°C for later use.

2.2.12.3 SDS-PAGE preparation

For second dimension gel electrophoresis PROTEAN® II System (BIO-RAD, UK) was used. The outer glass plate size 20x20 and the inner glass plate 16x20 were washed with hot water and detergent and rinsed with deionized water and cleaned with 70% ethanol, dried, assembled with 1.5 mm spacers and clipped into the casting frame according to Bio-Rad manufacture instruction. Assembled glasses were checked for any leakage by pouring deionized water between the two glass plates. Non-leakage system, the water tipped and the system was dried with hair dryer airflow. The gel solution 12% SDS PAGE was made with water, 1.5 M Tris-HCl and 30% acrylamide, the solution was placed in a flask and degassed for 15 minutes at ambient temperature. The TEMED, APS and SDS were added and mixed by stirring. The gel solution was poured in between glass plates, avoiding any air bubbles, to level 1 cm below the inner glass plate. The top of the

gels was covered with (water saturated isopropanol 80%) and allowed to polymerise overnight.

2.2.12.4 Equilibration of the IPG strips

In order to perform the second dimension gel run, IPG strips subjected to isoelectric focused proteins should be equilibrated and reduced. For each strip 20 ml of frozen equilibration buffer thawed. In one tube of 10 ml equilibration buffer 100 mg of DTT was added while in the other 10 ml equilibration buffer 250 mg of iodo-acetamide and left to mix gently. The strip incubated in equilibration buffer containing 1% DTT for 20s min and after that incubated with equilibration buffer that contain 4% iodo-acetamide for another 20 min. Both incubation steps were carried out at room temperature. The IPG strips were rinsed with 1X electrophoresis buffer and placed on the top of SDS-PAGE.

2.2.12.5 Assembly and running of second dimensional gel

Agarose sealing solution was heated to liquefy. IPG strips were trimmed from each end up to 0.6 cm thus giving a final length of 15.8 cm. A small square of paper electrode wick (2×3 cm half thickness) was loaded with 10 µl of molecular weight marker and placed on the top of left hand corner of the gel. IPG strip was placed on the top of 12% SDS PAGE gel with the acidic side facing the glass plate hinge and sealed with agarose solution, avoiding any air bubbles to be trapped between the strip and the top of the gel. Electrophoresis tank was filled with 2.5 L of gel running buffer. The gels with strips were removed from the casting assembly and clipped onto the core unit of the protean tank. The core unit was lifted into the tank, running buffer was added to the top of the upper buffer chamber and air bubbles were removed with a glass rod. The lid was fitted to the

tank and cables were connected to the power PAC (Bio-Rad, Power Pac 1000). Electrophoresis was carried out first at 50 volts for 30 minutes and then at 150 volts for about 4.5 hours or until the bromophenol blue dye front had reached to the lower end. The core unit was then removed from the tank, disassembled and gels were removed from the clamps. The spacers were loosened and one edge of the glass plate was lifted up with a spatula. Gel was placed in a glass container containing gel fixing solution.

2.2.12.6 Protein visualisation

For visualization of protein spots, a modified silver staining protocol was extracted from (Gromova & Celis, 2006). Gels were washed with deionized water and fixed overnight in fixing solution. After that the gel washed with 20% methanol for 20 minutes with changing the wash buffer three times. The gel sensitized with 0.02% sodium thiosulfate for 1 min and washed with deionized water twice, each for 1 minute. Staining was done with 0.2% silver nitrate solution for 20 mins followed by a careful wash twice with deionized water for a maximum of 1 min each time. The gels were developed with sodium carbonate 6% and 0.0004 sodium thiosulfate for 2-5 mins until spots appear, and reaction was stopped by add 12% acetic acid with constant shaking for 10 mins. The gels were stored in 1% acetic acid at 4⁰C.

2.2.12.7 Gel scanning and spot analysis

Gels were scanned using the scanner (Epson image scanner III) with Lab Scan 6.0 software. First the scanner was calibrated and set to use the transparent settings at 300 dpi

with the blue filter. The scanner surface was cleaned with 70% ethanol and a little purified water was poured on the surface. The gel was placed directly on the scanner, previewed and air bubbles were smoothed out if any. Scan area of the gel was then selected and scanned. Gel images were saved as mel and tif files. Scanned gel images were characterised with Progenesis SameSpot software package (Nonlinear Dynamics Limited, UK).

**CHAPTER 3: The role of the poly (ADP-ribose) polymerase inhibitor
PJ-34 on the expression of LPS receptors on THP-1 cells**

PART I: Immunofluorescence analysis of poly (ADP-ribose) polymer synthesis PMA-differentiated THP-1 cells in presence and absence of PJ-34 in response to H₂O₂

3.1.1 Introduction

Immunofluorescence (IF) or cell imaging techniques depend on the use of antibodies (Abs) to label a specific antigen with a fluorescent dye (termed fluorophores or fluorochromes), and require that cells be fixed. Cells are incubated, with antibody, allowing accurate detection of cognate cellular antigens. This is achieved by estimating the relative antibody affinity. Both monoclonal (mAb) and polyclonal Abs can be used to localise the antigen of interest. mAbs are more specific than polyclonal Abs, recognizing a specific epitope on an antigen. However, cross-reactivity of mAbs may still occur because the epitope recognised can be present on other proteins. Polyclonal Abs are generally less specific than mAbs, since they constitute a mixture of antibodies, each recognising a different epitope.

The nuclear enzyme PARP-1 converts β -nicotinamide adenine dinucleotide (NAD⁺) into polymers of poly (ADP ribose) (PAR), which participate in regulated nuclear homeostasis Schreiber et al., (2006). In the present study monoclonal anti-PAR antibody clone 10H has been used to detect the presence of PAR polymer, with confocal microscopy used to visualize the presence of PARP-1 activity in the human acute monocytic cell line THP-1 (Barbierato et al., 2012). Previous studies have indicated that, when activated, PARP-1 is involved in a cytotoxic pathway associated with tissue injury or inflammation, as evidenced by direct protein interaction with transcription factors (NF- κ B) and/or poly (ADP-ribosyl)ation of transcription factors. PARP-1 is a multifunctional protein which can regulate transcription in a variety of ways, and transcriptional control of the

inflammatory response. Primarily, PARP adds ADP-ribose units to transcription factors, preventing them re-binding to DNA. Modulation of transcription factor binding activation takes place via pathways for signal transduction and gene expression (Hao & O'Shea, 2012). The purpose of this chapter was to detect the activation of PARP-1 in THP-1 cells upon oxidative stress and synthesis of poly (ADP-ribose) polymer in response to H₂O₂. The role of the PARP inhibitor PJ-34 in protection against DNA damage and the effect of PJ-34 on THP-1 cells viability were assessed.

3.1.2 Method and materials

3.1.2.1 Confocal microscopic analysis

Confocal microscopy was used to detect PAR polymer upon PARP-1 and DNA damage of THP-1 cells. THP-1 cells were differentiated 5 ng/ml of PMA for 72 hours and then cells were treated with 0, 50, 100 and 250 μ m H₂O₂ for 10 min and cells fixed and stained as described in section 2.2.4.2. Confocal images were acquired by laser-scanning confocal microscopy with an Olympus microscope equipped with a Radiance 2000 confocal setup (Bio-Rad), as described in section 2.2.5.1.

3.1.2.2 The toxicity of PJ-34 on THP-1 cells

The cytotoxicity effects of PJ-34 on THP-1 cell viability were determined as following; THP-1 cell (5×10^4 cell/ml) incubation with 5, 10, 20 and 30 μ M PJ-34 for 48 hrs and the viability of THP-1 cells were assessed as mentioned in section 2.2.1.4.

3.1.3 Results

3.1.3.1 Poly ADP-ribose synthesis in THP-1 cells

Oxidative damage to DNA elicited by oxidative agents such as H_2O_2 , either at low or high concentration, is able to cause single DNA strand breaks. These activate PARP-1, which is a damage-responsive enzyme with a role in repair of single-stranded DNA (ssDNA), leading to poly-ADP-ribose synthesis (Fisher et al., 2007; Heeres & Hergenrother, 2007; Krietsch et al., 2012); PARP-1 is the major PAR-producing enzyme in eukaryotes. In this experiment, H_2O_2 was used to induce DNA-damage-dependent activation of PARP-1 and PAR polymer formation. Poly ADP-ribosylation was detected using indirect IF. THP-1 cells were treated with 50, 100 and 250 μ M H_2O_2 . Controls comprised untreated samples.

3.1.3.2 Poly ADP ribose synthesis in THP-1 cells after treatment with different concentrations of H_2O_2

Fluorescent images of THP-1 cells were obtained with a Bio-Rad confocal microscope (Fig. 3.1 A). Control cells, untreated with H_2O_2 , did not show any formation of PAR polymer. However, in cells treated with 50 μ M H_2O_2 (Fig. 3.1 B) a small amount of PAR

polymer was detected, as shown by the presence of fluorescence foci in the nucleus. Following treatment with 100 μM H_2O_2 , the amount of PAR polymer within nuclei significantly increased (Fig. 3.1 C). However, treatment with 250 μM H_2O_2 did not significantly raise PAR polymer synthesis (Fig. 3.1 D). This indicates the depletion of the cell energy. Therefore, maximal PAR polymer formation is induced in PMA-differentiated THP-1 cells after treatment with 100 μM H_2O_2 , so this concentration was used in all experiments (Fig.3.2). The presence of the PAR localization is reveal the distribution of chromatin-bound, PARP-1, PAR associated among various fraction sheared and nuclease-digested THP-1 cell chromatin in response to H_2O_2 . The increase in the size of the nuclei suggest that H_2O_2 .induce cell damage which associated with induction of various cell death program that could be involved directly in body defense reaction. The viability of PMA-differentiated THP-1 cell were examined in response to 100 MH_2O_2 with 4% exclusion trypan blue.

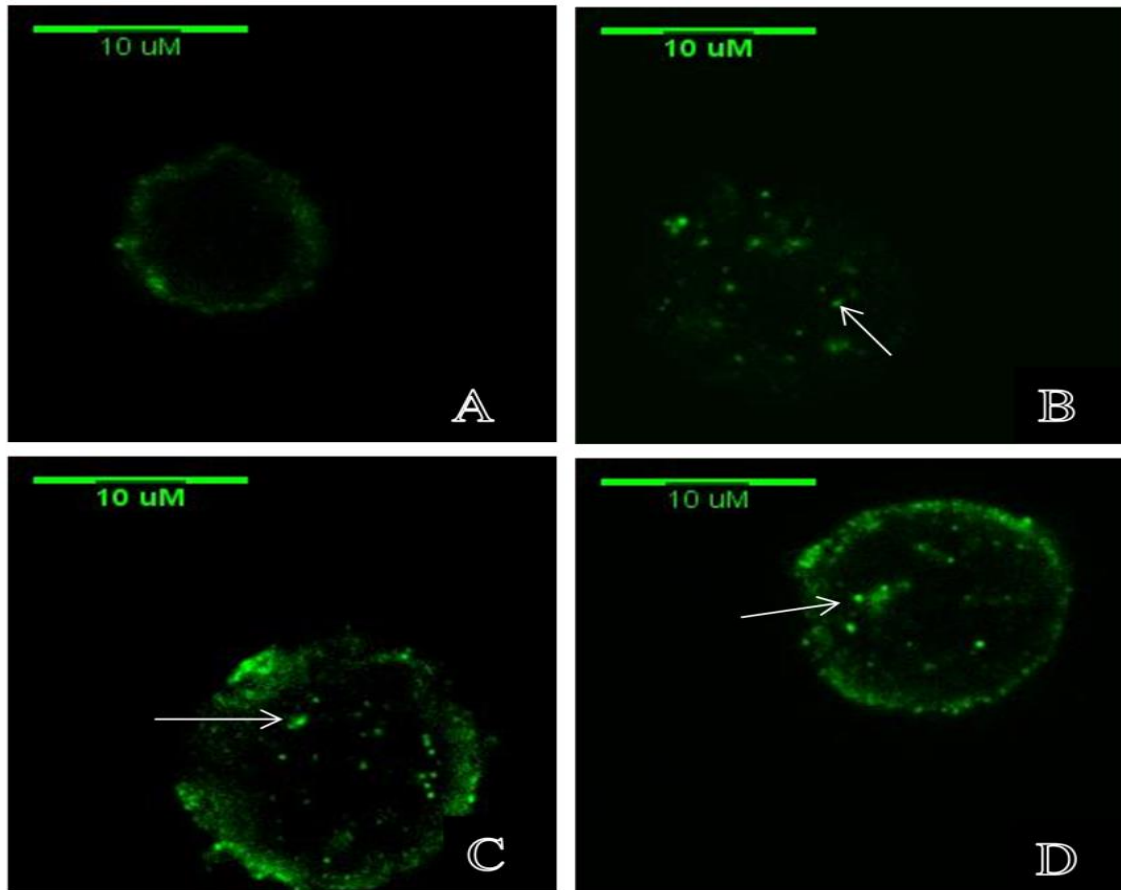


Figure 3-1: Poly ADP-ribose formation in PMA-differentiated THP-1 cells after treatment with different concentrations of H₂O₂. THP-1 cells were differentiated with 5 ng/ml phorbol 12-myristate 13-acetate on a cover slide for 72 hrs. Incubation of cells was then carried out with and without different concentrations of H₂O₂ (50, 100 and 250 μM) for 15 mins at 37°C. The cells were washed with PBS/BSA and cells were fixed with 4% (w/v) paraformaldehyde for 20 mins on ice, then permeabilised with 0.01% Triton X100 for 10 mins. Cells were washed and incubated with primary monoclonal antibody mouse anti-human PAR polymer (10H), followed by secondary antibody goat anti-mouse IgG labelled FITC. Green fluorescence images were obtained using a confocal microscope (Bio-Rad Radiance 2000) and analysed with Image-J software version 1.50g (National Institute of Health, USA). PAR polymers are indicated with a white arrow. **Panel A:** Fluorescence image of untreated cells. **Panel B:** Fluorescence image of cells treated with 50 μM of H₂O₂. **Panel C:** Fluorescence image of cells treated with 100 μM of H₂O₂. **Panel D:** Fluorescence image of cells treated with 250 μM of H₂O₂.

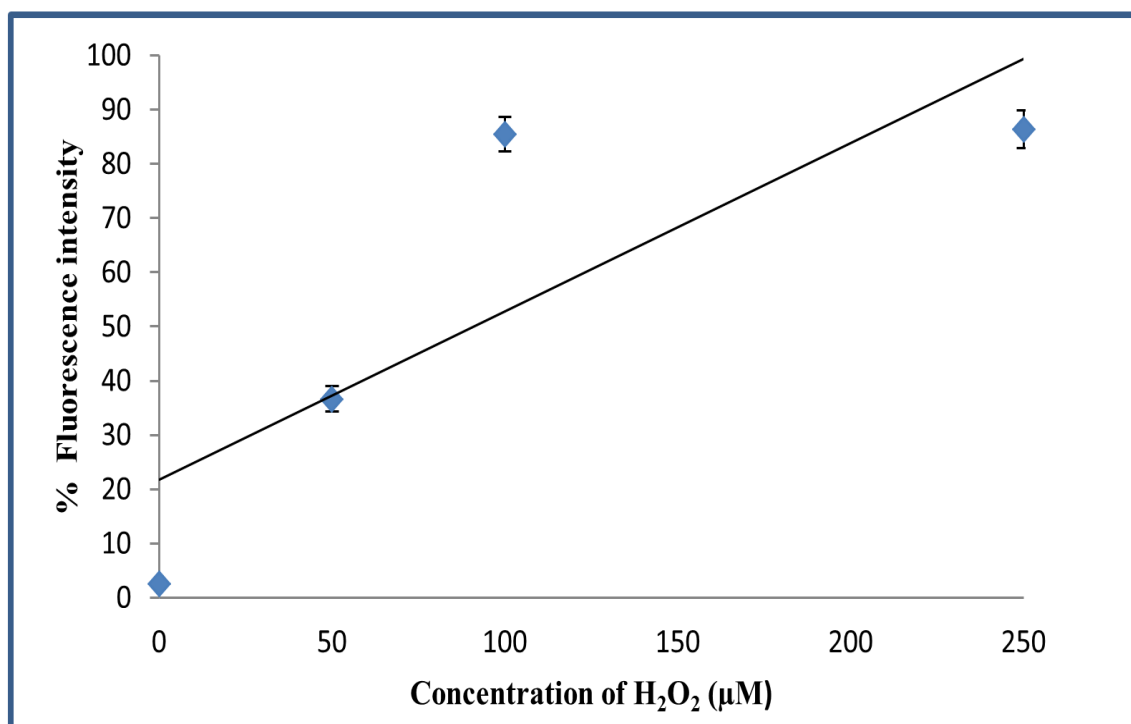


Figure 3-2: The effect of H₂O₂ on poly ADP-ribose formation in PMA-differentiated THP-1 cells. The percentage of integrated fluorescence intensity which is proportional to the poly ADP-ribose) synthesized upon treatment with different concentration of H₂O₂, was determined using the ImageJ software package (National institutes of health, USA). The fluorescence intensity obtained from cells treated with 100 µM H₂O₂ was set at 100%. The results represent the mean ± S.D. for three independent experiments.

3.1.3.3 The capacity of PJ-34 in lowering poly ADP ribose polymer synthesis in THP-1 cell following treatment with 100µM of H₂O₂

Monocytes differentiated into macrophages, they are the resident tissue phagocytes and sentinel cells of the innate immune response. THP-1 cells differentiated with PMA induced changes in cell morphology and strong adhere to the surface indicating of differentiation. These cells shows increased in cytoplasmic to nuclear ratio, increased mitochondrial and lysosomal numbers. Macrophages shows resistance to apoptotic stimuli, a high phagocytic and expressed a cytokine profile that resembled in response to

TLR ligands, in particular with marked TLR2 responses(Daigneault et al., 2010). This experiment was design to assess the capacity of PJ-34 to lower the level of PAR polymer formation induced by H₂O₂. This is desirable, since PAR polymer, a product of PARP-1 activity, is a cell death signal (Andrabi et al., 2006). Samples were observed using a Bio-Rad 2000 confocal scanning laser microscope (Bio-Rad, Inc, Hemel Hemstead).

As shown in figure 3.3, the control cells treated with 100 μ M H₂O₂ only. (Fig. 3.2 A) The effect of 1 μ M PJ-34 (Panel B) in THP-1 cells was limited, since the cells still produced a considerable amount of PAR polymer. PAR polymer, present in the nucleus, is manifested by fluorescence foci, indicated in figure 3.2 by a white arrow for comparison with control (cells treated with only 100 μ M H₂O₂, panel A). THP-1 cells treated with 10 μ M PJ-34 showed a significant decrease in PAR formation (Fig. 3.3, panel D) and the cells formed few fluorescence foci compared to control cells treated with 100 μ M H₂O₂ only. PAR polymer was not generated by cells treated with 20 and 30 μ M PJ-34 (Fig. 3.3, panels E and F). This result demonstrates that PJ-34 is a potent inhibitor of poly ADP-ribosylation. It was observed that inhibition of poly ADP-ribosylation increased proportionately with increasing concentration of PJ-34. Figure 3.4 shows the percentage of integrated fluorescence intensity of PAR polymer produced in response to 100 μ M H₂O₂. PAR polymer formation in cells was inhibited by 25% \pm and 69% \pm when cells were treated with 1 and 5 μ M PJ-34 prior to stimulation with 100 μ M H₂O₂. Cells treated with 10 μ M PJ-34 displayed decreased PAR polymer formation, peaking at 9%. Cells treated with 20 and 30 μ M PJ-34 exhibited an integrated fluorescence density of only 2% and 1% respectively.

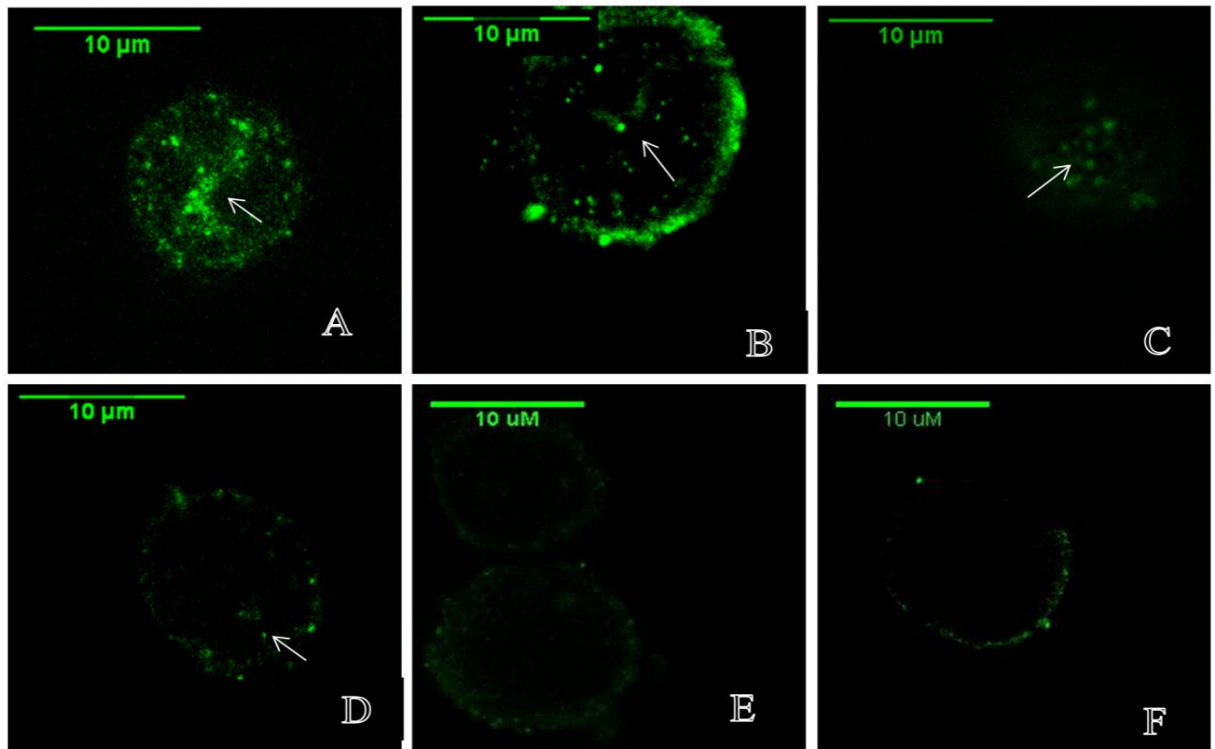


Figure 3-3: The effect of PJ-34 on poly ADP-ribose synthesis in PMA-differentiated THP-1 cells stimulated by H₂O₂. THP-1 cells were differentiated with PMA 5 ng/ml for 72 hrs. The cells were then incubated without or with 1, 5, 10, 20, 30 μM PJ-34 PARP inhibitor for 30 mins prior to stimulate with 100 μM of H₂O₂ for 15 min at 37^oC. The cells were washed with PBS/BSA and Cells were fixed with 4% (w/v) paraformaldehyde for 20 mins on ice, and then permeabilised with 0.01% Triton X100 for 10 mins. Cells were washed and incubated with primary monoclonal antibody mouse anti-human PAR polymer (10H), followed by secondary antibody goat anti-mouse IgG labelled FITC. Green fluorescence intensity was obtained using a confocal microscope (Bio-Rad Radiance 2000). PAR polymers are indicated with a white arrow. **Panel A:** Fluorescence intensity of cells treated with 100 μM of H₂O₂. **Panel B:** Fluorescence intensity of cells treated with 1 μM PJ-34 and 100 μM of H₂O₂. **Panel C:** Fluorescence intensity of cells treated with 5 μM PJ-34 and 100 μM of H₂O₂. **Panel D:** Fluorescence intensity of cells treated with 10 μM PJ-34 and 100 μM of H₂O₂. **Panel E:** Fluorescence intensity of cells treated with 20 μM PJ-34 and 100 μM of H₂O₂. **Panel F:** Fluorescence intensity of cells treated with 30 μM PJ-34 and 100 μM of H₂O₂.

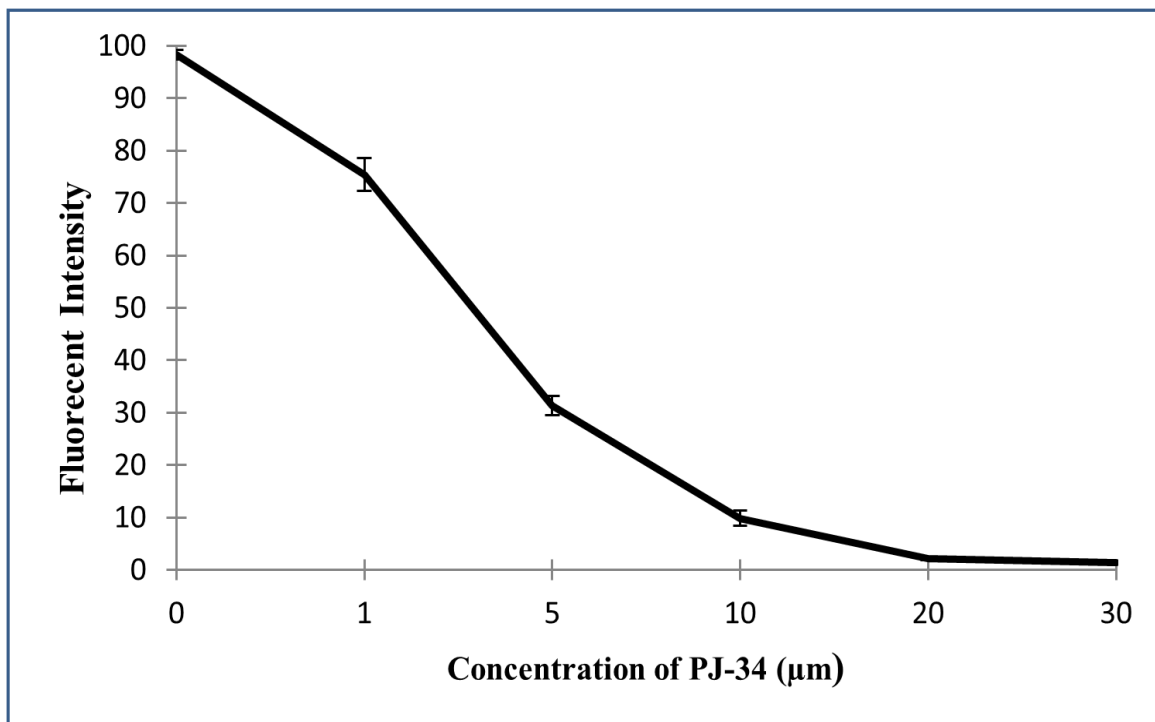


Figure 3-4: The effect of PJ-34 on poly ADP-ribose synthesis in PMA-differentiated THP-1 cells stimulated by H₂O₂. The fluorescence intensity obtained from PMA-differentiated THP-1 cells which is proportional to the poly ADP-ribose synthesized upon treatment with different concentration of PJ-34, is shown, following stimulation with 100 µM of H₂O₂. Data were analysed using the ImageJ software package (National institutes of health, USA). The fluorescence density for cells treated with 100 µM H₂O₂ was set at 100%. The results represent mean integrated fluorescence intensity (counts/µM²) ± S.D. for three independent experiments.

3.1.3.4 The effect of different concentrations of PJ-34 on THP-1 cell viability

Figure 3.5 shows that PJ-34, at concentration of 5 and 10 µM, had no effect on THP-1 cell viability at 24 and 48 hours from adding the inhibitor. In contrast, 20 and 30 µM PJ-34 significantly reduced THP-1 cell viability ($p < 0.05$). 20 µM PJ-34 reduced THP-1 cell viability by 20% and 35% at 24 and 48 h from incubation of the cells with PJ-34 respectively (Fig. 3.5). Furthermore, 30 µM PJ-34 also reduced the viability, the lowest viability peaking at 55% and 40% at 24 and 48 h from seeding time respectively ($p < 0.05$). Therefore the concentration of 10 µM PJ-34 to be used as a higher concentration

without affecting the cell viability when incubate with cells up to 48 hrs. Figure 3.6 shows cell viability of THP-1 cells treated with 10 μ M PJ-34 for 48 h, the viable cells remain unstained, whereas the dead cells stained blue colour. The data results suggest that

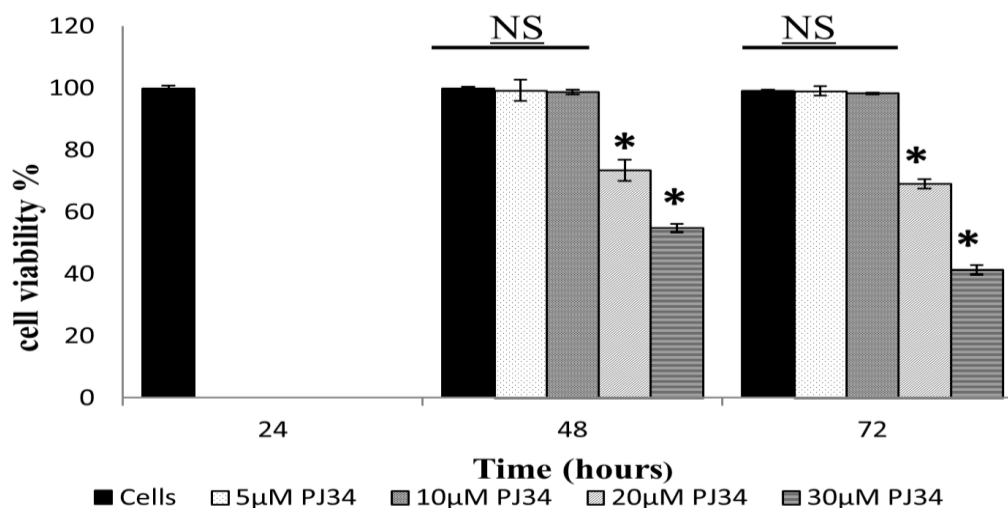


Figure 3-5: The effect of PJ-34 on THP-1 cell viability. THP-1 cells were cultured at a density of 5×10^4 cells/ml in RPMI-1640, supplemented with 10% (v/v) FCS, at 37°C, in a humidified atmosphere with 5% (v/v) CO₂. After 24 hrs, different concentrations of PJ-34 (0, 5, 10, 20 and 30 μ M) were added to the cell cultures. Control samples were left untreated. THP-1 cells were incubated at 37°C with different concentrations of PJ-34 for the indicated times. The significance different $P < 0.05$ vs. control (cells) is indicated with (*) and NS no significant difference. The data presented are the mean \pm SD of three independent experiments.

3.1.4 Conclusion

In this set of experiments it has been shown that PARP-1 activated upon treatment of THP-1 cells with H₂O₂, which caused DNA damage and formation of ADP-ribose polymers. A concentration of 100 μ M H₂O₂ was used as the highest concentration inducing DNA damage and induces maximal PAR polymer formation. The PJ-34 PARP inhibitor afforded a high level of protection against DNA damage induced by H₂O₂ 10 μ M PJ-34 was the highest concentration that blocked PARP activation upon H₂O₂-

induced DNA damage. Treatment of the cells with 20 and 30 μM PJ-34 had a strong adverse effect on THP-1 cell viability. Therefore, 10 μM PJ-34 was identified as the highest concentration of PJ-34 to inhibit PARP-1 activity in response to DNA damage without affecting cell viability, and this amount was used in subsequent experiments.

PART II: The role of PJ-34 in the expression of LPS receptors on differentiated THP-1 cell in response to LPS.

3.2.1 Introduction

The innate immune system utilizes protein receptors that are expressed on monocytes/macrophages, dendritic cells and some other cell types, including epithelial and endothelial cells. Pattern recognition receptors (PPRs); include Toll-like receptors (TLRs), RIG-I-like receptors, NOD-like receptors, and C-type lectin receptors. Lipopolysaccharide (LPS) is the major constituent of the outer cell wall of gram-negative bacteria and is the principal mediator of inflammatory responses to these pathogens. LPS is recognized by number of serum and cell surface PPRs, which cooperate to induce LPS signaling. The LPS signaling pathway is mediated through interaction between the acute phase protein CD14 and LPS-associated co-receptors. CD14 is unable to transduce LPS signaling alone, because it lacks a trans-membrane domain (Antal-Szalmaset al., 2000). Therefore, CD14 functions by binding to LPS and transferring it to other cell surface receptors to trigger LPS signaling (Hazoit, et al., 1996). LPS binding protein (LBP), a lipid transfer protein, recognizes and binds the lipid A portion of LPS and augments the immune response to LPS. LBP is an acute-phase protein that is synthesized principally in hepatocytes, and its production is greatly increased by stimulation with interleukin (IL)-1 or IL-6 (Gutsmann et al., 2001; Schröder & Schumann, 2005) . Consequently, elevated LBP serum levels have been described in severe sepsis (Blairon et al., 2003).

Toll-like receptor 4 (TLR4) is associated with CD14 in inflammatory responses to LPS. TLR4, a type 1 trans-membrane receptor, appears to associate with myeloid differentiation protein-2 (MD-2) on the cell surface. MD2 and TLR4 are involved in binding LPS, and make up the LPS receptor complex involved in the cellular recognition of and signaling by LPS (Miller et al., 2005). Recent studies have implicated high-

mobility group box 1 (HMGB1), a nuclear protein with inflammatory cytokine activities, in stimulating cytokine release (Andersson et al., 2002; Yang et al., 2002; Yamada & Maruyama, 2007). HMGB1 is released during cell injury and necrosis, or is actively secreted during immune cell activation, making it an important player in both sterile and infection-associated inflammation. To date, eight candidate receptors have been implicated in mediating biological responses to HMGB1. These are the receptor for advanced glycation end products (RAGE), TLR2, TLR4, TLR9, Mac-1, syndecan-1, phosphacan/protein-tyrosine phosphatase- ζ/β , and CD24. TLR4, a pivotal receptor for activation of innate immunity and cytokine release, is required for HMGB1-dependent activation of macrophage TNF- α release, but the mechanism of HMGB1-dependent cytokine release is unknown (Yang et al., 2002; Harris & Andersson, 2004; Yang & Tracey, 2010).

Monocytes express TLR2 which recognize products from gram negative and gram positive bacteria (Schaaf et al., 2009). MD-2 physically associates with both TLR4 and TLR2, but the association with TLR2 is weaker than with TLR4. Also, MD-2 and TLR2 and TLR4 enhance each other's expression (Dziarski & Gupta, 2000). The expression of TLR2 on monocytes up-regulated in response to LPS (Ashida et al., 2005). The TLR2-mediated response to stimulation was dependent on NF- κ B signalling, results in releasing of proinflammatory cytokines such as TNF- α and IL-1 β (Chowdhury *et al.*, 2006).

Scavenger receptors (SR) are another family of receptor proteins expressed on macrophages and recognize and bind both endogenous and exogenous molecules. SRs are structurally unrelated receptors functionally defined by their ability to recognise modified low-density lipoprotein (Mukhopadhyay and Gordon, 2004; Peiser et al., 2002). Macrophage receptor with collagenous domain (MARCO), a class-A SR, plays a pivotal

role in the transduction signaling of LPS via TLRs (Peiser et al., 2002; Bowdish & Gordon, 2009).

This study investigated the expression of innate recognition receptors expressed on differentiated and undifferentiated THP-1 cells, with or without stimulation with LPS. The effect of PJ-34 PARP inhibitor on the expression of these receptors in response to LPS was additionally investigated.

3.2.2 Methods

3.2.2.1 Cell differentiation

To enhance the expression of LPS recognition receptors, THP-1 cells were induced to become macrophage-like cells with different concentrations of PMA and Vit.D₃ (see section 2.2.2.3).

3.2.2.2 Cell culture assay

Undifferentiated and differentiated THP-1 cells were grown in RPMI-1640 medium containing 10 % FCS in 50 ml cell culture flasks at 37°C in a humidified 5 % CO₂ incubator.

3.2.2.3 Flow cytometry

Differentiated THP-1 cells were detached from the cell culture petri dish using accutase and undifferentiated THP-1 cells were washed with PBS, primary antibodies for anti-(CD14, TLR2, TLR4 and SR-MARCO) followed by incubation with secondary antibody conjugated FITC. Sorting was performed on a FACS Aria cell sorter (Becton Dickinson Biosciences), as outlined in section 2.2.3.1.

3.2.3 Results

3.2.3.1 Assessment of the expression of CD14, TLR2, TLR4 and MACRO in THP-1 cell in presence and absence of LPS

Cell lines provide an excellent and convenient tool for studying questions related to variety biological topics, including LPS recognition and signaling in septic shock. The THP-1 cell line is considered representative of the early stage of monocytic differentiation (Tsuchiya et al., 1980; Qin, 2012). THP-1 cells have been used to study the expression of the LPS recognition receptors CD14, TLR4, TLR2 and the macrophage SR MARCO (Diya Zhang et al., 2008). Cytokine profiles and the role of PJ-34 in regulating cytokine expression after LPS stimulation have also been studied (Pyriochou et al., 2008; Scalia et al., 2013; Wang et al., 2013).

The level of expression of protein receptors essential for LPS recognition was assessed in native THP-1 cells in the presence and absence of 100ng/ml LPS, with cells exposed to LPS for 4h hours. The cells were analysed on a BD Aria flow cytometer (Becton

Dickinson Biosciences) and the results analysed with Flow-Jo software. Antibody isotypes (negative control) used for detecting expression of the proteins studied are shown in Figure 3.7. Untreated cells (Fig. 3.7 A) showed that THP-1 cells express moderate levels of cell surface CD14, while TLR2, TLR4 and MARCO were expressed at low levels. However, after LPS stimulation for 4 h, the cells displayed a slight increase in CD14, TLR2 and TLR4 expression (Fig. 3.7 A, C and D). MARCO, by contrast, decreased upon stimulation with LPS (Fig. 3.7 B).

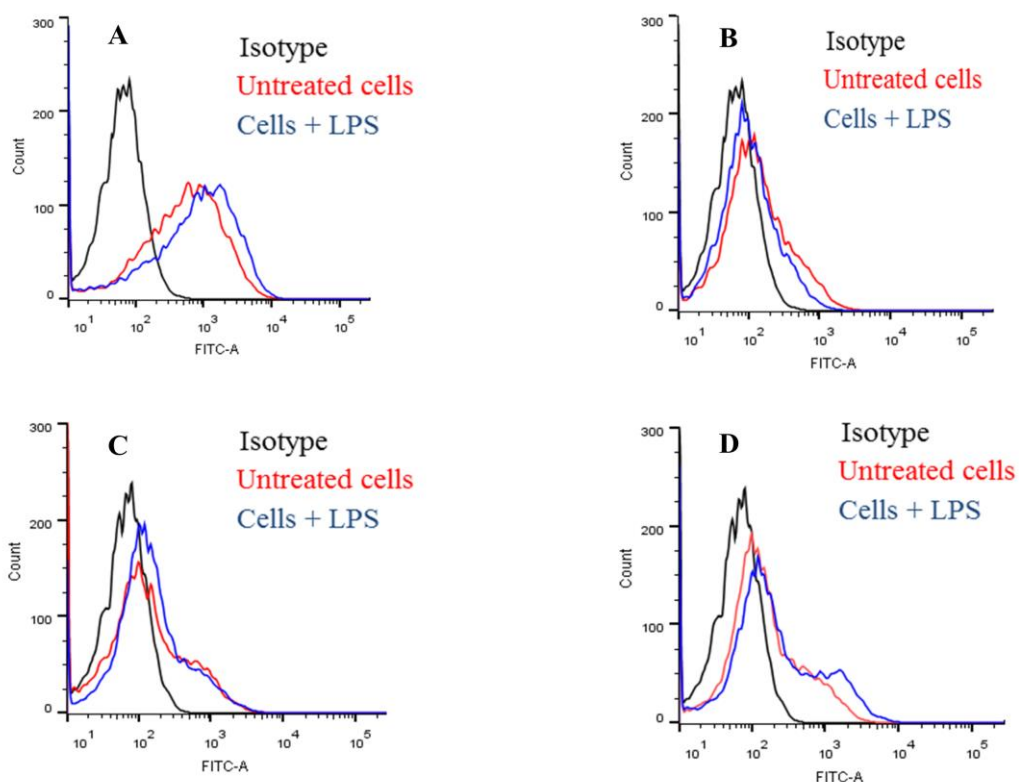


Figure 3-6: The expression of CD14, MARCO, TLR4 and TLR2 in THP-1 cells, assessed by flow cytometry. THP-1 cells were incubated with or without 100 ng/ml of LPS at 37⁰C in RPMI 1640 media supplemented with 10% (v/v) FCS for 4 hrs. Cells were washed and incubated with primary mouse anti-human (CD14 or MARCO or TLR4 and TLR2) monoclonal antibody for 45 mins, washed again, and then incubated with secondary antibody (goat anti-mouse IgG labelled FITC). IgG1 was used as the isotype for CD14 and MARCO, while IgG2b was used as the isotype for TLR2 and TLR4. Samples were analysed using an Aria flow cytometer (Becton Dickinson Biosciences) and Flow-Jo Vx.0.7 flow cytometry analysis software (Flow-Jo LLC, Ashland, USA) was used to analyse the data. **A:** represents CD14 expression **B:** represents MARCO expression. **C:** represents TLR2 expression and **D:** represents TLR4 expression. Black colour histograms represent isotypes. Red colour histograms represent receptors expression on untreated cells. Blue colour histograms represent receptor expression on THP-1 cells treated with LPS 100 ng/ml.

3.2.3.2 Differentiation of THP-1 cells induced by PMA and vit.D₃

The action of differentiation inducers was studied to investigate the effect of PJ-34 on LPS receptor expression and cytokine profiles in THP-1 cells. In these experiments, 1,

25-dihydroxyvitamin D₃ (Vit.D₃) and phorbol 12- myristate 13-acetate (PMA) were used to induce cell maturation. Figure 3.8 shows THP-1 cells in culture media RPMI-1640 supplement with 10% FCS. In the presence of PMA, the cells were spindle-like and strongly adhered to surfaces in comparison with cells treated with vit. D₃ caused a change in cell shape to that typical for macrophages and the cells were only slightly adhering.

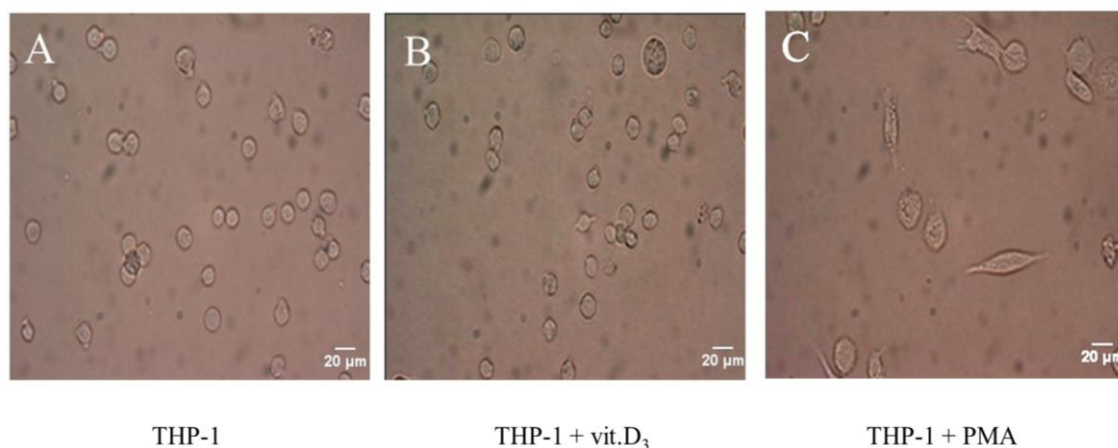


Figure 3-7: Differentiation of THP-1 cells with Vit.D₃ and PMA. Phase contrast photographs. (A) Untreated THP-1 cells, (B) differentiated THP-1 cells treated with 100 nM of vit.D₃ for 72 hours and (C) THP-1 cells treated with PMA 5 ng/ml for 72 hours.

Since maturation of monocytes is accompanied by changes in the levels expression of certain cell-surface markers, the effect of PMA and vit.D₃ on the expression of CD14, MARCO, TLR2 and TLR4 was examined (Fig. 3.8 and 3.10). Maturation of THP-1 cells was induced, with the cells exposed to different concentrations of PMA (0, 5, 10, 20 and 30 ng/ml) and vit.D₃ (0, 50, 100, 150 and 200 nM) for 72 hrs. Cell-surface expression of CD14, MARCO, TLR2 and TLR4 was detected on stained cells by indirect immunofluorescence. The cells were incubated with the correct concentration of specific primary monoclonal mouse anti- human antibodies for CD14, MARCO, TLR2 and TLR4 for 45 min, followed by incubation with goat anti mouse labelled FITC for 30 minutes.

The expression of protein receptors was detected using an Aria flow cytometer/sorter (Becton Dickinson Biosciences) with the data analysed using Flo-Jo software.

Differentiation of THP-1 cells with PMA and vit.D₃, up-regulate the expression of CD14, MARCO, TLR2 and TLR4; each of PMA and vit.D₃ had a different effect on the expression of each protein. The highest level of expression of all the proteins was detected in THP-1 cells treated with PMA 5 ng/ml and vit.D₃100 nM (Fig. 3. 8 & Fig. 3.10).

Figures 3.8 A, show that the expression of CD14 in PMA-differentiated THP-1 increased about tenfold. Whereas, vit.D₃ increased the expression of twice the amount of CD14 as that in THP-1 cells differentiated using PMA (Fig. 3.10 A). MARCO expression increased one fold in PMA-differentiated THP-1(Fig. 3.8 B) while, the cells differentiated with vit.D₃ showed an approximately eight fold increase of MARCO expression (Fig. 3.10 B). The expression of TLR4 and TLR2 in PMA-differentiated cells increased four and three fold respectively (Fig. 3.8 C & D). However, the expression of TLR4 and TLR2 in cells differentiated with vit.D₃ was much higher than in cells differentiated with PMA, roughly about 6 folds and 5 fold, respectively (Fig. 3.10 C & D). The FMI CD14, MARCO, TLR4 and TLR2 expression on THP-1 cells differentiated with PMA and vit.D₃ are represented in fig.3.9 and fig. 3.11. Subsequently, experiments of time course series was conducted for (24, 48, 72 and 96 h of differentiation), using PMA 5 ng/ml and Vit.D₃100 nM, was used to detect CD14, TLR4, TLR2 and MARCO expression in the cells. Receptor expression steadily increased over the time, peaking at 72 hrs, and then decreased at 96 hrs of differentiation

(Fig. 3.12), the results show that cells differentiated with vit.D₃ show higher expression of the receptors compared to PMA differentiated cells represented as bars (Fig. 3.12).

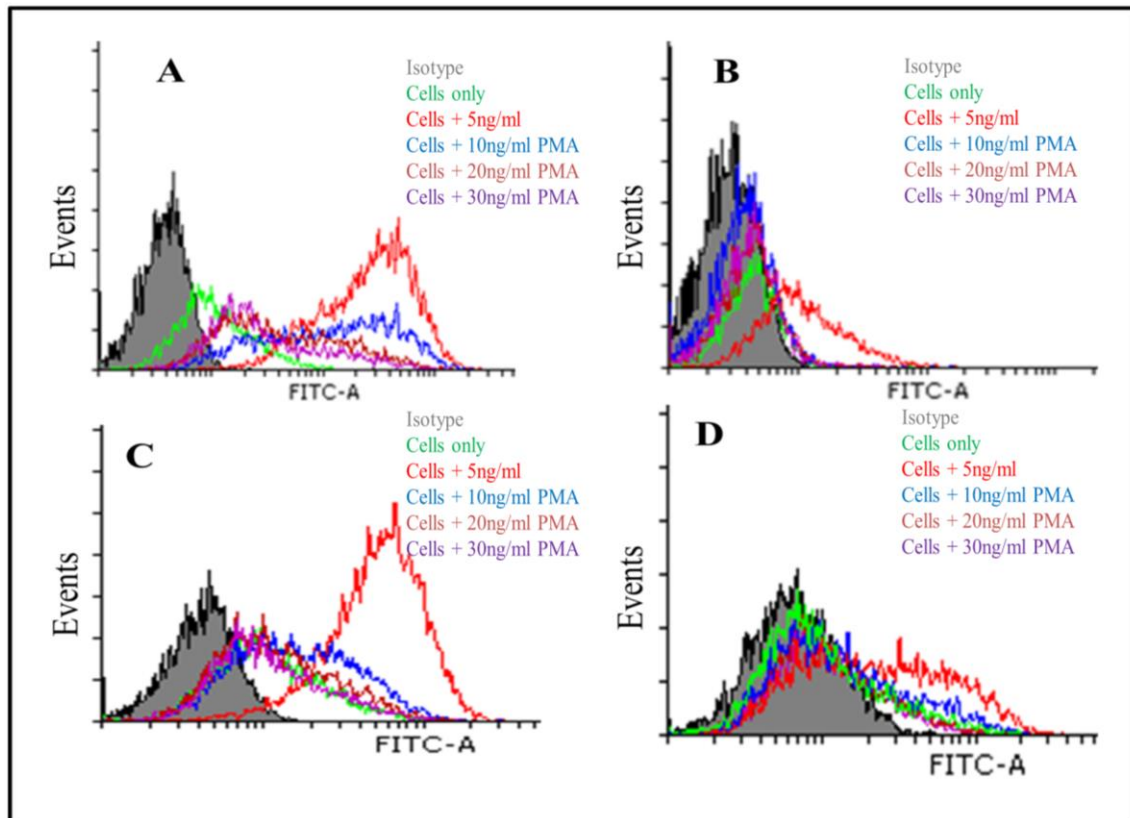


Figure 3-8: The effect of different concentrations of PMA on the expression of CD14, MARCO, TLR4 and TLR2 in THP-1 cells, assessed by flow cytometry. THP-1 cells (5×10^5 cells/ml) were incubated without or with 0, 5, 10, 20, 30 ng/ml of PMA d at 37°C in RPMI 1640 media supplemented with 10% (v/v) FCS for 72 hrs. Cells were washed and incubated with primary mouse anti-human (CD14 or TLR2 or TLR4 and MARCO) monoclonal antibody for 45 min, washed again, and then incubated with secondary antibody (goat anti-mouse IgG labelled FITC). IgG 1k was used as the isotype for CD14 and MARCO, while IgG 2b was used as the isotype for TLR2 and TLR4. Samples were analysed using an Aria flow cytometer (Becton Dickinson Biosciences) and Flowing software version 2.5.0 (Turku centre for biotechnology, University of Turku, Finland) was used to analyse the data. **A:** Represents the expression of CD14. **B:** Represents the expression of MARCO. **C:** Represents the expression of TLR4 and **D:** Represents the expression of TLR2. Grey histograms represent isotypes, green histograms represent untreated cells (control), red histograms represent cells treated 5 ng/ml of PMA, blue histograms represent cells treated with 10 ng/ml of PMA, brown histograms represent cells treated with 20 ng/ml of PMA and purple histograms represent cells treated with 30 ng/ml of PMA.

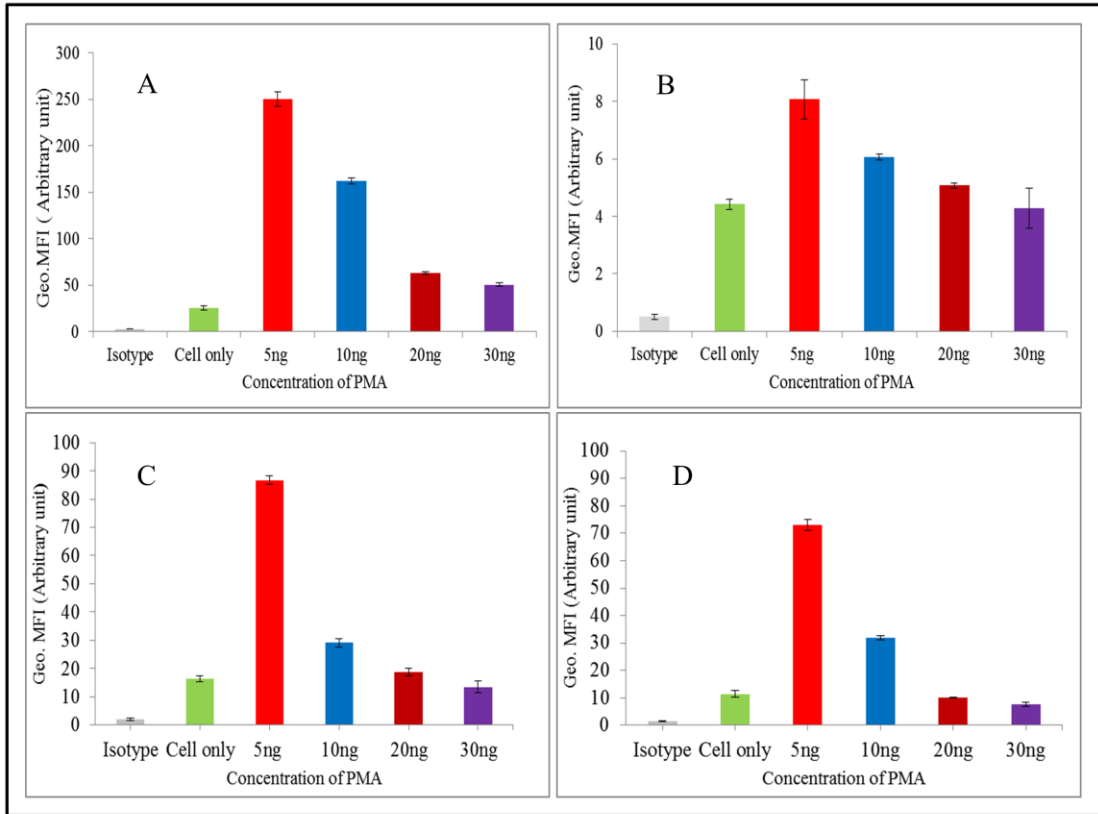


Figure 3.9: Bar figure represents the effect of different concentrations of PMA on the expression of CD14, MARCO, TLR4 and TLR2 in THP-1 cells, assessed by flow cytometry. A represents the expression of CD14, **B:** represent the expression of MARCO, **C:** represent the expression of TLR4 and **D:** represent the expression of TLR2. Bar colors represents, Gray isotype, green untreated cells, red cells treated 5 ng/ml PMA, blue cells treated 10ng/ml PMA, brown cells treated 20 ng/ml PMA, purple cells treated 30 ng/ml PMA. Values represent the mean \pm SD from three experiments.

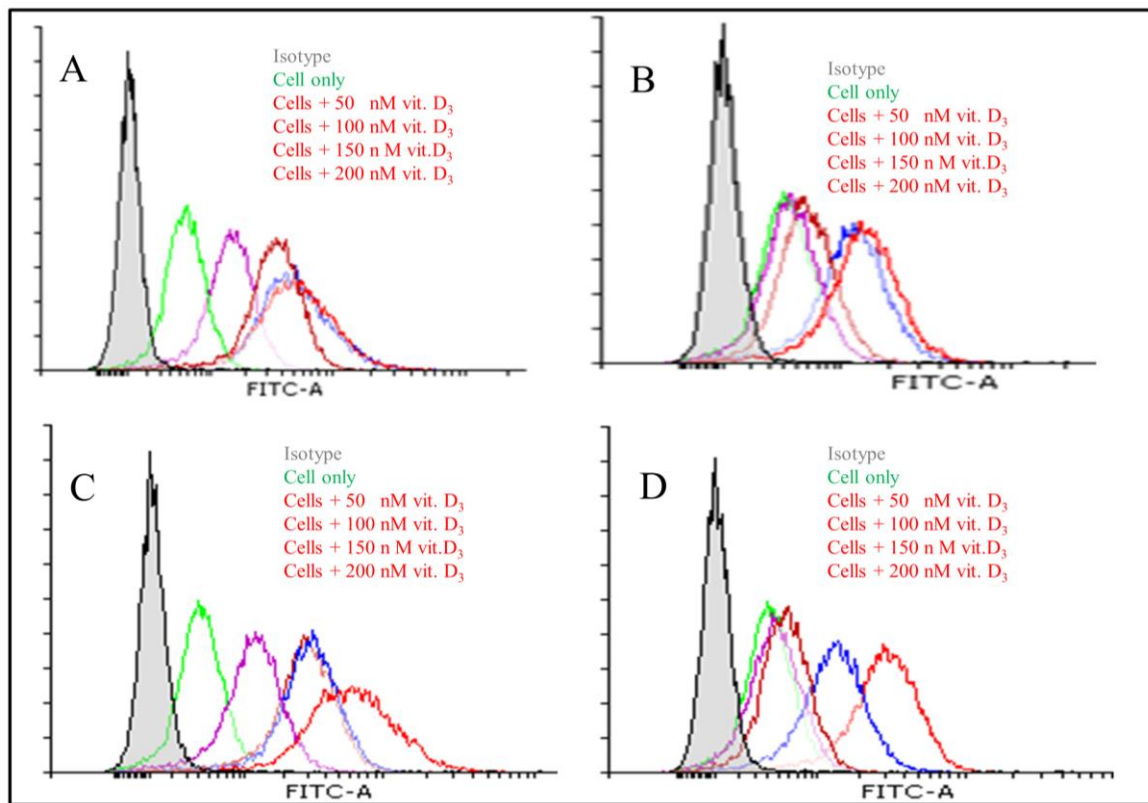


Figure 3-10: The effect of different concentrations of Vit. D₃ on the expression of CD14, MARCO, TLR4 and TLR2 in THP-1 cells, assessed with flow cytometry. THP-1 cells (5×10^5 cells/ml) were incubated without or with 0, 50, 100, 150 and 200 nM of vit.D₃ at 37°C in RPMI 1640 media supplemented with 10% (v/v) FCS for 72 hrs. Cells were washed and then incubated with primary mouse anti-human (CD14 or TLR2 or TLR4 and MARCO) monoclonal antibody for 45 mins, washed again, and then incubated with secondary antibody (goat anti-mouse IgG labelled FITC). IgG1k was used as the isotype for CD14 and MARCO, while IgG2b was used as the isotype for TLR2 and TLR4. Samples were analysed using an Aria flow cytometer (Becton Dickinson Biosciences) and Flowing software version 2.5.0 (Turku centre for biotechnology, University of Turku, Finland) was used to analyse the data. **A:** Represents the expression of CD14. **B:** Represents the expression of MARCO. **C:** Represents the expression of TLR4 and **D:** Represents the expression of TLR2. Grey histograms represent Isotypes, green histograms represent untreated cells (control), red histograms represent cells treated 50 nM of vit.D₃, blue histograms represent cells treated with 100 nM of vit. D₃, brown histograms represent cells treated with 150 nM of vit. D₃ and finally purple histograms represent cells treated with 200 nM of vit. D₃.

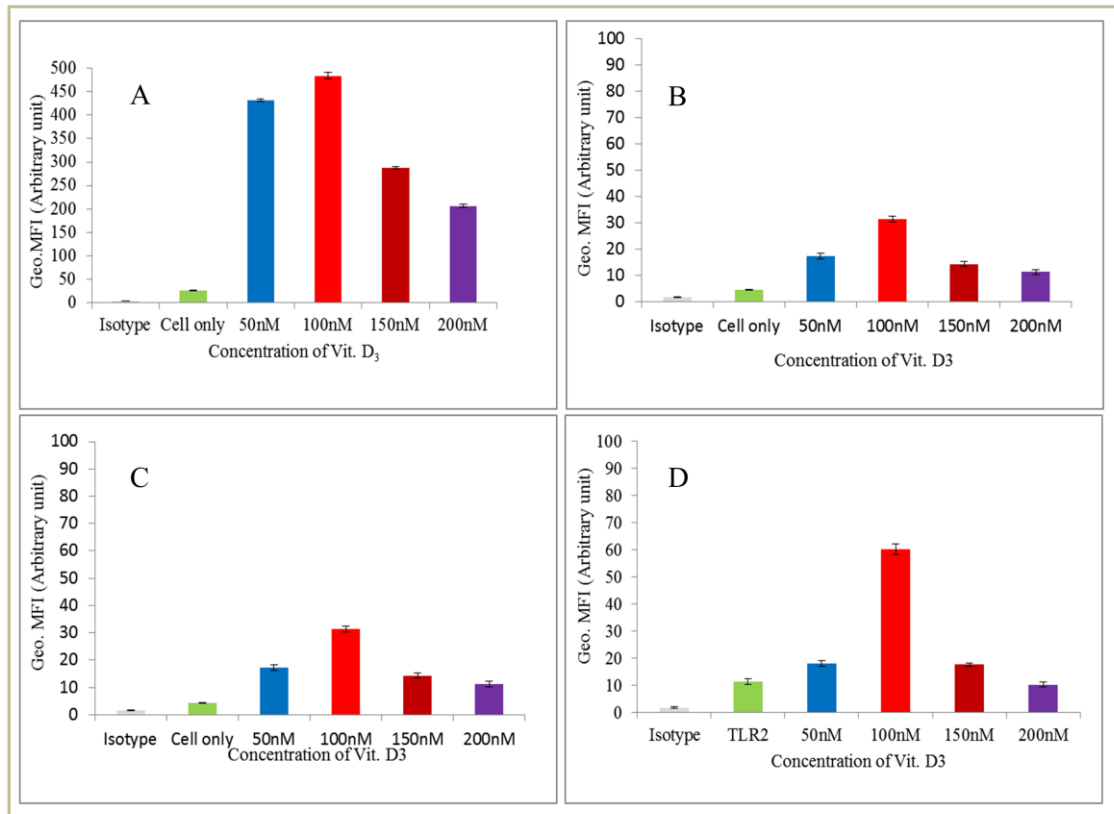


Figure 3-11: Bar figure represent the effect of different concentrations of vit.D₃ on the expression of CD14, MARCO, TLR4 and TLR2 in THP-1 cells assessed by flow cytometry. A: represent the expression of CD14, **B:** represent the expression of MARCO, **C:** represent the expression of TLR4 and **D:** represent the expression of TLR2. Bars represents; Gray isotype, green untreated cells, blue cells treated 50 nM vit.D₃, red cells treated 100 nM vit.D₃, brown cells treated 150 nM vit.D₃ and purpel cells treated 200 nM vit.D₃.Data represents three differentexperiments. Values represent the mean \pm SD from three experiments.

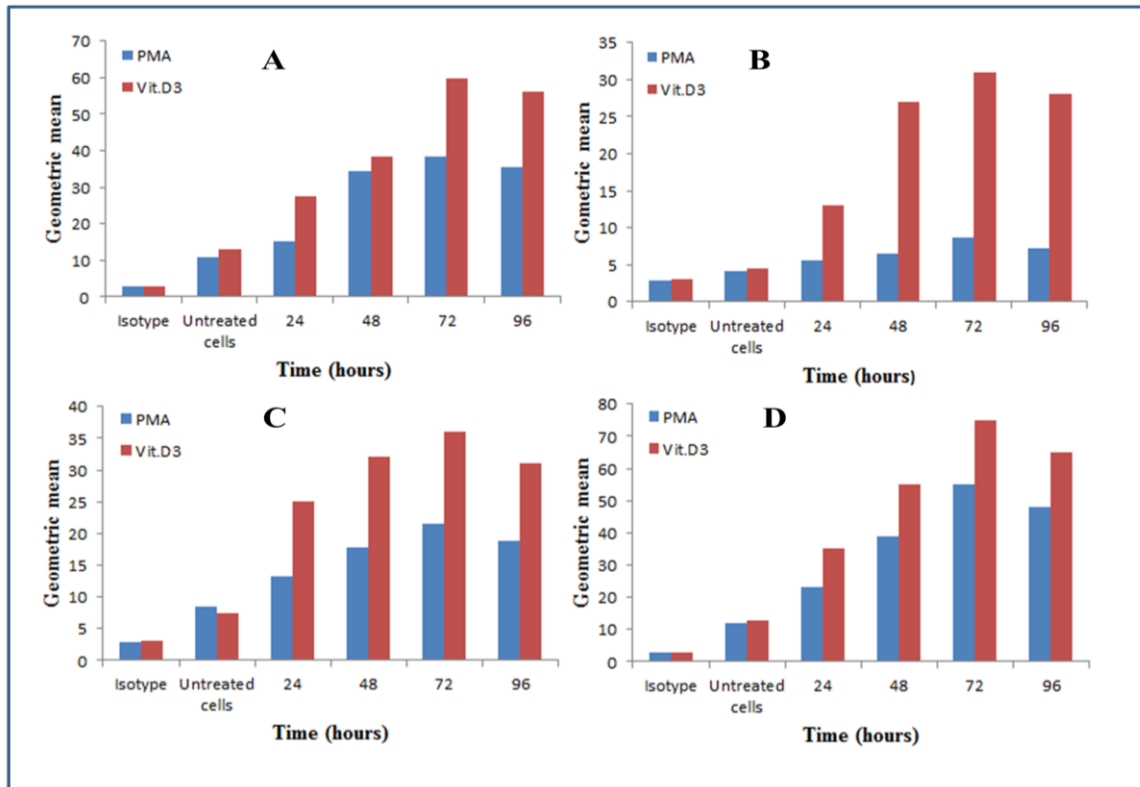


Figure 3-12: The expression of CD14, MARCO, TLR4 and TLR2 in THP-1 cells in response to PMA and vit.D₃ time course. THP-1 cells were differentiated in the presence of 5 ng/ml of PMA and 100 nM of vit.D₃ for the indicated times. The changes in the expression of receptors were detected using Aria flow cytometry (DB, Becton Dickinson Biosciences) and data analysed with flowing software version 2.5.0 (Turku centre for biotechnology, University of Turku, Finland). Results are plotted as the geometric mean of two independent experiments. Maximum expression of the receptors was achieved at 72 hrs. Differentiate of THP-1 cells with vit.D₃ results in greater expression of the receptors than cells differentiated with PMA. **A:** Represents the expression of CD14. **B:** Represents the expression of MARCO. **C:** Represents the expression of TLR4. **D:** Represents the expression of TLR2. Blue colour represents cells that treated with PMA and red colour represents cells that treated with vit.D₃.

3.2.3.3 The effect of PJ-34 on the expression of CD14, TLR2, TLR4 and MARCO in PD/THP-1 cells in response to LPS

To study the role of PJ-34 in membrane expression of CD14, MARCO, TLR4 and TLR2 in PD/ THP-1 cells, 25×10^4 cells/ml were incubated with or without 10 μ M of PJ-34 for 30 mins and then stimulated with LPS 100 ng/ml for 4 hrs. The cells were stained by indirect fluorescent staining using mouse anti-human monoclonal antibodies for CD14, MARCO, TLR4 and TLR2 proteins after a 45-mins incubation period. The cells were then incubated with FITC goat anti-mouse IgG for 30 minutes. Cells stained with IgG1k and IgG2b were used as isotype (negative) control. The samples were analysed using a FACS Aria cell sorter (Becton Dickinson Biosciences) and the data analysed by Flo-Jo software.

Figure 3.11 represents the expression of CD14, MARCO, TLR4 and TLR2 in PMA-differentiated THP-1 cells treated with or without 10 μ M PJ-34 for 30 mins prior to incubate with LPS 100 ng/ml for 4 hrs. Filled histograms (grey colour) represent the isotype control (negative control) column A, and non-filled histograms represent the expression of the receptors (Fig. 3.11 column B). The expression of CD14, TLR4 and TLR2 on PMA-differentiated THP-1 cells increased when the cells were incubated with LPS alone while the expression of MARCO decreased (Fig. 3.11 column C). Cells treated with PJ-34, prior to stimulate with LPS, exhibited a decrease in the expression of the CD14, TLR4 and TLR2 receptors (Fig. 3.11 column D). Whereas the expression of MARCO increased in cells treated with PJ-34 prior to stimulate with LPS (Fig.3.11 D). Figure 3.12 represents MFI of CD14, MARCO, TLR2, and TLR4 on PD/THP-1 cells in response to of LPS 100 ng/m in presence and absence of PJ-34 10 μ M.

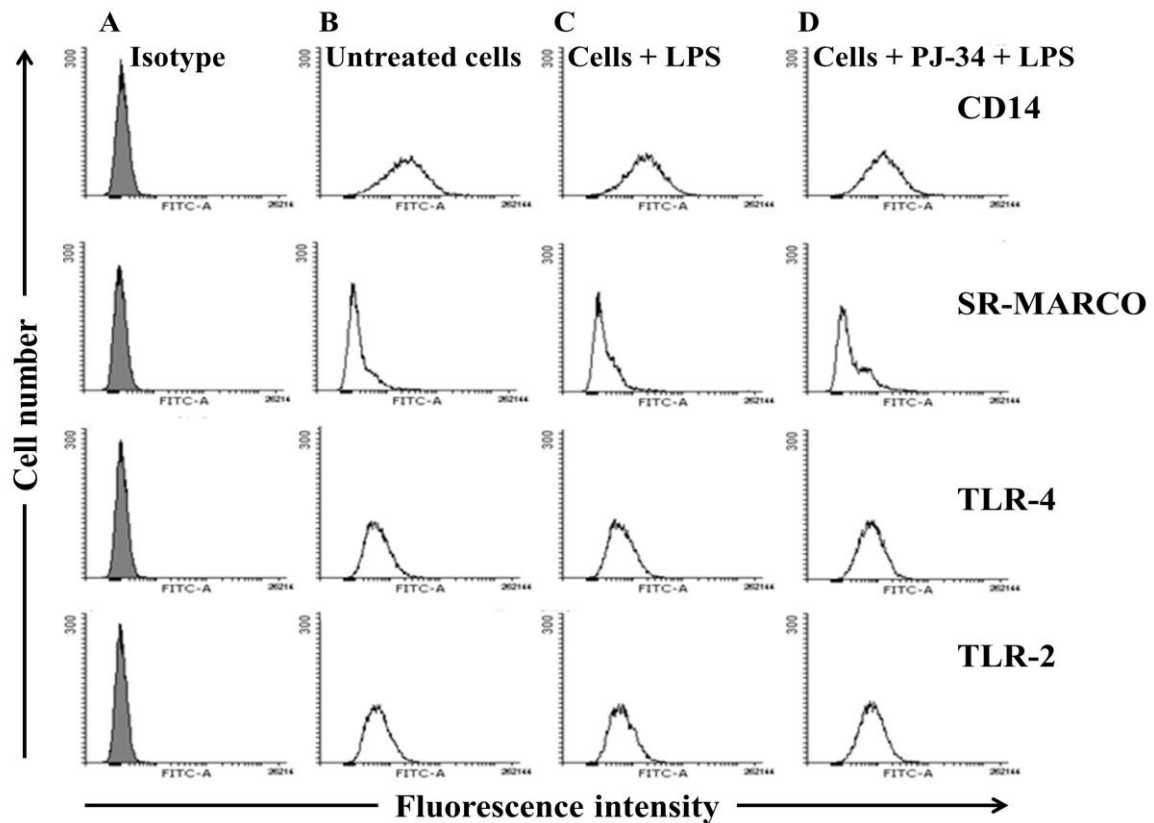


Figure 3-13: The effect of PJ-34 on CD14, MARCO, TLR4 and TLR2 expression in PD/THP-1 cells in response to LPS. THP-1 cells were differentiated with 5 ng/ml for 72 h, cells were incubated without or with 10 μ M of PJ-34 for 30 m prior to stimulation with LPS 100 ng/ml in RPMI 1640 media supplemented with 10% (v/v) FCS in a humidified atmosphere at 37°C for 4 hrs. Cells were washed and incubated with primary mouse anti-human (CD14 or TLR2 or TLR4 and MARCO) monoclonal antibody for 45 min, washed again, and then incubated with secondary antibody (goat anti-mouse IgG labelled FITC). IgG1K was used as the isotype for CD14 and MARCO, while IgG2b was used as the isotype for TLR2 and TLR4. Samples were analysed using an Aria flow cytometer (Becton Dickinson Biosciences) and Flowing Software v. 2.5.0 (Centre of biotechnology, Turku University, Finland) was used to analyse the data. **Column A:** Isotype (Negative control). **Column B:** Untreated cells. **Column C:** Cells treated with LPS. **Column D:** Cells treated with PJ-34 and then stimulated with LPS. Filled histograms represent isotypes and unfilled histograms represent expression of receptors.

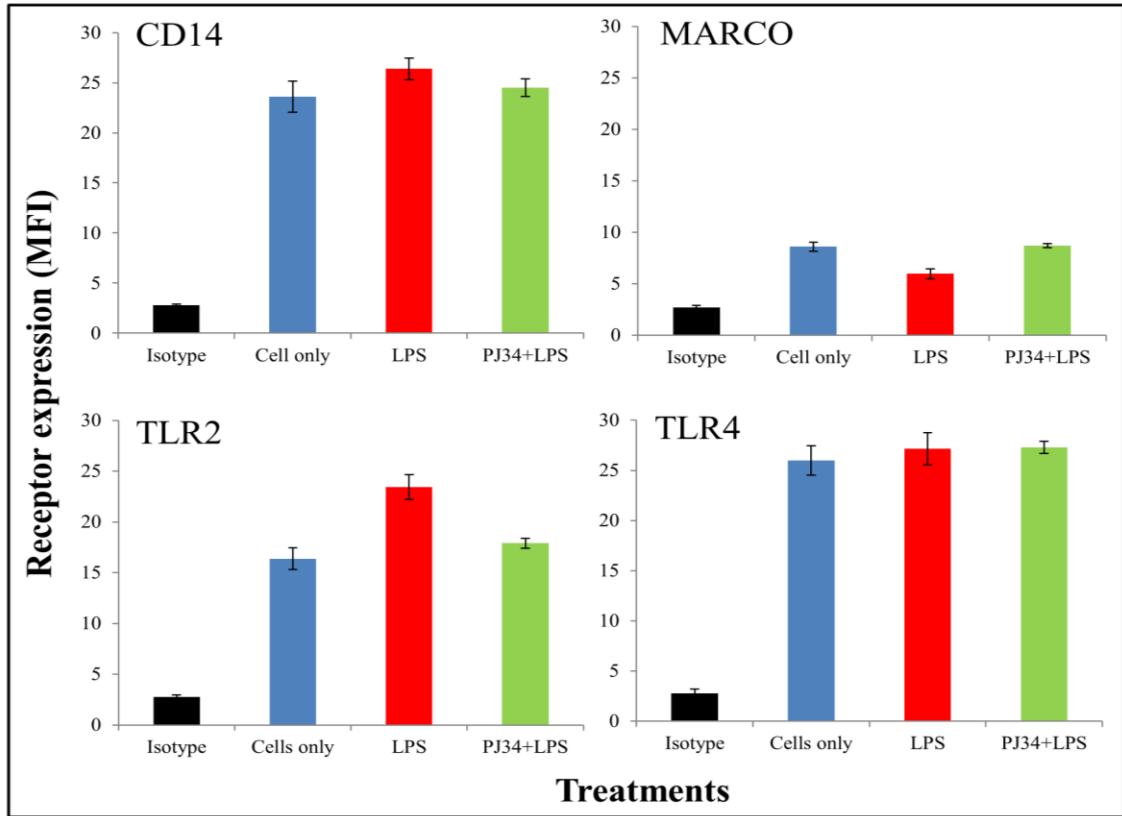


Figure 3-14: Bar figure represents the effect of PJ-34 on CD14, MARCO, TLR2 and TLR4 expression in PD/ THP-1 cells in response to LPS. Bar figure represents. Bars colors represents; Black isotype, blue untreated cells, red cells treated with LPS 100 ng/ml and green cells treated with PJ-34 10 μ M. Data represents three different experiments. Values represent the mean \pm SD from three experiments.

3.2.4 Conclusion

Native THP-1 cells express a moderate level of CD14 and low levels of MARCO, TLR4 and TLR2. The expression level of CD14, TLA4 and TLR2 slightly increased when THP-1 cells were stimulated with LPS 100 ng/ml. Whereas, MARCO expression decreased in LPS-treated cells.

In this study two different stimuli, PMA and vit.D₃ were used to differentiate THP-1 cells. PMA has greater differentiation effect as reflected by increased adherence and induce a higher level of proinflammatory cytokines in response to LPS. This was consistent with previous studies which identified the differentiation in PMA and vit.D₃ stimulated THP-1 cells (Daigneault et al., 2010). THP-1 cells differentiated with PMA and vit.D₃ shows Up-regulation in the expression of CD14, MARCO, TLR4 and TLR2 and released greater level of proinflammatory cytokines than non-differentiated cells. Although vit.D₃ differentiated cells shows higher receptors expression, PMA was used as its level of cytokines release was greater in cells, as this study investigate the role PARP enzyme in the regulation of LPS receptors and production of pro-inflammatory cytokines. The expression of CD14, TLR4 and TLR2 receptors increased in PMA-differentiated cells, when the cells were stimulated with LPS only. In contrast, cells treated with PJ-34, prior to LPS stimulation, showed a decrease in the expression of the receptors. Contrariwise, MARCO expression decreased in THP-1 cells treated only with LPS, and increased when the cells were treated with PJ-34 prior to exposure to LPS.

**CHAPTER 4: Measurement of production of cytokines and nitric oxide
by THP-1 cells**

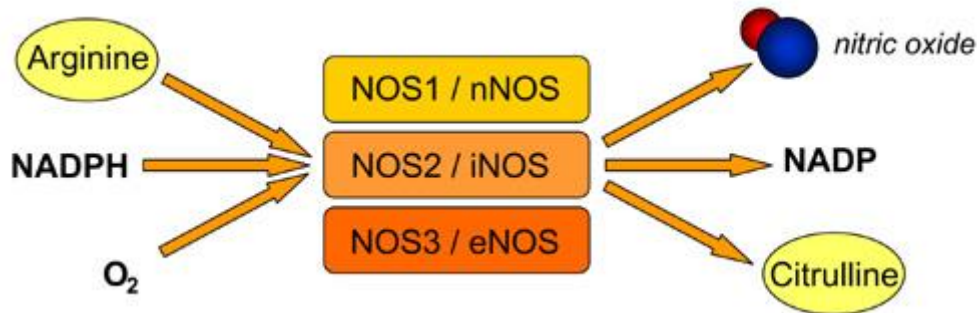
4.1 Introduction

Innate immunity is controlled by cytokines, which are produced predominantly by monocytes, macrophages and dendritic cells, with some released by other cell types such as T cells, NK cells, endothelial and epithelial cells. Proinflammatory cytokines such as tumour necrosis factor alpha (TNF- α) and interleukin 1 beta (IL-1 β) are essential in modulation of immunity and the inflammatory response. TNF- α is a notable inflammatory cytokine made mainly by mononuclear phagocytes, NK cells, activated lymphocytes and activated vascular endothelial cells. The mode of action of TNF- α is incumbent in septic shock after its release by macrophages activated by lipopolysaccharide (LPS) and other bacterial products. TNF- α also mediates acute inflammation by interaction with other inflammatory mediators such as IL-1 and IL-6 (Suharti et al., 2003; Lin & Tang, 2007; Rossol et al., 2011).

LPS, a component of the outer membrane of gram-negative bacteria, is one of the most potent innate activating stimuli known. The inflammatory mechanism of LPS involves the secretion of nitric oxide (NO) in various tissue as well as by monocytes and macrophages (Titheradge, 1999; Bultinck et al., 2006). NO is a small molecule with roles in many physiological and pathological responses, including circulation, blood pressure, platelet function, host defence and neurotransmission in the central nervous system and peripheral nerves (Moncada et al., 1991; Bogdan et al., 2000).

NO is produced at different levels by different types of cells, such as neurons, endothelial cells, platelets, and neutrophils, in response to inflammation. Its production controls many important functions of PMNs, including chemotaxis, adhesion, aggregation, apoptosis, and PMN-mediated bacterial killing (Sethi & Dikshit, 2000). NO is produced through the action of nitric oxide synthases (NOSs), a group of enzymes that generate NO from the amino acid L-arginine. NOSs convert arginine into citrulline, with NO produced during the process. Oxygen and NADPH are necessary co-factors. Three isoforms of NOS have

been identified, based on their activity: neuronal NOS (nNOS or NOS1), inducible NOS (iNOS or NOS2) and endothelial NOS (eNOS or NOS3). The general mechanism of NO production is as follows.



iNOS is expressed in many cell types, including macrophages, neutrophils, dendritic cells, endothelial cells and epithelial cells. NOS1 and NOS3 are less ubiquitous, but there is evidence to indicate they are critical for a normal physiology (Bogdan et al., 2000; O'Neill, 2011). iNOS is involved in the immune response, the production of NO by iNOS lasts much longer than from other isoforms of NOS. iNOS produces high concentrations of NO in the cell, this is because iNOS capability to bind tightly to calmodulin, even at very low cellular concentrations of calcium.

NO production plays a crucial role in host defence against intracellular pathogens. However, whether NO-dependent control of intracellular organisms primarily implicates cell-intrinsic or alternatively cell-extrinsic activity of NO is still not clear. For instance, NO production by infected phagocytes might enable these cells to individually control their pathogen burden. Alternatively, the ability of NO to diffuse across cell membranes may be critical for infection control (Olekhovitch et al., 2014).

Studies conducted by O'Neill, 2011; Seow et al., 2013, reported that the production of proinflammatory cytokines in response to LPS is regulated by the nuclear transcription

factor NF- κ B /Rel complex. When immune the cells treated or exposed to LPS, NF- κ B is activated and translocated into the nucleus from the cytoplasm. This results in expression of several critical transcriptional genes related to septic shock pathogenesis, such as TNF- α , interleukin 1 β , interferon- β (INF- β), adhesion molecules (ICAM-1 and E-selectin) and iNOS (Chandel et al., 2000; Bultinck et al., 2006; Jang et al., 2006; Rossol et al., 2011). PARP-1 is also involved in the regulation of inflammatory processes associated with NF- κ B (Chaitanya et al., 2010; Ohanna et al., 2011; Scalia et al., 2013)

The main objective of this part of the study was to determine the effect of LPS, and the involvement of PARP activity, on TNF- α , IL-1 β and NO production. Whether or not PARP activity is required for the induction of NF- κ B activation in THP-1 or in the PMA-differentiated THP-1 cells (PD/THP-1) was also examined.

4.2 Method

4.2.1 ELISA

The level of TNF- α and IL-1 β produced by undifferentiated THP-1 cells and THP-1 cells differentiated by treatment with PMA 5 ng/ml and vit.D₃ 100 nM of for 72 hrs, was measured by ELISA assay. Cells, at density 1x10⁶ cell/ ml, were stimulated with an increasing concentration of *E. Coli* EH100 (Ra mutant) LPS (10, 50, 100 and 1000 ng/ml) or 100 ng/ml of LPS in the presence and absence of 10 μ M PJ-34 or 1 μ g/ml of antibodies (anti-CD14, anti-TLR4, anti-TLR2, anti-MARCO, anti-NF- κ B or anti-JNK-1) for 30 mins. Control samples were left untreated. Samples were incubated at 37°C in a humidified tissue culture incubator with 5% (v/v) CO₂ for 4 hrs. The samples were centrifuged at hourly intervals at 1200 rpm (32 xg) for 5 mins. and the supernatants were

transferred to clean Eppendorf tubes and stored at -80°C . 100 μl of each sample was used to measure the TNF- α , and IL-1 β levels (see 2.2.7.1).

4.2.2 Western blotting

Undifferentiated THP-1 cells and PD/THP-1 were cultured in a 100 mm culture plate and were treated with or without 10 μM of PJ-34. After 30 mins prior to stimulation with LPS (1 $\mu\text{g}/\text{ml}$) for 15, 30, 60 and 120 mins., cells were lysed with a Nuclear Extract Kit (Active Motif, UK), and the manufacturer's protocol was followed to prepare the cytoplasmic or the whole cell lysate. Protein concentration in each sample was quantified with Bradford assay and plate was read with a plate reader (Versa max). The cell lysate was kept at -80°C until the analysis was carried out. Cell lysate from cytoplasmic extract, 15 μg , and whole cell lysate were loaded on a 12% SDS page-gel. After electrophoresis, protein was transferred to a polyvinylidene fluoride membrane (Immobilon-FL, Merck Millipore, Merck KGaA, and Darmstadt, Germany). Membranes were blocked with 5% w/v skimmed milk in PBS for 1 h. The membrane containing the cytoplasmic extract was probed with-rabbit anti-human NF- κB -65 (clone poly 6226, Biolegend , UK) at a dilution of 1:1000 μl in 5% skimmed milk in western wash buffer (tPBS). tPBS contain 2.42 g Tris base, 8g NaCl and was diluted to 1 L with distilled water, adjusted to pH 7.6, with 0.5 ml Tween-20 then added. The membrane containing whole-cell lysate was incubated with rabbit anti-human JNK-1 (clone poly6331, biolegend, UK), and incubated for 1-2 hrs on a rocker. The membranes were then washed three times with wash buffer; 10 mins each wash, changing the wash buffer. The membranes were subsequently incubated with secondary antibody, IRDye® 700CW Donkey anti-rabbit IgG, or IRDye® 800CW goat anti-mouse IgG (Li-Cor Bioescieces, Lincoln, NE, U.S.A), at a dilution of 1:10000 The

primary mAb, mouse anti-human α -Tubulin (clone 10D8, Biolegend, UK), was used as a control at a dilution of 1:1000. Membranes were scanned and analysed with a Li-Cor scanner infrared imaging system using Odyssey software (Li-Cor Bioscience).

4.2.3 Nitric oxide measurement

NO produced by the undifferentiated THP-1 cells and PD/THP-1 was evaluated by measuring nitrite/nitrate (NO_2^-) accumulation in culture supernatants using the Griess reaction. Cells were seeded at 2.5×10^5 cells/ml in RPMI-1640 medium supplemented with 10% (v/v) FCS in a 96-well plate. The plate was treated with 10 μM of PJ-34 for 30 mins, subsequently stimulated with 100 ng/ml LPS, and then incubated in a tissue culture incubator at 37°C in a humidified atmosphere of 5% (v/v) CO_2 . Following incubation, supernatants were collected by centrifuging the cells at 1200 rpm for 5 mins every hour and were stored at -80°C. Finally, 50 μl of each sample was used to measure nitrite concentration as described in section (2.2.6.1).

4.3 Results

4.3.1 Secretion of TNF- α and IL-1 β in undifferentiated and differentiated THP-1 cells in response to LPS

To investigate the inflammatory response of the human monocytic cell line THP-1 and PMA, vit.D₃ differentiated THP-1 cells to LPS, cells, at density of 1×10^6 cells/ml, were stimulated with increasing concentrations (0, 1, 10, 100, 1000 ng/ml) of *E. coli* EH100 (Ra mutant) LPS for 4 h and TNF- α and IL-1 β levels in culture supernatants determined

using ELISA. Figure 4.1 and 4.2, shows that native THP-1 cells and vit.D₃ and PD/THP-1 differentiated cells secreted more TNF- α than IL-1 β in response to LPS for the same incubation period.

As shown in figure 4.1, undifferentiated cells were found to respond weakly to LPS stimulation, producing approximately ~35 pg./ml of TNF- α , whereas THP-1 cells differentiated with vit.D₃ and PMA significantly produced higher level of TNF- α production in response to LPS. The production of TNF- α in vit.D₃ differentiated cells reached peak of 273 pg/ml, while the level in PD/THP-1 peaked at 600 pg/ml (Fig. 4.1). In addition the production of TNF- α by different types of cells increases with increasing LPS concentration and the maximum level produce in cells treated with 100 ng/ml LPS for 4 h (Fig. 4.1). Also the production amount of IL-1 β was significantly higher in differentiated cells than undifferentiated cells. In PD/THP-1 the level of IL-1 β produced was higher than vit.D₃ differentiated cells and reached level of 182.12 pg/ml and 63.12 pg./ml respectively while, undifferentiated cells produced only 21.87 pg/ml at 4 hrs incubation and obtained in cells incubated with LPS 100 ng/ml (Fig. 4.2).

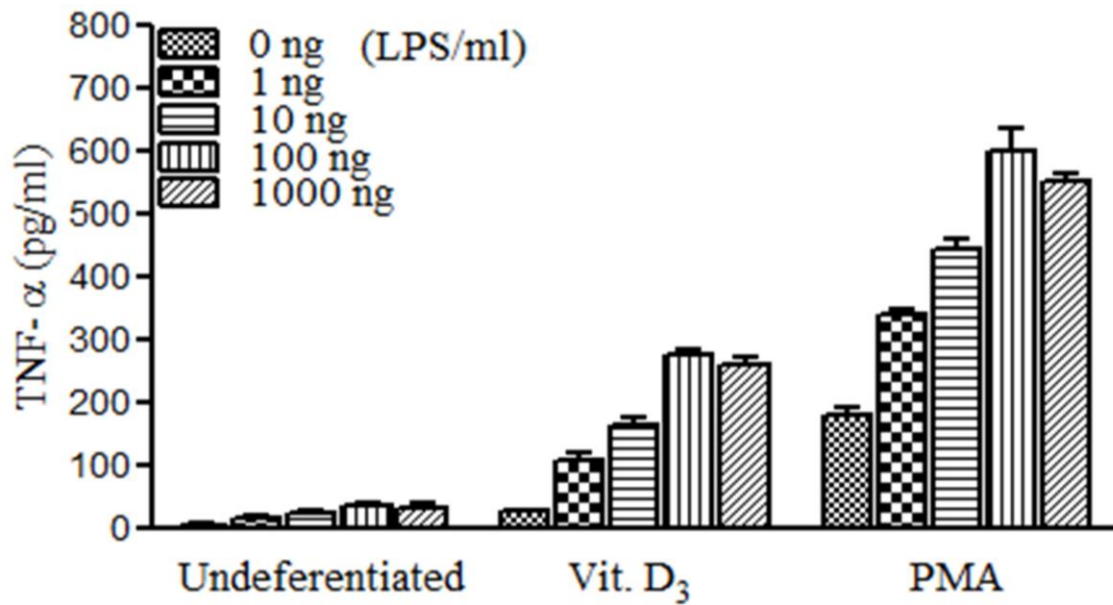


Figure 4-1: The TNF- α secretion by undifferentiated cells, vit.D₃ and PMA differentiated THP-1 cells in response to LPS. Untreated THP-1 cells, THP-1 cells differentiated with vit.D₃ 100 nM for 72 hrs THP-1 cells differentiated with PMA 5 ng/ml for 72 hrs, (1×10^6 cell/ml) were stimulated with the indicated concentration (0, 1, 10, 100 and 1000 ng/ml) of *E.coli* LPS for 4 hrs. TNF- α concentration in the cell-free culture supernatant was determined by ELISA. Values represent the mean \pm SD from three experiments.

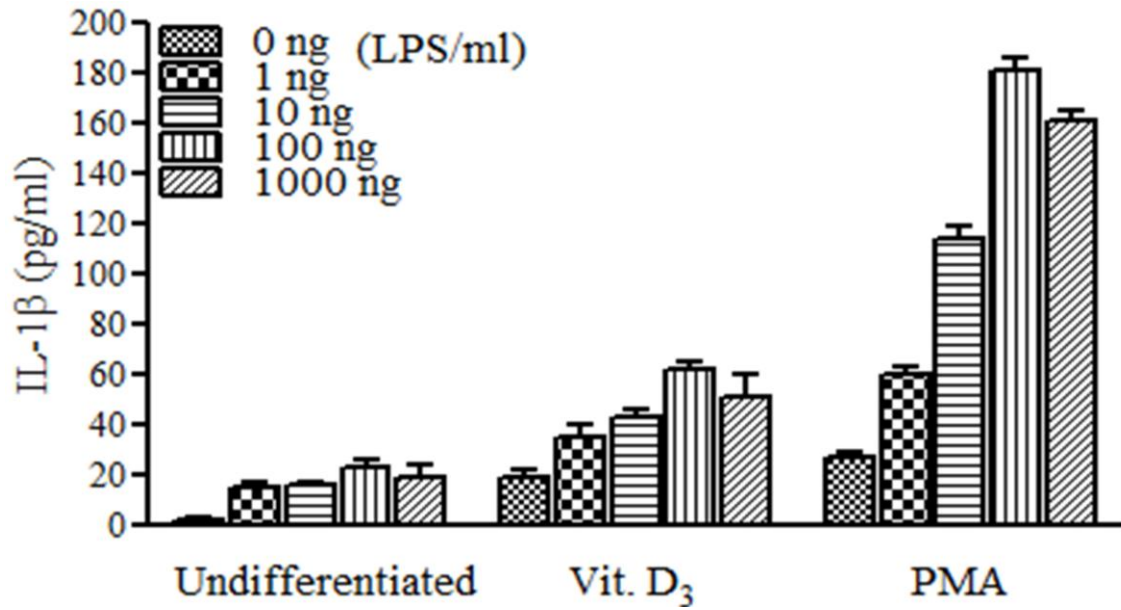


Figure 4-2: The IL-1 β - α secretion by undifferentiated cells, vit.D₃ and PMA differentiated THP-1 cells in response to LPS. Untreated THP-1 cells, THP-1 cells differentiated with vit.D₃ 100 nM for 72 hrs THP-1 cells differentiated with PMA 5 ng/ml for 72 hrs, (1×10^6 cell/ml) were stimulated with the indicated concentration (0, 1, 10, 100 and 1000 ng/ml) of *E.coli* LPS for 4 hrs. IL-1 β concentration in the cell-free culture supernatant was determined by ELISA. Values represent the mean \pm SD from three experiments.

4.3.2 The effect of PJ-34 on TNF- α and IL-1 β production by THP-1 and PD/THP-1 cells after LPS exposure.

In response to different stimuli PARP-1 is an enzyme in eukaryotic cells activated as a result of DNA damage and results in the release of transcription factors specific for the stimulant. LPS causes DNA damage and releases transcription factors for many cytokines such as TNF- α , IL-1 β and many others. In this set of experiments the effect of a potent PARP inhibitor (PJ-34) was investigated regarding activation of PARP upon DNA damage in response to LPS. This effect was measured over time incubation with LPS 100 ng/ml. Based on the literature the highest concentration of TNF- α release after 4 hrs exposure to LPS.

Figure 4.3 and Fig 4.4 show the level of TNF- α produced by THP-1 cells and PD/THP-1 cells, which were treated with or without 10 μ M PJ-34 for 30 mins prior to stimulation with 100 ng/ml LPS. TNF- α released by both cell lines in response to LPS was observed to increase with increasing incubation time. THP-1 cells produced very little TNF- α , roughly 5 pg/ml compared to cells differentiated with PMA, which produced about 50 pg/ml TNF- α (Fig. 4.4). Treatment of PD/THP-1 cells with PJ-34 had no significant effect; it reached a peak of ~18.49 pg/ml. In contrast, in PD/THP-1 cells TNF- α production was lowered by 33% and reached a peak of 400 pg/ml (Fig. 4.3 & Fig. 4.4)

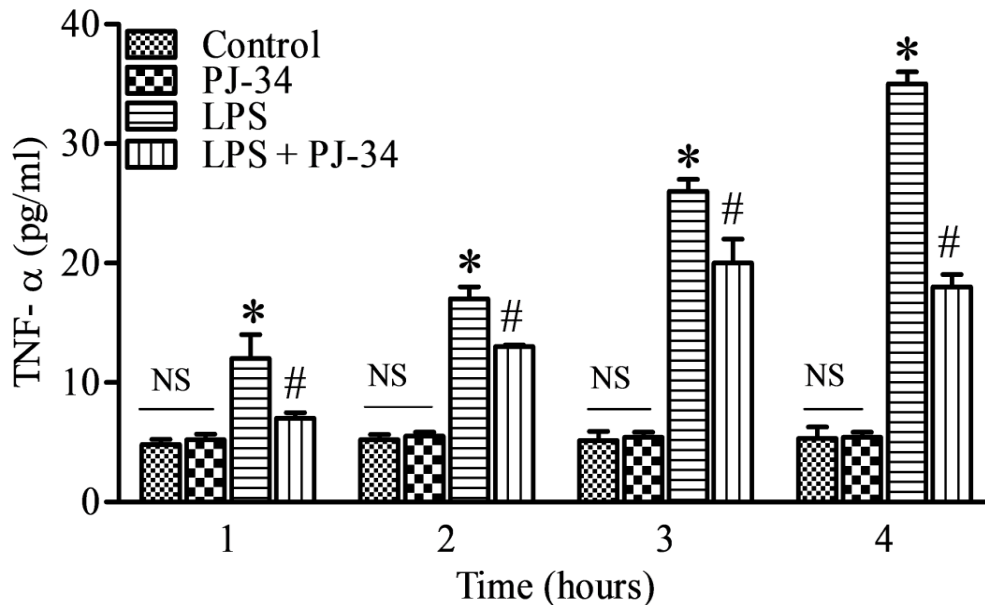


Figure 4-3: The effect of PJ-34 on TNF- α secretion by undifferentiated THP-1 cells in response to *E. coli* LPS. Undifferentiated THP-1 cells (1×10^6 cell/ml) were stimulated with LPS 100 ng/ml in presence and absence of 10 μ M of PJ34 for 30 mins for the indicated times. Supernatant was collected for TNF- α analysed by ELISA at the indicated time intervals. Data were analysed statically by two way analysis variance (ANOVA). (NS) non-significant difference, (*) Significant difference of cell treated with LPS V control, whereas (#) significant difference $p < 0.05$ cells treated with PJ-34 and LPS V cells treated with LPS. Values represent the mean \pm SD from three experiments.

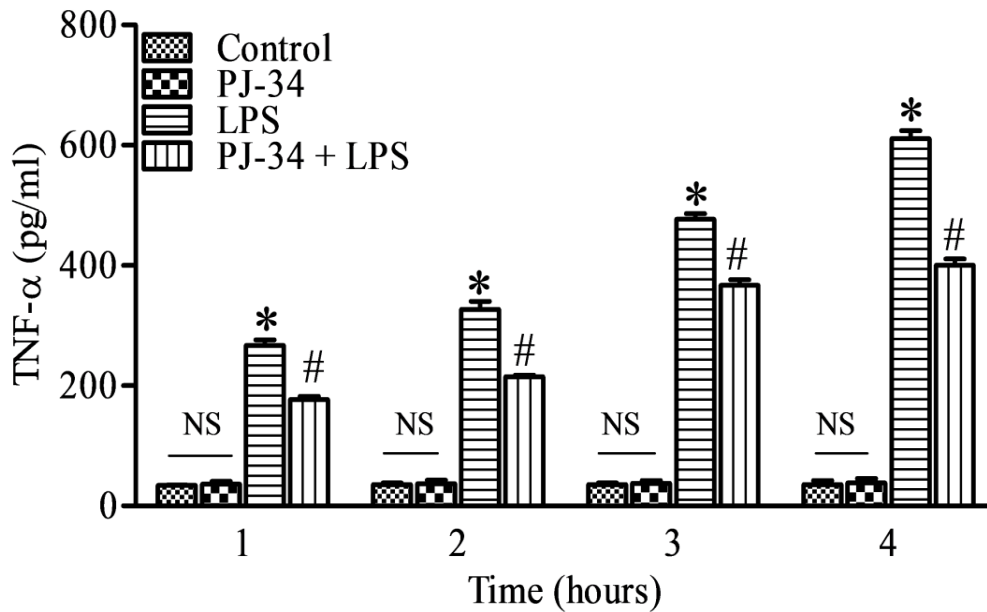


Figure 4-4: The effect of PJ-34 on TNF- α secretion by PMA-differentiated THP-1 cells in response to *E. coli* LPS. PMA-differentiated THP-1 cells (1×10^6 cell/ml) were stimulated with LPS 100 ng/ml in presence and absence of 10 μ M of PJ34 for 30 mins for the indicated times, Supernatant was collected for TNF- α analysed by ELISA at the indicated times. Data were analysed statically by two way analysis variance (ANOVA). (NS) non-significant difference, (*) Significant difference of cell treated with LPS V control, whereas (#) significant difference $p < 0.05$ cells treated with PJ-34 and LPS V cells treated with LPS. Values represent the mean \pm SD from three experiments.

Figures 4.5 & fig. 4.6, shows the cells treated with 10 μ M PJ-34 reduced the amount of IL-1 β produced by the both undifferentiated and PD/THP-1 cells in response to 100 ng/ml LPS. Figures 4.5 and 4.6 show that 10 μ M PJ34 had no effect on the amount of IL-1 β produced by both types of cells after LPS exposure, compared to non-treated cells. Production of IL-1 β increased significantly over the time incubation ($P < 0.05$) in response to 100 ng/ml LPS in both types of cells compared to non-treated cells. The highest amount of IL-1 β produced by THP-1 cells after 4 hrs of LPS stimulation was about 21.97 pg/ml (Fig. 4.5). Whereas the PD/THP-1 cells produced amount of IL-1 β reached the peaked of 181.93 pg/ml (Fig. 4.6).

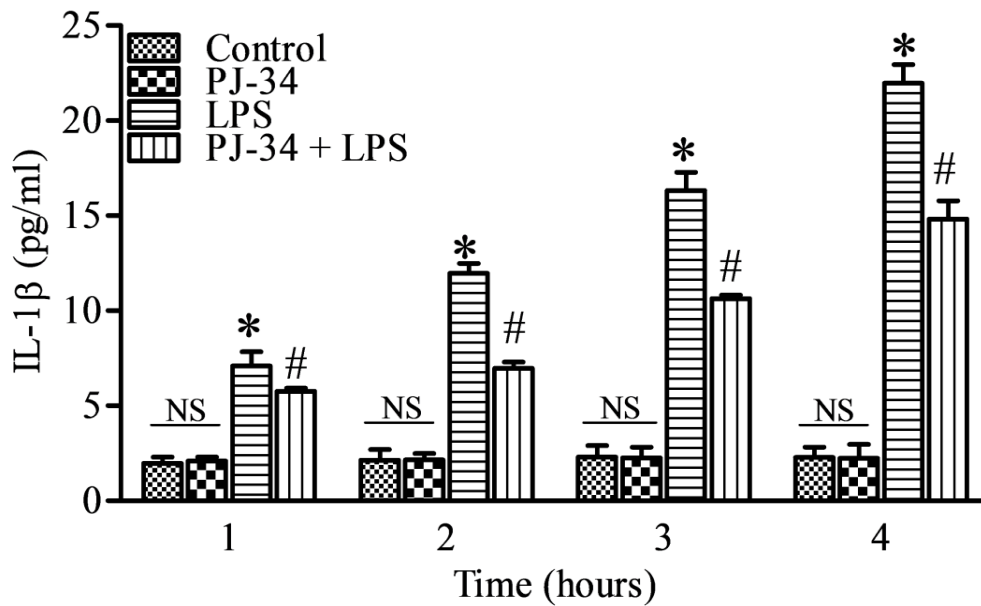


Figure 4-5: The effect of PJ-34 on IL-1 β secretion by undifferentiated THP-1 cells in response to *E. coli* LPS. Undifferentiated THP-1 cells (1×10^6 cell/ml) were stimulated with 100 ng/ml of LPS in presence and absence of 10 μ M of PJ34 for 30 minutes for the indicated times, supernatant was collected for IL-1 β analysis by ELISA at the times intervals shown. Data were analysed statically by two way analysis variance (ANOVA). (NS) non-significant difference, (*) Significant difference of cell treated with LPS V control, whereas (#) significant difference $p < 0.05$ cells treated with PJ-34 and LPS V cells treated with LPS. Values represent the mean \pm SD from three experiments

While, cells treated with 10 μ M of PJ-34 30 mins prior to LPS stimulation shows a significant reduction in the amount of IL-1 β produced ($p < 0.05$). Production of IL-1 β in native THP-1 cells was reduced by 33%, reaching 18.49 pg/ml (Fig. 4.5). PD/THP-1 cells produced only 127.85 pg/ml IL-1 β (Fig. 4.6).

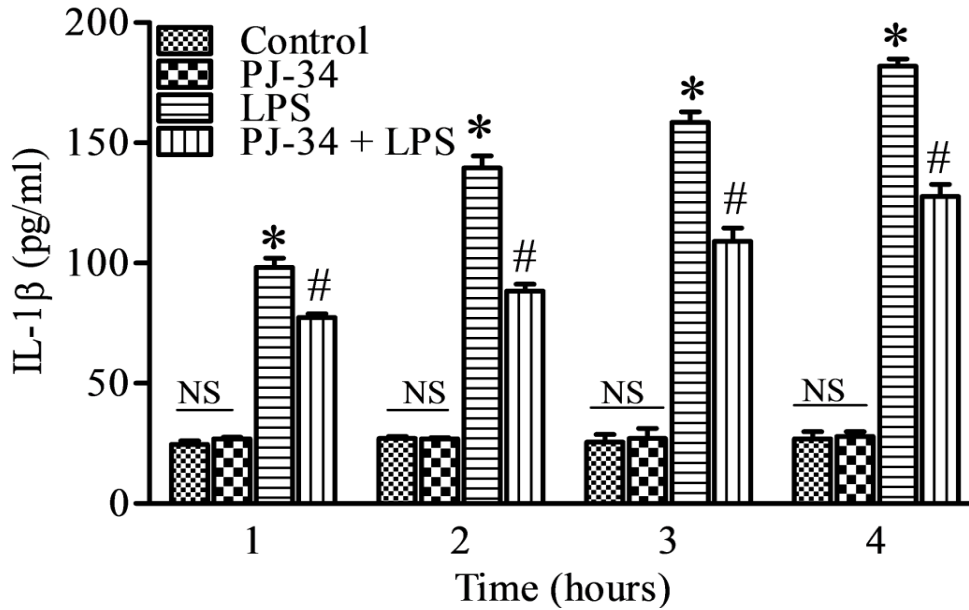


Figure 4-6: The effect of PJ-34 on IL-1 β secretion by PMA-differentiated THP-1 cells in response to *E. coli* LPS. PMA-differentiated THP-1 cells (1×10^6 cell/ml) were stimulated with 100 ng/ml LPS in presence and absence of 10 μ M of PJ34 for 30 mins for the indicated times, supernatant was collected for IL-1 β analysis by ELISA at the time intervals shown. Data were analysed statically by two way analysis variance (ANOVA). (NS) non-significant difference, (*) Significant difference of cell treated with LPS V control, whereas (#) significant difference $p < 0.05$ cells treated with PJ-34 and LPS V cells treated with LPS. Values represent the mean \pm SD from three experiments.

4.3.3 The role of CD14, TLR2, TLR4 and MARCO in the production of TNF- α and IL-1 β by PD/THP-1 cells in response to LPS

Differentiated THP-1 cells with PMA produced higher level of proinflammatory cytokine TNF- α and IL-1 β in response LPS compared with undifferentiated and vit.D₃ differentiated THP-1 cells (Fig. 4.1 and 4.2). This experiment was carried out to investigate the role of LPS receptors and the effect of PJ-34 on the production of TNF- α PD/THP-1 cells. Monocytes and macrophages express CD14, toll-like (TLRs) (Chávez-Sánchez et al., 2010) and MARCO (Gordon & Taylor, 2005) on the cell surface. CD14

has been proposed as the first host pattern recognition receptor involved in the recognition of most bacterial components (Triantafilou & Triantafilou, 2002) and facilitates the expression of inflammatory molecules via activation of the TLRs (Levy et al., 2009). Based on the inhibitory effect of antibodies to CD14, TLR2, TLR4 and MARCO on TNF- α and IL-1 β production in monocytes/macrophages, we suppose that these molecules are all important in the signal chain induced by LPS. It was found that levels of TNF- α secreted by PD/THP-1 cells increased over the times in response to LPS (100 ng/ml) and reached peak of ~ 611 pg/ml after 4 hrs LPS stimulation compared to untreated cells (Fig 4.7 & 4.8). Cells incubated with anti-human CD14(26ic) , TLR4(HTA 125) and TLR2 (TLR2.1) antibodies for 30 mins prior to stimulate with LPS, however, showed a reduced TNF- α production in response to LPS (Fig. 4.7).

Incubation of cells with anti-CD14 antibody minimized TNF- α secretion, although it slightly increased over the course of incubation, reaching ~180 pg/ml at 4 hrs of LPS stimulation (Fig. 4.7). While, more TNF- α was secreted after incubation of LPS-stimulated cells with anti-TLR4 and TLR2 antibodies. During the incubation period, anti-TLR2 contributed to a greater level of TNF- α production than anti-TLR4; where TNF- α levels reached ~ 440 and ~380 pg/ml respectively (Fig. 4.7).

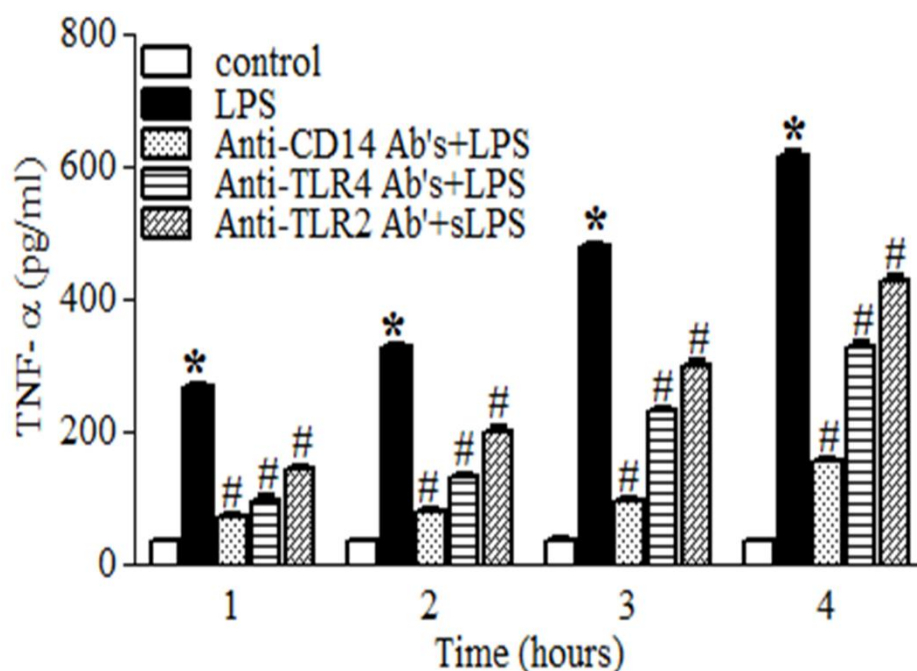


Figure 4-7: The TNF- α secretion by PMA-differentiated THP-1 cell in response to *E. coli* LPS.

THP-1 cells differentiated with PMA 5 ng/ml for 72 hrs were incubated with 10 μ g anti-human CD14, TLR4 and TLR2 monoclonal antibody for 30 mins prior to stimulation with LPS 100 ng/ml for 4 hrs. Supernatants of samples were collected hourly by centrifugation. The cell culture supernatant was transferred to a clean Eppendorf tube and kept in -80⁰C. The TNF- α level in culture supernatant was determined by ELISA. Data were analysed statically by two way analysis variance (ANOVA). (NS) non-significant difference, (*) Significant difference of cell treated with LPS V control, whereas (#) significant difference $p < 0.05$ cells treated with PJ-34 and LPS V cells treated with LPS. Values represent the mean \pm SD from three experiments.

Figure 4.8 shows that treatment of LPS-stimulated PD/THP-1 cells with anti-human MARCO antibody (PLK1) and PJ-34 significantly ($p < 0.05$) reduced the TNF- α levels over the incubation period, which reached ~ 460 and ~ 400 pg/ml, respectively. TNF- α level, in response to LPS, steadily increased over time, anti-MARCO antibody had little effect. In contrast, cells treated with PJ-34 showed steady reduction of TNF- α over the incubation period (Fig. 4.8).

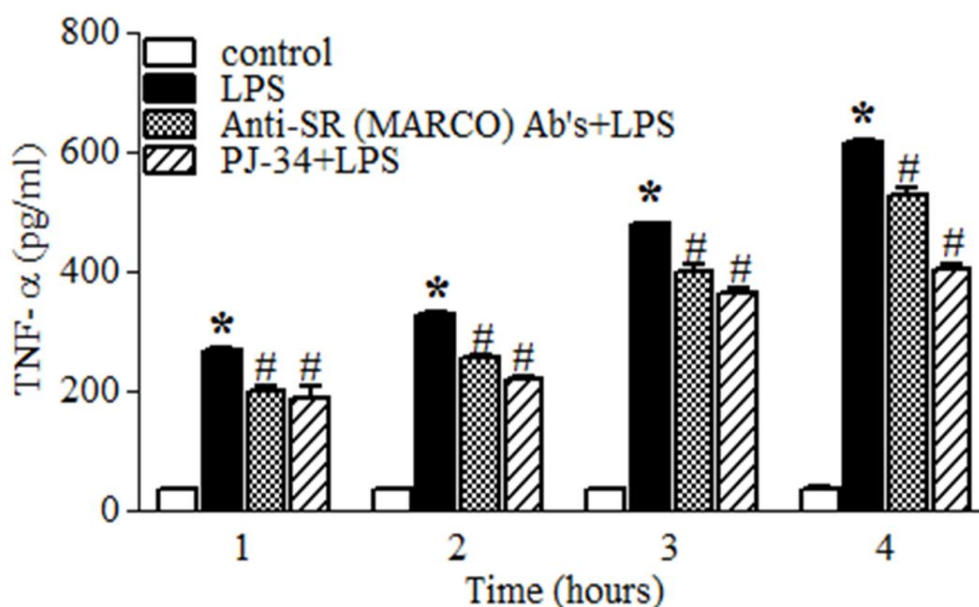


Figure 4-8: The TNF- α secretion by PMA-differentiated THP-1 cell in response to *E. coli* LPS.

THP-1 cells differentiated with PMA 5 ng/ml for 72 hrs were incubated with 10 μ g anti-human MARCO monoclonal antibody and 10 μ M PJ-34 for 30 mins prior to stimulation with LPS 100 ng/ml for 4 hrs. Supernatants of samples were collected hourly by centrifugation. The cell culture supernatant was transferred to a clean Eppendorf tube and kept in -80 $^{\circ}$ C. TNF- α level in culture supernatants was determined by ELISA. Data were analysed statically by two way analysis variance (ANOVA). (NS) non-significant difference, (*) Significant difference of cell treated with LPS V control, whereas (#) significant difference $p < 0.05$ cells treated with PJ-34 and LPS V cells treated with LPS. Values represent the mean \pm SD from three experiments.

The role of LPS receptors and the effect of PJ-34 on the production of IL-1 β by PD/THP-1 cells, following LPS treatment was analysed by ELISA (Fig. 4.9 and 4.10). LPS-stimulated THP-1 cells produced IL-1 β over time, peaking at ~181 pg/ml at 4 hrs stimulation with LPS (Fig. 4.9). In contrast, untreated cells (control) produced very little IL-1 β . Incubation of cells with anti-human CD14, TLR4 and TLR2 for 30 mins prior to stimulation with LPS cause to reduction in the amount of IL-1 β released ($p < 0.05$). This reduction was slightly increased over the incubation period. The greatest reduction of IL-1 β was observed during the first hr of incubation in THP-1 cells treated with anti-CD14

(Fig. 4.9). The IL-1 β level continued to fall, reaching ~92.1 pg/ml after 4 hrs stimulation with LPS. Cells treated with anti-TLR4 and anti-TLR2 antibodies released considerably higher levels of IL-1 β for same period of incubation with LPS compared to cells treated with anti-CD14 antibody. At 4 hours stimulation with LPS, cells treated with anti-TLR4 produced ~110 pg/ml IL-1 β . Cells incubated with anti-TLR2 the level of IL-1 β secreted peaked at ~159.5 pg/ml (Fig. 4.9).

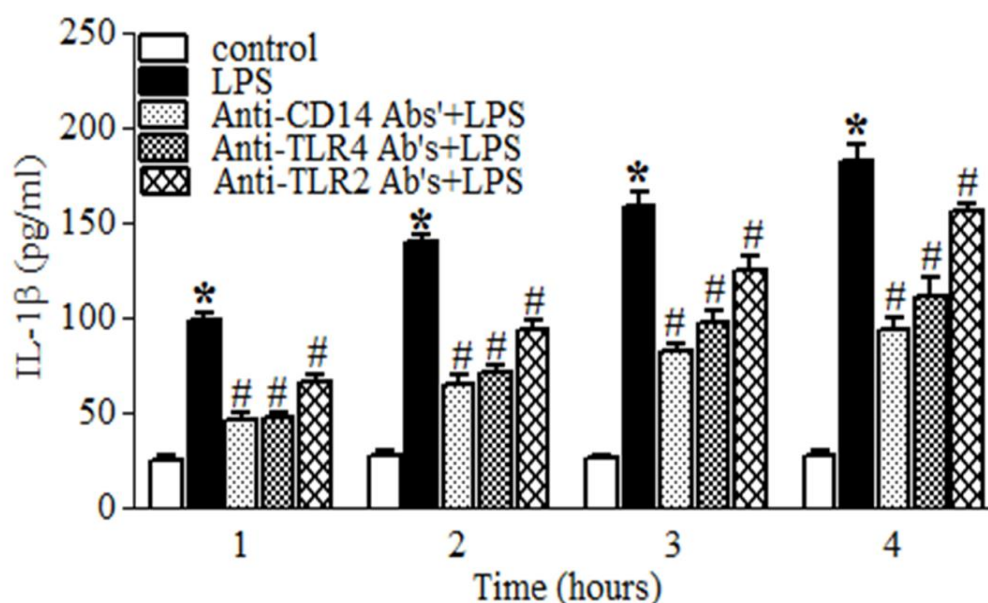


Figure 4-9: Secretion of IL-1 β by PMA-differentiated THP-1 cells in response to E. coli LPS.

THP-1 cells differentiated with PMA 5 ng/ml for 72 hours were incubated with 10 μ g anti-human CD14, TLR4, and TLR2 monoclonal antibody for 30 mins prior to stimulation with LPS 100 ng/ml for 4 hrs. Supernatants of samples were collected hourly by centrifugation. The cell culture supernatant was transferred to a clean Eppendorf tube and kept in -80 $^{\circ}$ C. The IL-1 β level in culture supernatants was determined by ELISA. Data were analysed statically by two way analysis variance (ANOVA). (NS) non-significant difference, (*) Significant difference of cell treated with LPS V control, whereas (#) significant difference p<0.05 cells treated with PJ-34 and LPS V cells treated with LPS. Values represent the mean \pm SD from three experiments.

When the cells were incubated with anti-MARCO antibody and PJ-34 a significant reduction of IL-1 β was observed, in response to LPS, at 4 hours. The level of IL-1 β reached was ~174.2 pg/ml and ~140.3 pg/ml, respectively, after anti-MARCO and PJ-34 treatment. Anti-MARCO antibody invoked little protection effect, in respect of limiting IL-1 β production in response to LPS, compared to anti-CD14, TLR4 and TLR2, and effect of this antibody declined over the time. PJ-34 increased the reduction of IL-1 β secretion over incubation time.

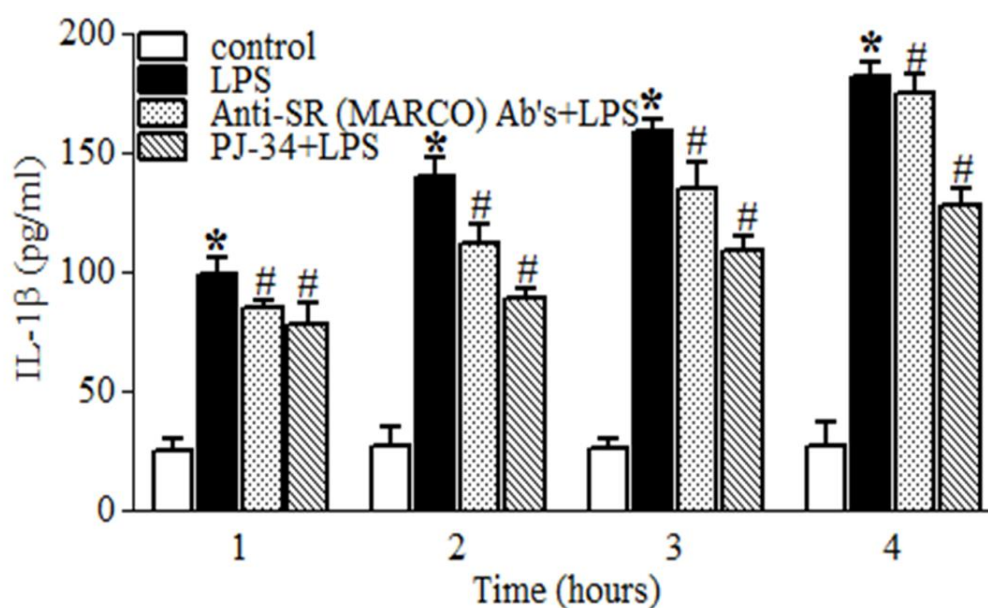


Figure 4-10: Secretion of IL-1 β by PMA-differentiated THP-1 cells in response to *E.coli* LPS.

PMA-differentiated THP-1 cells, treated with 5 ng/ml for 72 hrs, were incubated with 10 μ g anti-human SR (MARCO) monoclonal antibody and 10 μ M PJ-34 for 30 mins prior to stimulate with 100 ng/ml LPS for 4 hrs. Supernatants of samples were collected hourly by centrifugation. The cell culture supernatant was transferred to a clean Eppendorf tube and kept in -80 $^{\circ}$ C. The IL-1 β level in culture supernatant was determined by ELISA. Data were analysed statically by two way analysis variance (ANOVA). (NS) non-significant difference, (*) Significant difference of cell treated with LPS V control, whereas (#) significant difference p<0.05 cells treated with PJ-34 and LPS V cells treated with LPS. Values represent the mean \pm SD from three experiments.

4.3.4 The effect of PJ-34 and activation of NF- κ B and JNK on TNF- α and IL-1 β secretion by PD/THP-1 cells after LPS stimulation

NF- κ B has long been considered a prototypical proinflammatory signaling pathway, largely based on the activation of NF- κ B by proinflammatory cytokines such TNF- α and IL-1 β . CD14 recognize and bind to LPS then bind to TLRs and form LPS/CD14/TLRs complex. This complex trigger LPS signaling into cytoplasm and activate transcription factors such as NF- κ B (Uematsu & Akira, 2008) and MAPK signalling pathway(Guha & Mackman, 2001; Kim & Kim, 2014). Activation of NF- κ B by LPS signaling required TLRs such TLR2,4, result in activation of I κ B and free NF- κ B translocate into nucleus and cause DNA damage and subsequently activation of PARP-1, and release transcription factor gene of many proinflammatory cytokines (e.g. TNF- α and IL-1 β). Activation of c-Jun N-terminal kinase (JNK) member of MAPK family, mediate downstream signalling events leading to the activation of AP-1 and NF- κ B, which results in induction of a range of inflammatory cytokines (Guha & Mackman, 2001; Kim & Kim, 2014). Therefore, inhibition of the activation of MAPKs, Akt, NF- κ B and AP-1 may have potential therapeutic applications (Park et al., 2011). In this study induce inhibition of the NF- κ B transcription factor and JNK signal pathways in the production of TNF- α and IL-1 β , and the effect of PJ-34 in activating these pathways in response to LPS. PD/THP-1 cells were stimulated with LPS (100 ng/ml) for 4 hours in presence and absence of 10 μ g of anti- human NF- κ B antibody (poly 6226) and anti-human JNK antibody (poly 6331), or 10 μ M of PJ3-4. The levels of TNF- α and IL-1 β were determined with ELISA.

TNF- α level in LPS-stimulated PD/THP-1 cells increased over the incubation period compared to untreated cells (Fig. 4.11).Whereas, the cells treated with anti-human JNK anti-NF- κ B or PJ-34 prior to LPS stimulation displayed a reduction in the amount of TNF- α released over the incubation time. PD/THP-1 cells treated with anti-NF- κ B

showed a pronounced reduction in the level of TNF- α in response to LPS (85%) and roughly reaching 91.2 pg/ml at 4 hours of stimulation. Anti-JNK antibody had less effect and the cells displayed high levels of TNF- α compared to cells incubated with anti-NF- κ B antibody or the cells incubated with PJ-34. The level of TNF- α reached ~590.3 pg/ml at 4 hours of stimulation, but the amount produced by the cells treated with PJ-34 reached peak ~ 411.7 pg/ml at the same time (Fig.4.11).

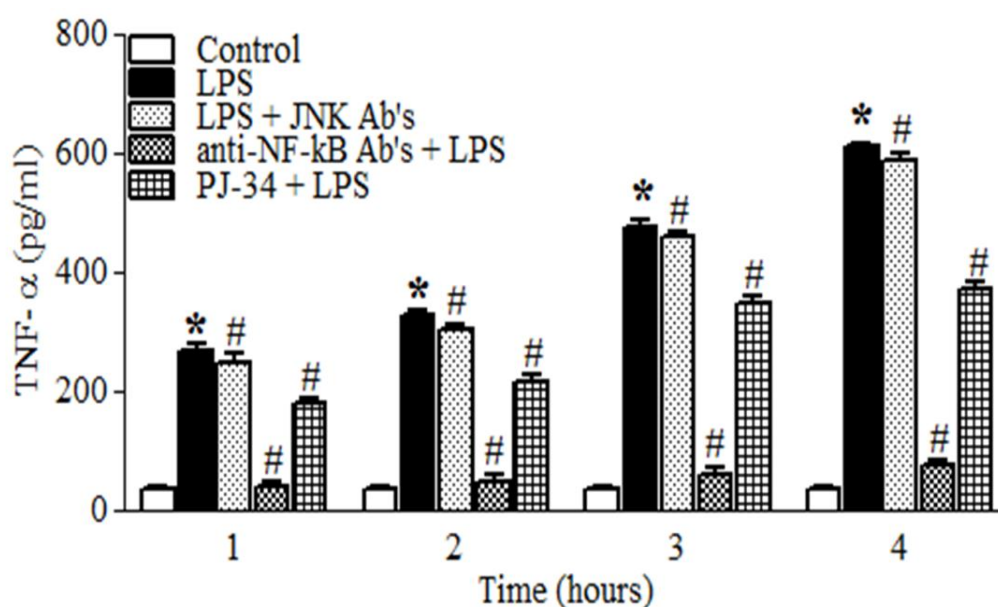


Figure4-11: The TNF- α production by PMA-differentiated THP-1 cells in response to *E. coli* LPS.

THP-1 cells differentiated with PMA 5 ng/ml for 72 hrs, were incubated with 10 μ g anti-human NF- κ B , anti-JNK monoclonal antibody or 10 μ M PJ-34 for 30 mins prior to stimulation with LPS 100 ng/ml for 4 hrs. Supernatants of samples were collected hourly by centrifugation. The cell culture supernatant was transferred to a clean Eppendorf tube and kept in -80 $^{\circ}$ C. TNF- α level in culture supernatants was determined by ELISA. Data were analysed statically by two way analysis variance (ANOVA). (NS) non-significant difference, (*) Significant difference of cell treated with LPS V control, whereas (#) significant difference p<0.05 cells treated with PJ-34 and LPS V cells treated with LPS. Values represent the mean \pm SD from three experiments.

The level of IL-1 β produced by PD/THP-1 cells in response to LPS increased over the period of LPS incubation compared to untreated (control) cells (Fig. 4.12) After 4 hrs LPS stimulation, the level of IL-1 β reached ~191 pg/ml. IL-1 β levels in LPS-stimulated cells peaked at ~143 pg/ml and 115 pg/ml after treatment with anti-JNK and anti-NF- κ B antibodies, respectively (Fig. 4.12), thus showing significant reduction in the amount of IL-1 β produced. The level of IL-1 β secreted by PJ-34-treated cells was ~113 pg/ml (Fig. 4.12). The level of IL-1 β released by PD/THP-1 might relate to availability of NF- κ B and subsequently release more IL-1 β transcription factor gene and producing more IL-1 β . Differentiated cells show an increase in cell size and amount of NF- κ B in the cytoplasm.

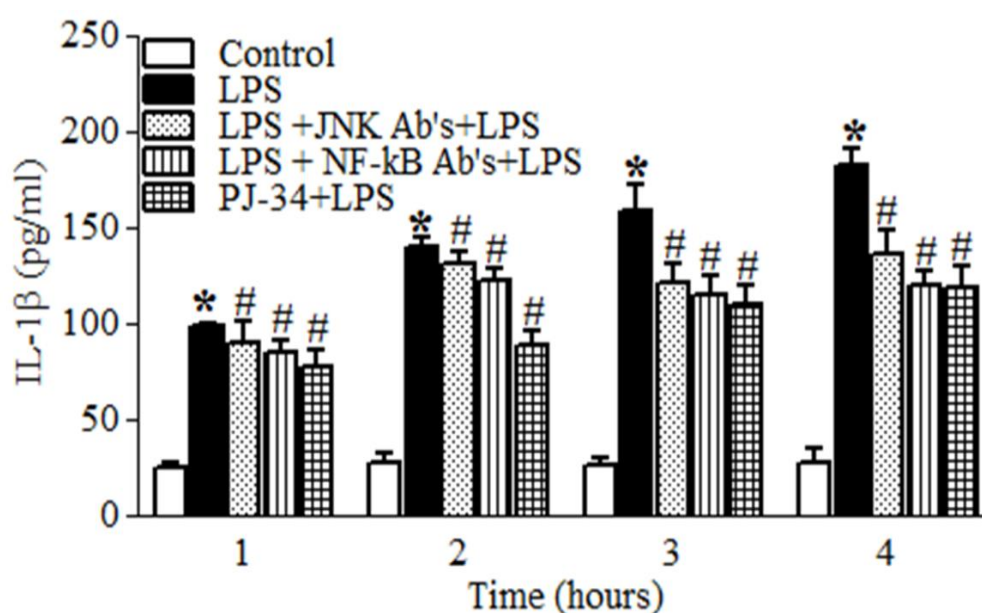


Figure 4-12: The production of IL-1 β by PMA-differentiated THP-1 cells in response to *E. coli* LPS.

THP-1 cells differentiated with PMA 5 ng/ml for 72 hrs, were incubated with 10 μ g anti-human NF- κ B, anti-JNK monoclonal antibody or 10 μ M PJ-34 for 30 mins prior to stimulation with 100 ng/ml LPS for 4 hrs. Sample supernatants were collected hourly by centrifugation. The cell culture supernatant was transferred to a clean Eppendorf tube and kept in -80 $^{\circ}$ C. IL-1 β levels in culture supernatants were determined by ELISA. Data were analysed statically by two way analysis variance (ANOVA). (NS) non-significant difference, (*) Significant difference of cell treated with LPS V control, whereas (#) significant difference p<0.05 cells treated with PJ-34 and LPS V cells treated with LPS. Values represent the mean \pm SD from three experiments.

4.3.5 Role of PJ-34 in NF- κ B and JNK activation in response to LPS

The effect of PJ-34 on NF- κ B and JNK activation (phosphorylation) in THP-1 and PD/THP-1 cells in response to LPS (100 ng/ml) was assessed by Western blotting (Figs 4.13 and 4.14). NF- κ B was detected by loading 15 μ g of cytoplasmic cell lysate, while JNK was detected in whole cell lysate. Proteins were separated by SDS-PAGE and then blotted on a PDVF membrane, which was probed with either primary polyclonal rabbit anti-human NF- κ B antibody or polyclonal rabbit anti-human JNK antibody and then the membrane were incubated with primary mouse anti-human α -tubulin (control). For detection of NF- κ B and JNK, membranes were incubated with secondary antibody IRDye® 700 CW PE donkey anti-rabbit antibody (Red). While, α -tubulin detected with IRDye® 800 CW FITC goat anti-mouse antibody (Green). Then the membrane was scanned on a LI-COR scanner using odyssey software.

Figure 4.13 shows the activation of NF- κ B in THP-1 and PD/THP-1 cells in response to LPS in the presence and absence of PJ-34. NF- κ B activation was detected by the presence of the bands at a molecular weight of 70 kDa. Differences of band intensity correlate roughly with the amount of expression of NF- κ B. Cells treated with PJ-34 only, showed no significant difference in the level of NF- κ B expressed in the cell cytoplasm. However cells treated with LPS showed reduction in the expression of cytosolic NF- κ B, indicating an increase in NF- κ B activation and its translocation into the nucleus. In contrast, cells treated with PJ34 for 30 mins prior to stimulation with LPS showed increased expression of NF- κ B, indicating its reduced activation and limited translocation into the nucleus (Fig. 4.13 [A & C]). The α -tubulin was used as controls to equalize the amount of proteins were loaded on the gels. NF- κ B expression was plotted (Fig. 4.13 B & D) after normalized the band intensity of the NF- κ B with its internal α -tubulin.

Figure 4.14 shows the expression of c-Jun N-terminal kinase (JNK-1) in THP-1 cells and PD/THP-1 cells. Increase in JNK activation detected by decreased in band intensity in response to LPS. Treatment of cells with PJ34 prior to their stimulation with LPS did not affect JNK expression in response to LPS. The expression of JNK was plotted (Fig. 4.14 B and D) after normalizing the band intensity with internal α -tubulin.

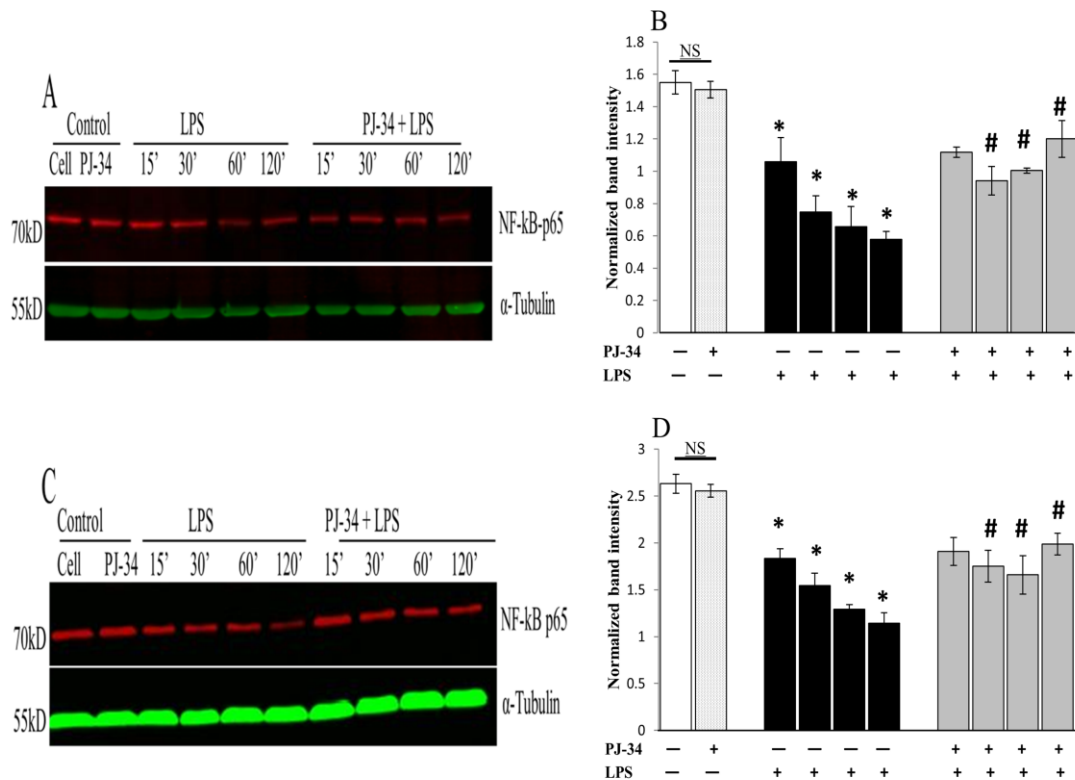


Figure 4-13: The effect of PJ-34 on the activation of NF- κ B in response to LPS. THP-1 cells, or THP-1 cells differentiated with 5ng ml PMA for 72 hrs, were left untreated or treated with 10 μ M of PJ-34 for 30 mins prior to stimulation with *E. coli* LPS (100 ng/ml) for the indicated times. Cytoplasmic extracts from the cells were separated by SDS-PAGE and then Western blotted with primary monoclonal antibody mouse anti-human α -tubulin (TU10D8) as a loading control and polyclonal rabbit-anti-human NF- κ B p65 antibody (Poly6226). The blotting membrane was then incubated with secondary antibody IRDye® 800CW goat anti-mouse IgG or IRDye® 700CW donkey anti-rabbit. Finally the membrane was scanned using a Li-COR infrared image scanner using odyssey software. [A & C] represents Western blot expression of NF- κ B and α -tubulin in THP-1 cells and PMA-differentiated THP-1 cells. [B & D] shows the level of NF- κ B expressed by the cell samples after normalized to it is relevant α tubulin band to avoid any loading error of the proteins. The percentage of was then calculated for each sample using Image Studio Lite software (LI-COR Biosciences). Data were analysed statically by two way analysis variance (ANOVA). (NS) non-significant difference, (*) Significant difference of cell treated with LPS V control, whereas (#) significant difference p<0.05 cells treated with PJ-34 and LPS V cells treated with LPS. Values represent the mean \pm SD from three experiments.

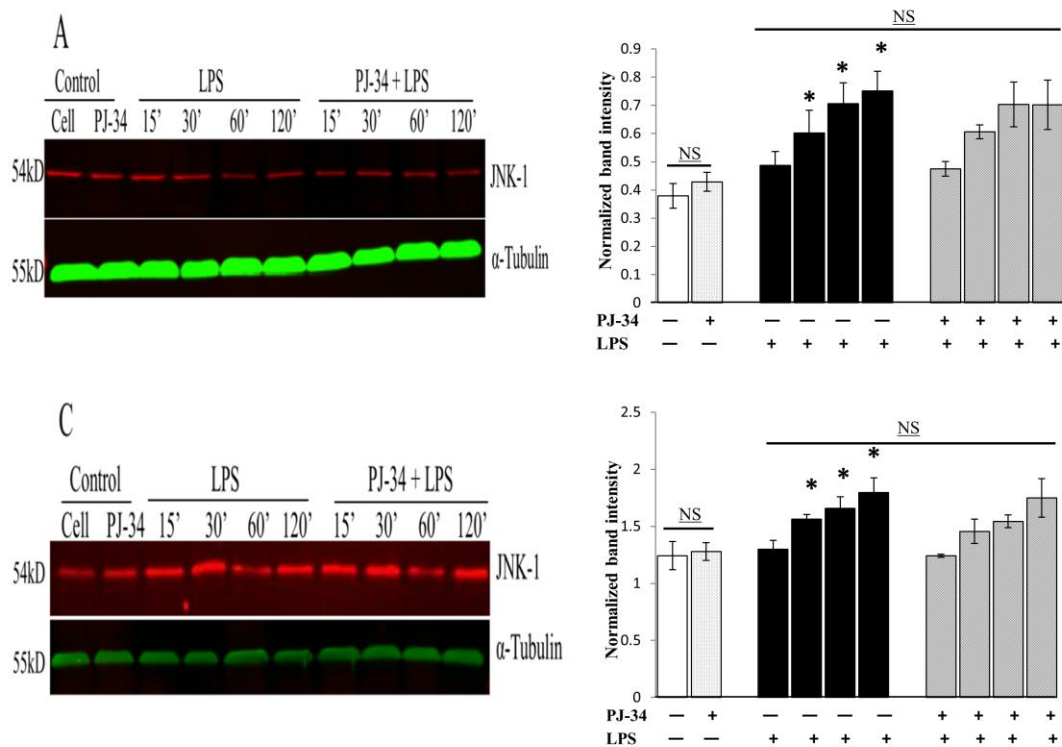


Figure4-14: The effect of PJ-34 on the activation of JNK-1 in response to LPS.

THP-1 cells or THP-1 cells differentiated with 5ng/ml PMA for 72 hrs were left untreated or treated with 10 μ M of PJ-34 for 30 mins prior to stimulation with *E. coli* LPS (100 ng/ml) for the indicated times. Cytoplasmic extracts from the cells were separated by SDS-PAGE and Western blotted with primary monoclonal antibody mouse anti-human α -tubulin (TU10D8) as a loading control and polyclonal antibody rabbit anti-human phosphorylated-JNK-1 antibody (Poly6331). The membrane was then incubated with secondary antibody IRDye® 800CW goat-anti-mouse IgG or IRDye® 700CW donkey anti-rabbit. Finally the membrane was scanned Li-COR infrared image scanner using odyssey software. [A & C] represents Western blot expression of JNK-1 and α -tubulin in THP-1 cells and PMA-differentiated THP-1 cells. [B & D] represents the levels of JNK-1 expressed by the cell samples after normalized to its relevant α -tubulin band to avoid any loading error of the proteins. The percentage was calculated for each sample using Image Studio Lite software (LI-COR Biosciences). Data were analysed statically by two way analysis variance (ANOVA). (NS) non-significant difference, (*) Significant difference of cell treated with LPS v control. The immunoblot image is a representative of three experiments.

4.3.6 The effect of PJ-34 on production of nitric oxide in response to LPS.

NO formation was investigated by measuring nitrite (NO_2^-), one of two primary, stable and nonvolatile breakdown products of NO. The Griess assay was used to measure NO_2^- . This technique relies on a diazotization reaction (Griess, 1879).

To ensure accurate nitrite quantitation, a reference curve was plotted, constructed using a nitrite standard solution. To assess NO production in untreated and PD/THP-1 cells (1×10^6) were stimulated with 100 ng/ml of LPS in the present and absence of 10 μM of PJ-34 for 6 hrs. A highest level of NO was produced by THP-1 cells in response to LPS at 6 hrs. In both native THP-1 and DP/THP-1 cells, NO concentration steadily increased over the time of incubation with LPS (Fig.4.15 A & B). PD/THP-1 cells produced a much higher concentration of NO than did native THP-1 cells. Untreated cells (control) did not produce NO. In contrast, cells incubated with 10 μM PJ-34 for 30 mins prior to LPS stimulation displayed significant reduction in NO production in both cell lines. High levels of NO produced by activated macrophages in response to LPS, represent a major cytotoxic principle of these cells (Connelly et al., 2003). In addition, higher concentrations of NO can directly interfere with the DNA damage of target cells, and excessive NO production by iNOS plays a crucial role in septic shock (Kitasato et al., 2007).

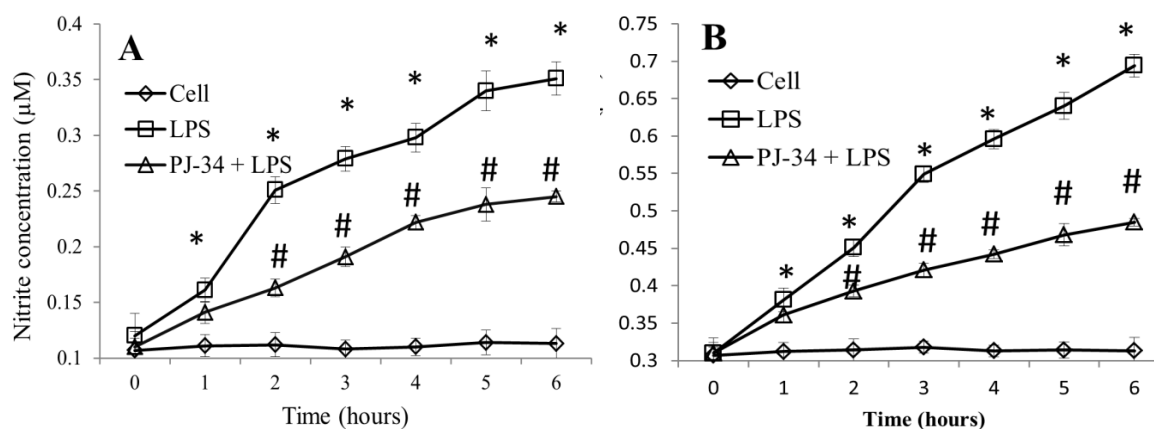


Figure 4-15: The effect of PARP inhibitor PJ-34 on NO production in THP-1 cells in response to LPS. The concentration of nitrite was calculated using a nitrite standard curve. **A:** Untreated cells and **B:** PMA-differentiated THP-1 cells (1×10^6 /ml) were stimulated with 100ng/ml of LPS in the presence and absence of 10µM PJ-34 for the times indicated. The supernatant was collected hourly by centrifugation of the cell culture and the supernatant was kept at -80°C until used. Data were analysed statically by two way analysis variance (ANOVA). (*) Significant difference of untreated cells V cells treated with LPS, whereas (#) significant difference $p < 0.05$ cells treated with PJ-34 and LPS V cells treated with LPS

4.4 Conclusion

Differentiated macrophages are the resident tissue phagocytes and patrol cells of the innate immune response. PMA and vit.D₃ are stimuli commonly used to induce macrophage differentiation in THP-1 cell line. The phenotype of the THP-1 cell line after differentiation utilising Vit.D₃ and PMA compared undifferentiated THP-1 cells, both stimuli induced changes in cell morphology indicative of differentiation. Activation of vit.D₃ or PMA differentiated THP-1 cells was induced by treating these cells with LPS for 4 hrs which resulted in production of high level of TNF- α and IL-1 β by the cells. While, undifferentiated THP-1 cells produced less amount of TNF- α and IL-1 β compared to differentiated THP-1 cells. The level of TNF- α produced by undifferentiated and vit.D₃ or PMA differentiated THP-1 cells was much higher than IL-1 β for the same incubation. The level TNF- α and IL-1 β produced by PD/THP-1 was much higher than vit.D₃

differentiated cells, therefore vit.D₃ differentiated cells were not investigated all experiment. The production of TNF- α and IL-1 β in both undifferentiated and PD/THP-1 cells with 100 ng/ml LPS were increased significantly over the incubation time. Whereas, incubation of cells with 10 μ M PJ-34 prior to stimulate with LPS shows a significant decrease in TNF- α and IL-1 β production in both groups of cells. Monocytes/macrophages express different LPS receptors served a variety role toward effecting TNF- α and IL-1 β production in response to LPS in undifferentiated and PD/THP-1 cells. In this study a significant reduction of TNF- α and IL-1 β production was observed in cells incubated with anti-CD14, anti-TLR4 and anti-TLR2 antibodies prior to LPS stimulation in compare with that stimulated with LPS alone. This finding is consistent with previous study which has shown that CD14 is LPS receptor, which it lacks a cytoplasmic domain and does not participate directly in LPS signalling(Gangloff et al., 2005). TLRs have recently been shown to be important components of the CD14/LPS signaling. TLR2 and TLR4 have been shown to contribute to the LPS response (Chowdhury et al., 2006). CD14/LPS/TLRs complex induce LPS signaling which results in NF- κ B activation and translocation into the nucleus. Activated NF- κ B bind DNA and subsequently activate PARP-1 and then release transcription factors gene of TNF- α and IL-1 β . Also our results show that incubation PD/THP-1 cells with anti-TLR2 and anti-TLR4 impaired NF- κ B activation which is required for LPS signaling. MARCO is another receptor which is needed for LPS-induced inflammatory responses in macrophages (Yu et al., 2012). MARCO bind to LPS and its association with TLR4 increase macrophages response to LPS. Incubated cells with anti-MARCO had less effect on TNF- α and IL-1 β production because of the NF- κ B activation-LPS signalling is not impaired by blocking MARCO receptor, this was thought to be due and LPS signaling activated NF- κ B via other LPS receptors. The effects of all antibodies declined over the time of incubation. In contrast, the cells that treated

with PJ-34 showed increased reduction of TNF- α of IL-1 β after LPS treatment. Activation of NF- κ B by LPS signals release of NO production which contributes to immune system controlling bacterial infection. Over production of NO it's harmful and might cause cell dysfunction. A significant reduction of NO production was observed in undifferentiated and PD/THP-1 cells in response to LPS and its effect intensified with increasing incubation time.

The role of LPS in activation of NF- κ B and JNK signalling pathway of TNF- α and IL-1 β production were examined. Incubation of undifferentiated and PD/THP-1 cells with anti-NF- κ B antibody, prior to exposure to LPS, significantly reduced TNF- α and IL-1 β production, while anti-JNK-1 antibody was less effective than anti-NF- κ B in reducing production of these cytokines. The effectiveness of the antibodies slightly reduced over the time of incubation. In contrast, cells treated with PJ-34 showed increased TNF- α and IL-1 β secretion in response to LPS over time incubation period. These results reveal that activation of NF- κ B is more essential for TNF- α and IL-1 β production in response to LPS than the JNK-1 pathway. The Western blot results show that PJ-34 had a significant role in prolonging NF- κ B activation in response to LPS, but it had very little effect on JNK-1 activation in response to LPS.

**CHAPTER 5: The role of CD14 and MARCO receptors in response to
LPS**

5.1 Introduction

The Mammalian innate immune system relies on numbers of receptors molecules known as pathogen recognition receptors (PRPs) which have ability to recognize specific molecules expressed by the invaded microorganism known as pathogen-associated molecules patterns (PAMPs) and directly activate array of anti-microbial immune responses via induction of various proinflammatory cytokines, chemokines. These immune responses also play a vital role for initiate long term adaptive immunity through B, T lymphocytes cells. These receptors in addition to CD14 the main receptor for invaded microbial molecules include toll like receptors family (TLRs) (Uematsu & Akira, 2008; Kumar et al., 2011).

Septic shock, and inflammatory response syndrome remain one of the main reason causes of death in intensive care units, for example in united states there is more than 750,000 patients admitted to intensive care unit annually and resulting in 215,000 deaths(Angus et al., 2001) . Lipopolysaccharide (LPS) the major component of outer membrane of gram negative bacteria, is play a critical role in inducing sepsis during infection with gram negative bacteria. When it reach blood stream will recognised and bind to LPS receptors expressed on monocytes and macrophages and slightly less on other type of cells mainly CD14 (Schaaf et al., 2009; Thorgersen et al., 2013), CD14 is upregulated by exposure to LPS in both in *vivo* and in *vitro* (Landmann et al., 1996; Thorgersen et al., 2013). The mechanism by which LPS induce septic shock relies on its ability to bind to CD14 and initiate a signal transduction pathway, since CD14 it lacks a transmembrane domain; therefore it is incapable to trigger a signal downstream into the cytoplasm. It believed that LPS bind CD14 signal cascade initiate via TLR4 and resulting in activation of NF- κ B , subsequently release transcriptional factor gene of many proinflammatory cytokines

(Schaaf et al., 2009). LPS internalization by CD14 is dependent on the physical state in which LPS presented to the cell (Kitchens & Munford, 1998).

MARCO is expressed by monocytes/macrophages and dendritic cells and certain endothelial cells. It is well known that SRs involved in lipid metabolism and bind modified low-density lipoproteins, and they play a vital role in uptake and clearance of modified host molecules and apoptotic cells. In addition they recognise bind and internalising products of gram positive bacteria such as lipoteichoic acid, lipopolysaccharide product of Gram-negative bacteria and initiate an immune response which result in secretion of proinflammatory cytokines such as TNF- α and IL-1, implicated in pathogenesis of sepsis and alter the expression and morphology of the cells (El Khoury et al., 1996; Peiser et al., 2002; Canton et al., 2013). Studies show in a murine model of pneumococcal pneumonia, MARCO^{-/-} mice displayed an impaired ability to clear bacteria from the lungs, increased pulmonary inflammation and cytokine release, and diminished survival. In vitro binding of *Streptococcus pneumoniae* and in vivo uptake of unopsonized particles by MARCO^{-/-} AMs were dramatically impaired, indicating an important role of MARCO in mounting an efficient and appropriately regulated innate immune response against pathogens (Arredouani et al., 2006; Goh et al., 2010; Uza et al., 2011)

In this chapter PMA-differentiated THP-1 cells was used to investigate the relation between CD14 and SR MARCO and possible role of PARP inhibitor PJ-34 in the membranous and gene expression of these receptors and LPS up-take by MARCO in response to LPS.

5.2 Methods

5.2.1 Flow cytometry

The level expression of CD14 and SR MARCO were assessed on PMA-differentiated THP-1 cell in presence and absence of 10 μ M PJ-34 in response to LPS. Briefly, 25×10^4 cells treated with or without PJ-34 for 30 minutes prior to stimulate with LPS for 6 hours. Cells were prepared for flow cytometry assay as described in section 2.2.3.1 and samples were read with flow cytometry Accuri 6 and the results were analysed with flow-jo software.

5.2.2 Colocalisation

5.2.2.1 Immunofluorescence staining

Un-differentiated THP-1 cells or THP-1 cells differentiated in the Lab-Tek chamber slides (Nunc) with PMA (5 ng/ml) for 72 hrs and monolayer cells were incubated with or without PARP inhibitor PJ-34 10 μ M for 30 mins prior to stimulate with 100 ng/ml LPS (Sigma Aldrich, UK) for 2 hours. Untreated cells (control cells) left to grow in culture media only. Cells were immunofluorescently stained as previously described in section 2.2.4.3.

5.2.2.2 Confocal microscopy

Cells which stained with immunofluorescent probes were imaged at single cell level for colocalisation studies as described in section 2.2.5.2.

5.2.2.3 Colocalisation analysis and visuatisation

Comprehensive technique for colocalisation analysis and visualisation of data results already mentioned in section 2.2.5.3 & 2.2.5.4.

5.2.3 Real time PCR (qRT-PCR)

Differentiated THP-1 cells with 5 ng/ml PMA for 72 hours were cultured on glass culture plate until confluent (10^7 - 10^8 cells/plate), treated with 100 ng/ml of LPS in presence and absence of 10 μ M PJ-34 for 15 mins, 30 mins, 1 hr, 2 hrs, 3 hrs and 4 hrs. Afterward the RNA was extracted with TRI reagent see section 2.2.8.2 and cDNA for sample conditions were prepared as described in section 2.2.8.3. PCR primer pairs for CD14, MARCO and cyclophilin were designed with pearl primer software to span intron-exon splice sites to avoid amplification of any genomic DNA. To amplify each gene of CD14 and SR MARCO, cyclophilin was used as house-keeping gene. The qRT-PCR reaction (20 μ l) per sample was prepared as following; Master mix SYBR green 10 μ l, sterile double distilled water 7.4 μ l, 1.6 μ l from mixed primers of forward and reverse each at concentration of (5 μ M), cDNA 1 μ l were aliquot in 96 well PCR well plate in triplicate and qRT-PCR plate sealed with an qRT-PCR film seal and the plate spun briefly to insure that the liquid placed in the bottom of the wells and then the plate was placed on the qRT-PCR machine (CFX 96, Bio-Rad) The results were analysed with CFX manager software. Following gene sequences was designed with pearl primer software and three steps PCR condition was used, first step is denaturing at 95°C for 2 minutes then second step involve 39 cycles each cycle started at 95°C for 0.10 seconds and 60°C for 0.10 seconds and 72°C

for 0.10 seconds and then 95 for 0.10 seconds and finally melting temperature from 65°C to 95°C from 0.05-0.5 seconds plus plate read.

CD14 (F): 5'AAAGAAGCTAAAGCACTTCCAG3'

CD14(R):'CAGCGGAAATCTTCATCGTC5'

SR (MARCO) (F): 5'ATTCTGATGCCATTGTCTTCTG3'

SR (MARCO) (R):3'ACACTGAACATTATCCAGCC5'

Cyclophilin (F): 5' TGGCACAGGAGGAAAGAGCATC3'

Cyclophilin (R):3' AAAGGGCTTCTCCACATCGAT5'

5.2.4 Immunoprecipitation

The interaction between CD14 and SR MARCO in response to LPS and the effect of PJ-34 on this interaction were assessed with immunoprecipitation assay. Briefly, THP-1 and PMA-differentiated THP-1 cells, at density of 7×10^6 per culture plate were treated with 100 ng/ml of LPS for 4 hrs in present and absence of 10 μ M PJ-34. Cells then lysate and equal amount of each sample were load on 12% SDS page gel and separated in electrophoresis apparatus. Protein interaction was detected with infrared LICOR image scanner using odyssey software see section 2.2.10.1.

5.3 Results

5.3.1 The effect of PJ-34 on the expression of CD14 and SR (MARCO) in response to LPS

A figure [5.1&5.2] represents PMA-differentiated THP-1 cells stimulated with LPS in present and absence of PARP inhibitor PJ-34. Expression of CD14 was increased in response to LPS over time incubation in the cells that stimulated with LPS alone. Whereas, the cells that treated with PJ-34 for 30 mins prior to stimulate with LPS shows decrease in the level expression of CD14 fig. 5.1. However the situation was completely different with cells that incubated with anti-human MARCO antibody, fig. 5.2 shows decrease in the expression of MARCO receptor on the cells that stimulated with LPS alone over the time incubation. In other hand the cells that treated with PJ-34 prior to stimulate with LPS shows increase in the level.

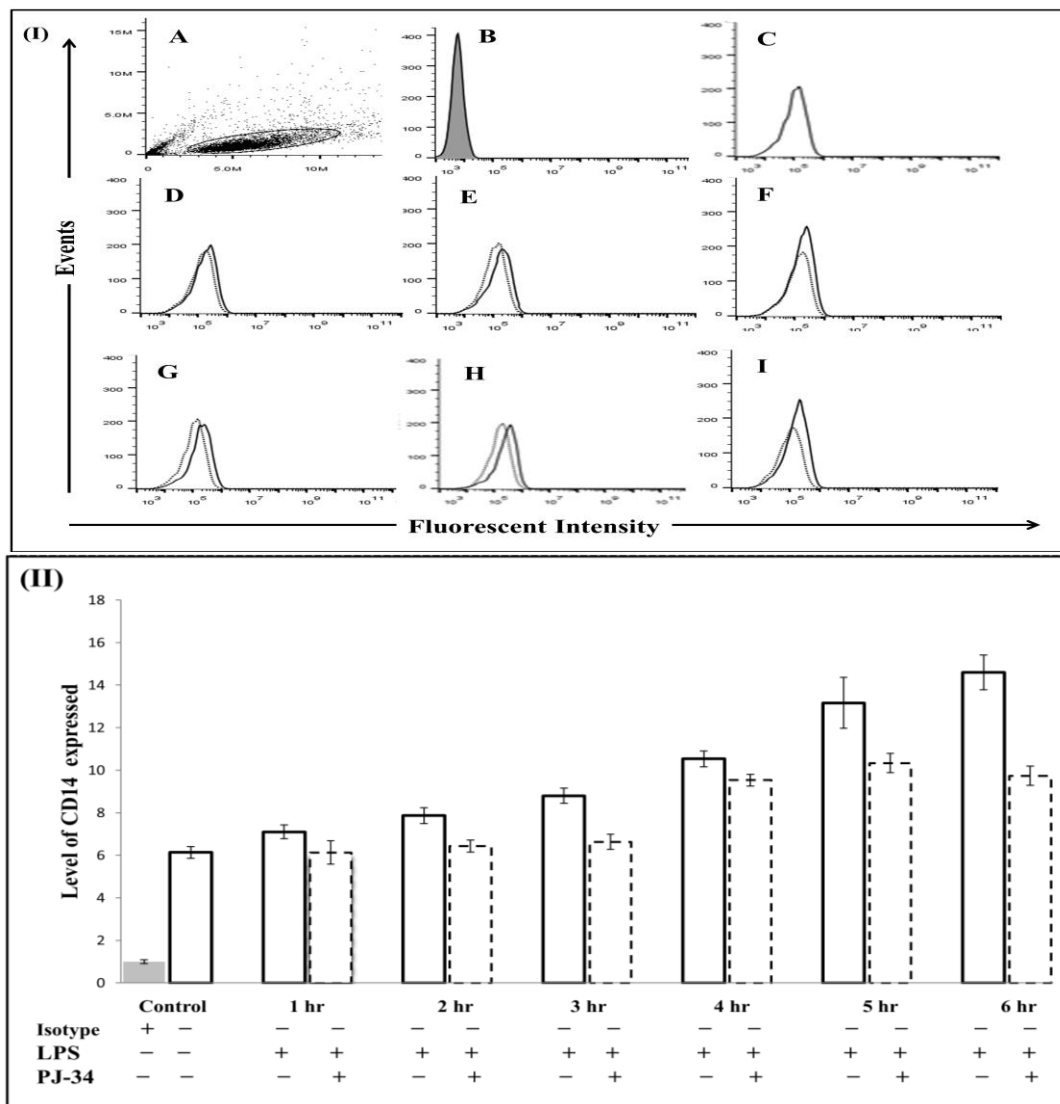


Figure 5-1 (I) & (II): Represents the expression of CD14 on PMA-differentiated THP-1 cells in response to LPS in presence and absence of PJ-34. THP-1 cells were differentiated with PMA 5 ng/ml for 72 hrs. Cells were incubated without or with 10 μ M of PJ-34 for 30 mins prior to stimulation with LPS 100 ng/ml in RPMI 1640 media supplemented with 10% (v/v) FCS in humidified atmosphere at 37⁰C for 6 hrs. Cells were washed and incubated with primary mouse anti-human CD14 monoclonal antibody for 45 mins. Following washing cells incubated with secondary antibody (Goat anti-mouse IgG labelled FITC) for 30 mins and washed. IgG1K was used as the isotype for CD14. Samples were analysed using Accuri6 flow cytometer (DB Biosciences) and Flow-Jo Software v.10 (Centre of biotechnology, Turku University, Finland) was used to analyse the data. **A:** Dot plot Column, **B:** Isotype (negative control), **C:** Untreated cells, **D, E, F, G, H** and **I** represents cells treated with PJ-34 and then stimulated with LPS for 1, 2, 3, 4, 5 and 6 hours respectively. Filled histograms represents isotypes, blacks histograms represent CD14 expression on cells stimulated with 100ng/ml LPS and dotted histograms represent CD14 expression on cells treated with 10 μ M PJ-34 prior to simulate with 100ng/ml LPS.

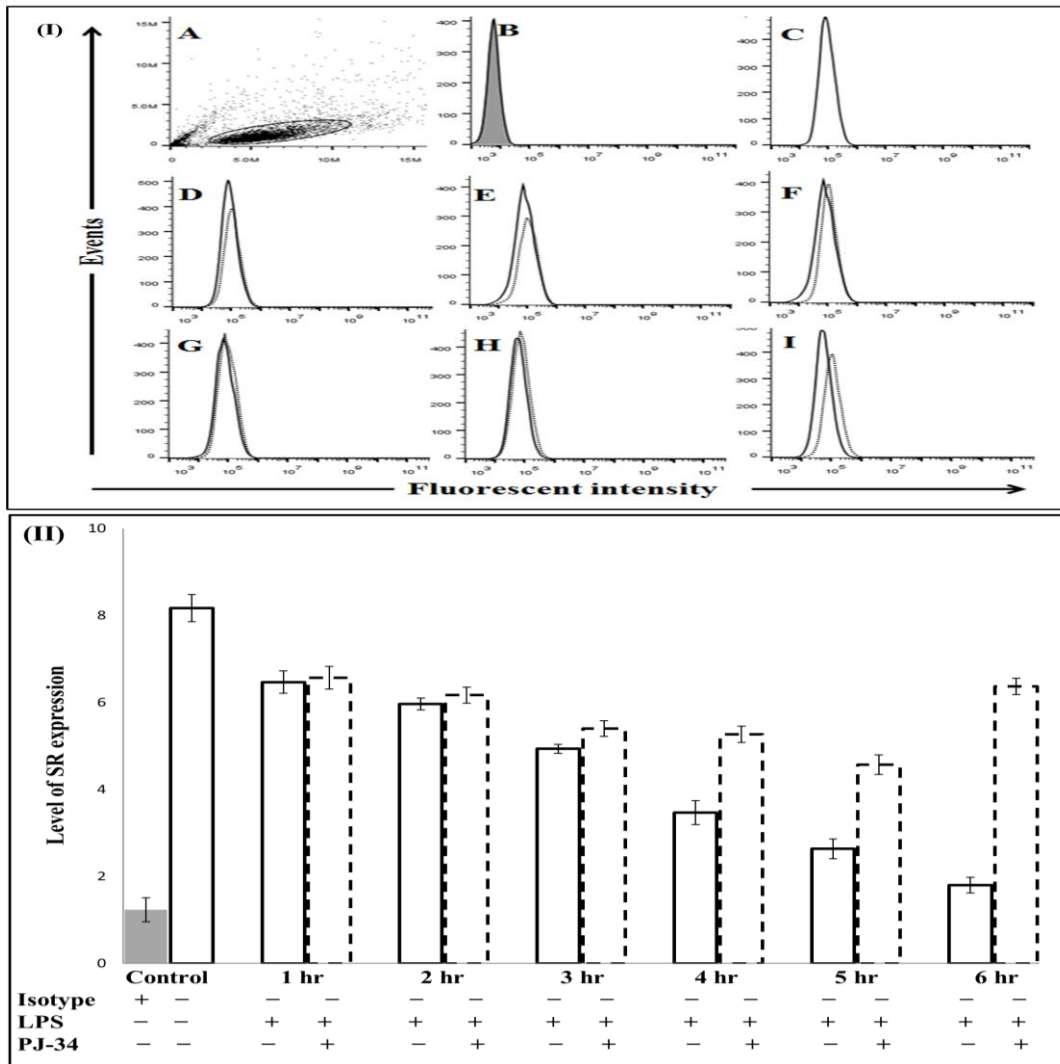


Figure 5.2(I) & (II): Represents the expression of SR (MARCO) on PMA-differentiated THP-1 cells in response to LPS in presence and absence of PJ-34. THP-1 cells were differentiated with PMA (5 ng/ml) for 72 hrs, and then cells were incubated without or with 10 μ M of PJ-34 for 30 mins prior to stimulation with LPS 100 ng/ml in RPMI 1640 media supplemented with 10% (v/v) FCS in humidified atmosphere at 37^oC for 6 hrs. Cells were washed and incubated with primary mouse anti-human MARCO monoclonal antibody for 45 min. Following washing cells incubated with secondary antibody (Goat anti-mouse IgG labelled FITC) for 30 mins and washed. IgG1K was used as the isotype for MARCO. Samples were analysed using Accuri6 flow cytometer (DB Biosciences) and Flow-Jo Software v.10 (Centre of biotechnology, Turku University, Finland) was used to analyse the data. **A:** Dot plot Column, **B:** Isotype (negative control), **C:** Untreated cells, **D, E, F, G, H** and **I** represents cells treated with PJ-34 and then stimulated with LPS for 1, 2, 3, 4, 5 and 6 hours respectively. Filled histograms represents isotypes, blacks histograms represents MARCO expression on cells stimulated with LPS 100ng/ml and dotted histograms represents MARCO expression on cells treated with 10 μ M PJ-34 prior to simulate with 100ng/ml LPS.

5.3.2 Confocal microscopy

Immunofluorescently stained cells were imaged at single-cell level and surface receptors were visualised individually with different wavelength, appearing as green and red spots in the image (Figure 5.3). Confocal microscopic images of cells shows CD14 and SR MARCO receptors labelled with antibodies appeared as masses of spherical blurred spots distributed all over the cell surface. Each CD14 and SR (MARCO) receptors pair under study, antibody-labelled surface receptors were imaged separately at different wavelengths, resulting as diffraction-limited isotropic spots of identical size in each channel. As the resolution is poorer in axial (z) direction than laterally (xy), the 3D receptors appear as cigar-shaped (Fig. 5.3). For CD14 and SR (MARCO) receptors colocalisation study, CD14 was labelled with rabbit anti-human antibody Alexa Fluor cy555 seen as red spots and SR (MARCO) was labelled with Alexa 488 and seen as green spots, while yellow/orange spots indicates co-expressed of CD14 and SR (MARCO) on THP-1. The negative control samples were stained with mouse IgG isotype and secondary antibodies and no signals above background fluorescence are observed. The cell nucleus stained with DAPI (blue colour) figure 5.4.

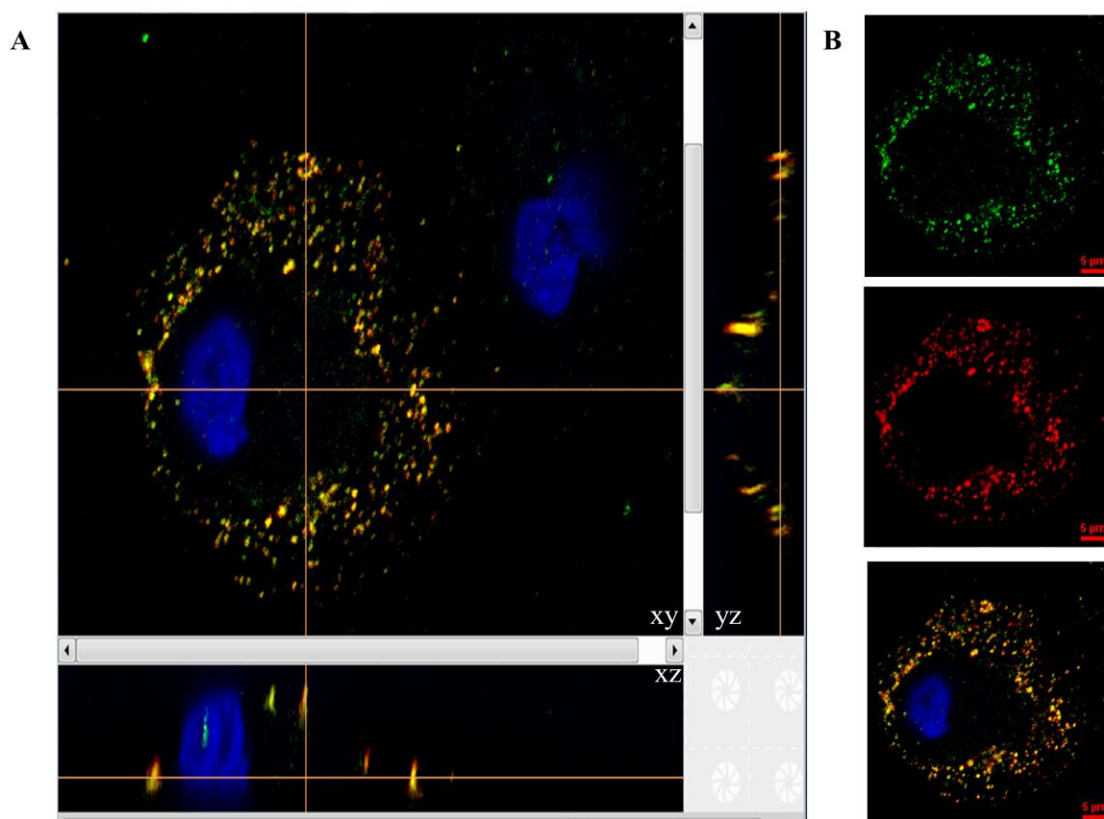


Figure 5-3: A representative of single cell image acquired by Nikon confocal microscope. Monocytic leukaemia cell stained for SR (MARCO) (green) and CD14 (red). Colocalised receptors appear yellow. **A:** represents 3D view of single plane of THP-1 cell in the xy, yz and xz direction. The cutting planes are indicated by the grey horizontal and vertical lines. **B:** represents single channel staining of SR (MARCO) green and CD14 red and colocalised receptors appear in yellow. Scale bar 5 μmTHP-1.

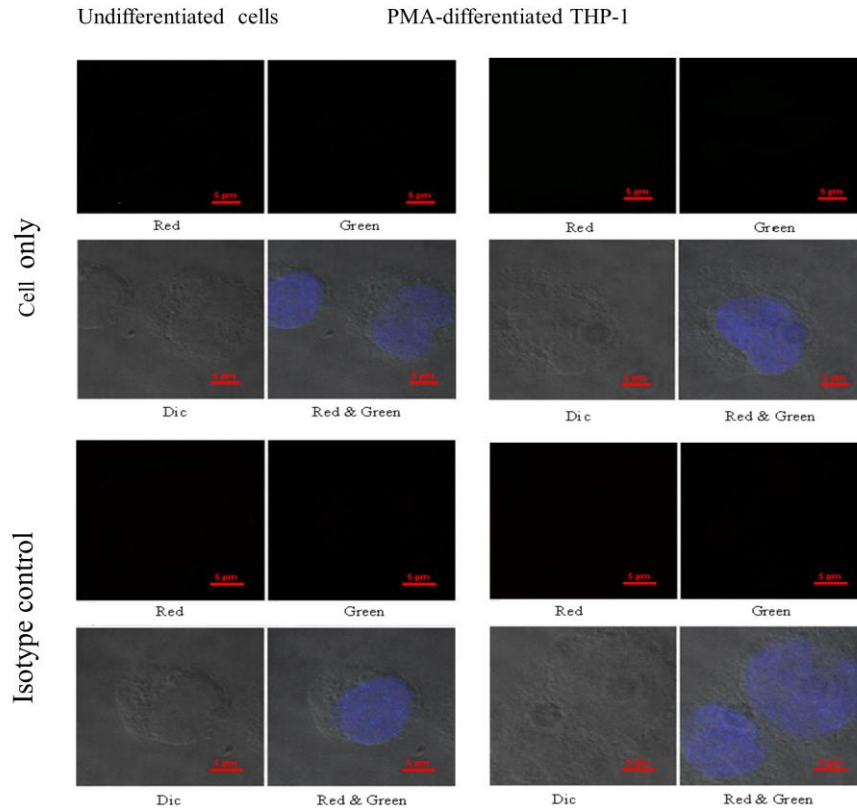


Figure 5-4: Confocal microscopy images of unstained cells and negative control samples of undifferentiated and PMA-differentiated THP-1 cells. Cell only images, represents cells stained with green 488nm and red 555nm wavelength lasers to quantify the cell auto fluorescence. Isotype control images, represents cells stained with Isotype control IgG primary and Alexa Flour 488 and Alexa Fluor 555 secondary antibodies Blue colour shows DAPI stained cell nucleus stained with DAPI (blue colour), whereas DIC is differential interference contrast image of corresponding cell. Scale bar 5µm.

5.3.2.1 Colocalisation analysis of CD14 and SR (MARCO)

Monocytic leukaemia cell line THP-1 cell were used in this study to investigate whether CD14 and SR (MARCO) receptors colocalising in response to LPS, and also to assess the role of PARP inhibitor PJ-34 in this colocalisation since the both receptors express by the cell line. Undifferentiated and PMA-differentiated THP-1 cells were immunostained with suitable primary antibody followed by a secondary antibody. CD14 was labelled with Alexa Fluor® (red) and SR (MARCO) was labelled with Alexa Fluor® (green). Merging the green and the red channels considered the colocalisation of two receptors. To analyse the colocalisation of CD14/SR a novel method mentioned in Jabeen et al (2013) and Obara et al (2013) was followed. Figure 5-5 3D images represents the colocalisation of CD14/SR the 3D on cell surface of undifferentiated and PMA-differentiated THP-1 cells in response to LPS in presence or absence of PARP inhibitor PJ-34, which were acquired in stack, with z-direction step size 0.14 μm using NIS element. This method of colocalisation analysis calculate the total number of CD14 and SR receptors per cell and the number of colocalized CD14/SR receptor pairs per cell. Red and green receptors colocalized on the surface of individual cells using a threshold ranging between 0.059-0.21 μm .

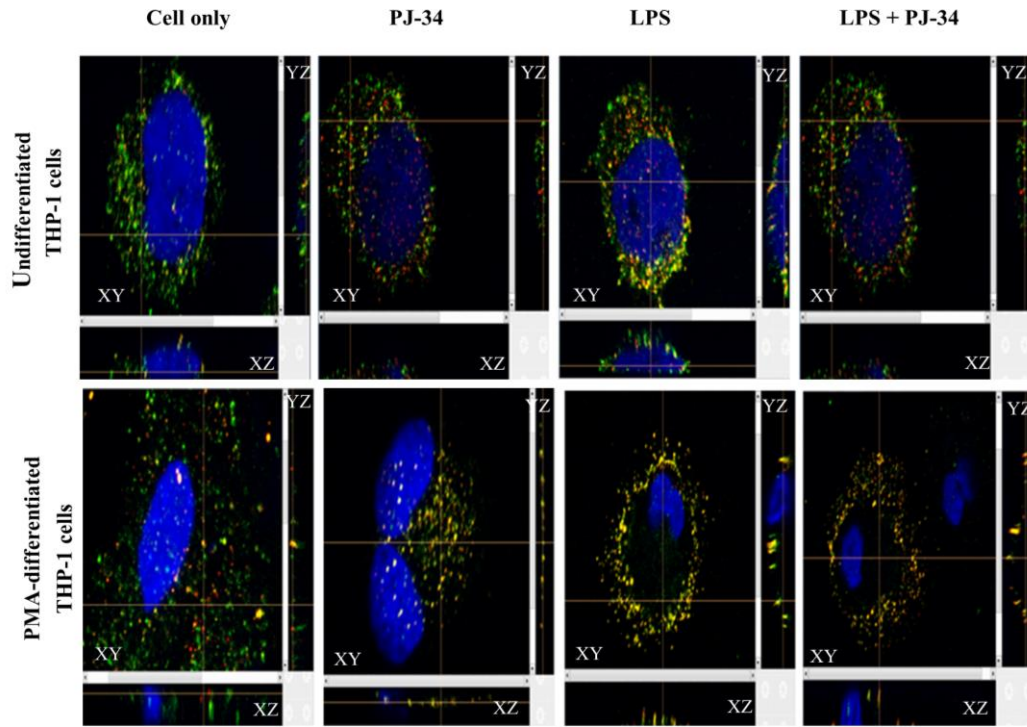


Figure 5-5: Localisation of CD14 and SR (MARCO) on the cell surface of undifferentiated and PMA-differentiated THP-1 cells, determined by confocal microscopy analysis. Green and red indicate pairings as follows: SR (MARCO) green and CD14 (red). Yellow/orange fluorescence reveals the potential colocalisations of CD14/SR. 3D images were acquired in stacks, with z-direction step size 0.14 μm . Single-plane section of z-stack is shown in three directions as xy, yz and zx. The cutting planes of the

Figure 5-6 shows the colocalisation percentage of CD14 and SR receptors on undifferentiated and PMA-differentiated THP-1 cells. The average percentage CD14/SR (Average of CD14/SR counted on each cells) colocalisation in undifferentiated cells (cell only) was $16.99\% \pm 4.23\%$, whereas PMA-differentiated cells (cell only) was $25.31\% \pm 5.32\%$. Both undifferentiated and PMA-differentiated THP-1 cells treated with PARP inhibitor PJ-34 alone shows no effect on the percentage of CD14/SR colocalisation. Both cell line shows a significant increase in CD14/SR colocalisation in response to LPS indicated with (*) $p < 0.05$ and reached peak of $22.73\% \pm 2.418$ and $36.57\% \pm 3.647\%$ in Undifferentiated and PMA-differentiated THP-1 cells respectively. The cells that incubated with PJ-34 for 30 min prior to stimulate with LPS shows a significant reduction in the number of CD14/SR receptors colocalized in response to LPS indicated with # $p < 0.05$ and reached level of $14.39\% \pm 2.34$ for undifferentiated cells and level of $17.43\% \pm 7.18\%$ for PMA-differentiated cells.

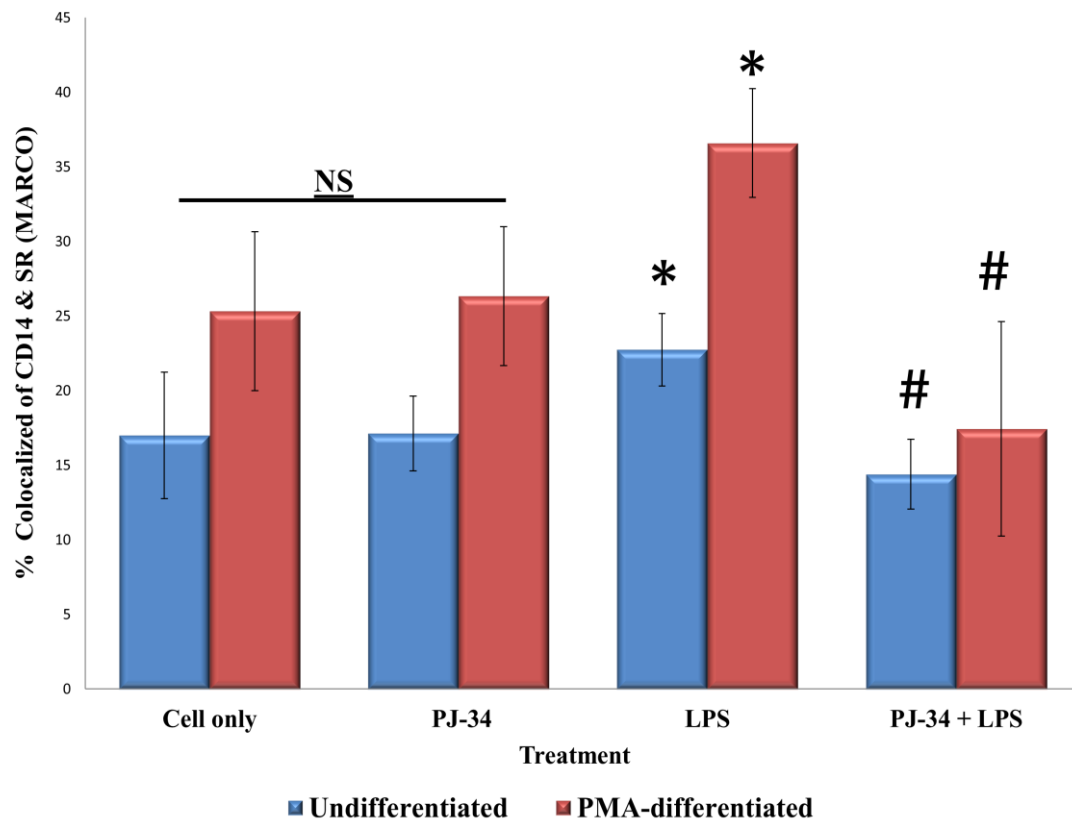


Figure 5-6: The effect of PJ-34 on the localisation percentage of CD14 and SR (MARCO) receptors by undifferentiated and PMA-differentiated THP-1 cells in response to LPS. Comparison of fractions of CD14/SR receptors colocalisation, between undifferentiated THP-1 cells (Blue bars) and PMA-differentiated THP-1 cells (Red bars) stimulate with LPS in presence or absence of PJ-34. Cell only (untreated) or cells treated with PJ-34 used as (control). Each data point represents mean \pm SD of three independent experiments. Data were statistically analysed using two ways ANOVA. (NS) non-significant difference, (*) $p < 0.05$ represents the significant difference of cells treated with LPS V cells only. Whereas (#) $p < 0.05$ represents the significant difference of cells treated PJ-34/LPS V cells treated with LPS only. Values represent three different experiments.

5.3.3 Interaction of CD14 and SR (MARCO) in response to LPS

To assess whether a physical protein-protein association occurs entirely between the human CD14 and SR (MARCO) receptors on both undifferentiated and PD/THP-1 cells in response to LPS and determine the role of PARP inhibitor PJ-34 in this protein association. A co-immunoprecipitation technique was used to carry out this investigation. Cell lysate was extracted from undifferentiated and PD/THP-1 cells cultivated in the RPMI 1694 supplement with 10% of FCS left untreated (control) or stimulated with LPS in presence or absence of PJ-34. The lysate from undifferentiated and PD/THP-1 cells were incubated with anti-CD14 afterward incubated with protein A/G loaded on a gel and blotted on PDVF membrane. Finally the membrane incubated either with anti-CD14 antibody for immunoprecipitation of CD14 or anti-SR (MARCO) antibody for co-immunoprecipitation between CD14 and SR (MARCO).

CD14 first pulled down by immunoprecipitation in undifferentiated and PD/THP-1 cells (Fig. 5.7 A & 5.8 A). The protein interaction of CD14 and SR (MARCO) were demonstrated by co-immunoprecipitation (Fig. 5.7 B & 5.8 B) revealed that CD14 interacted with SR (MARCO) in both undifferentiated and PD/THP-1 cell. In general the interaction between CD14 and SR (MARCO) is less on undifferentiated THP-1 cells in comparison with cells differentiated with PMA. Furthermore, this interaction even increased on both cell lines in response to LPS which can be detected with increasing in band intensity. The cells that treated with PJ-34 prior to stimulate with LPS shows decrease in the band intensity. Bands of CD14 and SR (MARCO) are corresponding for the antibody coupled to the magnetic beads, were observed in all the samples. In addition no bands were observed with protein G beads alone, which were loaded as the negative control (Lane 2).

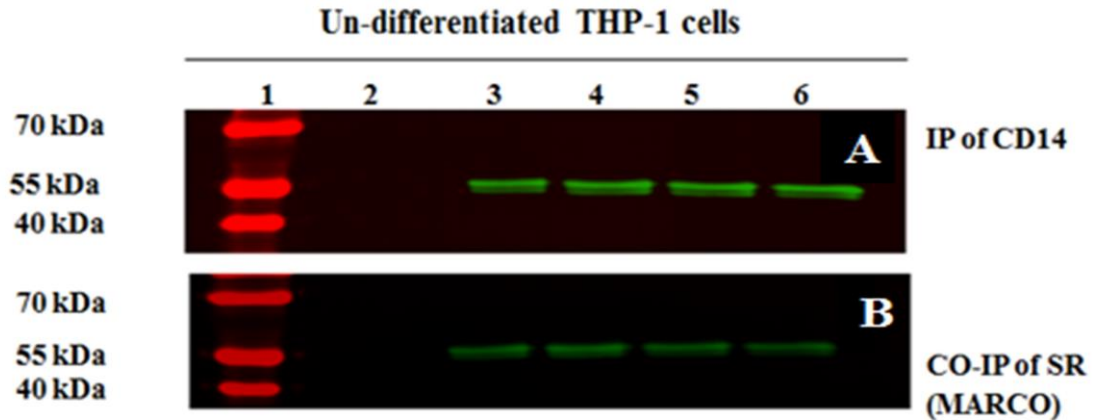


Figure 5- 7: Immunoprecipitation of CD14 and co-immunoprecipitation to study the interaction of CD14 and SR (MARCO) in undifferentiated THP-1 cells. Cell lysates from undifferentiated THP-1 cells was separated by 12% SDS-PAGE. Blots were probed with mouse anti-human CD14 and mouse anti-human SR (MARCO) antibodies. **(A)** Immunoprecipitation was subjected to pull down CD14 from the cells lysate. **(B)** Co-IP was applied to study the interaction of CD14/SR (MARCO). Lane 1: represents molecular mass in kDa, lane 2: G beads only with no cell lysate (negative control), lane 3: cell only, lane 4: cell treated PJ-34, lane 5: cells treated LPS and lane 6: cells incubated with PJ-34 for 30 min and the stimulated with LPS. Data represent three different experiments.

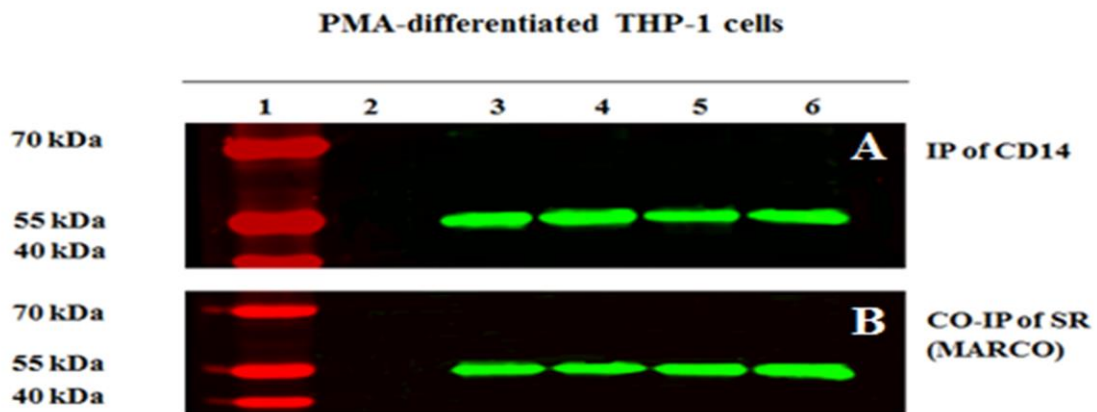


Figure 5-8: Immunoprecipitation (IP) of CD14 and coimmunoprecipitation (Co-IP) to study the interaction of CD14 and SR (MARCO) in PMA-differentiated THP-1 cells. Cell lysates from PMA-differentiated THP-1 cells was separated by 12% SDS-PAGE. Blots were probed with mouse anti-human CD14 and mouse anti-human SR (MARCO) antibodies. **(A)** Immunoprecipitation was subjected to pull down CD14 from the cells lysate. **(B)** Co-IP was applied to study the interaction of CD14/SR (MARCO). Lane 1: represents molecular mass in kDa, lane 2: G beads only with no cell lysate (negative control), lane 3: cell only, lane 4: cell treated PJ-34, lane 5: cells treated LPS and lane 6: cells incubated with PJ-34 for 30 min and the stimulated with LPS. Data represent three different experiments

5.3.4 The effect of PJ34 on mRNA CD14 and mRNA SR (MARCO) expression in response LPS

The purpose of this experiment was to investigate the effect of PARP inhibitor PJ-34 on the on the expression of CD14 and SR (MARCO) at gene level in cells treated with LPS. THP-1 cells differentiated with PMA was stimulated with 100 ng/ml of LPS in presence and absence of PJ-34 for (15 mins, 30 mins, 1 hr, 2 hrs, 3 hrs and 4 hrs), RNA was extracted and cDNA prepared as mentioned previously. Quantitive real time PCR was conducted see section 5.2.3. Figure 5-9 represent cells stimulated with LPS which show a significant increase in the level expression of CD14 mRNA in compare with control (untreated cells) and this expression increased with time incubation and indicated with (*) $p < 0.05$ and the highest level of mRNA CD14 was reached at 4 hrs incubation with LPS. Whereas, the cells that treated with PARP inhibitor PJ-34 prior to stimulate with LPS shows significant decrease in the level expression and it is continued with time incubation indicated with (#) $p < 0.05$.

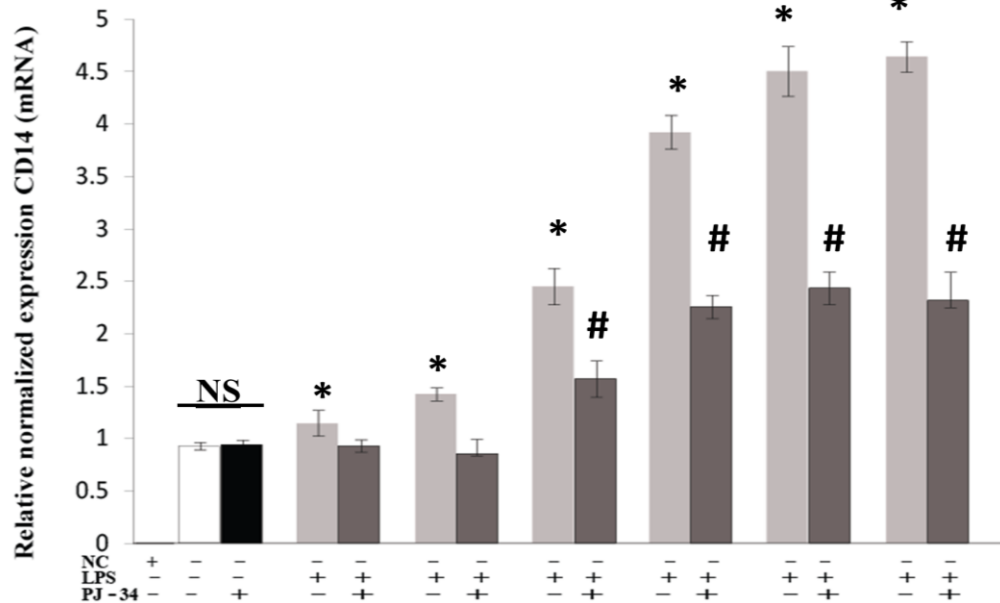


Figure 5-9: Expression of CD14 mRNA in PMA-differentiated THP-1 in response to LPS in presence and absence of PJ-34 using RT-qPCR. RT-qPCR was performed on the cDNA obtained from PMA-differentiated THP-1 cells using Master mix SYBR green 10 μ l, PCR reaction. a. *Cyclophilin* was used as the housekeeping gene to normalise the target genes (CD14) and the expression values were used to construct bar figure. Sample designed as following; untreated cells and cells treated with PJ-34 or negative control used as a control, cells treated with LPS in presence and absence of PJ-34 30 mins prior to stimulate with LPS. Two way-ANOVA analysis performed to calculate the significance difference, NS represents non-significant difference. (*) $p < 0.05$ represents the significant differences of mRNA CD14 expression by cells treated with LPS only V control. Whereas (#) $p < 0.05$ represents the significant differences of mRNA CD14 expression by the cells treated with PJ-34 and stimulated with LPS V cells treated with LPS only.

The cells show a significant decrease in the level expression of SR (MARCO) mRNA in response to LPS and this decreasing continued the time incubation indicated with (*) $p < 0.05$ and the lowest level of mRNA MARCO expression was detected at 4 hrs incubation with LPS. While, the cells treated with PARP inhibitor PJ-34 prior to stimulate by LPS shows significant increase in the level expression of SR (MARCO) mRNA indicated with (#) $p < 0.05$ and this continuous with increasing the time incubation (Fig.5-10).

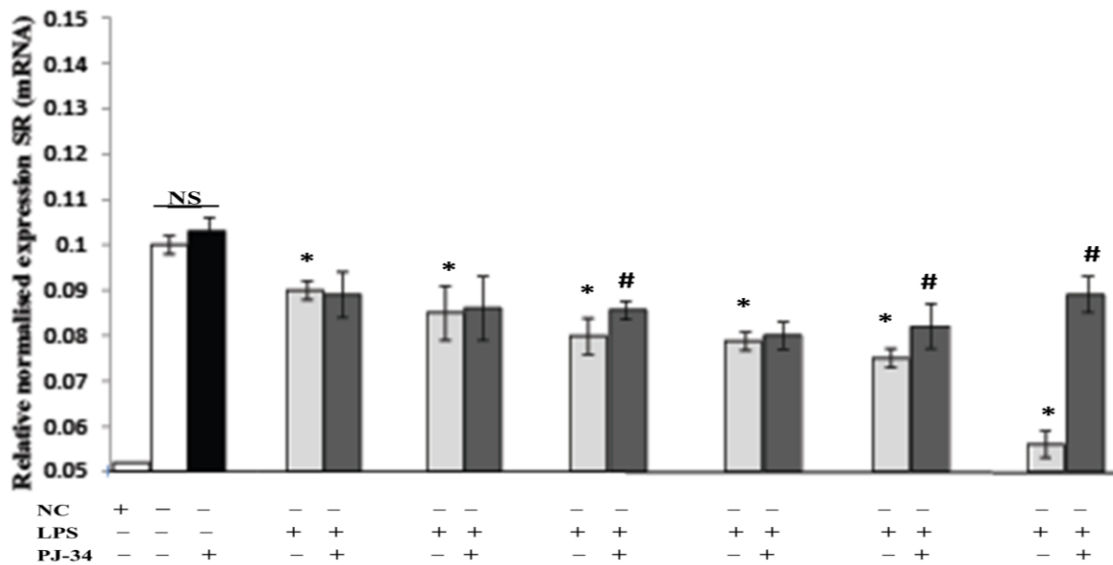


Figure 5-10: Expression of MARCO mRNA in PMA-differentiated THP-1 in response to LPS in presence and absence of PJ-34 using RT-qPCR. RT-qPCR was performed on the cDNA obtained from PMA-differentiated THP-1 cells using Master mix SYBR green 10 μ l, PCR reaction. *Cyclophilin* was used as the housekeeping gene to normalise the target genes (CD14) and the expression values were used to construct bar figure. Sample designed as following; untreated cells and cells treated with PJ-34 or negative control used as a control, cells treated with LPS in presence and absence of PJ-34 30 mins prior to stimulate with LPS. Two way-ANOVA performed to calculate the significance difference, Two way-ANOVA performed to calculate the significance difference, NS represents non-significant difference. (*) $p < 0.05$ represents the significant differences of SR (MARCO) mRNA expression by the cells treated with LPS only V control. Whereas (#) $p < 0.05$ represents the significant differences of SR (MARCO) mRNA expression by cells treated with PJ-34 and stimulated with LPS V cells treated with LPS only.

5.3.5 The effect of PJ-34 on LPS uptake

Since scavenger receptors are expressed by monocytes/macrophages cells and play a vital role in immune regulation in response to LPS. Human alveolar macrophages (AM), express scavenger MARCO which play a vital role in defense against inhaled particles and pathogens, was inhibited by anti-human MARCO antibody (PLK1). This experiment was designed to investigate the role of SR (MARCO) in uptake of LPS-labelled FITC (100ng/ml) in presence and absence of 10 μ l of PJ-34 for (15', 30', 60', and 120'). The LPS uptake was

observed by fluorescent microscopy (Nikon widefield). Figure (5.11) the uptake of LPS was detected with a fluorescence tag bound to LPS (Arredouani et al., 2005). The uptake of LPS was great at 15 and 30 mins of incubation (Fig. 5.11 [B&C]) and the uptake slightly reduced at 60 mins. The maximum reduction of LPS uptake was observed at 120 min after incubation (Fig. 5.11 E). No fluorescence was detected in PD/THP-1 cells incubated with PJ-34 only (negative control) (Fig. 5.11 A1). In contrast, PD/THP-1 cells incubated with PJ-34, then with LPS shows increase in LPS uptake for 60 min and 120 min of incubation compared with the cells that stimulated with LPS only (Fig. 5.11 D1& E1).

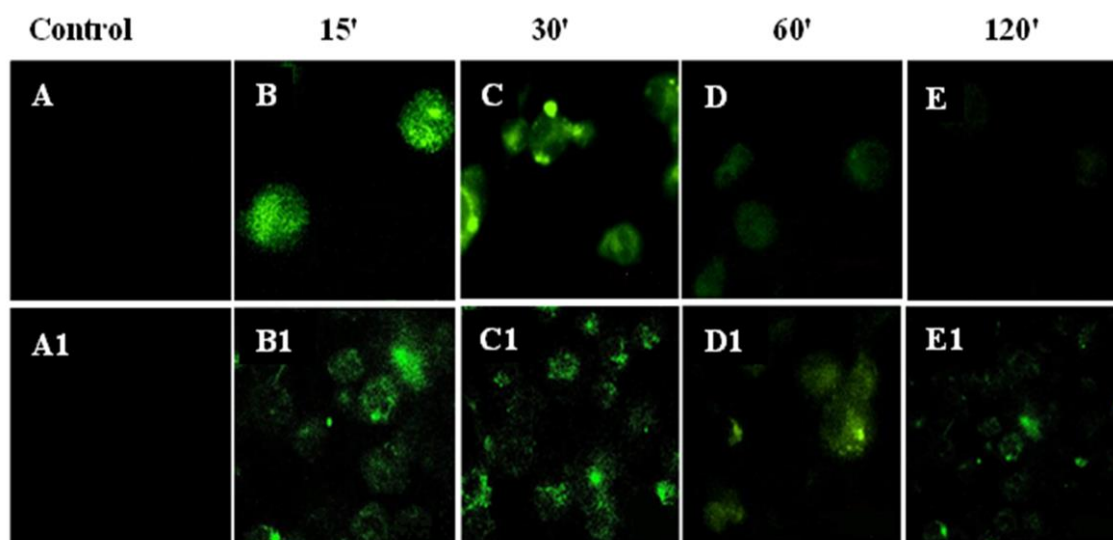


Figure 5-11: The effect of PARP inhibitor PJ-34 on the up taking of LPS labelled FITC by SR (MARCO). THP-1 cells at density of 25×10^3 were differentiated with PMA in LabTek 8-well chamber slide for 72 hours and the media replaced with media free serum (RPMI 1640). Cells then stimulated with LPS labelled FITC in absence or presence of PARP inhibitor PJ-34 for indicated times. **A-** Represents cell only (negative control), whereas (**B, C, D, and E**) represents cells treated with LPS only. **A1-** Represents cells treated with PJ-34 (negative control), while (**B1, C1, D1, and E1**) represents cells that treated with PJ-23 for 30min prior to stimulate with LPS. The data represent three different experiments. Scale bar 10 μ m.

5.4 Conclusion

PD/differentiated THP-1 cells were stimulated with LPS 100ng/ml in presence and absence of PARP inhibitor PJ-34 and subjected for flow cytometry examination and the cell that treated with LPS alone shows increase in the expression of CD14 and decrease in the expression of MARCO receptor with increasing the incubation time. Whereas, the cells incubated with PJ-34 30 min prior to stimulate with LPS shows decrease in CD14 expression and increase of MARCO with time incubation. The physical association between CD14 and MARCO was investigated with confocal microscopy on undifferentiated and PD/THP-1 cells in response to LPS in presence and absence of PJ-34. Undifferentiated cells show minor interaction between CD14 and MARCO, while in PD/THP-cells (without treatment) was increased with no significant effect of PJ-34 on this interaction in both undifferentiated and PD/THP-1 cells. Cells treated with LPS significantly upregulated the interaction between CD14 and MARCO, whereas, PJ-34 down regulated this interaction significantly. This interaction was confirmed by immunoprecipitation technique which detects the intracellular interaction between CD14 and MARCO. Undifferentiated and PD/THP-1 cells shows increases CD14 mRNA in response to LPS with increased time of incubation, while MARCO mRNA decreased with increased incubation time. In contrast, PJ-34 down regulates the expression of CD14 mRNA in response to LPS, while it increases the expression of MARCO mRNA in response to LPS with incubation time. MARCO has an important role in LPS clearance and this property was investigated by confocal microscopy which showed decreased in fluorescence intensity (which represents the LPS uptake) at 60 min and disappeared at 120 min of incubation. In contrast treatment with PJ-34 prior to LPS treatment there was continues LPS uptake even after 120 min of incubation.

**CHAPTER 6: Proteomic analysis of PMA-differentiated THP-1 cells
stimulated with LPS in presence and absence of PJ-34**

6.1 Introduction

The aim of proteomics is to characterise the proteome, the entire complement of proteins produced by an organism, system, or biological context, including modifications made to specific proteins. Proteomes vary under different conditions and at different times and the goal of proteomics is to analyse the varying proteomes, highlighting the differences among them. Proteomics has three main categories or subdivisions. Structural proteomics seeks to define the 3-dimensional structure of each protein encoded by a given genome. Expression proteomics is the study of dysregulated proteins as a function of stimulation or condition. Interaction proteomics aims to distinguish interactions between proteins and to characterise protein complexes in order to determine function. Proteomics data can provide important clues to the nature of mechanisms involved in the complex process of LPS recognition and signaling.

Two-dimensional gel electrophoresis (2-DE), which facilitates the separation of complex protein samples, has become a powerful and widely used technique for proteomic analyses. 2-DE accommodates a large mass range and is able to resolve all peptide components of a complex mixture by separating proteins by two stages. Proteins are first separated by isoelectric focusing (IEF) using an immobilized pH-gradient (IPG), the first dimension. This is followed by the second dimension, sodium dodecyl sulphate-polyacrylamide gel electrophoresis (SDS-PAGE) The resolved proteins are identified by mass spectrometry (MS) or tandem mass spectrometry (MS/MS) (Issaq & Veenstra, 2008).

Resolved protein spots can be analysed with suitable software for comparison among different samples and can be used for MS analysis. However, this method has some disadvantages, such as the occurrence of gel-to-gel variation (Goldfarb, 2007). Low

protein solubility and a high tendency for aggregation may additionally result in protein absorption and aggregation during application of both IEF and gel protein separation. Use of thiourea in addition to urea as a chaotrope, and of zwitterionic amphiphilic compounds such as chaps is able to resolve protein solubility problems (Natarajan et al., 2005; Trevino et al., 2008).

The proteome is very dynamic in nature because of post-translational modifications (Gupta et al., 2007; Witze et al., 2007; Kamath et al., 2011). Therefore, in order to recognize the physiological and pathological events that occur in health and disease, it is important to detect and analyse proteins from their native proteome.

The 2-DE technique was here used to investigate the effect of the PARP-1 inhibitor PJ-34 on the immune response of THP-1-cells after pre-treatment with LPS. The ExPASy tool (<http://web.expasy.org/tagident/>) was used to identify and quantify THP-1 cell proteins expressed. This investigation will assist understanding of the molecular aspects septic shock and potential use of PARP inhibitors in the treatment of severe sepsis and septic shock.

6.2 Methods

6.2.1 Cells growth conditions

THP-1 cells were cultured in 100 mm cell culture dishes (Nunc) and differentiated with PMA 5 ng/ml for 72 hours. Then the media was replaced with fresh media and the cells rested for 24 hours. The cells were then either left untreated (control) or treated with 100 ng/ml LPS in presence or absence of PJ-34 for 2 h hours. Protein concentrations were quantified as mentioned in section 2.2.12.1 and 2.2.6.1.

6.2.2 Two-Dimensional gel electrophoresis

Lysate from PMA-differentiated cells exposed or not exposed to PJ-34 was used for 2-DE as mentioned previously (section 2.2.12.1).

6.3 Results

6.3.1 Two dimensional gel analysis of the effect of PJ-34 on PMA-differentiated THP-1 cells in response to LPS

THP-1 cells have been used in this study as a model for septic shock and to study differential expression of the THP-1 proteome in the presence and absence of PJ-34 following LPS pre-treatment. 2D-gel-based proteomic analysis was employed, followed by protein spot analysis. Total proteins in samples of cell lysate were separated by first dimension isoelectric focusing on the basis of the isoelectric point (IP) of the proteins. The isoelectrically focused proteins are then resolved by second dimension SDS-PAGE on the basis of their molecular weight (Figure 6.1). An ultrasensitive silver stain method was used to visualise proteins spots in the SDS-PAGE gels. 2-DE gels of LPS-treated THP-1 cells treated or not treated (control) with PJ-34 are shown in figure 6.1. Gel images from three independent experiments were analysed using Progenesis SameSpot software (Nonlinear Dynamics Limited). Image analysis was performed by comparison of control gels and gels loaded with samples. This revealed differentially expressed proteins in LPS and PJ-34-treated cells. Differentially expressed polypeptide spots are indicated in figure 6.2 by a blue line and a spot number is given to each spot. The 3D view tool in Progenesis SameSpot was used to visualise and analyse protein spots resolved because of different experimental conditions (Fig. 6.3). Table 6.1 shows differentially expressed

spots on the reference gel image (untreated cells), with IP and molecular weight shown. Treatment of PMA-differentiated cells resulted in disappearance of many polypeptide spots, disappearing in response to LPS. These protein spots were present on gels loaded with samples from THP-1 cells treated with LPS that had been pre-treated with PJ-34 (Table 6.2). The results from this analysis provide initial data on the effect of PJ-34 on differential polypeptides expression after LPS exposure.

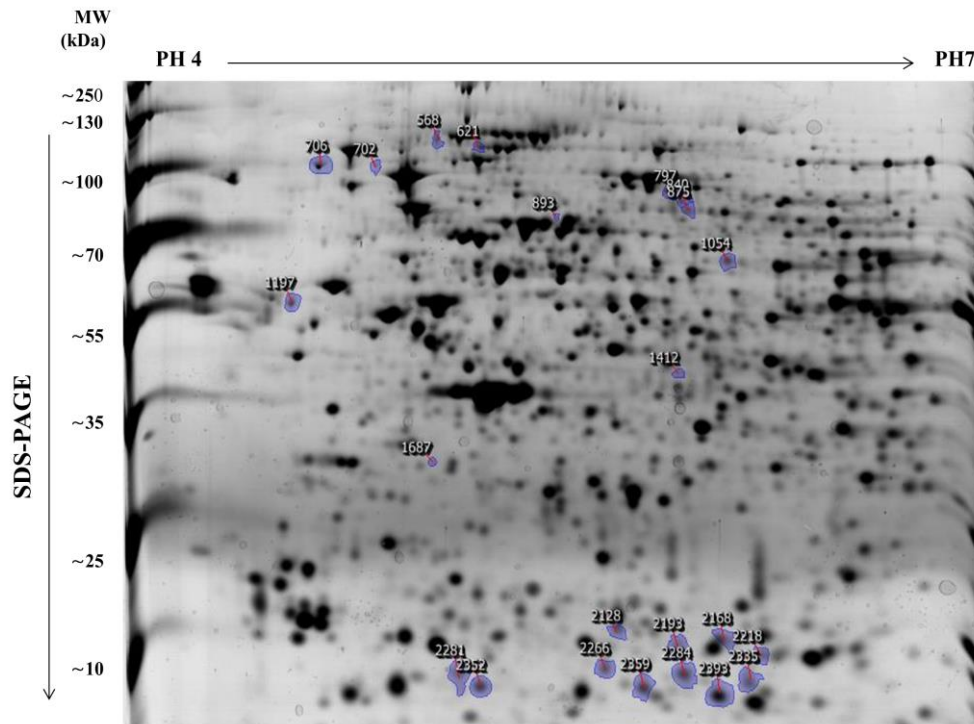


Figure 6-2: Reference image of cells only (control) showing all differentially expressed polypeptide spots. The reference image of PMA-differentiated cell only was used for analysis using Progenesis SameSpot software to compare the potential differentially expressed protein spots on cells stimulated with LPS in presence and absence of the PARP inhibitor PJ-34. Isoelectric points IP range represents protein separation based on pH) shown at the top. The left side shows the molecular weight and second dimension (SDS-PAGE) and protein separation based on molecular weight, indicated with arrow.

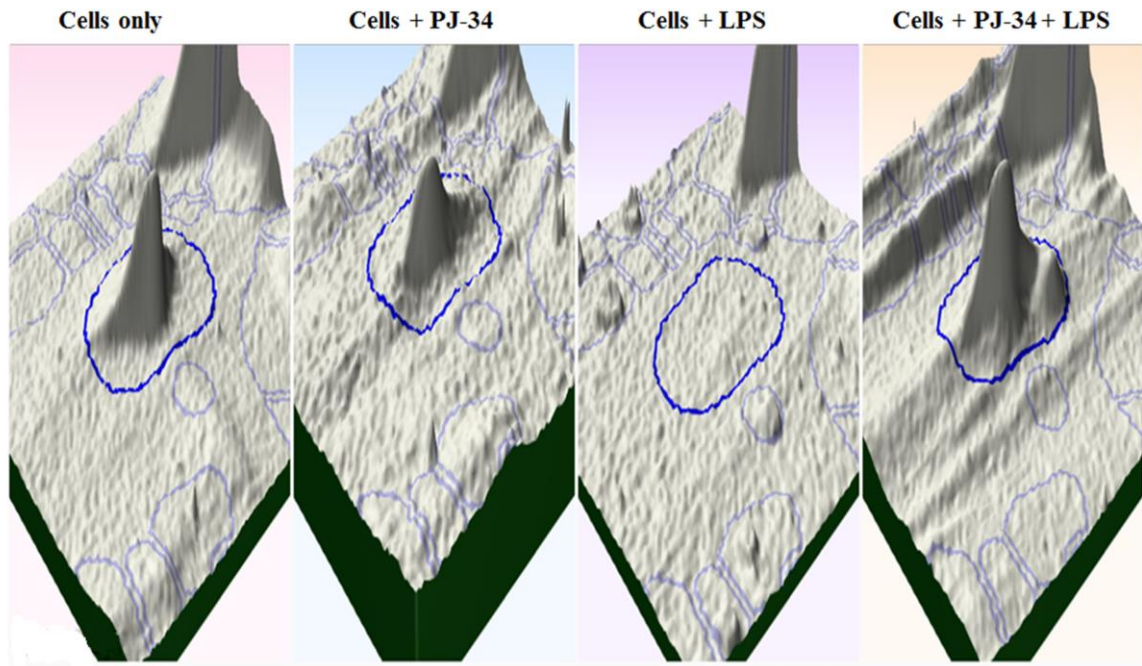


Figure 6.3: 3dimensional views of polypeptide spots derived from PMA-differentiated THP-1 cells, analysed by Progenesis SameSpot software. Three-dimensional views of protein spots show the different protein expression in untreated PMA-differentiated THP-1 cells (control) and THP-1 cells treated with LPS in the presence and absence of PARP inhibitor PJ-34. The image shows that PJ-34 protects against protein degradation in response to LPS.

PMA-differentiated THP-1 cells

Spot Number	PI (PH)	Molecular weight (kDa)	Spot Number	PI (PH)	Molecular weight (kDa)
568	5	120	2128	5.7	125
621	5.2	115	2168	6.1	12
702	4.7	110	2193	5.8	11.5
706	5.9	108	2218	6.2	11.5
797	6	103	2266	5.6	11
840	6	100	2281	5.1	10.5
875	6	90	2284	5.9	10
893	5.4	76	2335	6.3	11
1054	6.1	70	2352	5.2	8
1197	4.5	60	2359	5.7	9
1412	6	45	2393	6.1	5
1687	5	32			

Table 6.1: Summary of the polypeptides found using the reference image showing all differentially expressed spots derived from untreated PMA-differentiated THP-1 cell lysate (Control) by their IP and molecular weight.

Average normalised volumes of PMA-differentiated THP-1 cells spots analysed with Progenesis SameSpot software				
Spot Number	Untreated cells (Control)	cells + PJ-34 (10 μ M)	Cells + LPS (100 ng/ml)	Cells + PJ-34 + LPS
568	Spot +	Spot +	Spot -	Spot +
621	Spot +	Spot +	Spot -	Spot +
702	Spot +	Spot +	Spot -	Spot +
797	Spot +	Spot +	Spot -	Spot +
840	Spot +	Spot +	Spot -	Spot +
875	Spot +	Spot +	Spot -	Spot +
893	Spot -	Spot -	Spot -	Spot +
1054	Spot +	Spot +	Spot -	Spot +
1197	Spot +	Spot +	Spot -	Spot +
1687	Spot -	Spot -	Spot -	Spot +
2128	Spot +	Spot +	Spot -	Spot +
2168	Spot +	Spot +	Spot -	Spot +
2193	Spot +	Spot +	Spot -	Spot +
2118	Spot +	Spot +	Spot -	Spot +
2266	Spot +	Spot +	Spot -	Spot +
2281	Spot +	Spot +	Spot -	Spot +
2284	Spot +	Spot +	Spot -	Spot +
2335	Spot +	Spot +	Spot -	Spot +
2359	Spot +	Spot +	Spot -	Spot +
2393	Spot +	Spot +	Spot -	Spot +

Table 6.2: Representative and Comparison of polypeptides spots expressed by untreated PMA-differentiated THP-1 cells (control) and cells treated with LPS in the presence and absence of PJ-34 PARP inhibitor. PMA-differentiated THP-1 cells were either untreated or stimulated with 100 ng/ml LPS in presence and absence of 10 μ M of PJ-34 PARP inhibitor for 2 hrs. Cell lysate from all cell condition was subjected to isoelectric focusing (first dimension). The second dimension of protein separation was performed using a 12% SDS-PAGE. Protein spots were visualised by staining the gel with silver stain and then scanning with a gel scanner. Gel images were analysed by Progenesis SameSpot software. A plus sign (+) indicates the presence of protein spots before or after treatment, while a minus sign (-) indicates the absence of protein spots before or after treatment. Four spots out of 23 polypeptide spots (highlighted in bold) were selected randomly and analysed using ExPASy tool.

6.4 Conclusion

Proteomic analysis of 2-DE gels loaded with proteins from LPS-treated PMA-differentiated THP-1 cells, performed using Progenesis SameSpot software, revealed a number of polypeptides expressed by PJ-34-untreated cells which were not expressed by PJ-34-treated cells. These polypeptide proteins are present in THP-1 cells incubated with PJ-34 30 minutes prior to LPS exposure. Some spots were not present in untreated cells, or cells treated with PJ-34, or in cells treated with LPS alone. However, these spots appear in the cells that had been incubated with PJ-34 30 minutes prior to stimulation with LPS. It was found that PJ-34 PARP inhibitor imparts a protective effect, allowing sustained cell survival after LPS was administered. Further study of the polypeptide proteins found to be differentially expressed is now necessary in order to establish their role in sepsis, and to assess the role of PJ-34 in cell survival during LPS-induced toxemia

CHAPTER 7: Discussion

7.1 Discussion

The innate immune system recognises microbial infections and products and activates the first line of defence following infection. Innate immunity involves the production of proinflammatory cytokines such as TNF- α , IL-1 β and NO and activation of transcription factors such as NF- κ B and interferon regulatory factor 3. This study investigated the immunomodulation of PRRs in human monocyte/macrophage (THP-1) cells by the nuclear enzyme PARP-1, within the context of the innate immune response triggered by the LPS component of the Gram-negative bacterial cell wall. LPS is the prototypical endotoxin, binding to the CD14/TLR4/MD2 receptor complex especially in monocytes, macrophages, dendritic cells and B cells. CD14 and TLR4, and also TLR2 and the scavenger receptor MARCO play a crucial role in the protective functions of the macrophage/monocyte lineage. They are also important in the pathogenesis of sepsis and septic shock and other inflammatory diseases (Szabo et al. 1997; Oliver et al., 1999, Jiang et al., 2000). In this study, the PARP-1 inhibitor PJ-34 was used to investigate the role of PARP in septic shock via regulation of the LPS receptors CD14, TLR2, TLR4 and MARCO, and LPS-induced transcriptional activation.

LPS is an outer membrane component of all Gram-negative bacteria with an essential barrier function. It is recognised by PRRs, including TLRs that invoke the production of pro- and anti-inflammatory mediators (Ulevitch and Tobias, 1995). It has been established that production of proinflammatory cytokines and activation of NF- κ B, following stimulation of monocytes/macrophages with LPS, involves CD14, TLR4, TLR2 and MARCO. However, the regulations of these receptors are still unclear. In this study, the expression of CD14, TLR4, TLR2 and MARCO in THP-1 cells was investigated to determine whether they interact between each other and also to study the effect of PARP on the expression of these receptors. In addition, the role of the PJ-34 on the activation of

NF- κ B and JNK was examined. The production of TNF- α and IL-1 β by THP-1 and PMA-differentiated cells stimulated with LPS was also measured.

The first stage of this research entailed establishing an *in vitro* cell line suitable to provide reproducible and testable data that served as a model system. The human monocytic leukemia THP-1 cell line is isolated from the peripheral blood of a 1-year old male patient suffering from acute monocytic leukemia (Tsuchiya et al., 1980). This cell line has been widely used to study immune responses while cells are not only in the monocyte state but also can be differentiate in the macrophage-like state THP-1 macrophages, when stimulated with LPS, expressed MD2, CD14 and MyD88 genes, which are also required for LPS signaling in vivo (Daigneault et al., 2010). THP-1 cell line is easy and safe to use as it has been reported that there is no evidence for the presence of infectious viruses or toxic products, and also it can be cultured in vitro up to 25 passages without changes of cell sensitivity and activity (Mangan & Wahl, 1991). THP-1 cells can be stored for a number of years can be recovered without any obvious effects on monocyte–macrophage features and cell viability. The disadvantages of the use of cell lines is that the malignant background and the cultivation of cells under controlled conditions (outside their natural environment) might possibly result in different sensitivities and responses compared to normal somatic cells in their natural environment (Schildberger et al., 2013). Also, possibly relevant interactions between the target cells and surrounding cells, as in natural tissues, cannot be easily mimicked. However, in vitro co-cultivation of THP-1 cells with neighbouring cells might be an option to overcome this drawback.

It has been reported that oxidative reagents might cause irreversible DNA damage, and cell recovery from DNA oxidative damage is related to its extent (Stewart et al., 2000; Norbury & Zhivotovsky, 2004; Duan et al., 2005). In this study, the cytotoxic effect of PMA-differentiated THP-1 cells treated with H₂O₂ was clearly observed. PARP-1 binds

to DNA via two zinc-finger domains (Zn I and Zn II); the second determines specificity for single-strand breaks in DNA. DNA binding activates PARP-1's catalytic domain (bearing an NAD⁺ binding site), which cleaves NAD⁺ into nicotinamide and ADP-ribose polymers. The newly synthesised ADP-ribose chains are added to a number of nuclear acceptor proteins including histones, transcription factors and PARP-1 itself. Over activation of PARP in the presence of extensive DNA damage can lead to NAD⁺ depletion. To redress this loss, cells use ATP to synthesize more NAD⁺. This is thought, ultimately, to lead to an energy crisis that causes cell death (Ha & Snyder, 1999; Kim et al., 2004; Putt & Hergenrother, 2004; Pacher & Szabo 2007; Lou and Kraus, 2012). Consistent with this mechanism, the results demonstrated heightened activation of PARP-1 in the presence of major H₂O₂-induced DNA damage, which was dependent on the concentration of H₂O₂. It was observed here that 100µM of H₂O₂ was the maximum concentration causing PARP activation without adversely affecting cellular function, and this should be used in future experiments. Previously published research has shown that a decrease in NAD⁺ content and energy charge does not seem implicated within the context of PARP inhibition in conditions such as haemorrhagic shock, colitis, and cerebral ischemia, which has no deleterious effect (Popoff et al., 2002; Liaudet et al., 2002; Paschen & Doutheil, 1999). In conclusion, it has been shown that H₂O₂ caused DNA oxidative damage of PMA-differentiated THP-1 cells. The present results appear to be consistent with those of Szabo et al. (1996), regarding the activation level of PARP in the presence of intensive DNA damage, which was dependent on the concentration of H₂O₂.

The role of PJ-34 PARP inhibitor in the attenuation of PARP activity induced by H₂O₂ was studied. It was first necessary to ensure that the concentration of PJ-34 used would not interfere with the obtained results due to its possible toxic effect.

High concentrations of PJ-34 are toxic, since complete arrest of PARP-1 activity leads to cell dysfunction (Carrillo et al., 2005; Cepeda et al., 2006; Peralta-Leal et al., 2009; Krishnakumar & Kraus, 2010; Murai et al., 2012). This reveals the importance of PARP-1 in normal cell growth and cell survival (Wang et al., 1997; Herceg & Wang, 2001; Yelamos et al., 2011; Luo & Lee Kraus, 2012). 10 μ M of PJ-34 was found to be the highest concentration of PJ-34 that blocked PARP activity with lower or no effect on PMA-differentiated THP-1 cell viability. Therefore, this concentration was used as the maximum dose in all experiments

NF- κ B has been reported to be essential for the transcription of cyclin D1, which promotes cell growth (Joyce *et al.*, 2001; Arnold & Papanikolaou, 2005). PARP-1 acts as co-activator for NF- κ B (Veres *et al.*, 2003; Hassa et al., 2001; Geraets et al., 2007; Hunter et al., 2012). Thus, the effect of PJ-34 on cell growth might be explained by the attenuation of NF- κ B activation, as caused by the inhibition of PARP. Given the fact that PARP activity plays an important role in genomic stability, it is also possible that PARP inhibition, caused by a high concentration of PARP inhibitor, leads to chromosomal instability. This could affect cell growth and survival (Wang et al., 1997; Patel et al., 2011; Murai et al., 2012).

The use of PARP inhibitors below their toxic threshold has beneficial effects, and they have been used in treatment of inflammatory, neurodegenerative and ischemia-reperfusion-based diseases (Refs). Two mechanisms are responsible for their beneficial impact. First, PARP inhibitors inhibit cell death due to over activation of PARP-1. Second, PARP inhibitors inhibit signal transduction and the production of

proinflammatory mediators through interaction with number of transcription factors such as NF- κ B. (Erdelyi et al., 2005; Racz et al., 2010).

In order to investigate the effect of PJ-34 on PRR levels and cytokines secretion in response to LPS, the expression of receptors that are essential for LPS recognition was assessed in undifferentiated and differentiated THP-1 cells. Undifferentiated THP-1 cells show a moderate expression of CD14, TLR2, TLR4 and MARCO. The levels of these receptors were slightly up-regulated in response to LPS 100 ng/ml.

To enhance the expression of CD14, TLR2, TLR4 and MARCO, THP-1 cells were treated with PMA and Vit.D₃, known to be potent inducers of differentiation (Kohro et al., 2004; Huang et al., 2008; Aldo et al., 2013). PMA-differentiated THP-1 cells display a macrophage-like morphology, are strongly adherent and do not proliferate. Vit.D₃-differentiated THP-1 cells exhibit a rounded morphology, are weakly adherent and are proliferative. Both PMA and Vit.D₃ increased PRR expression in THP-1 cells after LPS exposure. The level of PRR expression was greater in cells differentiated with Vit.D₃.

Fluorescence analysis of PMA-differentiated THP-1 cells revealed that CD14, TLR2 and TLR4 proteins were up-regulated after treatment with 100 ng/ml LPS for 4 h. In contrast, cells that treated with PJ-34 showed reduced expression of these receptors in response to LPS. MARCO expression was down-regulated in PMA-differentiated THP-1 cells when treated with LPS, while the presence of PJ-34 resulted in up-regulation of MARCO after treatment with LPS in the same cells. Thus, it appears that PARP activity prohibits the expression of LPS receptors in THP-1 cells in response to LPS. Inhibition of PARP activity resulted in reduced expression of CD14, TLR2 and TLR4 but not of MARCO.

Many studies have studied the role of PARP-1 in the pathogenesis of LPS-induced inflammation, which focused on the relationship between PARP-1 and NF- κ B . Using the electrophoretic mobility shift assay, Chang and Alvarez-Gonzalez (2001), studied the molecular mechanism by which PARP-1 activates the sequence-specific binding of NF- κ B to its oligo deoxynucleotide, NF- κ B-p50 DNA binding was dependent on the presence of β NAD⁺. NF- κ B transcriptional activity was dependant on the availability of β NAD⁺. PJ-34 has the ability to block the enzymatic activity of PARP enzyme. Therefore It is possible that NF- κ B activity is dependent upon the enzymatic activity of PARP by facilitating the binding of NF- κ B -P50 to its DNA by inhibiting protein-protein interaction between NF- κ B -P50 and PARP-1.

Oliver et al. (1999) reported that cells from PARP-1-deficient mice exhibit defective NF- κ B activation, leading to abrogation of TNF- α , IL-1 β and iNOS expression. Treatment of mice with anti-TNF- α or anti-IL-1 β reduced the effect of LPS, and lead to an increase of CD14 on the cell membrane and CD14 messenger RNA (Kimura et al., 2000; Vives-Pi et al., 2003; Jessen et al., 2007). This finding may suggest that inhibition of PARP-1 activity disrupts indirect LPS up-regulation of innate receptors via abrogating the NF- κ B dependant transcription of these inflammatory cytokines.

The CD14 gene promoter includes binding sites for the SP-1 and AP-1 nuclear binding proteins, which are believed to be vital for CD14 transcriptional regulation (Zhang et al., 1994; Wheeler & Thurman, 2003; Fujioka et al., 2004; Nareika et al., 2008). The transcription factor AP-1 has a serves to increase CD14 expression in epithelial cells after Gram-negative bacterial infection (Iwahashi et al., 2000). It has been shown in many studies that the activity of a number of transcription factors involved in LPS signaling,

such as NF- κ B , SP-1 and AP-1 in glia cells, is altered by poly (ADP-ribose) polymerase activity (Ha et al., 2002; Virág, 2005). The activation of transcription factors such as NF- κ B and AP-1 is attenuated by PARP-1 inhibitors, including, 4 hydroxyquinazoline (4-HQN), during LPS-induced endotoxic shock (Veres, 2004). In addition, PARP-1 inhibition is able to abolish the DNA-binding activity of AP-1 in murine macrophages (Andreone et al., 2003).

CD14 bind to lipid A moiety of LPS, hence many studies show that CD14 is one of LPS receptor and involves in LPS stimulation of CD14 positive cells such as macrophage and neutrophil. Stimulated macrophages by LPS produce prostaglandin E₂ (PGE₂), which stimulate gene expression of CD14 via protein kinase A, also PGE₂ has the ability to stimulate AP-1-mediated expression of CD14 in mouse macrophages via cAMP-dependent protein kinase A. Iwahashi et al., (2000) showed that PGE₂ both *in vitro* and *in vivo* can activate the transcription of CD14 gene in mouse macrophages by activating AP-1. Also Hofer et al. (2004) showed that PGE₂ can stimulate the expression of LPS receptors in the human Mono Mac 6 cell line.

Innate immunity is regulated by cytokines, which are produced mainly by monocyte/macrophage lineage cells and dendritic cells. In this study two different cytokines TNF- α and IL-1 β , which are key regulators of innate immune and proinflammatory responses have been studied. This study demonstrated that PARP activity regulates the production of TNF- α and IL-1 β and the release of NO in LPS stimulated THP-1 cells *in vitro*. These cells produced low level of TNF- α , IL-1 β and NO in response to LPS, while THP-1 cells differentiated with Vit. D₃ or PMA produced higher levels. The highest concentration of TNF- α , IL-1 β and NO, following LPS-exposure, was observed in PMA-differentiated

cells. The data obtained indicate that PJ-34 has the capacity to decrease the production of TNF- α , IL-1 β and NO in response to LPS.

These results clearly demonstrate that activation of NF- κ B and JNK-1 in response to LPS is regulated by TNF- α , IL-1 β and NO production. This regulation could be as a result of suppression effect of PARP inhibitor on the activation of NF- κ B, a key transcription factor which is involved in chemokine generation in immunostimulated cells. These results are consistent with previous work by; (Shaposhnikov et al., 2011; Castri et al., 2014) which investigated the regulation of the JNK-1 dependent transcriptional pathway. Haskó and coworkers (2002) showed that the production of TNF- α was suppressed in both PARP deficient mice and in the presence of PARP inhibitor. The production of inducible NO synthase by many types of cells in response to inflammatory stress (Olivenza et al., 2000; Lamon et al., 2010; Peng et al., 2012) was suppressed by PARP inhibition of the endotoxin-induced NO pathway in macrophages (Huang, 2009).

LPS-induced iNOS expression in human monocytes is reduced in the presence of the PARP inhibitors DPQ and PJ-34 (Scalia et al., 2013). PARP inhibition also reduces edema formation within the context septic and non-septic models of lung inflammation by reducing the level of NO in plasma (Sidorkina et al., 2003; Murakami et al., 2004).

The present study highlights the role of LPS receptors in production of TNF- α and IL-1 β , and in NO production. Blocking CD14, MARCO, TLR2 and TLR4 with appropriate monoclonal antibody resulted in much lowered LPS-induced production of TNF- α , IL-1 β , and NO. The LPS receptors (CD14, MARCO, TLR2 and TLR4) act differentially in production of proinflammatory cytokines. These findings reflected the importance of these receptors in LPS signaling. LPS-induced TNF- α release was partially inhibited by TLR4 blockade, suggesting that LPS utilizes both TLR4-dependent and independent

mechanism. Blockade of CD14 also resulted in inhibition of TNF- α release, confirming that CD14 is essential for production of TNF- α (Eva et al., 2009). Therefore, this study indicates that TNF- α production depends on LPS binding to CD14 not only association with TLR4, but also with other TLR2 and/or MD2. Blockage of LPS receptors could help to prevent the release of proinflammatory cytokines and prevent the harmful effect of inflammatory responses caused by Gram-negative bacteria (O Neil 2003). The transcription factor NF- κ B plays a vital role in regulation of proinflammatory cytokines production in response to LPS signaling.

The mechanism by which LPS induces septic shock involves its ability to activate NF- κ B /Rel family transcription factor members, which results in expression of several critical genes involved in septic shock pathogenesis, including TNF- α , IL-1 β and NO (Reimer et al., 2008; Schreck et al., 2009; Vallabhapurapu & Karin, 2009; Ghosh & Hayden, 2008). NF- κ B is consist of P65 and P50 proteins subunits.(Gupta et al., 2010) NF- κ B in unstimulated cells localised in cytoplasm by binding to I-KB α and I-KB β to prevent nuclear translocation (Gamble et al., 2012). Activation of cells with LPS leads to phosphorylation of I-kB kinase, which results in degradation of NF- κ B and translocation to the nucleus where it binds to region of target gene which is responsible for production of different proinflammatory cytokines such as TNF- α , IL1 β , IL-6 and IL-8 (Bonizzi & Karin, 2004b; Lawrence, 2009; Gupta et al., 2010). In agreement with previously published results, it was observed that PJ-34 was able to inhibit the translocation of NF- κ B into the nucleus (Soriano et al., 2001; Pacher et al., 2002; Pacher & Szabó, 2005).

The role of PARP in regulating the expression of inflammatory mediators has been intensively investigated. Many studies have focused on whether the catalytic activity of

PARP or the presence of the protein itself is required for inflammatory gene expression. Binding of NF- κ B to DNA has been found to depend on the availability of NAD⁺; this activity is blocked in the presence of PARP inhibitor. This indicates that this binding is protein poly (ADP-ribosyl)ation dependent (Hassa et al., 2001). The present results show that regulation of TNF- α , IL-1 β and NO and activation of NF- κ B by PARP-1 depends on the activity of the PARP enzyme. Consistent with previous studies, PJ-34 was found to regulate the expression of TNF- α , IL-1 β (Oliver et al., 1999; Liaudet et al., 2002b; Leung et al., 2012).

The scavenger receptor MARCO is expressed by macrophages and binds and is regulated by LPS (Kraal et al., 2000; Perez et al., 2010; Thelen et al., 2010). It has been suggested that MARCO has a role in microbial recognition and phagocytosis (Peiser et al., 2000; Areschoug & Gordon, 2009). MARCO may also modulate TLR4-mediated responses to LPS, since SR-A-mediated internalization of LPS leads to its degradation, but does not induce cellular activation (Chen et al., 2010). It has been found that SR-A knockout mice are more sensitive to LPS (Arredouani et al., 2006; Mukhopadhyay et al., 2006). The finding that MARCO is down-modulated in THP-1 cells in response to LPS may in part be due to LPS-induced TNF- α biosynthesis; most of the inhibitory activity of LPS on the macrophage scavenger receptors can be blocked with an antibody to TNF- α , (van Lenten & Fogelman, 1992; Hsu et al., 1996; Buechler et al., 2000) indicating that TNF- α mediates the LPS effect. It has been proposed that TNF- α regulates macrophage scavenger receptor expression in macrophage-like PD/THP-1 cells by transcriptional and post-transcriptional mechanisms (Hsu et al., 1996), but principally by destabilization of macrophage scavenger receptor mRNA. This interpretation was supported, in that the half-life of MARCO mRNA was significantly reduced in cells treated with TNF- α relative to untreated cells. Up-regulation of MARCO, caused by PJ-34-induced PARP-

inactivation that results in inference of NF- κ B activation, may thus be correlated with down-modulation of TNF- α expression. The real time PCR shows that the expression of CD14 and MARCO were regulated at mRNA level in response to LPS.

CD14 is the major innate receptor that recognizes and binds LPS and it has a vital role in the LPS signaling pathway (Triantafilou & Triantafilou, 2002b; Jiang *et al.*, 2005; Anas *et al.*, 2010). CD14 is anchored on the plasma membrane by GPI tail and has no intracellular signaling moiety. Signaling is initiated through TLR4 after LPS binds to CD14 and forms a complex of LPS-CD14, bypassing this barrier. LPS signalling trigger activation of NF- κ B, inducing production of proinflammatory cytokines. MARCO, expressed in monocytes/macrophages, plays an importance role in the clearing of circulating LPS (Peiser *et al.*, 2002b; Plüddemann *et al.*, 2009). Hence, MARCO knockout mice are susceptible to LPS induced lethality (Mukhopadhyay *et al.*, 2006).

This study obtained the first evidence indicating physical interaction between CD14 and MARCO on the cell surface of THP-1 cells. The colocalisation of cell-surface CD14 and MARCO increased upon the differentiation PMA. It further increased in response to LPS. Treatment of THP-1 cells with PJ-34 prior to stimulation with LPS led to a reduction in the number of CD14 and MARCO molecules colocalized on THP-1 cell and DP/THP-1 cells. The average percentage of each CD14 and MARCO receptor colocalized was calculated out of the total colocalized receptors. The ratio of receptor pairs colocalized was calculated by considering total colocalized molecules out of total red and green spots per cell. This calculation approach allowed a comparison to be made between treated and untreated groups. The relative ratio of colocalized CD14 and MARCO increased in response to LPS treatment in both THP-1 cells and DP/THP-1 cells. In contrast, cells treated with PJ-34 prior to stimulation with LPS showed significant

reduction in the number of receptors colocalized in response to LPS. This physical association of CD14 and MARCO in response to LPS might play a vital role in modulation of the immunoresponse to LPS, since MARCO-deficient mice are susceptible to LPS induced lethality.

The physical association of CD14 and MARCO was detected through immunoprecipitation and co-immunoprecipitation of cell extracts from untreated THP-1 cells and cells treated with LPS. The LPS-treated cells displayed heightened expression of CD14 and MARCO. However, cells treated with PJ-34 showed a reduction in the number of CD14 and MARCO proteins colocalized in response to LPS. The role of MARCO in the DP/THP-1, in terms of its ability to take up LPS, and the effect of PJ-34 in this process, were studied. THP-1 cells were treated with PJ-34 30 min before stimulation with FITC-labelled LPS. Clearance of LPS was found to be reduced with increasing of time incubation (Fig. 5-11). MARCO LPS clearance activity peaked between 15 min and 30 min, declined at 1 h and was abolished at 2 h. The time-course data for cells treated with PJ-34 differ, showing continuous up-take of LPS during 2 h incubation with LPS. This indicates that MARCO has an important role in binding of LPS, but there is a noteworthy discordance between the low expression level of MARCO and its high binding capacity which might be due to LPS molecules size which are large enough to engage MARCO receptor (Arredouani et al., 2004). LPS clearance is mediated by phagocytosis, a process that is either opsonin-dependent or opsonin-independent (Mukhopadhyay et al., 2006 ; Benard et al., 2014). Recent studies on opsonin-independent recognition of microorganisms and apoptotic cells have shown involvement of scavenger receptors, including SR-AI/II. MARCO, however, is identified as a main

receptor for binding unopsonized microorganisms and particles, and this indicates an important function of MARCO in human host defence (Arredouani et al., 2013).

The proteomic study of the effect of PJ-34 in DP/THP-1 cells in response to LPS, using 2-D gel electrophoresis, was performed to identify the differences between untreated and treated DP/THP-1 cells after exposure to LPS. The effect of PJ-34 on the cells prior to stimulation with LPS was initially investigated. Amongst the 2-D PAGE-resolved proteins 23 protein spots were identified in DP/THP-1 cells as interesting spots suitable for further analysis, based on IP and MW (Table 6-1). The ExPASy tool, a UniProtKB programme with high-quality and free accessible recourse of protein sequence and functional information, yielded several potential useful results, and was used to analyse four random selected polypeptide spots, highlighted in Table 6.1. For example, polypeptide spot number 568 correlated with a member of the histone deacetylase (HDAC) class of enzymes, which have an IP of ~5 and a MW of 120 kDa. It is believed that HDACs play a role in innate immunity. This is based on the observation that HDAC inhibition by HDAC inhibitor (LAQ824) alters TLR4-dependent activation and the function of macrophages and dendritic cells (Brogdon et al., 2007). Enzymes such as histone acetyltransferases and HDACs regulate the dynamics of chromatin structure and function by removing acetyl groups from a ϵ -N-acetyl lysine amino acid. This process is essential in modulating gene transcription through chromatin organization, and plays an important role in many key biological processes. Disruption of this process results in aberrant gene transcription and causes diseases (Huang et al., 2003). Non-histone transcription factors such as p53, HSP90, and STAT3, have been identified as substrates of HDACs, indicating a novel mechanism of action of HDACs in modulating gene function (Minucci & Pelicci, 2006).

The polypeptide spot 875 is believed to be related to mitogen-activated protein kinase (MAPK) which has an IP of ~6 and a MW of 90 kDa. MAPK proteins that play a crucial role in signal transduction pathways and gene expression in response to cell stimulants.

Polypeptide spot number 797, which has an IP of ~ 6 and a MW of 103 kDa, shares similarity to the 80-kDa LPS-binding membrane protein (LMP80). This is expressed in monocytes, erythrocytes, and in endothelial cells and interacts with LPS (El-Samalouti et al., 1999). LMP80 is similar to CD55, the decay-accelerating factor (DAF). CD55 is a complement regulatory molecule that is present in almost all cells that are in contact with the blood stream (Alegretti et al., 2010). It protects the cells from autologous complement lysis by accelerating the decay of the C3 convertases of the classical and the alternative complement pathways (Harris et al., 2006).

The polypeptide spot 2266, which has an IP of ~ 5.6 and a MW of 11 kDa, is similar to cytochrome c (Cyt_c) and cytochrome c oxidase (COX), which catalyses the terminal reaction of the mitochondria electron transport chain (ETC), through which the reduction of oxygen to water occurs. Both Cyt_c and COX play a crucial role in health and disease together with ATP synthase, which provides the vast majority of cellular energy and drives all cellular processes. Under stress conditions, the ETC generates reactive oxygen species, which cause cell damage and trigger death processes. In acute inflammation (e.g. sepsis), COX is inhibited, leading to energy depletion due phosphorylation of COX. In ischemia/reperfusion injury the hyperactive ETC complexes generate pathologically high mitochondrial membrane potentials, leading to excessive ROS production, with cell death occurring via energy deprivation or ROS-triggered apoptosis (Hüttemann et al., 2012) .

The current study has found a number of proteins in the sepsis model system that is differentially expressed in response to LPS action; it has examined the effect of PARP inhibitor in the regulation of these proteins. The data presented here could be used as baseline for further detailed investigation. In this regard, functional assays need to be employed to further validate the data presented. Further analysis by mass spectrometry is also required to identify protein sequences and differentially observed polypeptide spots.

In this study PARP activation has been found to upregulate the expression of CD14, TLR2 and TLR4 in response to stimulation with LPS and the expression of SR (MARCO) was down regulated. This was proven by blocking PARP enzyme with PJ-34 a potent PARP inhibitor. Inhibition of PARP with PJ-34 does not overcome the effect of the LPS. The confocal microscopy results have shown the association between CD14 and MARCO which has been increased in response to LPS and down regulated by inhibition of PARP activity.

References

- Aderem A, Ulevitch RJ (2000) Toll-like receptors in the induction of the innate immune response. *Nature*, **406**, 782–787.
- Ahel I, Ahel D, Matsusaka T, Clark AJ, Pines J, Boulton SJ, West SC (2008) Poly(ADP-ribose)-binding zinc finger motifs in DNA repair/checkpoint proteins. *Nature*, **451**, 81–85.
- Akashi S, Ogata H, Kirikae F et al. (2000) Regulatory roles for CD14 and phosphatidylinositol in the signaling via toll-like receptor 4-MD-2. *Biochemical and biophysical research communications*, **268**, 172–177.
- Akira S, Uematsu S, Takeuchi O (2006) Pathogen Recognition and Innate Immunity. *Cell*, **124**, 783–801.
- Alano CC, Garnier P, Ying W, Higashi Y, Kauppinen TM, Swanson RA (2010) NAD⁺ depletion is necessary and sufficient for poly(ADP-ribose) polymerase-1-mediated neuronal death. *The Journal of neuroscience : the official journal of the Society for Neuroscience*, **30**, 2967–78.
- Aldo PB, Craveiro V, Guller S, Mor G (2013) Effect of culture conditions on the phenotype of THP-1 monocyte cell line. *American Journal of Reproductive Immunology*, **70**, 80–86.
- Alegretti AP, Mucenic T, Merzoni J, Faulhaber GA, Silla LM, Xavier RM (2010) Expression of CD55 and CD59 on peripheral blood cells from systemic lupus erythematosus (SLE) patients. *Cellular Immunology*, **265**, 127–132.
- Anas AA, Hovius JWR, Van 't Veer C, van der Poll T, de Vos AF (2010) Role of CD14 in a mouse model of acute lung inflammation induced by different lipopolysaccharide chemotypes. *PloS one*, **5**, e10183.
- Andersson U, Erlandsson-Harris H, Yang H, Tracey KJ (2002) HMGB1 as a DNA-binding cytokine. *Journal of leukocyte biology*, **72**, 1084–1091.
- Andonegui G, Goyert SM, Kubes P (2002) Lipopolysaccharide-induced leukocyte-endothelial cell interactions: a role for CD14 versus toll-like receptor 4 within microvessels. *Journal of immunology (Baltimore, Md. : 1950)*, **169**, 2111–2119.
- Andrabi S, Kim N, Yu S et al. (2006) Poly(ADP-ribose) (PAR) polymer is a death signal. *Proceedings of the National Academy of Sciences*, **103**, 18308–18313.
- Andreakos E, Sacre SM, Smith C et al. (2004) Distinct pathways of LPS-induced NF- κ B activation and cytokine production in human myeloid and nonmyeloid cells defined by selective utilization of MyD88 and Mal/TIRAP. *Blood*, **103**, 2229–2237.
- Andreone TL, O'Connor M, Denenberg A, Hake PW, Zingarelli B (2003) Poly(ADP-ribose) polymerase-1 regulates activation of activator protein-1 in murine fibroblasts. *Journal of immunology (Baltimore, Md. : 1950)*, **170**, 2113–2120.
- Angus DC, Linde-Zwirble WT, Lidicker J, Clermont G, Carcillo J, Pinsky MR (2001) Epidemiology of severe sepsis in the United States: analysis of incidence, outcome, and associated costs of care. *Critical care medicine*, **29**, 1303–1310.
- Annane D, Bellissant E, Cavaillon J-M (2005) Septic shock. *Lancet*, **365**, 63–78.
- Antal-Szalm??'s P (2000) Evaluation of CD14 in host defence. *European Journal of*

- Clinical Investigation*, **30**, 167–179.
- Antoniades CG, Berry PA, Wendon JA, Vergani D (2008) The importance of immune dysfunction in determining outcome in acute liver failure. *Journal of hepatology*, **49**, 845–861.
- Arbour NC, Lorenz E, Schutte BC et al. (2000) TLR4 mutations are associated with endotoxin hyporesponsiveness in humans. *Nature genetics*, **25**, 187–191.
- Areschoug T, Gordon S (2009) Scavenger receptors: Role in innate immunity and microbial pathogenesis. *Cellular Microbiology*, **11**, 1160–1169.
- Arnold A, Papanikolaou A (2005) Cyclin D1 in breast cancer pathogenesis. *Journal of Clinical Oncology*, **23**, 4215–4224.
- Arredouani M, Yang Z, Ning Y, Qin G, Soininen R, Tryggvason K, Kobzik L (2004) The scavenger receptor MARCO is required for lung defense against pneumococcal pneumonia and inhaled particles. *The Journal of experimental medicine*, **200**, 267–272.
- Arredouani MS, Palecanda A, Koziel H et al. (2005) MARCO Is the Major Binding Receptor for Unopsonized Particles and Bacteria on Human Alveolar Macrophages. *The Journal of Immunology*, **175**, 6058–6064.
- Arredouani MS, Yang Z, Imrich A, Ning Y, Qin G, Kobzik L (2006) The macrophage scavenger receptor SR-AI/II and lung defense against pneumococci and particles. *American Journal of Respiratory Cell and Molecular Biology*, **35**, 474–478.
- Arredouani MS, Palecanda A, Koziel H et al. (2013) MARCO Is the Major Binding Receptor for Unopsonized.
- Arroyo-Espliguero R, Avanzas P, Jeffery S, Kaski JC (2004) CD14 and toll-like receptor 4: a link between infection and acute coronary events? *Heart (British Cardiac Society)*, **90**, 983–8.
- Ashida K, Miyazaki K, Takayama E et al. (2005) Characterization of the Expression of TLR2 (Toll-like Receptor 2) and TLR4 on Circulating Monocytes in Coronary Artery Disease. *Journal of Atherosclerosis and Thrombosis*, **12**, 53–60.
- Auerbuch V, Brockstedt DG, Meyer-Morse N, O’Riordan M, Portnoy DA (2004) Mice lacking the type I interferon receptor are resistant to *Listeria monocytogenes*. *The Journal of experimental medicine*, **200**, 527–33.
- Auffray C, Sieweke MH, Geissmann F (2009) Blood monocytes: development, heterogeneity, and relationship with dendritic cells. *Annual review of immunology*, **27**, 669–92.
- Bandow K, Kusuyama J, Shamoto M, Kakimoto K, Ohnishi T, Matsuguchi T (2012) LPS-induced chemokine expression in both MyD88-dependent and -independent manners is regulated by Cot/Trp12-ERK axis in macrophages. *FEBS Letters*, **586**, 1540–1546.
- Barbierato M, Argentini C, Skaper SD (2012) Indirect immunofluorescence staining of cultured neural cells. *Methods in Molecular Biology*, **846**, 235–246.
- Basta G, Schmidt AM, De Caterina R (2004) Advanced glycation end products and vascular inflammation: Implications for accelerated atherosclerosis in diabetes. *Cardiovascular Research*, **63**, 582–592.
- Beishuizen A, Thijs LG (2003) Endotoxin and the hypothalamo-pituitary-adrenal (HPA)

- axis. *Journal of Endotoxin Research*, **9**, 3–24.
- Benard EL, Roobol SJ, Spaink HP, Meijer AH (2014) Phagocytosis of mycobacteria by zebrafish macrophages is dependent on the scavenger receptor Marco, a key control factor of pro-inflammatory signalling. *Developmental and Comparative Immunology*, **47**, 223–233.
- Beutler B (2000) Tlr4: Central component of the sole mammalian LPS sensor. *Current Opinion in Immunology*, **12**, 20–26.
- Blairon L, Wittebole X, Laterre PF (2003) Lipopolysaccharide-binding protein serum levels in patients with severe sepsis due to gram-positive and fungal infections. *J Infect Dis*, **187**, 287–291.
- Blanchet C, Jouvion G, Fitting C, Cavaillon JM, Adib-Conquy M (2014) Protective or deleterious role of scavenger receptors SR-A and CD36 on host resistance to *Staphylococcus aureus* depends on the site of infection. *PLoS ONE*, **9**.
- Bogdan C, Rölinghoff M, Diefenbach a (2000) The role of nitric oxide in innate immunity. *Immunological reviews*, **173**, 17–26.
- Bogoyevitch MA (2005) Therapeutic promise of JNK ATP-noncompetitive inhibitors. *Trends in Molecular Medicine*, **11**, 232–239.
- Bonizzi G, Karin M (2004) The two NF-kappaB activation pathways and their role in innate and adaptive immunity. *Trends in immunology*, **25**, 280–8.
- . Bowdish DME, Gordon S (2009) Conserved domains of the class A scavenger receptors: Evolution and function. *Immunological Reviews*, **227**, 19–31.
- Brogdon JL, Xu Y, Szabo SJ, An S, Buxton F, Cohen D, Huang Q (2007) Histone deacetylase activities are required for innate immune cell control of Th1 but not Th2 effector cell function. *Blood*, **109**, 1123–1130.
- Buechler C, Ritter M, Orsó E, Langmann T, Klucken J, Schmitz G (2000) Regulation of scavenger receptor CD163 expression in human monocytes and macrophages by pro- and anti-inflammatory stimuli. *Journal of leukocyte biology*, **67**, 97–103.
- Bultinck J, Sips P, Vakaet L, Brouckaert P, Cauwels A (2006) Systemic NO production during (septic) shock depends on parenchymal and not on hematopoietic cells: in vivo iNOS expression pattern in (septic) shock. *The FASEB journal : official publication of the Federation of American Societies for Experimental Biology*, **20**, 2363–2365.
- Bürkle A (2005) Poly(ADP-ribose): The most elaborate metabolite of NAD⁺. *FEBS Journal*, **272**, 4576–4589.
- Canton J, Neculai D, Grinstein S (2013) Scavenger receptors in homeostasis and immunity. *Nature reviews. Immunology*, **13**, 621–34.
- Carrillo A, Monreal Y, Ramirez P et al. (2005) Establishment of an immortalized PARP-1^{-/-} murine endothelial cell line: A new tool to study PARP-1 mediated endothelial cell dysfunction. *Journal of Cellular Biochemistry*, **94**, 1163–1174.
- Carty M, Goodbody R, Schröder M, Stack J, Moynagh PN, Bowie AG (2006) The human adaptor SARM negatively regulates adaptor protein TRIF-dependent Toll-like receptor signaling. *Nature immunology*, **7**, 1074–81.
- Cagri P, Lee Y ja, Ponzio T, Maric D, Spatz M, Bembry J, Hallenbeck J (2014) Poly(ADP-ribose) polymerase-1 and its cleavage products differentially modulate

- cellular protection through NF- κ B-dependent signaling. *Biochimica et Biophysica Acta - Molecular Cell Research*, **1843**, 640–651.
- Cepeda V, Fuertes M a, Castilla J, Alonso C, Quevedo C, Soto M, Pérez JM (2006) Poly(ADP-ribose) polymerase-1 (PARP-1) inhibitors in cancer chemotherapy. *Recent patents on anti-cancer drug discovery*, **1**, 39–53.
- Chaitanya G V, Steven AJ, Babu PP (2010) PARP-1 cleavage fragments: signatures of cell-death proteases in neurodegeneration. *Cell Commun Signal*, **8**, 31.
- Chandel NS, Trzyna WC, McClintock DS, Schumacker PT (2000) Role of Oxidants in NF- B Activation and TNF- Gene Transcription Induced by Hypoxia and Endotoxin. *The Journal of Immunology*, **165**, 1013–1021.
- Chávez-Sánchez L, Madrid-Miller A, Chávez-Rueda K, Legorreta-Haquet M V., Tesoro-Cruz E, Blanco-Favela F (2010) Activation of TLR2 and TLR4 by minimally modified low-density lipoprotein in human macrophages and monocytes triggers the inflammatory response. *Human Immunology*, **71**, 737–744.
- Chen F (2012) JNK-induced apoptosis, compensatory growth, and cancer stem cells. *Cancer Research*, **72**, 379–386.
- Chen Y, Wermeling F, Sundqvist J, Jonsson AB, Tryggvason K, Pikkarainen T, Karlsson MCI (2010) A regulatory role for macrophage class A scavenger receptors in TLR4-mediated LPS responses. *European Journal of Immunology*, **40**, 1451–1460.
- Chen X, Yang X, Liu T et al. (2012) Kaempferol regulates MAPKs and NF- κ B signaling pathways to attenuate LPS-induced acute lung injury in mice. *International Immunopharmacology*, **14**, 209–216.
- Chevanne M, Zampieri M, Caldini R et al. (2010) Inhibition of PARP activity by PJ-34 leads to growth impairment and cell death associated with aberrant mitotic pattern and nucleolar actin accumulation in M14 melanoma cell line. *Journal of Cellular Physiology*, **222**, 401–410.
- Chowdhury P, Sacks SH, Sheerin NS (2006) Toll-like receptors TLR2 and TLR4 initiate the innate immune response of the renal tubular epithelium to bacterial products. *Clinical and Experimental Immunology*, **145**, 346–356.
- Cie??lar-Pobuda A, Saenko Y, Rzeszowska-Wolny J (2012) PARP-1 inhibition induces a late increase in the level of reactive oxygen species in cells after ionizing radiation. *Mutation Research - Fundamental and Molecular Mechanisms of Mutagenesis*, **732**, 9–15.
- Cleveland MG, Gorham JD, Murphy TL, Tuomanen E, Murphy KM (1996) Lipoteichoic acid preparations of gram-positive bacteria induce interleukin-12 through a CD14-dependent pathway. *Infection and Immunity*, **64**, 1906–1912.
- Cohausz O, Althaus FR (2009) Role of PARP-1 and PARP-2 in the expression of apoptosis-regulating genes in HeLa cells. *Cell Biology and Toxicology*, **25**, 379–391.
- Cohen J (2002) The immunopathogenesis of sepsis. *Nature*, **420**, 885–891.
- Connelly L, Jacobs AT, Palacios-Callender M, Moncada S, Hobbs AJ (2003) Macrophage endothelial nitric-oxide synthase autoregulates cellular activation and pro-inflammatory protein expression. *Journal of Biological Chemistry*, **278**, 26480–26487.
- Cuzzocrea S (2005) Shock, inflammation and PARP. *Pharmacological Research*, **52**, 72–82.

- Czerkies M, Borzecka K, Zdioruk MI, Płóciennikowska A, Sobota A, Kwiatkowska K (2013) An interplay between scavenger receptor A and CD14 during activation of J774 cells by high concentrations of LPS. *Immunobiology*, **218**, 1217–1226.
- Daigneault M, Preston JA, Marriott HM, Whyte MKB, Dockrell DH (2010) The identification of markers of macrophage differentiation in PMA-stimulated THP-1 cells and monocyte-derived macrophages. *PLoS ONE*, **5**.
- Diya Zhang, Lili Chen, Shenglai Li, Zhiyuan Gu, Jie Yan (2008) Lipopolysaccharide (LPS) of *Porphyromonas gingivalis* induces IL-1beta, TNF-alpha and IL-6 production by THP-1 cells in a way different from that of *Escherichia coli* LPS. *Innate immunity*, **14**, 99–107.
- Doyle SE, O'Connell RM, Miranda G a et al. (2004) Toll-like receptors induce a phagocytic gene program through p38. *The Journal of experimental medicine*, **199**, 81–90.
- Dreskin SC, Thomas GW, Dale SN, Heasley LE (2001) Isoforms of Jun Kinase Are Differentially Expressed and Activated in Human Monocyte/Macrophage (THP-1) Cells. *The Journal of Immunology*, **166**, 5646–5653.
- Duan J, Duan J, Zhang Z, Tong T (2005) Irreversible cellular senescence induced by prolonged exposure to H₂O₂ involves DNA-damage-and-repair genes and telomere shortening. *International Journal of Biochemistry and Cell Biology*, **37**, 1407–1420.
- Dufour C, Corcione A, Svahn J et al. (2003) TNF-alpha and IFN-gamma are overexpressed in the bone marrow of Fanconi anemia patients and TNF-alpha suppresses erythropoiesis in vitro. *Blood*, **102**, 2053–2059.
- Duncan L, Yoshioka M, Chandad F, Grenier D (2004) Loss of lipopolysaccharide receptor CD14 from the surface of human macrophage-like cells mediated by *Porphyromonas gingivalis* outer membrane vesicles. *Microbial Pathogenesis*, **36**, 319–325.
- Dunne DW, Resnick D, Greenberg J, Krieger M, Joiner KA (1994) The type I macrophage scavenger receptor binds to gram-positive bacteria and recognizes lipoteichoic acid. *Proceedings of the National Academy of Sciences of the United States of America*, **91**, 1863–7.
- Dziarski R, Gupta D (2000) Role of MD-2 in TLR2- and TLR4-mediated recognition of Gram-negative and Gram-positive bacteria and activation of chemokine genes. *Journal of endotoxin research*, **6**, 401–405.
- Dziarski R, Viriyakosol S, Kirkland TN, Gupta D (2000) Soluble CD14 enhances membrane CD14-mediated responses to peptidoglycan: Structural requirements differ from those for responses to lipopolysaccharide. *Infection and Immunity*, **68**, 5254–5260.
- Van Eck M, Pennings M, Hoekstra M, Out R, Van Berkel TJ (2005) Scavenger receptor BI and ATP-binding cassette transporter A1 in reverse cholesterol transport and atherosclerosis. *Current opinion in lipidology*, **16**, 307–315.
- Edrees AF, Misra SN, Abdou NI (2005) Anti-tumor necrosis factor (TNF) therapy in rheumatoid arthritis: Correlation of TNF-alpha serum level with clinical response and benefit from changing dose or frequency of infliximab infusions. *Clinical and Experimental Rheumatology*, **23**, 469–474.
- El-Samalouti VT, Schletter J, Chyla I et al. (1999) Identification of the 80-kDa LPS-binding protein (LMP80) as decay-accelerating factor (DAF, CD55). *FEMS*

Immunology and Medical Microbiology, **23**, 259–269.

- Elass E, Coddeville B, Guérardel Y, Kremer L, Maes E, Mazurier J, Legrand D (2007) Identification by surface plasmon resonance of the mycobacterial lipomannan and lipoarabinomannan domains involved in binding to CD14 and LPS-binding protein. *FEBS Letters*, **581**, 1383–1390.
- Enkhbayar P, Kamiya M, Osaki M, Matsumoto T, Matsushima N (2004) Structural Principles of Leucine-Rich Repeat (LRR) Proteins. *Proteins: Structure, Function and Genetics*, **54**, 394–403.
- Erdelyi K, Bakondi E, Gergely P, Szabó C, Virág L (2005) Pathophysiologic role of oxidative stress-induced poly(ADP-ribose) polymerase-1 activation: Focus on cell death and transcriptional regulation. *Cellular and Molecular Life Sciences*, **62**, 751–759.
- Esposito E, Cuzzocrea S (2009) TNF-alpha as a therapeutic target in inflammatory diseases, ischemia-reperfusion injury and trauma. *Current medicinal chemistry*, **16**, 3152–67.
- Ferrante MC, Raso GM, Bilancione M, Esposito E, Iacono A, Melia R (2008) Differential modification of inflammatory enzymes in J774A.1 macrophages by ochratoxin A alone or in combination with lipopolysaccharide. *Toxicology Letters*, **181**, 40–46.
- Ferrero E, Jiao D, Tsuberi BZ, Tesio L, Rong GW, Haziot A, Goyert SM (1993) Transgenic mice expressing human CD14 are hypersensitive to lipopolysaccharide. *Proceedings of the National Academy of Sciences of the United States of America*, **90**, 2380–4.
- Finch KE, Knezevic CE, Nottbohm AC, Partlow KC, Hergenrother PJ (2012) Selective small molecule inhibition of poly(ADP-ribose) glycohydrolase (PARG). *ACS Chemical Biology*, **7**, 563–570.
- Fisher AEO, Hohegger H, Takeda S, Caldecott KW (2007) Poly(ADP-ribose) polymerase 1 accelerates single-strand break repair in concert with poly(ADP-ribose) glycohydrolase. *Molecular and cellular biology*, **27**, 5597–5605.
- Frazier WJ, Xue J, Luce WA, Liu Y (2012) MAPK Signaling Drives Inflammation in LPS-Stimulated Cardiomyocytes: The Route of Crosstalk to G-Protein-Coupled Receptors. *PLoS ONE*, **7**.
- Freeman BD, Natanson C (2000) Anti-inflammatory therapies in sepsis and septic shock. *Expert opinion on investigational drugs*, **9**, 1651–63.
- Frink M, van Griensven M, Kobbe P et al. (2009) IL-6 predicts organ dysfunction and mortality in patients with multiple injuries. *Scandinavian journal of trauma, resuscitation and emergency medicine*, **17**, 49.
- Fujioka S, Niu J, Schmidt C et al. (2004) NF-kappaB and AP-1 connection: mechanism of NF-kappaB-dependent regulation of AP-1 activity. *Molecular and cellular biology*, **24**, 7806–19.
- Furusako S, Takahashi T, Mori S, Takahashi Y, Tsuda T, Namba M, Mochizuki H (2001) Protection of mice from LPS-induced shock by CD14 antisense oligonucleotide. *Acta Medica Okayama*, **55**, 105–115.
- Gamble C, McIntosh K, Scott R, Ho KH, Plevin R, Paul A (2012) Inhibitory kappa B kinases as targets for pharmacological regulation. *British Journal of Pharmacology*, **165**, 802–819.

- Gangloff SC, Zahringer U, Blondin C, Guenounou M, Silver J, Goyert SM (2005) Influence of CD14 on Ligand Interactions between Lipopolysaccharide and Its Receptor Complex. *The Journal of Immunology*, **175**, 3940–3945.
- Garcia Soriano F, Virág L, Jagtap P et al. (2001) Diabetic endothelial dysfunction: the role of poly(ADP-ribose) polymerase activation. *Nature medicine*, **7**, 108–113.
- Gauglitz GG, Callenberg H, Weindl G, Korting HC (2012) Host defence against *Candida albicans* and the role of pattern-recognition receptors. *Acta Dermato-Venereologica*, **92**, 291–298.
- Geraets L, Moonen HJJ, Brauers K, Gottschalk RWH, Wouters EFM, Bast A, Hageman GJ (2007) Flavone as PARP-1 inhibitor: Its effect on lipopolysaccharide induced gene-expression. *European Journal of Pharmacology*, **573**, 241–248.
- Ghosh S, Hayden MS (2008) New regulators of NF-kappaB in inflammation. *Nature Reviews Immunology*, **8**, 837–848.
- Di Gioia M, Zanoni I (2015) Toll-like receptor co-receptors as master regulators of the immune response. *Molecular Immunology*, **63**, 143–152.
- Godon C, Cordelières FP, Biard D, Giocanti N, Mégnin-Chanet F, Hall J, Favaudon V (2008) PARP inhibition versus PARP-1 silencing: Different outcomes in terms of single-strand break repair and radiation susceptibility. *Nucleic Acids Research*, **36**, 4454–4464.
- Goh JWK, Tan YS, Dodds AW, Reid KBM, Lu J (2010) The class A macrophage scavenger receptor type I (SR-AI) recognizes complement iC3b and mediates NF-??B activation. *Protein and Cell*, **1**, 174–187.
- Goldfarb M (2007) Computer analysis of two-dimensional gels. *Journal of Biomolecular Techniques*, **18**, 143–146.
- Gonzalez-Quintela A, Alonso M, Campos J, Vizcaino L, Loidi L, Gude F (2013) Determinants of Serum Concentrations of Lipopolysaccharide-Binding Protein (LBP) in the Adult Population: The Role of Obesity. *PLoS ONE*, **8**.
- Gordon S (2002) Pattern recognition receptors: Doubling up for the innate immune response. *Cell*, **111**, 927–930.
- Gordon S, Taylor PR (2005) Monocyte and macrophage heterogeneity. *Nature Reviews Immunology*, **5**, 953–964.
- Gough PJ, Greaves DR, Gordon S (1998) A naturally occurring isoform of the human macrophage scavenger receptor (SR-A) gene generated by alternative splicing blocks modified LDL uptake. *J Lipid Res*, **39**, 531–543.
- Granucci F, Petralia F, Urbano M, Citterio S, Di Tota F, Santambrogio L, Ricciardi-Castagnoli P (2003) The scavenger receptor MARCO mediates cytoskeleton rearrangements in dendritic cells and microglia. *Blood*, **102**, 2940–2947.
- Greaves DR, Gordon S (2005) Thematic review series: the immune system and atherogenesis. Recent insights into the biology of macrophage scavenger receptors. *J Lipid Res*, **46**, 11–20.
- Gregory AP, Dendrou CA, Attfield KE et al. (2012) TNF receptor 1 genetic risk mirrors outcome of anti-TNF therapy in multiple sclerosis. *Nature*, **488**, 508–11.
- Griffin JD, Ritz J, Nadler LM, Schlossman SF (1981) Expression of myeloid differentiation antigens on normal and malignant myeloid cells. *The Journal of*

- clinical investigation*, **68**, 932–41.
- Gromova I, Celis JE (2006) Protein Detection in Gels by Silver Staining : A Procedure Compatible with Mass Spectrometry. 219–223.
- Gronow S, Brade H (2001) Lipopolysaccharide biosynthesis: which steps do bacteria need to survive? *Journal of endotoxin research*, **7**, 3–23.
- Guha M, Mackman N (2001) LPS induction of gene expression in human monocytes. *Cellular Signalling*, **13**, 85–94.
- Gupta N, Tanner S, Jaitly N et al. (2007) Whole proteome analysis of post-translational modifications: Applications of mass-spectrometry for proteogenomic annotation. *Genome Research*, **17**, 1362–1377.
- Gupta SC, Sundaram C, Reuter S, Aggarwal BB (2010) Inhibiting NF- κ B activation by small molecules as a therapeutic strategy. *Biochimica et Biophysica Acta - Gene Regulatory Mechanisms*, **1799**, 775–787.
- Gupta S, Sundaram C, Reuter S, Aggarwal B (2011) Inhibiting NF- κ B Activation by Small Molecules As a Therapeutic Strategy. *Biochim Biophys Acta*, **1799**, 775–787.
- Gustot T, Durand F, Lebrec D, Vincent JL, Moreau R (2009) Severe sepsis in cirrhosis. *Hepatology*, **50**, 2022–2033.
- Gutsmann T, Müller M, Carroll SF, MacKenzie RC, Wiese A, Seydel U (2001) Dual role of lipopolysaccharide (LPS)-binding protein in neutralization of LPS and enhancement of LPS-induced activation of mononuclear cells. *Infection and Immunity*, **69**, 6942–6950.
- Gutsmann T, Haberer N, Carroll SF, Seydel U, Wiese A (2001) Interaction between lipopolysaccharide (LPS), LPS-binding protein (LBP), and planar membranes. *Biological Chemistry*, **382**, 425–434.
- Ha HC, Snyder SH (1999) Poly(ADP-ribose) polymerase is a mediator of necrotic cell death by ATP depletion. *Proceedings of the National Academy of Sciences of the United States of America*, **96**, 13978–82.
- Ha HC, Hester LD, Snyder SH (2002) Poly(ADP-ribose) polymerase-1 dependence of stress-induced transcription factors and associated gene expression in glia. *Proceedings of the National Academy of Sciences of the United States of America*, **99**, 3270–3275.
- Hacker J, Carniel E (2001) Ecological fitness, genomic islands and bacterial pathogenicity A Darwinian view of the evolution of microbes. *EMBO reports*, **2**, 376–381.
- Hacker J, Kaper JB (2000) PATHOGENICITY ISLANDS AND THE EVOLUTION OF MICROBES. *Annu. Rev. Microbiol*, **54**, 641–79.
- Hagelueken G, Clarke BR, Huang H et al. (2015) A coiled-coil domain acts as a molecular ruler to regulate O-antigen chain length in lipopolysaccharide. *Nature Structural & Molecular Biology*, **22**, 50–56.
- Hamann L, Alexander C, Stamme C, Zähringer U, Schumann RR (2005) Acute-phase concentrations of lipopolysaccharide (LPS)-binding protein inhibit innate immune cell activation by different LPS chemotypes via different mechanisms. *Infection and Immunity*, **73**, 193–200.
- Hao N, O'Shea EK (2012) Signal-dependent dynamics of transcription factor

- translocation controls gene expression. *TL - 19. Nature structural & molecular biology*, **19** VN-r, 31–39.
- Harris HE, Andersson U (2004) The nuclear protein HMGB1 as a proinflammatory mediator. *European Journal of Immunology*, **34**, 1503–1512.
- Harris CL, Pettigrew DM, Lea SM, Morgan BP (2006) Decay-Accelerating Factor Must Bind Both Components of the Complement Alternative Pathway C3 Convertase to Mediate Efficient Decay. *The Journal of Immunology*, **178**, 352–359.
- Hassa PO, Hottiger MO (2005) A role of poly (ADP-ribose) polymerase in NF-kappaB transcriptional activation. *Biological chemistry*, **380**, 953–959.
- Hassa PO, Covic M, Hasan S, Imhof R, Hottiger MO (2001) The Enzymatic and DNA Binding Activity of PARP-1 Are Not Required for NF-??B Coactivator Function. *Journal of Biological Chemistry*, **276**, 45588–45597.
- Hassa PO, Haenni SS, Buerki C et al. (2005) Acetylation of poly(ADP-ribose) polymerase-1 by p300/CREB-binding protein regulates coactivation of NF-κB-dependent transcription. *Journal of Biological Chemistry*, **280**, 40450–40464.
- Haworth R, Platt N, Keshav S et al. (1997) The macrophage scavenger receptor type A is expressed by activated macrophages and protects the host against lethal endotoxic shock. *The Journal of experimental medicine*, **186**, 1431–1439.
- Haziot A, Ferrero E, Köntgen F et al. (1996) Resistance to endotoxin shock and reduced dissemination of gram-negative bacteria in CD14-deficient mice. *Immunity*, **4**, 407–414.
- Heeres JT, Hergenrother PJ (2007) Poly(ADP-ribose) makes a date with death. *Current Opinion in Chemical Biology*, **11**, 644–653.
- Heidenreich S, Schmidt M, August C, Cullen P, Rademaekers A, Pauels HG (1997) Regulation of human monocyte apoptosis by the CD14 molecule. *Journal of immunology (Baltimore, Md. : 1950)*, **159**, 3178–88.
- Heinzmann A, Dietrich H, Deichmann KA (2003) Association of uteroglobulin-related protein 1 with bronchial asthma. *International Archives of Allergy and Immunology*, **131**, 291–295.
- Hereg Z, Wang ZQ (2001) Functions of poly(ADP-ribose) polymerase (PARP) in DNA repair, genomic integrity and cell death. *Mutation Research - Fundamental and Molecular Mechanisms of Mutagenesis*, **477**, 97–110.
- Hinz M, Arslan SÇ, Scheidereit C (2012) It takes two to tango: IκBs, the multifunctional partners of NF-κB. *Immunological Reviews*, **246**, 59–76.
- Hiomura K, Furuhashi M, Minami K, Miyazaki K, Yoshida K, Kuno N, Ishikawa K (2007) Life-threatening septic shock in a pregnant woman with ileus. *The journal of maternal-fetal & neonatal medicine : the official journal of the European Association of Perinatal Medicine, the Federation of Asia and Oceania Perinatal Societies, the International Society of Perinatal Obstetricians*, **20**, 491–493.
- Hodgkinson CP, Laxton RC, Patel K, Ye S (2008) Advanced glycation end-product of low density lipoprotein activates the toll-like 4 receptor pathway implications for diabetic atherosclerosis. *Arteriosclerosis, Thrombosis, and Vascular Biology*, **28**, 2275–2281.
- Hofer TP, Bitterle E, Beck-Speier I, Maier KL, Frankenberger M, Heyder J, Ziegler-Heitbrock L (2004) Diesel exhaust particles increase LPS-stimulated COX-2

- expression and PGE2 production in human monocytes. *Journal of Leukocyte Biology*, **75**, 856–864.
- Holgate ST, Bodey KS, Janezic A, Frew AJ, Kaplan AP, Teran LM (1997) Release of RANTES, MIP-1 α , and MCP-1 into asthmatic airways following endobronchial allergen challenge. *American Journal of Respiratory and Critical Care Medicine*, **156**, 1377–1383.
- Hsu HY, Nicholson AC, Hajjar DP (1996) Inhibition of macrophage scavenger receptor activity by tumor necrosis factor-alpha is transcriptionally and post-transcriptionally regulated. *The Journal of biological chemistry*, **271**, 7767–73.
- Huang FC (2009) Upregulation of salmonella-induced IL-6 production in caco-2 cells by PJ-34, parp-1 inhibitor: Involvement of PI3K, p38 MAPK, ERK, JNK, and NF- B. *Mediators of Inflammation*, **2009**.
- Huang C, Sloan EA, Boerkoel CF (2003) Chromatin remodeling and human disease. *Curr Opin Genet Dev*, **13**, 246–252.
- Huang Z, Wang C, Wei L et al. (2008) Resveratrol inhibits EMMPRIN expression via P38 and ERK1/2 pathways in PMA-induced THP-1 cells. *Biochemical and Biophysical Research Communications*, **374**, 517–521.
- Huang G, Shi LZ, Chi H (2009) Regulation of JNK and p38 MAPK in the immune system: Signal integration, propagation and termination. *Cytokine*, **48**, 161–169.
- Huang L, Xuan Y, Koide Y, Zhiyentayev T, Tanaka M, Hamblin MR (2012) Type I and Type II mechanisms of antimicrobial photodynamic therapy: An in vitro study on gram-negative and gram-positive bacteria. *Lasers in Surgery and Medicine*, **44**, 490–499.
- Huber A, Bai P, Murcia JM De, Murcia G De (2004) PARP-1, PARP-2 and ATM in the DNA damage response: Functional synergy in mouse development. *DNA Repair*, **3**, 1103–1108.
- Huber M, Kalis C, Keck S et al. (2006) R-form LPS, the master key to the activation of TLR4/MD-2-positive cells. *European Journal of Immunology*, **36**, 701–711.
- Hunter JD, Doddi M (2010) Sepsis and the heart. *British Journal of Anaesthesia*, **104**, 3–11.
- Hunter JE, Willmore E, Irving J a E, Hostomsky Z, Veuger SJ, Durkacz BW (2012) NF- κ B mediates radio-sensitization by the PARP-1 inhibitor, AG-014699. *Oncogene*, **31**, 251–264.
- Husemann J, Loike JD, Anankov R, Febbraio M, Silverstein SC (2002) Scavenger receptors in neurobiology and neuropathology: Their role on microglia and other cells of the nervous system. *GLIA*, **40**, 195–205.
- Hussell T, Bell TJ (2014) Alveolar macrophages: plasticity in a tissue-specific context. *Nature reviews. Immunology*, **14**, 81–93.
- Hüttemann M, Lee I, Gao X et al. (2012) Cytochrome c oxidase subunit 4 isoform 2-knockout mice show reduced enzyme activity, airway hyporeactivity, and lung pathology. *The FASEB Journal*, **26** VN-r, 3916–3930.
- Iovine N, Eastvold J, Elsbach P, Weiss JP, Gioannini TL (2002) The carboxyl-terminal domain of closely related endotoxin-binding proteins determines the target of protein-lipopolysaccharide complexes. *Journal of Biological Chemistry*, **277**, 7970–7978.

- Issaq HJ, Veenstra TD (2008) Two-dimensional polyacrylamide gel electrophoresis (2D-PAGE): Advances and perspectives. *BioTechniques*, **44**, 697–700.
- Iwahashi H, Takeshita A, Hanazawa S (2000) Prostaglandin E2 stimulates AP-1-mediated CD14 expression in mouse macrophages via cyclic AMP-dependent protein kinase A. *J Immunol*, **164**, 5403–5408.
- Iwasaki A, Medzhitov R (2004) Toll-like receptor control of the adaptive immune responses. *Nature immunology*, **5**, 987–95.
- Jabeen A, Miranda-Sayago JM, Obara B et al. (2013) Quantified colocalization reveals heterotypic histocompatibility class I antigen associations on trophoblast cell membranes: relevance for human pregnancy. *Biology of reproduction*, **89**, 94.
- Janeway C, Medzhitov R (2000) Viral interference with IL-1 and toll signaling. *Proceedings of the National Academy of Sciences of the United States of America*, **97**, 10682–10683.
- Janeway CA, Medzhitov R (2002) Innate immune recognition. *Annual review of immunology*, **20**, 197–216.
- Jang CH, Choi JH, Byun MS, Jue DM (2006) Chloroquine inhibits production of TNF- α , IL-1 β and IL-6 from lipopolysaccharide-stimulated human monocytes/macrophages by different modes. *Rheumatology*, **45**, 703–710.
- Jerala R (2007) Structural biology of the LPS recognition. *International Journal of Medical Microbiology*, **297**, 353–363.
- Jessen KM, Lindboe SB, Petersen AL, Eugen-Olsen J, Benfield T (2007) Common TNF- α , IL-1 β , PAI-1, uPA, CD14 and TLR4 polymorphisms are not associated with disease severity or outcome from Gram negative sepsis. *BMC infectious diseases*, **7**, 108.
- Jiang Z, Georgel P, Du X et al. (2005) CD14 is required for MyD88-independent LPS signaling. *Nature immunology*, **6**, 565–570.
- Jiang Y, Oliver P, Davies KE, Platt N (2006) Identification and characterization of murine SCARA5, a novel class A scavenger receptor that is expressed by populations of epithelial cells. *The Journal of biological chemistry*, **281**, 11834–45.
- Johnson GL, Johnson GL, Lapadat R, Lapadat R (2002) Mitogen-Activated Protein Kinase Pathways Mediated by ERK, JNK, and p38 Protein Kinases. *Science*, **298**, 1911–1912.
- Joyce D, Albanese C, Steer J, Fu M, Bouzahzah B, Pestell RG (2001) NF- κ B and cell-cycle regulation: The cyclin connection. *Cytokine and Growth Factor Reviews*, **12**, 73–90.
- Kaisho T, Takeuchi O, Kawai T, Hoshino K, Akira S (2001) Endotoxin-induced maturation of MyD88-deficient dendritic cells. *Journal of immunology (Baltimore, Md. : 1950)*, **166**, 5688–94.
- Kamath KS, Vasavada MS, Srivastava S (2011) Proteomic databases and tools to decipher post-translational modifications. *Journal of Proteomics*, **75**, 127–144.
- Kanno S, Furuyama A, Hirano S (2007) A murine scavenger receptor MARCO recognizes polystyrene nanoparticles. *Toxicological Sciences*, **97**, 398–406.
- Karlsson MCI, Guinamard R, Bolland S, Sankala M, Steinman RM, Ravetch J V (2003) Macrophages control the retention and trafficking of B lymphocytes in the splenic

- marginal zone. *The Journal of experimental medicine*, **198**, 333–340.
- Kasimanickam RK, Kasimanickam VR, Olsen JR, Jeffress EJ, Moore D a, Kastelic JP (2013) Associations among serum pro- and anti-inflammatory cytokines, metabolic mediators, body condition, and uterine disease in postpartum dairy cows. *Reproductive biology and endocrinology : RB&E*, **11**, 103.
- Kawai T, Akira S (2007) Signaling to NF- κ B by Toll-like receptors. *Trends in Molecular Medicine*, **13**, 460–469.
- Kawai T, Akira S (2010) The role of pattern-recognition receptors in innate immunity: update on Toll-like receptors. *Nature immunology*, **11**, 373–84.
- Kawai T, Adachi O, Ogawa T, Takeda K, Akira S (1999) Unresponsiveness of MyD88-deficient mice to endotoxin. *Immunity*, **11**, 115–122.
- Kellermayer Z, Fisi V, Mihalj M, Berta G, Kóbor J, Balogh P (2014) Marginal Zone Macrophage Receptor MARCO Is Trapped in Conduits Formed by Follicular Dendritic Cells in the Spleen. *The journal of histochemistry and cytochemistry : official journal of the Histochemistry Society*, **62**, 436–449.
- El Khoury J, Hickman SE, Thomas CA, Cao L, Silverstein SC, Loike JD (1996) Scavenger receptor-mediated adhesion of microglia to beta-amyloid fibrils. *Nature*, **382**, 716–719.
- Kim D, Kim JY (2014) Anti-CD14 antibody reduces LPS responsiveness via TLR4 internalization in human monocytes. *Molecular Immunology*, **57**, 210–215.
- Kim J, Krueger JG (2015) The Immunopathogenesis of Psoriasis. *Dermatologic Clinics*, **33**, 13–23.
- Kim MY, Mauro S, G??vry N, Lis JT, Kraus WL (2004) NAD⁺-dependent modulation of chromatin structure and transcription by nucleosome binding properties of PARP-1. *Cell*, **119**, 803–814.
- Kim JI, Chang JL, Mi SJ, Lee CH, Paik SG, Lee H, Lee JO (2005) Crystal structure of CD14 and its implications for lipopolysaccharide signaling. *Journal of Biological Chemistry*, **280**, 11347–11351.
- Kim MY, Zhang T, Kraus WL (2005) Poly(ADP-ribosyl)ation by PARP-1: “PAR-laying” NAD⁺ into a nuclear signal. *Genes and Development*, **19**, 1951–1967.
- Kim ML, Jeong HG, Kasper CA, Arrieumerlou C (2010) IKK γ contributes to canonical NF- κ B activation downstream of Nod1-mediated peptidoglycan recognition. *PLoS ONE*, **5**.
- Kimura S, Tamamura T, Nakagawa I, Koga T, Fujiwara T, Hamada S (2000) CD14-dependent and independent pathways in lipopolysaccharide-induced activation of a murine B-cell line, CH12.LX. *Scandinavian Journal of Immunology*, **51**, 392–399.
- Kitasato A, Tajima Y, Kuroki T, Tsutsumi R, Adachi T, Mishima T, Kanematsu T (2007) Inflammatory cytokines promote inducible nitric oxide synthase-mediated DNA damage in hamster gallbladder epithelial cells. *World Journal of Gastroenterology*, **13**, 6379–6384.
- Kitchens RL, Munford RS (1998) CD14-dependent internalization of bacterial lipopolysaccharide (LPS) is strongly influenced by LPS aggregation but not by cellular responses to LPS. *Journal of immunology (Baltimore, Md. : 1950)*, **160**, 1920–1928.

- Kitchens RL, Thompson P a (2005) Modulatory effects of sCD14 and LBP on LPS-host cell interactions. *Journal of endotoxin research*, **11**, 225–229.
- Kitchens RL, Thompson PA, Viriyakosol S, O’Keefe GE, Munford RS (2001) Plasma CD14 decreases monocyte responses to LPS by transferring cell-bound LPS to plasma lipoproteins. *Journal of Clinical Investigation*, **108**, 485–493.
- Knoll P, Schlaak J, Uhrig A, Kempf P, zum Büschenfelde KHM, Gerken G (1995) Human Kupffer cells secrete IL-10 in response to lipopolysaccharide (LPS) challenge. *Journal of Hepatology*, **22**, 226–229.
- Kobayashi Y, Miyaji C, Watanabe H et al. (2000) Role of macrophage scavenger receptor in endotoxin shock. *The Journal of pathology*, **192**, 263–72.
- Kohro T, Tanaka T, Murakami T, Wada Y, Aburatani H, Hamakubo T, Kodama T (2004) A comparison of differences in the gene expression profiles of phorbol 12-myristate 13-acetate differentiated THP-1 cells and human monocyte-derived macrophage. *Journal of atherosclerosis and thrombosis*, **11**, 88–97.
- Koppolu P, Durvasula S, Palaparthi R, Rao M, Sagar V, Reddy SK, Lingam S (2013) Estimate of CRP and TNF-alpha level before and after periodontal therapy in cardiovascular disease patients. *Pan African Medical Journal*, **15**.
- Kraal G, Van Der Laan LJW, Elomaa O, Tryggvason K (2000) The macrophage receptor MARCO. *Microbes and Infection*, **2**, 313–316.
- Kraus WL, Hottiger MO (2013) PARP-1 and gene regulation: Progress and puzzles. *Molecular Aspects of Medicine*, **34**, 1109–1123.
- Kravchenko V V, Kaufmann GF, Mathison JC et al. (2008) Modulation of gene expression via disruption of NF-kappaB signaling by a bacterial small molecule. *Science (New York, N.Y.)*, **321**, 259–263.
- Krietsch J, Caron M-C, Gagné J-P et al. (2012) PARP activation regulates the RNA-binding protein NONO in the DNA damage response to DNA double-strand breaks. *Nucleic acids research*, **40**, 10287–301.
- Krishnakumar R, Kraus WL (2010) The PARP Side of the Nucleus: Molecular Actions, Physiological Outcomes, and Clinical Targets. *Molecular Cell*, **39**, 8–24.
- Kumagai Y, Akira S (2010) Identification and functions of pattern-recognition receptors. *Journal of Allergy and Clinical Immunology*, **125**, 985–992.
- Kumar H, Kawai T, Akira S (2011) Pathogen recognition by the innate immune system. *International reviews of immunology*, **30**, 16–34.
- Kumar PA, Chitra PS, Lu C, Sobhanaditya J, Menon R (2014) Growth hormone (GH) differentially regulates NF-kB activity in preadipocytes and macrophages: Implications for GH’s role in adipose tissue homeostasis in obesity. *Journal of Physiology and Biochemistry*, **70**, 433–440.
- Kumar A, Singh UK, Kini SG et al. (2015) JNK pathway signaling: a novel and smarter therapeutic targets for various biological diseases. *Future medicinal chemistry*, **7**, 2065–86.
- De La Garza R (2005) Endotoxin- or pro-inflammatory cytokine-induced sickness behavior as an animal model of depression: Focus on anhedonia. *Neuroscience and Biobehavioral Reviews*, **29**, 761–770.
- Laird MHW, Rhee SH, Perkins DJ, Medvedev AE, Piao W, Fenton MJ, Vogel SN (2009)

- TLR4/MyD88/PI3K interactions regulate TLR4 signaling. *Journal of leukocyte biology*, **85**, 966–77.
- Lamkanfi M, Festjens N, Declercq W, Vanden Berghe T, Vandenabeele P (2007) Caspases in cell survival, proliferation and differentiation. *Cell death and differentiation*, **14**, 44–55.
- Lamon BD, Upmacis RK, Deeb RS, Koyuncu H, Hajjar DP (2010) Inducible nitric oxide synthase gene deletion exaggerates MAPK-mediated cyclooxygenase-2 induction by inflammatory stimuli. *American journal of physiology. Heart and circulatory physiology*, **299**, H613–H623.
- Landmann R, Knopf HP, Link S, Sansano S, Schumann R, Zimmerli W (1996) Human monocyte CD14 is upregulated by lipopolysaccharide. *Infection and Immunity*, **64**, 1762–1769.
- Langelier MF, Planck JL, Roy S, Pascal JM (2011) Crystal structures of poly(ADP-ribose) polymerase-1 (PARP-1) zinc fingers bound to DNA: Structural and functional insights into DNA-dependent PARP-1 activity. *Journal of Biological Chemistry*, **286**, 10690–10701.
- Laudisi F, Sambucci M, Pioli C (2011) Poly (ADP-ribose) polymerase-1 (PARP-1) as immune regulator. *Endocrine, metabolic & immune disorders drug targets*, **11**, 326–33.
- Lawrence T (2009) The nuclear factor NF-kappaB pathway in inflammation. *Cold Spring Harbor perspectives in biology*, **1**.
- Lee MS, Kim Y-J (2007) Pattern-recognition receptor signaling initiated from extracellular, membrane, and cytoplasmic space. *Molecules and cells*, **23**, 1–10.
- Lee JD, Kravchenko V, Kirkland TN et al. (1993) Glycosyl-phosphatidylinositol-anchored or integral membrane forms of CD14 mediate identical cellular responses to endotoxin. *Proc Natl Acad Sci U S A*, **90**, 9930–9934.
- van Lenten BJ, Fogelman AM (1992) Lipopolysaccharide-induced inhibition of scavenger receptor expression in human monocyte-macrophages is mediated through tumor necrosis factor-alpha. *Journal of immunology (Baltimore, Md. : 1950)*, **148**, 112–116.
- Leon-Ponte M, Kirchhof MG, Sun T, Stephens T, Singh B, Sandhu S, Madrenas J (2005) Polycationic lipids inhibit the pro-inflammatory response to LPS. *Immunology Letters*, **96**, 73–83.
- Leung A, Todorova T, Ando Y, Chang P (2012) Poly(ADP-ribose) regulates post-transcriptional gene regulation in the cytoplasm. *RNA biology*, **9**, 542–8.
- Levy E, Xanthou G, Petrakou E, Zacharioubaki V, Tsatsanis C, Fotopoulos S, Xanthou M (2009) Distinct roles of TLR4 and CD14 in LPS-induced inflammatory responses of neonates. *Pediatric Research*, **66**, 179–184.
- Li Q, Verma IM (2002) NF-kappaB regulation in the immune system. *Nature reviews. Immunology*, **2**, 725–34.
- Liaudet L, Mabley JG, Pacher P et al. (2002) Inosine exerts a broad range of antiinflammatory effects in a murine model of acute lung injury. *Ann Surg*, **235**, 568–578.
- Liaudet L, Pacher P L, Mabley JG, Virag L, Soriano FG, Hask G, Szab C (2002) Activation of poly(ADP-ribose) polymerase-1 is a central mechanism of

- lipopolysaccharide-induced acute lung inflammation. *American Journal of Respiratory and Critical Care Medicine*, **165**, 372–377.
- Lin JY, Tang CY (2007) Interleukin-10 administration inhibits TNF- α and IL-1 β , but not IL-6, secretion of LPS-stimulated peritoneal macrophages. *Journal of Food and Drug Analysis*, **15**, 48–54.
- Linton MF, Fazio S (2001) Class A scavenger receptors, macrophages, and atherosclerosis. *Curr Opin Lipidol*, **12**, 489–495.
- Liu L, Ke Y, Jiang X et al. (2012) Lipopolysaccharide activates ERK-PARP-1-RelA pathway and promotes nuclear factor- κ B transcription in murine macrophages. *Human Immunology*, **73**, 439–447.
- Lizundia R, Sauter K-S, Taylor G, Werling D (2008) Host species-specific usage of the TLR4-LPS receptor complex. *Innate immunity*, **14**, 223–231.
- Loutet SA, Flannagan RS, Kooi C, Sokol PA, Valvano MA (2006) A complete lipopolysaccharide inner core oligosaccharide is required for resistance of *Burkholderia cenocepacia* to antimicrobial peptides and bacterial survival in vivo. *Journal of Bacteriology*, **188**, 2073–2080.
- Lu Y-C, Yeh W-C, Ohashi PS (2008) LPS/TLR4 signal transduction pathway. *Cytokine*, **42**, 145–151.
- Lu Y, Suh SJ, Kwak CH et al. (2012) Saucerneol F, a new lignan, inhibits iNOS expression via MAPKs, NF- κ B and AP-1 inactivation in LPS-induced RAW264.7 cells. *International Immunopharmacology*, **12**, 175–181.
- Luo X, Lee Kraus W (2012) On par with PARP: Cellular stress signaling through poly(ADP-ribose) and PARP-1. *Genes and Development*, **26**, 417–432.
- Manassero G, Repetto IE, Cobianchi S, Valsecchi V, Bonny C, Rossi F, Vercelli A (2012) Role of JNK isoforms in the development of neuropathic pain following sciatic nerve transection in the mouse. *Molecular Pain*, **8**, 39.
- Mangan DF, Wahl SM (1991) Differential regulation of human monocyte programmed cell death (apoptosis) by chemotactic factors and pro-inflammatory cytokines. *J Immunol*, **147**, 3408–3412.
- Manukyan M, Triantafilou K, Triantafilou M et al. (2005) Binding of lipopeptide to CD14 induces physical proximity of CD14, TLR2 and TLR1. *European Journal of Immunology*, **35**, 911–921.
- Martinez FO (2008) Macrophage activation and polarization. *Frontiers in Bioscience*, **13**, 453.
- Martínez VG, Moestrup SK, Holmskov U, Mollenhauer J, Lozano F (2011) The conserved scavenger receptor cysteine-rich superfamily in therapy and diagnosis. *Pharmacological reviews*, **63**, 967–1000.
- Mazzone GL, Nistri A (2011) Effect of the PARP-1 inhibitor PJ 34 on excitotoxic damage evoked by kainate on rat spinal cord organotypic slices. *Cellular and Molecular Neurobiology*, **31**, 469–478.
- Meder VS, Boeglin M, de Murcia G, Schreiber V (2005) PARP-1 and PARP-2 interact with nucleophosmin/B23 and accumulate in transcriptionally active nucleoli. *Journal of cell science*, **118**, 211–222.
- Mehan S, Meena H, Sharma D, Sankhla R (2011) JNK: A stress-activated protein kinase

- therapeutic strategies and involvement in Alzheimer's and various neurodegenerative abnormalities. *Journal of Molecular Neuroscience*, **43**, 376–390.
- Miller SI, Ernst RK, Bader MW (2005) LPS, TLR4 and infectious disease diversity TL - 3. *Nature Reviews Microbiology*, **3** VN-re, 36–46.
- Min W, Wang Z-Q (2009) Poly (ADP-ribose) glycohydrolase (PARG) and its therapeutic potential. *Frontiers in bioscience : a journal and virtual library*, **14**, 1619–1626.
- Minucci S, Pelicci PG (2006) Histone deacetylase inhibitors and the promise of epigenetic (and more) treatments for cancer. *Nature reviews Cancer*, **6**, 38–51.
- Mishra AK, Driessen NN, Appelmeik BJ, Besra GS (2011) Lipoarabinomannan and related glycoconjugates: Structure, biogenesis and role in Mycobacterium tuberculosis physiology and host-pathogen interaction. *FEMS Microbiology Reviews*, **35**, 1126–1157.
- Moncada S, Higgs EA, Hodson HF et al. (1991) The l-Arginine: Nitric Oxide Pathway. *Journal of Cardiovascular Pharmacology*, **17**, S1&hyhen;S9.
- Moore KJ, Andersson LP, Ingalls RR et al. (2000) Divergent response to LPS and bacteria in CD14-deficient murine macrophages. *The Journal of Immunology*, **165**, 4272–4280.
- Mukhopadhyay S, Chen Y, Sankala M et al. (2006) MARCO, an innate activation marker of macrophages, is a class A scavenger receptor for Neisseria meningitidis. *European Journal of Immunology*, **36**, 940–949.
- Murai J, Huang SYN, Das BB et al. (2012) Trapping of PARP1 and PARP2 by clinical PARP inhibitors. *Cancer Research*, **72**, 5588–5599.
- Murakami K, Enkhbaatar P, Shimoda K et al. (2004) Inhibition of poly (ADP-ribose) polymerase attenuates acute lung injury in an ovine model of sepsis. *Shock*, **21**, 126–133.
- Murray PJ, Wynn TA (2011) Protective and pathogenic functions of macrophage subsets. *Nature Reviews Immunology*, **11**, 723–737.
- Naito M, Kodama T, Matsumoto A, Doi T, Takahashi K (1991) Tissue distribution, intracellular localization, and in vitro expression of bovine macrophage scavenger receptors. *Am J Pathol*, **139**, 1411–1423.
- Nakajima H (2004) Critical role of the automodification of poly(ADP-ribose) polymerase-1 in nuclear factor-[kappa]B-dependent gene expression in primary cultured mouse glial cells. *J. Biol. Chem.*, **279**, 42774–42786.
- Nakamura K, Funakoshi H, Miyamoto K, Tokunaga F, Nakamura T (2001) Molecular cloning and functional characterization of a human scavenger receptor with C-type lectin (SRCL), a novel member of a scavenger receptor family. *Biochemical and biophysical research communications*, **280**, 1028–35.
- Nakamura A, Mori Y, Hagiwara K et al. (2003) Increased susceptibility to LPS-induced endotoxin shock in secretory leukoprotease inhibitor (SLPI)-deficient mice. *The Journal of Experimental Medicine*, **197**, 669–674.
- Nareika A, Im Y Bin, Game BA et al. (2008) High glucose enhances lipopolysaccharide-stimulated CD14 expression in U937 mononuclear cells by increasing nuclear factor ??B and AP-1 activities. *Journal of Endocrinology*, **196**, 45–55.
- Natarajan S, Xu C, Caperna TJ, Garrett WM (2005) Comparison of protein solubilization

- methods suitable for proteomic analysis of soybean seed proteins. *Analytical Biochemistry*, **342**, 214–220.
- Nedredal GI, Elvevold KH, Ytrebo LM, Olsen R, Revhaug A, Smedsrod B (2003) Liver sinusoidal endothelial cells represents an important blood clearance system in pigs. *Comp Hepatol*, **2**, 1.
- Nguewa PA, Fuertes MA, Valladares B, Alonso C, Perez JM (2005) Poly(ADP-ribose) polymerases: homology, structural domains and functions. Novel therapeutical applications. *Prog. Biophys. Mol. Biol.*, **88**, 143–172.
- Norbury CJ, Zhivotovsky B (2004) DNA damage-induced apoptosis. *Oncogene*, **23**, 2797–2808.
- O'Neill LAJ (2011) A critical role for citrate metabolism in LPS signalling. *The Biochemical journal*, **438**, e5-6.
- O'Neill LAJ, Golenbock D, Bowie AG (2013) The history of Toll-like receptors - redefining innate immunity. *Nature reviews. Immunology*, **13**, 453–60.
- Ohanna M, Giuliano S, Bonet C et al. (2011) Senescent cells develop a parp-1 and nuclear factor- κ B-associated secretome (PNAS). *Genes and Development*, **25**, 1245–1261.
- Olivenza R, Moro M a, Lizasoain I et al. (2000) Chronic stress induces the expression of inducible nitric oxide synthase in rat brain cortex. *Journal of neurochemistry*, **74**, 785–791.
- Oliver FJ, Ménessier-de Murcia J, Nacci C et al. (1999) Resistance to endotoxic shock as a consequence of defective NF- κ B activation in poly (ADP-ribose) polymerase-1 deficient mice. *EMBO Journal*, **18**, 4446–4454.
- Pacher P, Szabó C (2007) Role of poly(ADP-ribose) polymerase 1 (PARP-1) in cardiovascular diseases: The therapeutic potential of PARP inhibitors. *Cardiovascular Drug Reviews*, **25**, 235–260.
- Pacher P, Szabó C (2005) Role of poly(ADP-ribose) polymerase-1 activation in the pathogenesis of diabetic complications: endothelial dysfunction, as a common underlying theme. *Antioxidants & Redox Signaling*, **7**, 1568–1580.
- Pacher P, Liaudet L, Soriano FG, Mabley JG, Szabó C, Szabó C (2002) The role of poly(ADP-ribose) polymerase activation in the development of myocardial and endothelial dysfunction in diabetes. *Diabetes*, **51**, 514–521.
- Palecanda a, Paulauskis J, Al-Mutairi E et al. (1999) Role of the scavenger receptor MARCO in alveolar macrophage binding of unopsonized environmental particles. *The Journal of experimental medicine*, **189**, 1497–1506.
- Park HS, Jung HY, Park EY, Kim J, Lee WJ, Bae YS (2004) Cutting edge: direct interaction of TLR4 with NAD(P)H oxidase 4 isozyme is essential for lipopolysaccharide-induced production of reactive oxygen species and activation of NF- κ B. *Journal of immunology (Baltimore, Md. : 1950)*, **173**, 3589–3593.
- Park BS, Song DH, Kim HM, Choi B-S, Lee H, Lee J-O (2009) The structural basis of lipopolysaccharide recognition by the TLR4-MD-2 complex. *Nature*, **458**, 1191–5.
- Park HY, Han MH, Park C et al. (2011) Anti-inflammatory effects of fucoidan through inhibition of NF- κ B, MAPK and Akt activation in lipopolysaccharide-induced BV2 microglia cells. *Food and Chemical Toxicology*, **49**, 1745–1752.

- Paschen W, Doutheil J (1999) Disturbances of the functioning of endoplasmic reticulum: a key mechanism underlying neuronal cell injury? *Journal of cerebral blood flow and metabolism : official journal of the International Society of Cerebral Blood Flow and Metabolism*, **19**, 1–18.
- Patel AG, Sarkaria JN, Kaufmann SH (2011) Nonhomologous end joining drives poly(ADP-ribose) polymerase (PARP) inhibitor lethality in homologous recombination-deficient cells. *Proceedings of the National Academy of Sciences of the United States of America*, **108**, 3406–11.
- Peiser L, Gough PJ, Kodama T, Gordon S (2000) Macrophage class A scavenger receptor-mediated phagocytosis of *Escherichia coli*: Role of cell heterogeneity, microbial strain, and culture conditions in vitro. *Infection and Immunity*, **68**, 1953–1963.
- Peiser L, Mukhopadhyay S, Gordon S (2002) Scavenger receptors in innate immunity. *Current Opinion in Immunology*, **14**, 123–128.
- Peng J, Yuan Q, Lin B et al. (2010) SARM inhibits both TRIF- and MyD88-mediated AP-1 activation. *European Journal of Immunology*, **40**, 1738–1747.
- Peng Y-L, Liu Y-N, Liu L, Wang X, Jiang C-L, Wang Y-X (2012) Inducible nitric oxide synthase is involved in the modulation of depressive behaviors induced by unpredictable chronic mild stress. *Journal of neuroinflammation*, **9**, 75.
- Peralta-Leal A, Rodríguez-Vargas JM, Aguilar-Quesada R, Rodríguez MI, Linares JL, de Almodóvar MR, Oliver FJ (2009) PARP inhibitors: New partners in the therapy of cancer and inflammatory diseases. *Free Radical Biology and Medicine*, **47**, 13–26.
- Perera PY, Mayadas TN, Takeuchi O, Akira S, Zaks-Zilberman M, Goyert SM, Vogel SN (2001) CD11b/CD18 acts in concert with CD14 and Toll-like receptor (TLR) 4 to elicit full lipopolysaccharide and taxol-inducible gene expression. *Journal of immunology (Baltimore, Md. : 1950)*, **166**, 574–581.
- Perez A, Wright MB, Maugeais C et al. (2010) MARCO, a macrophage scavenger receptor highly expressed in rodents, mediates dalcetrapib-induced uptake of lipids by rat and mouse macrophages. *Toxicology in Vitro*, **24**, 745–750.
- Peri F, Piazza M (2012) Therapeutic targeting of innate immunity with Toll-like receptor 4 (TLR4) antagonists. *Biotechnology Advances*, **30**, 251–260.
- Peri F, Piazza M, Calabrese V, Damore G, Cighetti R (2010) Exploring the LPS/TLR4 signal pathway with small molecules [Review]. *Biochemical Society Transactions*, **38**, 1390–1395.
- Platt N, Suzuki H, Kodama T, Gordon S (2000) Apoptotic thymocyte clearance in scavenger receptor class A-deficient mice is apparently normal. *Journal of immunology (Baltimore, Md. : 1950)*, **164**, 4861–4867.
- Plüddemann A, Neyen C, Gordon S (2007) Macrophage scavenger receptors and host-derived ligands. *Methods*, **43**, 207–217.
- Plüddemann A, Mukhopadhyay S, Sankala M et al. (2009) SR-A, MARCO and TLRs differentially recognise selected surface proteins from *neisseria meningitidis*: An example of fine specificity in microbial ligand recognition by innate immune receptors. *Journal of Innate Immunity*, **1**, 153–163.
- Popoff I, Jijon H, Monia B, Tavernini M, Ma M, McKay R, Madsen K (2002) Antisense oligonucleotides to poly(ADP-ribose) polymerase-2 ameliorate colitis in interleukin-

- 10-deficient mice. *J Pharmacol Exp Ther*, **303**, 1145–1154.
- Postel S, Kemmerling B (2009) Plant systems for recognition of pathogen-associated molecular patterns. *Seminars in Cell and Developmental Biology*, **20**, 1025–1031.
- Putt KS, Hergenrother PJ (2004) An enzymatic assay for poly(ADP-ribose) polymerase-1 (PARP-1) via the chemical quantitation of NAD⁺: Application to the high-throughput screening of small molecules as potential inhibitors. *Analytical Biochemistry*, **326**, 78–86.
- Pyriochou A, Olah G, Deitch EA, Szabo C, Papapetropoulos A (2008) Inhibition of angiogenesis by the poly(ADP-ribose) polymerase inhibitor PJ-34. *International Journal of Molecular Medicine*, **22**, 113–118.
- Qi J, Qiao Y, Wang P, Li S, Zhao W, Gao C (2012) MicroRNA-210 negatively regulates LPS-induced production of proinflammatory cytokines by targeting NF- κ B1 in murine macrophages. *FEBS Letters*, **586**, 1201–1207.
- Qin Z (2012) The use of THP-1 cells as a model for mimicking the function and regulation of monocytes and macrophages in the vasculature. *Atherosclerosis*, **221**, 2–11.
- Qiu R, Sun BG, Li J, Liu X, Sun L (2013) Identification and characterization of a cell surface scavenger receptor cysteine-rich protein of *Sciaenops ocellatus*: bacterial interaction and its dependence on the conserved structural features of the SRCR domain. *Fish & shellfish immunology*, **34**, 810–818.
- Racz B, Hanto K, Tapodi A et al. (2010) Regulation of MKP-1 expression and MAPK activation by PARP-1 in oxidative stress: A new mechanism for the cytoplasmic effect of PARP-1 activation. *Free Radical Biology and Medicine*, **49**, 1978–1988.
- Raetz CRH, Reynolds CM, Trent MS, Bishop RE (2007) Lipid A modification systems in gram-negative bacteria. *Annual review of biochemistry*, **76**, 295–329.
- Ramakrishnan P, Clark PM, Mason DE, Peters EC, Hsieh-Wilson LC, Baltimore D (2013) Activation of the transcriptional function of the NF-kappaB protein c-Rel by O-GlcNAc glycosylation. *Sci Signal*, **6**, ra75.
- Raman M, Chen W, Cobb MH (2007) Differential regulation and properties of MAPKs. *Oncogene*, **26**, 3100–3112.
- Reimer T, Brcic M, Schweizer M, Jungi TW (2008) poly(I:C) and LPS induce distinct IRF3 and NF-kappaB signaling during type-I IFN and TNF responses in human macrophages. *Journal of leukocyte biology*, **83**, 1249–1257.
- Reyes RE, Saad HR, Galicia CS, Herrera MO, Jiménez VRC (2009) Mechanisms involved in O antigen variability in gram negative bacteria. *Mecanismos involucrados en la variabilidad del antígeno O de bacterias gram negativas*, **51**, 32–43.
- Rice KC, Bayles KW (2008) Molecular control of bacterial death and lysis. *Microbiol.Mol.Biol.Rev.*, **72**, 85–109, table.
- Rossol M, Heine H, Meusch U, Quandt D, Klein C, Sweet MJ, Hauschildt S (2011) LPS-induced Cytokine Production in Human Monocytes and Macrophages. *Critical ReviewsTM in Immunology*, **31**, 379–446.
- Roux PP, Blenis J (2004) ERK and p38 MAPK-activated protein kinases: a family of protein kinases with diverse biological functions. *Microbiology and molecular biology reviews : MMBR*, **68**, 320–44.

- Ruppert J, Friedrichs D, Xu H, Peters JH (1991) IL-4 decreases the expression of the monocyte differentiation marker CD14, paralleled by an increasing accessory potency. *Immunobiology*, **182**, 449–464.
- Sabroe I, Read RC, Whyte MKB, Dockrell DH, Vogel SN, Dower SK (2003) Toll-like receptors in health and disease: complex questions remain. *Journal of immunology (Baltimore, Md. : 1950)*, **171**, 1630–1635.
- Salminen A, Huuskonen J, Ojala J, Kauppinen A, Kaarniranta K, Suuronen T (2008) Activation of innate immunity system during aging: NF- κ B signaling is the molecular culprit of inflamm-aging. *Ageing Research Reviews*, **7**, 83–105.
- Sankala M, Brännström A, Schulthess T et al. (2002) Characterization of recombinant soluble macrophage scavenger receptor MARCO. *Journal of Biological Chemistry*, **277**, 33378–33385.
- Sarnico I, Lanzillotta A, Boroni F et al. (2009) NF- κ B p50/RelA and c-Rel-containing dimers: Opposite regulators of neuron vulnerability to ischaemia. *Journal of Neurochemistry*, **108**, 475–485.
- Sarrias MR, Grønlund J, Padilla O, Madsen J, Holmskov U, Lozano F (2004) The Scavenger Receptor Cysteine-Rich (SRCR) domain: an ancient and highly conserved protein module of the innate immune system. *Critical reviews in immunology*, **24**, 1–37.
- Sasaki CY, Barberi TJ, Ghosh P, Longo DL (2005) Phosphorylation of RelA/p65 on serine 536 defines an I κ B γ -independent NF- κ B pathway. *Journal of Biological Chemistry*, **280**, 34538–34547.
- Sbodio JI, Lodish HF, Chi N-W (2002) Tankyrase-2 oligomerizes with tankyrase-1 and binds to both TRF1 (telomere-repeat-binding factor 1) and IRAP (insulin-responsive aminopeptidase). *The Biochemical journal*, **361**, 451–459.
- Scalia M, Satriano C, Greca R, Stella AMG, Rizzarelli E, Spina-Purrello V (2013) PARP-1 inhibitors DPQ and PJ-34 negatively modulate proinflammatory commitment of human glioblastoma cells. *Neurochemical Research*, **38**, 50–58.
- Schaaf B, Luitjens K, Goldmann T et al. (2009) Mortality in human sepsis is associated with downregulation of Toll-like receptor 2 and CD14 expression on blood monocytes. *Diagnostic Pathology*, **4**, 12.
- Schildberger, A., Rossmannith, E., Eichhorn, T., Strassl, K & Weber V (2013) Monocytes, Peripheral Blood Mononuclear Cells, and THP-1 Cells Exhibit Different Cytokine Expression Patterns following Stimulation with Lipopolysaccharide. *Mediators of inflammation*, **2013**, 10.
- Schnabl B, Brandl K, Fink M et al. (2008) A TLR4/MD2 fusion protein inhibits LPS-induced pro-inflammatory signaling in hepatic stellate cells. *Biochemical and Biophysical Research Communications*, **375**, 210–214.
- Schortgen F, Charles-Nelson A, Bouadma L, Bizouard G, Brochard L, Katsahian S (2015) Respective impact of lowering body temperature and heart rate on mortality in septic shock: mediation analysis of a randomized trial. *Intensive Care Medicine*, **41**, 1800–1808.
- Schreck R, Albermann K, Baeuerle PA (2009) Nuclear Factor κ B: An Oxidative Stress-Responsive Transcription Factor of Eukaryotic Cells (A Review). *Free Radical Research Communications*, **17**, 221–237.

- Schreiber V, Amé JC, Dollé P et al. (2002) Poly(ADP-ribose) polymerase-2 (PARP-2) is required for efficient base excision DNA repair in association with PARP-1 and XRCC1. *Journal of Biological Chemistry*, **277**, 23028–23036.
- Schreiber V, Dantzer F, Ame J-C, de Murcia G (2006) Poly(ADP-ribose): novel functions for an old molecule. *Nature reviews. Molecular cell biology*, **7**, 517–28.
- Schröder NWJ, Schumann RR (2005) Non-LPS targets and actions of LPS binding protein (LBP). *Journal of endotoxin research*, **11**, 237–242.
- Schrohm AB, Brandenburg K, Loppnow H, Moran AP, Koch MHJ, Rietschel ET, Seydel U (2000) Biological activities of lipopolysaccharides are determined by the shape of their lipid A portion. *European Journal of Biochemistry*, **267**, 2008–2013.
- Schumann RR (1992) Function of lipopolysaccharide (LPS)-binding protein (LBP) and CD14, the receptor for LPS/LBP complexes: a short review. *Research in Immunology*, **143**, 11–15.
- Schuster M, Annemann M, Plaza-Sirvent C, Schmitz I (2013) Atypical IκB proteins - nuclear modulators of NF-κB signaling. *Cell communication and signaling : CCS*, **11**, 23.
- Sekine Y, Yumioka T, Yamamoto T et al. (2006) Modulation of TLR4 Signaling by a Novel Adaptor Protein Signal-Transducing Adaptor Protein-2 in Macrophages. *The Journal of Immunology*, **176**, 380–389.
- Seow V, Lim J, Iyer A et al. (2013) Inflammatory responses induced by lipopolysaccharide are amplified in primary human monocytes but suppressed in macrophages by complement protein C5a. *Journal of immunology (Baltimore, Md. : 1950)*, **191**, 4308–16.
- Sethi S, Dikshit M (2000) Modulation of Polymorphonuclear Leukocytes Function by Nitric Oxide. *Thrombosis Research*, **100**, 223–247.
- Shall S, De Murcia G (2000) Poly(ADP-ribose) polymerase-1: What have we learned from the deficient mouse model? *Mutation Research - DNA Repair*, **460**, 1–15.
- Shaposhnikov M V, Moskalev AA, Plyusnina EN (2011) Effect of PARP-1 overexpression and pharmacological inhibition of NF-κB on the lifespan of *Drosophila melanogaster*. *Advances in gerontology = Uspekhi gerontologii / Rossiiskaia akademiia nauk, Gerontologicheskoe obshchestvo*, **24**, 405–419.
- Shi H, Kokoeva M V, Inouye K, Tzameli I, Yin H, Flier JS (2006) TLR4 links innate immunity and fatty acid – induced insulin resistance. *The journal of clinical investigation*, **116**, 3015–3025.
- Shifu C, Gengyu C (2005) Photocatalytic degradation of organophosphorus pesticides using floating photocatalyst TiO₂ / SiO₂/beads by sunlight. *Solar Energy*, **79**, 1–9.
- Shuto T, Kato K, Mori Y et al. (2005) Membrane-anchored CD14 is required for LPS-induced TLR4 endocytosis in TLR4/MD-2/CD14 overexpressing CHO cells. *Biochemical and Biophysical Research Communications*, **338**, 1402–1409.
- Sidorkina O, Espey MG, Miranda KM, Wink DA, Laval J (2003) Inhibition of poly(ADP-ribose) polymerase (PARP) by nitric oxide and reactive nitrogen oxide species. *Free Radical Biology and Medicine*, **35**, 1431–1438.
- Silva E, Leitão S, Henriques S et al. (2010) Gene transcription of TLR2, TLR4, LPS ligands and prostaglandin synthesis enzymes are up-regulated in canine uteri with cystic endometrial hyperplasia-pyometra complex. *Journal of Reproductive*

- Immunology*, **84**, 66–74.
- Da Silva Correia J, Soldau K, Christen U, Tobias PS, Ulevitch RJ (2001) Lipopolysaccharide is in close proximity to each of the proteins in its membrane receptor complex. Transfer from CD14 to TLR4 and MD-2. *Journal of Biological Chemistry*, **276**, 21129–21135.
- Singh BP, Chauhan RS, Singhal LK (2003) Toll-like receptors and their role in innate immunity. *October*, **85**.
- Skurnik M, Bengoechea JA (2003) The biosynthesis and biological role of lipopolysaccharide O-antigens of pathogenic *Yersinia*. *Carbohydrate Research*, **338**, 2521–2529.
- Sodhi RK, Singh N, Jaggi AS (2010) Poly(ADP-ribose) polymerase-1 (PARP-1) and its therapeutic implications. *Vascular Pharmacology*, **53**, 77–87.
- Soldani C, Scovassi AI (2002) Poly(ADP-ribose) polymerase-1 cleavage during apoptosis: An update. *Apoptosis*, **7**, 321–328.
- Song PI, Abraham T a, Park Y et al. (2001) The expression of functional LPS receptor proteins CD14 and toll-like receptor 4 in human corneal cells. *Investigative ophthalmology & visual science*, **42**, 2867–2877.
- Soriano FG, Pacher P, Mabley J, Liaudet L, Szabo C (2001) Rapid reversal of the diabetic endothelial dysfunction by pharmacological inhibition of poly(ADP-ribose) polymerase. *Circ Res*, **89**, 684–91.
- Souza KLA, Gurgul-Convey E, Elsner M, Lenzen S (2008) Interaction between pro-inflammatory and anti-inflammatory cytokines in insulin-producing cells. *Journal of Endocrinology*, **197**, 139–150.
- Stewart VC, Sharpe MA, Clark JB, Heales SJR (2000) Astrocyte-derived nitric oxide causes both reversible and irreversible damage to the neuronal mitochondrial respiratory chain. *Journal of Neurochemistry*, **75**, 694–700.
- Suharti C, Van Gorp ECM, Dolmans WM V, Setiati TE, Hack CE, Djokomoeljanto RJ, Van Der Meer JWM (2003) Cytokine patterns during dengue shock syndrome. *European Cytokine Network*, **14**, 172–177.
- Surh Y-J, Chun K-S, Cha H-H, Han SS, Keum Y-S, Park K-K, Lee SS (2001) Molecular mechanisms underlying chemopreventive activities of anti-inflammatory phytochemicals: down-regulation of COX-2 and iNOS through suppression of NF- κ B activation. *Mutation Research/Fundamental and Molecular Mechanisms of Mutagenesis*, **480–481**, 243–268.
- Symons A, Beinke S, Ley SC (2006) MAP kinase kinases and innate immunity. *Trends in Immunology*, **27**, 40–48.
- Szabo G (2002) Poly(ADP-ribose) polymerase inhibition reduces reperfusion injury after heart transplantation. *Circ. Res.*, **90**, 100–106.
- Szabo C (2007) Poly (ADP-ribose) polymerase activation and circulatory shock. *Novartis Foundation Symposium*, **280**, 92-97-164.
- Szabó G, Liaudet L, Hagl S et al. (2004) Poly(ADP-ribose) polymerase activation in the reperfused myocardium. *Cardiovasc. Res.*, **61**, 471–480.
- Takeda K, Akira S (2004) TLR signaling pathways. *Seminars in Immunology*, **16**, 3–9.
- Tanimura N, Saitoh S, Matsumoto F, Akashi-Takamura S, Miyake K (2008) Roles for

- LPS-dependent interaction and relocation of TLR4 and TRAM in TRIF-signaling. *Biochemical and Biophysical Research Communications*, **368**, 94–99.
- Tanouchi Y, Lee AJ, Meredith H, You L (2013) Programmed cell death in bacteria and implications for antibiotic therapy. *Trends in Microbiology*, **21**, 265–270.
- Tentori L, Graziani G (2005) Chemopotential by PARP inhibitors in cancer therapy. *Pharmacological Research*, **52**, 25–33.
- Teo ZP, Hughes D (2003) The Role of Macrophages in Apoptosis : Initiator , Regulator , Scavenger. *Reviews in Undergraduate Research*, **2**, 7–11.
- Terpstra V, van Berkel TJC (2000) Scavenger receptors on liver Kupffer cells mediate the in vivo uptake of oxidatively damaged red blood cells in mice. *Blood*, **95**, 2157–2163.
- Thelen T, Hao Y, Medeiros AI et al. (2010) The class A scavenger receptor, macrophage receptor with collagenous structure, is the major phagocytic receptor for *Clostridium sordellii* expressed by human decidual macrophages. *Journal of immunology (Baltimore, Md. : 1950)*, **185**, 4328–4335.
- Thomas CA, Li Y, Kodama T, Suzuki H, Silverstein SC, El Khoury J (2000) Protection from lethal gram-positive infection by macrophage scavenger receptor-dependent phagocytosis. *The Journal of experimental medicine*, **191**, 147–56.
- Thompson PA, Tobias PS, Viriyakosol S, Kirkland TN, Kitchens RL (2003) Lipopolysaccharide (LPS)-binding protein inhibits responses to cell-bound LPS. *Journal of Biological Chemistry*, **278**, 28367–28371.
- Thorgersen EB, Pischke SE, Barratt-Due A et al. (2013) Systemic CD14 inhibition attenuates organ inflammation in porcine *Escherichia coli* sepsis. *Infection and Immunity*, **81**, 3173–3181.
- Titheradge M a (1999) Nitric oxide in septic shock. *Biochimica et biophysica acta*, **1411**, 437–55.
- Trent MS, Stead CM, Tran AX, Hankins J V (2006) Diversity of endotoxin and its impact on pathogenesis. *Journal of endotoxin research*, **12**, 205–223.
- Trevino SR, Scholtz JM, Pace CN (2008) Measuring and increasing protein solubility. *Journal of Pharmaceutical Sciences*, **97**, 4155–4166.
- Triantafilou M, Triantafilou K (2002a) Lipopolysaccharide recognition: CD14, TLRs and the LPS-activation cluster. *Trends in Immunology*, **23**, 301–304.
- Triantafilou M, Triantafilou K (2002b) Lipopolysaccharide recognition: CD14, TLRs and the LPS-activation cluster. *Trends in Immunology*, **23**, 301–304.
- Tsuchiya S, Yamabe M, Yamaguchi Y, Kobayashi Y, Konno T, Tada K (1980) Establishment and characterization of a human acute monocytic leukemia cell line (THP-1). *International Journal of Cancer. Journal International Du Cancer*, **26**, 171–176.
- Tsukamoto H, Fukudome K, Takao S, Tsuneyoshi N, Kimoto M (2010) Lipopolysaccharide-binding protein-mediated Toll-like receptor 4 dimerization enables rapid signal transduction against lipopolysaccharide stimulation on membrane-associated CD14-expressing cells. *International Immunology*, **22**, 271–280.
- Uematsu S, Akira S (2008) Pathogen recognition by innate immunity. *Skin Research*, **7**,

1–11.

- Uza N, Nakase H, Yamamoto S et al. (2011) SR-PSOX/CXCL16 plays a critical role in the progression of colonic inflammation. *Gut*, **60**, 1494–1505.
- Vallabhapurapu S, Karin M (2009) Regulation and function of NF-kappaB transcription factors in the immune system. *Annual review of immunology*, **27**, 693–733.
- Veckman V (2007) *Microbe-Induced Activation of Inflammatory Cytokine Response in Human Cells*.
- Verbon A, Joost CMM, Spek CA et al. (2003) Effects of IC14, an Anti-CD14 Antibody, on Coagulation and Fibrinolysis during Low-Grade Endotoxemia in Humans. *The Journal of infectious diseases*, **187**, 55–61.
- Veres B (2004) Regulation of kinase cascades and transcription factors by a poly(ADP-ribose) polymerase-1 inhibitor, 4-hydroxyquinazoline, in lipopolysaccharide-induced inflammation in mice. *J. Pharmacol. Exp. Ther.*, **310**, 247–255.
- Veres B, Gallyas F, Varbiro G et al. (2003) Decrease of the inflammatory response and induction of the Akt/protein kinase B pathway by poly-(ADP-ribose) polymerase 1 inhibitor in endotoxin-induced septic shock. *Biochemical Pharmacology*, **65**, 1373–1382.
- Veuger SJ, Hunter JE, Durkacz BW (2009) Ionizing radiation-induced NF-kappaB activation requires PARP-1 function to confer radioresistance. *Oncogene*, **28**, 832–42.
- Vilá LM, Molina MJ, Mayor AM, Cruz JJ, Ríos-Olivares E, Ríos Z (2007) Association of serum MIP-1 α , MIP-1 β , and RANTES with clinical manifestations, disease activity, and damage accrual in systemic lupus erythematosus. *Clinical Rheumatology*, **26**, 718–722.
- Virág L (2005) Structure and function of poly(ADP-ribose) polymerase-1: role in oxidative stress-related pathologies. *Current vascular pharmacology*, **3**, 209–14.
- Visintin A, Halmen KA, Latz E, Monks BG, Golenbock DT (2005) Pharmacological inhibition of endotoxin responses is achieved by targeting the TLR4 coreceptor, MD-2. *J Immunol.*, **175**, 6465–6472.
- Vives-Pi M, Somoza N, Fernandez-Alvarez J et al. (2003) Evidence of expression of endotoxin receptors CD14, toll-like receptors TLR4 and TLR2 and associated molecule MD-2 and of sensitivity to endotoxin (LPS) in islet beta cells. *Clinical and Experimental Immunology*, **133**, 208–218.
- Wanecek M, Weitzberg E, Rudehill A, Oldner A (2000) The endothelin system in septic and endotoxin shock. *European Journal of Pharmacology*, **407**, 1–15.
- Wang ZQ, Stingl L, Morrison C, Jantsch M, Los M, Schulze-Osthoff K, Wagner EF (1997) PARP is important for genomic stability but dispensable in apoptosis. *Genes and Development*, **11**, 2347–2358.
- Wang L, Wang Q, Reeves PR (2010) The variation of O antigens in gram-negative bacteria. *Sub-Cellular Biochemistry*, **53**, 123–152.
- Wang G, Huang X, Li Y, Guo K, Ning P, Zhang Y (2013) PARP-1 inhibitor, DPQ, attenuates LPS-induced acute lung injury through inhibiting NF- κ B-mediated inflammatory response. *PLoS ONE*, **8**.
- Ward TL, Goto K, Altosaar I (2014) Ingested soluble CD14 contributes to the functional

- pool of circulating sCD14 in mice. *Immunobiology*, **219**, 537–546.
- Wheeler MD, Thurman RG (2003) Up-regulation of CD14 in liver caused by acute ethanol involves oxidant-dependent AP-1 pathway. *Journal of Biological Chemistry*, **278**, 8435–8441.
- Widmann C, Gibson S, Jarpe MB, Johnson GL (1999) Mitogen-Activated Protein Kinase: Conservation of a Three-Kinase Module From Yeast to Human. *Physiol Rev*, **79**, 143–180.
- Witze ES, Old WM, Resing KA, Ahn NG (2007) Mapping protein post-translational modifications with mass spectrometry. *Nature methods*, **4**, 798–806.
- Wright SD, Ramos RA, Tobias PS, Ulevitch RJ, Mathison JC (1990) CD14, a receptor for complexes of lipopolysaccharide (LPS) and LPS binding protein. *Science*, **249**, 1431–1433.
- Wu A, Hinds CJ, Thiemermann C (2004) High-density lipoproteins in sepsis and septic shock: metabolism, actions, and therapeutic applications. *Shock (Augusta, Ga.)*, **21**, 210–221.
- Wurfel MM, Hailman E, Wright SD (1995) Soluble CD14 acts as a shuttle in the neutralization of lipopolysaccharide (LPS) by LPS-binding protein and reconstituted high density lipoprotein. *The Journal of experimental medicine*, **181**, 1743–1754.
- Xagorari A, Chlichlia K (2008) Toll-like receptors and viruses: induction of innate antiviral immune responses. *The open microbiology journal*, **2**, 49–59.
- Xiao Y, Wang YC, Li LL, Jin YC, Sironi L, Wang Y (2014) Lactones from *Ligusticum chuanxiong* Hort. reduces atherosclerotic lesions in apoE-deficient mice via inhibiting over expression of NF- κ B -dependent adhesion molecules. *Fitoterapia*, **95**, 240–246.
- Xu H, Liew LN, Kuo IC, Huang CH, Goh DLM, Chua KY (2008) The modulatory effects of lipopolysaccharide-stimulated B cells on differential T-cell polarization. *Immunology*, **125**, 218–228.
- Yamada S, Maruyama I (2007) HMGB1, a novel inflammatory cytokine. *Clinica Chimica Acta*, **375**, 36–42.
- Yang H, Tracey KJ (2010) Targeting HMGB1 in inflammation. *Biochimica et Biophysica Acta - Gene Regulatory Mechanisms*, **1799**, 149–156.
- Yang H, Wang H, Czura CJ, Tracey KJ (2002) HMGB1 as a cytokine and therapeutic target. *Journal of Endotoxin Research*, **8**, 469–72.
- Yelamos J, Farres J, Llacuna L, Ampurdanes C, Martin-Caballero J (2011) PARP-1 and PARP-2: New players in tumour development. *American journal of cancer research*, **1**, 328–346.
- Yi H, Bai Y, Zhu X et al. (2014) IL-17A Induces MIP-1 α Expression in Primary Astrocytes via Src/MAPK/PI3K/NF- κ B Pathways: Implications for Multiple Sclerosis. *Journal of Neuroimmune Pharmacology*, **9**, 629–641.
- Ying W, Garnier P, Swanson RA (2003) NAD⁺ repletion prevents PARP-1-induced glycolytic blockade and cell death in cultured mouse astrocytes. *Biochemical and Biophysical Research Communications*, **308**, 809–813.
- Yu H, Ha T, Liu L et al. (2012) Scavenger receptor A (SR-A) is required for LPS-induced TLR4 mediated NF- κ B activation in macrophages. *Biochimica et Biophysica Acta* -

- Molecular Cell Research*, **1823**, 1192–1198.
- Yu X, Guo C, Fisher PB, Subjeck JR, Wang XY (2015) Scavenger Receptors: Emerging Roles in Cancer Biology and Immunology. *Advances in Cancer Research*, **128**, 309–364.
- Yung TMC, Sato S, Satoh MS (2004) Poly(ADP-ribosyl)ation as a DNA damage-induced post-translational modification regulating poly(ADP-ribose) polymerase-1-topoisomerase I interaction. *Journal of Biological Chemistry*, **279**, 39686–39696.
- Zanoni I, Granucci F (2013) Role of CD14 in host protection against infections and in metabolism regulation. *Frontiers in cellular and infection microbiology*, **3**, 32.
- Zanoni I, Ostuni R, Capuano G et al. (2009) CD14 regulates the dendritic cell life cycle after LPS exposure through NFAT activation. *Nature*, **460**, 264–268.
- Zhang DE, Hetherington CJ, Gonzalez DA, Chen HM, Tenen DG (1994) Regulation of CD14 expression during monocytic differentiation induced with 1 alpha,25-dihydroxyvitamin D3. *Journal of immunology (Baltimore, Md. : 1950)*, **153**, 3276–84.
- Zhong X, Li X, Liu F, Tan H, Shang D (2012) Omentin inhibits TNF- α -induced expression of adhesion molecules in endothelial cells via ERK/NF- κ B pathway. *Biochemical and Biophysical Research Communications*, **425**, 401–406.
- Züllig S, Neukomm LJ, Jovanovic M et al. (2007) Aminophospholipid Translocase TAT-1 Promotes Phosphatidylserine Exposure during *C. elegans* Apoptosis. *Current Biology*, **17**, 994–999.
- Luo X, Lee Kraus W (2012) On par with PARP: Cellular stress signaling through poly(ADP-ribose) and PARP-1. *Genes and Development*, **26**, 417–432.